Three Dimensional Perfused Cell Culture for *In Vitro* Toxicity Testing

Department of Engineering Science

University of Oxford

Jie Yang

St. Cross College

Thesis Submitted for the Degree of Doctor of Philosophy

Trinity Term, 2011

Abstract

Three Dimensional Perfused Cell Culture for In Vitro Toxicity Testing

A thesis submitted for the Degree of Doctor of Philosophy

Jie Yang St. Cross College Trinity Term, 2011

This study describes the development of a novel method of three dimensional perfused cell culture for in vitro toxicity testing. Multiple parallel perfused microbioreactors (TissueFlex^{TM}) were adopted to provide a well-controlled cell culture environment. Alginate and collagen type I, commonly used as hydrogel scaffolds to support cell culture, were tested as the scaffolding materials for this application. Alginate supports cell proliferation, but does not support cell attachment. Collagen gel (type I), good for cell attachment but with poor mechanical strength, could be used at the high concentration of 5mg/ml to prevent the degradation of the gel. Improvement of collagen biomechanical property by a purpose-designed compressor to physically induce cross-linking showed promising results and merits further study. The suitability of alamarBlue® assay, a common non-toxic non-destructive viability assay method, was confirmed for this study and the protocol was optimised. To demonstrate the effectiveness of three dimensional perfused cell culture, human mesenchymal stem cells (MSC) seeded in collagen type I were employed to test the cell inhibition of two antibiotics, trimethoprim and pyrimethamine. The results displayed the perfusion system has greater advantage and sensitivity than the static system, as does these of 3D scaffolds, compared with 2D. Such differences are related to the continuous supply of fresh culture medium to keep cells at a stable pH, temperature, oxygen, and a more physiological like environment. The cytotoxicity of two stereoisomer compounds,

obtained confidentially from Pfizer. Ltd., was assessed using the developed method and compared to conventional 2D static and perfused culture by using rat adipose mesenchymal stem cells. The results successfully distinguished toxic and non-toxic compounds and also demonstrated that the 3D perfused system improved the prediction of drug toxicity over 2D culture. 3D perfused bioreactors were applied to hepatotoxicity study using freshly isolated rat hepatocytes. Only algimatrix^{TM} supported hepatocyte spheroid formation among those tested including collagen type I, alginate beads, poly lactic acid fibres, and Algimatrix^{TM}. A new variation of TissueFlex^{TM} bioreactor with micro-patterned surface, designed specifically for hepatocyte self-assembly culture without use of any scaffold, was tested. The results demonstrated that, compared with the standard sandwich culture, the self-assembly culture in the micro-patterned bioreactors showed high cell viability, biomarkers expression, as well as more physiological immunocytochemistry. Moreover, the differential gene expression indicated that self-assembly culture could provide more relevant information regarding metabolising processes than the 2D sandwich culture, which would potentially improve hepatotoxicity prediction. In conclusion, 3D perfused cell culture for *in vitro* toxicity testing improved the predictivity, reliability and physiological relevance of drug toxicity compared to traditional 2D culture.

Acknowledgements

I would like to thank my supervisor, Professor Zhanfeng Cui, who introduced me to the field of tissue engineering, and supported me continuously throughout my DPhil time at Oxford University. I would also like to thank Dr. Xia Xu, who co-supervised me for the first two years of my research, but left to pursue an academic career in China. Other members in the group, I would like to thank Dr. Nuala Trainor, Pierre-Alexis Mouthuy, Jinnan Zhang, and Nikolas Weissmueller. Special thanks to Dr. Cathy Ye, Dr. Julian Gorge, Dr. Yasser El-sherbini and Dr. Ryan Cawood for their help in discussing my thesis, and proof reading. Also, thanks to Jim Fisk and Roger Lewis for all machining work. Also thanks to Dr. Annamaria Rossi, my supervisor in Pfizer, Sandwich, where I spent the last year of my DPhil research. Without her guidance and support, I would not be able to complete my research there on time. And others Jon Hichcock, Graham Gandy, Kathryn Hedley, Gareth Philips and Elodie Philips, Clare Gardener, Ben Sidders and Clarisse Dubray thanks for always helping me with whatever techniques I need. Meanwhile, I would like to thank Dr. Zhaohui Li, Dr. David Hughes and Dr. Tim Hart from Zyoxel Ltd, for their discussion and following up with my research progress and allowing me to have the first work experience prior to Pfizer. Last but not least, I would like to express my deepest gratitude to my parents, who have been encouraging me all the time, and supporting me by all means! And my friends who have accompanied me for the past a few years in Oxford, thank you all for making my life rich and beautiful!

Table of Contents

List of figures

List of tables

List of Equations

List of Abbreviations

2D: two dimensional
3D: three dimensional
AB: AlamarBlue®
ADMSC: Adiposed derived mesenchymal stem cell
ALT: Alanine transaminase
AST: Aspartate aminotransferase
ATP: adenosine triphosphate
Calcein-AM: calcein acetoxymethyl
cDNA: complementary DNA
CK18: Cytokeratin 18
CMFDA: 5-chloromethylfluorescein diacetate
Dapi: 4,6-diamidino-2-phenylindole-dihydrochloride
Dex: dexamethasone
DMEM: Dulbecco's modified Eagle's medium
DMSO: dimethylsulphoxide
DNA: deoxyribonucleic acid
DNase: Deoxyribonuclease I
ECM: extracellular matrix
EDTA: ethylenediaminetetraacetic acid
EGF: Epidermal growth factor
Eqn: Equation
ES cells: Embryonic stem cells
FBS: Foetal bovine serum
FDA: food and drug administration
GLDH: Glutamate dehydrogenase
GO: Gene oncology
HBSS: Hank's Balanced Salt Solution
HEPES: 4-(2-hydroxyethyl)-1-piperazineethanesulfonic acid
HGF: Hepatocyte growth factor
hMSC: Human mesenchymal stem cells
HNF-4: Hepatocyte nuclear factor-4
LDH: Lactate dehydrogenase
MALB: Microalbumin
MP: Micro-patterned
MPM: multiphoton microscope
MSCs: mesenchymal stem cells
MTT: 3-(4,5-dimethyldiazol-2-yl)-2,5 diphenyl tetrazolium bromide
NADPH: Nicotinamide adenine dinucleotide phosphate
PBS: Phosphate buffered saline
PCA: Principle Component Analysis
PDMS: polydimethylsiloxane

PEG: Poly(ethylene glycol)
PET: poly (ethylene terepthalate)
PGA: polyglycolide
PI: Propidium iodide
PLA: polylactide
PLGA: poly(D,L-lactide-co-glycolide)
PPARα: Peroxisome proliferators-activated receptors alpha
RNA: ribonucleic acid
RNA: Ribonucleic acid
w/v: Weight per volume
ZO-1: Zona occludens-1
αMEM: alpha-minimum essential medium

Chapter 1 Introduction

Drug development is a long, expensive and complicated process. It generally involves drug identification, validation and optimisation, followed by pre-clinical trials in vitro and in animals and then finally to be proved by clinical trials. However, it is widely known that where drugs have failed in clinical trials, this is in many cases due to the adverse effect in humans. Therefore, improving drug safety and efficacy in the pre-clinical trial would certainly contribute to the success of clinical trials. Traditionally, a cell-based monolayer culture is used in the pre-clinical stage to evaluate the toxicity. However, there are some disadvantages of monolayer culture: lack of the cellular hierarchy structure, cell-cell contacts, different cell morphology, different gene expression, pH changes, insufficient nutrition supply, as well as being labour intensive. All of those limitations of the culture would hamper the development of toxicity testing. There is a great demand in in vitro toxicity testing to have a better platform, which improves the predictivity and accuracy of drugs in pre-clinical trials, which would ultimately reduce animal use.

1.1 Aims and Objectives

The aim of the work described in this thesis is to employ perfused bioreactors as a novel

tool to apply to cellular based toxicity testing. The main work is composed of several aspects listed below.

1) The use of mesenchymal stem cells and scaffolds, together with Tissueflex^{TM} bioreactor to develop a novel method to test known compounds' toxicity. For this purpose, culture conditions and assay conditions in 3D were optimised.
2) The use of adipose derived mesenchymal stem cells to test the toxicity of two compounds supplied confidentially by Pfizer was evaluated. Blind testing was carried out to test if any of the compounds was toxic and if the perfused bioreactor predicted better toxicity.
3) The use of primary liver hepatocytes to create a self-assembly spheroid culture in the modified perfused bioreactor with potential application to drug toxicity testing. Varieties of scaffold materials were also taken into consideration. The comparison between novel spheroid culture and traditional sandwich culture was carried out.

1.2 Scope of Thesis

The whole thesis is composed of 6 chapters. To begin with, a comprehensive literature review states the current situation of drug development, the demand of a better platform to predict cellular based toxicity, the different approaches to evaluate toxicity, as well as three dimensional scaffolds and perfused bioreactors. The following chapter (Chapter 3)

describes the development of the mesenchymal stem cell-based model for toxicity testing, by employing the perfused bioreactor. Scaffolds development, culture conditions and assay optimisation are discussed in detail. After the platform was developed, the perfused bioreactor was then applied to two compounds supplied confidentially by Pfizer ltd. by using adipose derived mesenchymal stem cells (Chapter 4). According to Pfizer, the cytotoxicity of oxazolidinones via inhibition of mitochondrial protein expression is induced by isomers with cis (Compound A), but not trans (Compound B), stereo chemistry on the heterocyclic materials. 3D perfused bioreactors significantly improved the prediction of toxicity. A modified version of the perfused bioreactors, micro-patterned (MP) bioreactors, were utilised to facilitate the primary hepatocyte culture (Chapter 5). Selection of scaffold materials and optimisation of self-assembly culture conditions were investigated. Comparison between traditional methods of hepatocyte culture and novel self-assembly culture by using MP bioreactors was discussed. Results include the viability test, functional tests, cellomics microscope imaging, confocal microscope imaging, immocytochemistry and gene analysis of two models, which indicate great potential for toxicity testing. The final chapter summarises the work described above and discusses future work.

Chapter 2 Development of *In Vitro* Toxicity Testing-Literature Review

2.1Introduction

In this chapter, a comprehensive literature review states the current situation of drug development, and the demands to develop a better cellular based model for in vitro toxicity testing during the preclinical stage to predict general or organ specific toxicity such as hepatotoxicity. Toxicity testing may be measured via viability, functional testing, genomics, as well as imaging approaches. Three dimension cell culture shows the advantages of cellular hierarchy structure, better cell-cell contacts, *in vivo* like cell morphology and closer gene expression. By applying perfused medium in bioreactors, with the three dimension system, cell culture maintains a stable pH and a sufficient nutrition supply, as well as less time consuming labour. All of these advantages would contribute to the development of toxicity testing, which potentially improves the predictivity and accuracy of drugs in preclinical trials.

2.2 Background

The entire discovery and development of every single drug, from the formation of molecular structure, to US Food and Drug Administration (FDA) approval, then finally

putting it on the market, usually takes 12-15 years to complete, with an average cost of more than a billion US dollars. There are 5 stages in drug development: discovery, pre-clinical trials, clinical trials, FDA approval and manufacturing and marketing. Initially, around 5,000 to 10,000 chemical molecules are designed to target the disease and selected as drug candidates to go through high throughput screening (Ukelis et al, 2008). 1 in around 250 subsequently undergoes pre-clinical trials. At this stage, lead compounds are evaluated and optimised to meet the drug efficacy and safety conditions using *in vitro* (bench) and then animal testing. The number of compounds remaining at the end of the pre-clinical trials is around 10-20. These first 2 stages usually take 3-7 years in total and may cost around US$25 million. Before entering the clinical stage, an Investigational New Drug Application needs to be submitted to the FDA to allow human exposure to the compounds for clinical trials. Clinical trials are human-based testing, which consists of 3 phases to test the compounds' efficacy and safety, can last 3-7 years, and cost up to $5 million. Ultimately 1 or 2 compounds will survive for FDA approval and manufacturing (Zambrowicz, 2003; Tonkens, 2005).

It is widely known that where drugs have failed in clinical trials, this is in many cases due to an adverse effect in humans. Traditionally, in the pre-clinical stage, drug efficacy and safety are evaluated in both in vitro and *in vivo* toxicity testing, which requires a large number of animals, high financial cost and long period of time. Olson et al reported from pharmaceutical companies worldwide in 2000, that 57% of drug toxicity in humans does not correspond to toxicity in experimental animals, because of various

pharmacokinetic differences among species (Olson H, 2000, Akhtar et al, 2008; Price et al, 2008). Meanwhile, some systematic reviews by de Boo, and Knight indicate that only 2 in 20 reviews show significant contributions towards human clinical trials made by using an animal-based *in vivo* model, the poor productivity in humans also indicating the pre-clinical model needs an alternative method (De Boo, 2005; Knight, A. 2007a, 2007b). The use of animals in toxicity and biomedical research also raises ethical issues, leading to public concern as seen in animal rights protests. In 1959 Russell and Burch originated the three Rs concept, encompassing reduction, refinement and replacement of usage of laboratory animals (Russell and Burch, 1959), which has been widely accepted throughout the world. 'Reduction' refers to reducing the numbers of animals used, 'refinement' involves refining the protocol to minimise the potential pain and stress suffered by the animals, while 'replacement' concerns replacing the current *in vivo* animal tests with *in vitro* tests which do not require living animals (Gad, 1990; Balls et al. 1995; Fielder et al. 1997). There is a need to develop *in vitro* testing in pre-clinical trials to improve the reliability and predictability of drug toxicity (Combes et al, 2002; Combes, 2005).

2.3 Stem Cells and Hepatocytes

2.3.1 Toxicity Testing Using Stem Cells

In order to reduce the use of animals before clinical trials on humans, cell-based models are widely exploited in the first 3 stages of development to identify, validate and optimise the drug. Cell lines are reproducible and able to retain the capacity to proliferate; however, they still failed on human clinical trials to mimic the human functional systems due to abnormal genotype, growth in culture, and physiological response (Rolletschek et al., 2004; Améen, 2008; Thiede 2009). Primary cell-based models are physiologically and genomically more relevant to *in vivo* systems, but batches vary and a whole animal is required to supply the tissue continuously. However, some cell functions are complex; once outside the living body, their proliferation capacity and viability decrease rapidly which results in the functions being quickly lost; therefore, the *in vitro* model does not completely correlate to the human, and cannot represent the human disorders (Senthil, 2010).

Stem cells as a source of models can be investigated for drug discovery, toxicity testing and mechanism study to circumvent the problems stated above. The main areas of stem cell based toxicity testing for preclinical usage are to predict heptatotoxicity, cardiotoxicity, neurotoxicity and nephrotoxicity.

Stem cells are undifferentiated cells which have high proliferation ability (self renewing

ability) and differentiation ability under the influence of certain growth factors. They are relatively stable and contain normal genetic structure. In a controlled environment, they are able to fully differentiate into a variety of cell lineages which positively display specific tissue markers and characteristic morphology (Jones and Fuller, 2004). They also can be derived from specific patients, which is more relevant to the disease; this should be able to predict toxicity more reliably for early efficacy and safety in pre-clinical development, along with the reduction of adverse effects on clinical development (Davila et al, 2004; Rubin LL, 2008; Pouton, 2005 Pouton, 2007).

Stem cells from the undifferentiated and differentiated stages are all widely used in toxicity testing. Embryonic stem cells were directly employed to test the embryotoxic hazards of chemical compounds (Bremer et al. 2002). The Murine Embryonic Stem Cell Test (EST) for drug toxicity has been designed and validated by the European Centre for the Validation of Alternative Methods (ECVAM) (Zuang, 2007; Marx-Stoelting et al., 2009). Paquette et al. stated that the pharmaceutical industry has been using such a model to assess the toxicity of known toxic compounds in the in-house library (Paquette, 2008). Cezar used human ES cells and hES cell-derived neural precursors to perform metabolite profiling as a tool to discover novel biomarkers with predictive drug efficacy and safety (Cezar, 2007). Stem cell based gene therapy also offers promising potentials to cure conditions like aging-related dysfunction, hematopoietic, cardiovascular, musculoskeletal, pulmonary, ocular, urogenital, neurodegenerative and skin disorders (Mimeault, 2009)

Embryonic Stem Cells

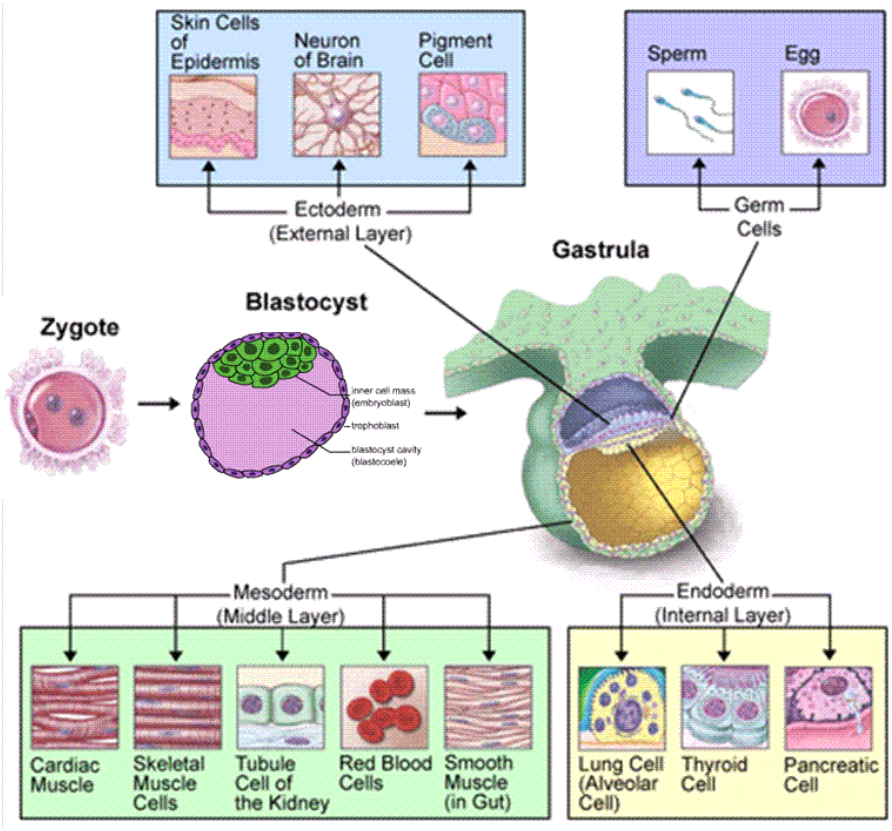

Figure 2.1 Development of Blastocyst (Adapted from the National Centre for Biotechnology Information)

Embryonic stem cells are derived from embryos 4 or 5 days after fertilisation. At this stage, the embryo consists of a blastocyst, comprising the trophoblast or outer layer of cells, the blastocoele (or inner cavity) and the inner cell mass. There are approximately 30 undifferentiated embryonic stem cells in the inner cell mass. The embryo develops three layers: the ectoderm, the mesoderm and the endoderm. The external layer (ectoderm) develops into skin, nails, teeth, lens of eyes, the nerves, the brain as well as the spinal cord. The internal layer forms organs such as the liver, lungs and gall bladder. The middle layer (mesoderm) develops into musculoskeletal, fat, and bone marrow.

Mesenchymal Stem Cells

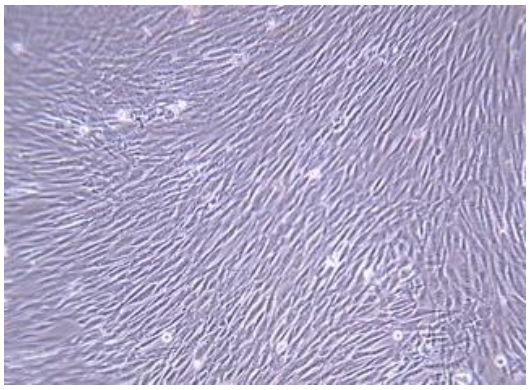

Figure 2.2 Human Mesenchymal Stem Cell

(Adapted from Alpha Stem Source)

Mesenchymal Stem Cells (MSCs) were first identified and characterized in 1966 in studies by Friedenstein and Petrakova, who isolated bone/cartilage-forming progenitor cells from rat bone marrow cells with fibroblast-like morphology (Kemp, 2005). MSCs are mostly derived from bone marrow (Figure 2.2). They are multipotent stem cells that can be purified, expanded and differentiated into a variety of cell types including osteoblasts, chondrocytes, myocytes, adipocytes, and as described recently, into beta-pancreatic islet cells (Darko, 2004). They have also been suggested to transdifferentiate into neuronal cells and hepatocyte-like cells (Pittergen, 1999). Although some scientists doubt whether adult stem cells such as MSCs can give rise to genuine pluripotent cells (Alvarez-Dolgado et al., 2003), efforts have been made to utilise adult stem cells for better efficacy (Ahuja, 2007). MSCs, apart from their promising potential for cell therapies and regenerative medicine, could be potential candidates for producing model tissue for drug and toxicity testing. Because of their multi-potency and self-renewal ability, they are suitable for forming a variety of tissues from the same cell source. A single cell source, therefore, would possibly offer specific

tissue toxicity testing with fewer ethical issues (Cui, 2007).

2.3.2 Cellular Systems for Hepatotoxicity Testing

The liver plays a most important role in the living body in terms of eliminating drugs and other harmful substances from the bloodstream, and is a most sensitive organ in response to toxic chemicals. Liver toxicity is one of the leading contributors to failure of clinical trials in humans, which is most often caused by the byproducts of drug metabolism which perturbate the cellular functions and lead to liver injury. In recent years, over two thirds of drugs withdrawn from the market were withdrawn because of hepatotoxicity and cardiovascular toxicity in humans (Schuster, 2005). Therefore, hepatotoxicity reflects the most common adverse effect and testing for it has been extensively used in drug discovery and development (Lucena, 2008; Tuschl, 2008).

Current models for hepatotoxicity testing are primary hepatocytes, standard cell lines, and differentiated stem cells (both embryonic and adult stem cells)

Primary Hepatocytes

In the liver, 70% of the cellular population are hepatocytes, which are important for metabolising xenobiotics (Nguyen, 2004). The source of primary hepatocytes may be from animals, humans or cryopreservation. Primary human hepatocytes, considered as the ‘gold-standard’, are the most precious of all primary sources, with potentially the best predictivity of drug toxicity in humans. However, due to ethical and economic

reasons, in conjunction with patient donor variations and gender variation (Delongchamp, 2005), use of primary hepatocytes is mainly limited to Phase I clinical trials of new chemical entities (LeCluyse, 2005; Sahu, 2007)

When hepatocytes were isolated from liver, three quarters of cytochrome P450 (CYP450) enzyme expression and other liver-specific functions were lost during the first 24 hours (Davila and Morris, 1999; LeCluyse, 2001). Therefore, it is essential to optimise the primary hepatocyte culture conditions before drug toxicity study. Sandwich culture configuration and culture medium optimisation are the major contributions to long-term culture of hepatocytes (Gómez-Lechón, 1998). Use of natural extracellular matrix (eg. collagen type I) (Dunn et al.,1991; Ezzell et al., 1993; Kern et al., 1997) or matrigel (Hamilton et al., 2001; Moghe et al., 1997) as pre-coated flasks/petri-dishes enhanced the signalling molecules (eg. heparan-sulfate proteoglycans) secreted by the cells (Farkas and Tannembaum, 2005). Meanwhile, low concentrations of insulin and dexamethasone in a serum free medium maintain liver-specific functions and gene expression level for primary hepatocyte culture, as well as cell morphology (LeCluyse, 1999; LeCluyse, 2001; Davila and Morris, 1999; Chandra, 2001;Rechert et al., 2006).

Cryopreservation of primary human hepatocytes offers the advantage of storing the cells for short or long periods, which provides the opportunity to use cells from the same source to increase the reproductivity (Lawrence and Benford, 1991). However, the conditions for maintaining human hepatocytes after thawing need to be optimised, since

the cells' viability, liver-specific metabolism and protein expression have been reduced readily and rapidly (Guillouzo, 1999; Miyamoto, 2006). Also, it would be difficult to validate the data obtained from *in vitro* cryopreserved hepatocytes to in vivo (Sahu, 2007).

Advantages and limitations of using primary hepatocytes are listed below (adapted from Gómez-Lechón 2010; Sahu, 2007).

Advantages

- Easy to use for both short term (acute toxicity) and long term culture, up to two weeks.
- Viability and functional studies
- Potential use for long term studies
- Detection of metabolism-mediated hepatotoxicity
- Reasonable resemblance to in vivo liver phenotype
- Possible to use in long-term chronic toxicity study for drug metabolism and drug-drug interactions
- Possibility of 3D culture (transport studies)
- Co-culture with other hepatic cells
- In vivo like morphology
- Cell-cell contacts and cell-matrix interaction (depending on culture condition)
- Interspecies studies

Limitations

- Culture conditions need to be take into consideration
- Poor phenotypic and functional match to in vivo human hepatocytes
- Not a single culture has fully expressed metabolism enzymes
- Short life span of differentiated phenotype
- Inconsistency between different preparations
- Batch to batch variations/patients variations
- Ethical issues e.g. animal usage
- Purity of cells
- Limited sources for human primary cells
- High influence of culture conditions (survival, morphology and functions, as well as gene expression level)
- Cryopreservation needs to be improved

Cell Lines

Cell lines, derived from human or animal tumour, or genetically engineered, can be employed for the prediction of hepatotoxicity. HepG2, as one of the most popular cell lines used at the present, was originally isolated from a 15-year-old male Caucasian in the early 1980s (Aden, 1979; Scheers et al, 2001). Some research has shown the HepG2 cell line increased phase I metabolism enzyme expression such as CYP1A, CYP2B and CYP3A, while other expressions, CYP2E1 for instance, were reduced, as well as some other phase II enzymes in the toxicity testing (Knasmüller, 2004). Other hepatic cell

lines such as rat clone-9, isolated from normal 4-week old male Sprague-Dawley rat; Mouse BNL CL.2, isolated from embryonic liver of a BALB/c mouse; WIF 12-1 with its sub clone cells line: WIF-B9 cells, both derived from Fao rat hepatoma cells together with WI38 human fibroblasts; HUH-7, hepatocytes derived from cellular carcinoma cells originally from a 57-year old Japanese man in 1982, MH1C1, isolated from rat hepatoma liver and HepaRG, recently derived from human hepatoma cells are all widely used in hepatotoxicity and drug metabolism studies (Aninat, 2006; Barhoumi et al, 2002; Kajsa, 2008; Sahu, 2010). Apart from organ directly derived cell lines, transfected cells or CYP-engineered cells are designed specifically to highly express certain enzymes, but lack the other expressions, which can be used to predict an isolated mechanism of metabolism (Sahu, 2007).

Advantages and limitations of using cell lines are listed below: (Adapted from: Gómez-Lechón, 2010, Sahu, 2007)

Advantages:

- Unlimited source
- Easy to use and robust
- Highly reproducible and high throughput
- Possible to manipulate the genes for specific enzyme or drug transporter studies

Limitations:

- Lacking of phenotypic and functional concordance to primary cells/ in vivo hepatocytes

- Only a small amount of hepatic function is expressed. Absent or reduced expression of other/ other key/ other basal hepatic functions
- Unstable genotype

Stem Cell Derived Hepatocytes

Hepatocytes can be differentiated from embryonic stem cells and adult stem cells. Embryonic stem cells are the original cell source that can be differentiated into all derivative cells, and preliminary data has already shown the ESCs differentiated into hepatic-like cells, with positive expression of hepatic markers (Lavon et al, 2004; Rambhatla et al, 2003; Shirahashi et al, 2004). The presence of FGF, BMP, HGF, and sodium butyrate would also keep hepatic-like cells in culture and to express hepatic characteristic makers such as alpha-fetoprotein, albumin, HNF4 as well as CYP450 activities (Cai et al, 2007; Hay et al, 2007). However, due to ethical issues of using embryonic stem cells, especially human embryonic stem cells, adult stem cells have shown advantages in academic research and industry (Henningson, 2003).

Both adipose and bone marrow derived stem cells are also able to differentiate into hepatocytes *in vitro* (Gimble et. al, 2008). Lee, Okumoto and Schwartz have successfully differentiated bone marrow derived stem cells of human origin into functional hepatocytes, with the presence of some growth factors such as hepatocyte growth factor, oncostatin M, fibroblast growth factor 2 and nicotinamide (Lee KD, 2004; Okumoto, 2003; Schwartz, 2002; Ouchi 1998; Shi, 2005). Especially for human bone

marrow derived mesenchymal stem cells, it has been reported that after being expanded in vitro, MSCs were differentiated and transplanted back into the same patient (Henningson, 2003; Kazemnejad, 2008). Meanwhile, adipose-derived stem cells of both human (Banas, 2007; Talens-Visconti, 2006; Seo 2005) and rat (Sgodda, 2007) origin have shown the same differentiation.

Advantages and limitations of using stem cell differentiated hepatocytes for hepatotoxicity are listed below (adapted from Abpi, 2006)

Advantages:

- Long term cell source can be used routinely
- Highly characterised cell source
- phenotypes and functions match closely to in vivo
- High drug metabolising capacity
- Longer life span of differentiated phenotype
- High consistency between experiments
- Reducing the animal usage

Limitations:

- At the moment, the methods and protocols need to be modified to produce highly purified and highly functional adult stem cell differentiated hepatocytes
- Ethical issues of using embryonic stem cells to differentiate hepatocytes
- Limited supplies, availability

2.4 Biomarkers and Functional Assays

2.4.1 Generic Cytotoxicity Assays

Cytotoxicity is the quality of being toxic to the cells. Cytotoxicity testing is performed to measure the level of toxicity of cells exposed to the compound. Cytotoxicity testing is commonly used in drug development in the secondary validation after the initial screening. Conventional testing is based on the cell-line in monolayer cultures. Cell viability and toxicity are usually tested. A considerable number of quantitative assays have been done to assess proliferation and survival of somatic cells. The easiest way to obtain quantitative values is visual counting of individual cells that were cultured in different conditions under a light microscope; for example, in the trypan blue exclusion test, dead cells do not possess intact cell membranes that take up trypan blue dye (Strober, 2001). This approach, however, has numerous limitations besides low reproducibility (S.Al-Nasiry, 2007). Alternatively, some sophisticated approaches such as spectrophotometry, flow cytometry and radiometry, have been used to quantify appropriately labelled cells.

Traditionally, there are several commonly used methods to detect *in vitro* cytotoxicity as the end points (Slater, 2001). Cell viability evaluation is one of the most common methods. It is based on analysing the cellular membrane integrity and mitochondrial activities, such as neutral red assay, 3-[4,5-dimethylthiazol-2-yl]-2,5-diphenyl tetrazolium bromide (MTT) assay and 2,3-bis[2-methyloxy-4-nitro-5-sulfophenyl]

-2H-tetrazolium-5-carb-oxanilide (XTT) assay, lactate dehydrogenase (LDH) assay, AlamarBlue® assay and adenosine triphosphate (ATP) assay.

Neutral Red Assay

Neutral red assay (3-amino-7-dimethylamino-2-methylphenazine hydrochloride) is one of the simplest assays that can be employed to determine cytotoxicity/viability (Borenfreund and Puerner, 1984) in primary cells (Fautz et al., 1991) and other cell lines (Morgan et al., 1991). It is a cationic dye that easily penetrates the live cell membrane and enters lysosomes where dye accumulation takes place over time (Green et al, 2001). The accumulation of the assay can be quantified to measure the cell viability by employing a spectrophotometer. The intensity of the colour corresponds to the numbers of live cells.

MTT Assay and XTT Assay

One of the classical assessments is called the MTT assay, (3-[4,5-dimethylthiazol-2-yl] -2,5-diphenyl tetrazolium bromide), the cleavage of water soluble tetrazolium salts, and modified version, MTS, 3-(4,5-dimethylthiazol-2yl)-5-(3-carboxymethoxyphenyl) -2-(4-sulfophenyl)-2H-tetra-zolium, inner salt (Rotunda et al. 2004). These are both colorimetric indicators that are commonly used to detect mitochondrial activity, an assay which is commonly applied to mammal cells (Hart et al., 1999) and cell lines (Tully et al., 2000, Mosmann, 1983). It is a two step reaction. In the first step, the water soluble tetrazolium salt is reduced to an insoluble purple formazan product by succinate

dehydrogenase in the mitochondria. However the purple formazan product is insoluble and impermeable to the cell membrane and it only accumulates within live cells. Then, an organic solvent needs to be used to solubilise the formazan product that can be evaluated under spectrophotometry.

Similarly, XTT (2,3-bis[2-methyloxy-4-nitro-5-sulfophenyl]-2H-tetrazolium-5-carb -oxanilide) assay also measures the mitochondrial activity by reducing yellow tetrazolium salts into orange water-soluble formazan rather than the insoluble product that MTT produced. Because the XTT assay results in water soluble dye, it can be measured directly by spectrophotometry without the solubilising solution which MTT requires as second step (Wang, 1996).

Lactate Dehydrogenase Assay

The lactate dehydrogenase (LDH) release assay is also commonly harnessed in *in vitro* toxicity studies as an endpoint. This enzyme is released from the cytoplasm of dying/dead cells into the culture supernatant. The measurement of this assay is based on the LDH activity (Fotakis and Timbrell, 2006). LDH catalyses the reduction of pyruvate to l-lactate which results in the oxidation of NADH to NAD (See Equation 2.1). The oxidation rate, which is from NADH to NAD, was measured by evaluating the decrease in absorbance at 340nm, and it is directly proportional to LDH activity (Parker and Holbrook, 1981). Not only LDH leaked from the damaged membrane, but other

enzymes were also released such as adenylate kinase (Olsson et al., 1983) or glyceraldehyde-3-phosphate dehydrogenase (GAPDH) (Corey et al., 1997) that can be used to evaluate the membrane integrity (Cho, 2008).

$$\text{Pyruvate} + \text{NADH} \xrightarrow{\text{Lactase Dehydrogenase}} \text{L} - \text{lactate} + \text{NAD} + \text{H}$$

Equation 2.1 LDH Assay Reaction

AlamarBlue® Assay

The assessments in drug testing require an assay which is not toxic itself and preferably not radioactive, but simple, easy to operate and sensitive enough to support accurate values. AlamarBlue®, a water soluble dye, has been previously used for quantifying cell viability and variety *in vitro* (Fields RD and Lancaster, 1993). It is an oxidation-reduction indicator when added to cell cultures. When it enters living cells, alamarBlue® causes a visible colour change of the growth medium reduction, behaving as an intermediate electron acceptor by accepting electrons from NADPH, FADH, FMNH, NADH from mitochondrial enzyme activity as well as from the cytochromes. This process happens in viable cells between the final reduction of oxygen and cytochrome oxidate, and can be substituted for molecular oxygen for most oxidoreductases that can use molecular oxygen as an electron transporter (Shahan TA, 1994). Nonviable cells rapidly lose metabolic capacity, and cannot reduce the indicator dye for the assay phenomenon (Technical bulletin). Therefore, the absorbance of alamarBlue® at the specific wavelength changes with a reduction in the mitochondrial

electron transport system (Ahmed SA, 1994), it is accumulated in the culture medium as cell growth progresses.

Another fluorescent dye, CFDA-AM (5-carboxyfluorescein diacetate acetoxymethyl ester), is also able to measure plasma membrane integrity and non-toxicity, and has a similar incubation time to alamarBlue® while using a different wavelength (Schirmer et al, 1997).

Adenosine Triphosphate Content Measurement

ATP is produced within mitochondria, which supply 90% of essential energy for cellular functions (Wallace, 1997) and plays a central role in energy exchanges in the living body (Slater, 2001). The mitochondrial inner membrane contains several complex proteins and enzymes which provide the ATP metabolism. Cellular function is maintained through free energy released from the membrane when ATP undergoes rapid hydrolysis from ATP to ADP or AMP (Drew and Leeuwenburgh, 2003). ATP content assay is based on the bioluminescent detection of firefly luciferase reaction. With the substrates of luciferin, oxygen and ATP, released from lysed membrane and Mg^{2+} and luciferase catalysed, oxyluciferin was produced, together with AMP, Pi, CO_2, and energy/light. The light emission can be quantitatively recorded by chemiluminometer (See Equation 2.2). The content of ATP is subject to the number of living cells proportionally.

$$\mathrm{ATP} + \mathrm{Luciferin} + \mathrm{Oxygen} \xrightarrow{\mathrm{Luciferase+Mg2+}} \mathrm{Oxyluciferin} + \mathrm{AMP} + \mathrm{Pi} + \mathrm{CO2} + \mathrm{Light}$$

Equation 2.2 ATP Assay Reaction

2.4.2 Hepatotoxicity Assays

To predict organ-specific toxicity, specific biomarkers are used to estimate the target organs. For example, aspartate aminotransferase (AST) and alanine aminotransferase (ALT), cytosolic enzymes leaked from damaged membrane, are used as the biomarkers for hepatic viability test/ hepatotoxicity testing (Gómez-Lechón, 2010). They are both used as indicators of liver damage, rather than hepatic dysfunction (Kew, 2000).

Alanine Aminotransferase Measurement

Alanine Aminotransferase (ALT) is predominantly located in the liver, specifically the cytoplasm (Schmidt and Schmidt, 1979, 1988), therefore, measuring the quantity of ALT in blood, serum or plasma can be used to diagnose and monitor hepatic diseases. ALT assay is a liver-specific assay (Clampitt 1978, Lindena et al, 1980), and is based on the fact that ALT catalyses the transfer of alanine from the a-amino group to a-keto group of ketoglutaric acid, resulting in pyruvic acid. ALT firstly leaks from the damaged cell membranes into plasma, with the presence of L-Alanine and α-Ketoglutarate; pyruvate and L-glutamate were then formed during catabolism. LDH catalysed the second reaction; pyruvate was reduced to lactate, NADH was oxidised to NAD. The resulting rate, which is the NADH oxidation rate, is directly proportional to the ALT

activity rate (See Equation 2.3).

$$\mathrm{L-Alanine} + \alpha - \mathrm{Ketoglutarate} \xrightarrow{\mathrm{ALT}} \mathrm{Pyruvate} + \mathrm{L-Glutamte}$$

$$\mathrm{Pyruvate} + \mathrm{NADH} \xrightarrow{\mathrm{LDH}} \mathrm{Lactate} + \mathrm{NAD} + \mathrm{H}$$

Equation 2.3 ALT Assay Reaction

Aspartate Aminotransferase Measurement

Similarly, AST is also present in high concentrations in the liver, four fifths of total intercellular enzyme is present in the mitochondria and the rest can be found in the cytoplasm (Rej, 1978). But, unlike ALT, AST is not a liver-specific enzyme. It can be found in many different tissues; liver, heart, skeletal muscles, as well as red blood cells (Batzakis and Briere, 1979). However, AST measurement is more sensitive than ALT measurement, due to the large amount of AST in the liver (Berg, 2006). It is also a cellular integrity assay. AST catalyses L-Aspartic acid to α-Ketoglutarate, resulting in the formation of oxalacetate and L-glutamate. Meanwhile, NADH and oxalacetate are catalysed by MDH to yield NAD and malate. The resulting rate is proportional to AST activity (See Equation 2.4).

$$\mathrm{L-Aspatate} + \alpha - \mathrm{Ketoglutarate} \xrightarrow{\mathrm{AST}} \mathrm{Oxalacetate} + \mathrm{L-Glutamte}$$

$$\mathrm{Oxalacetate} + \mathrm{NADH} \xrightarrow{\text{Malate Dehydrogenase}} \mathrm{Malate} + \mathrm{NAD}$$

Equation 2.4 AST Assay Reaction

Glutamate Dehydrogenase Measurement

Glutamate Dehydrogenase (GLDH) is a key liver-specific enzyme predominantly found

in mitochondria of liver cells (Schmidt and Schmidt, 1988), and is vital in amino acid oxidation and urea production (O'Brien, 2002). Increasing GLDH values are caused by damage to hepatocytes. It also can be used as an indicator of hepatic necrosis if a large quantity of GLDH is released from the liver (Schmidt and Schmidt, 1988). Some preliminary studies have demonstrated that GLDH assay is similar in sensitivity or even more sensitive, than other hepatic biomarkers such as ALT or AST, and should be used while evaluating hepatic injuries (Carakostas et al. 1986; O'Brien et al. 2000). Unlike AST and ALT, GLDH deaminates amino acid to free ammonia, rather than transferring the amino group from one to another substrate, and the reaction is highly reversible depending on the concentration of each substrate. The decrease in NADH is directly proportional to the GLDH activity (See Equation 2.5).

$$\alpha - \text{Ketoglutarate} + \text{NADH} + \text{NH4} + \xrightarrow{\text{GLDH}} \text{Glutamate} + \text{NAD} + +\text{H2O}$$

Equation 2.5 GLDH Assay Reaction

Albumin Secretion

Functional assays need to be used to assess toxicity as the second step after viability evaluation has taken place. For example, for liver injury, change in albumin and urea secretion would indicate the mental effect on the fundamental functions for hepatotoxicity measurement (Gómez-Lechón, 2010). Important liver functions include bile production, protein production and ammonia clearance, xenobiotic metabolism and detoxification as well as storage. The liver synthesises and secretes thousands of enzymes for metabolic functions. Serum albumin is the most abundant protein in

humans with a synthetic rate of 40~50 g/L. Albumin maintains the colloid osmotic pressure of plasma to keep the equilibrium system between plasma volume and tissue fluid. Plasma albumin is also responsible for transporting many substances in the blood, for example free fatty acids and some drugs. Albumin secretion reduction induced by liver injury may lead to oedema. Therefore detecting the rate of albumin secretion would aid the evaluation of hepatotoxicity.

Urea Secretion

Another pivotal functional assay is to evaluate urea synthesis. The liver also produces urea ammonia, which is derived from protein degradation and nucleic acid catabolism. Ammonia plays an important role in nitrogen metabolism. Usually, ammonia concentration in the liver is 10 times higher than the plasma ammonia level, and ammonia metabolism is a major liver function. A high level of ammonia circulating in the plasma may lead to brain disorders and result in coma, due to high neurotoxicity and deficient hepatic functions. Thus it is essential to reduce the high concentration of ammonia in the blood by urea synthesis in the liver, and ultimately by its excretion from the body via the kidneys.

2.4.3 Genomics

One of the key approaches to assess toxicity due to drug induced liver injury is to understand the mechanisms of gene expression. DNA microarrays offer the opportunity

to track the changes of gene expression among hundreds of thousands of genes simultaneously (Hewitt et al, 2007). Assays of microscopic cDNA spots on a solid surface. The microarrays detect the fluorescence from hybridisation of fluorescent labelled samples. After quality criteria and data analysis, all regulated genes from global gene expression profiling, including up and down regulated genes, are expressed to illustrate the difference of the mechanism from the tested samples (Kienhuis, 2006). Apart from the toxicogenomics by assessing the individual test compounds *in vivo* (Hengstler et al., 2006) or *in vitro*, it is also important to take gene expression into consideration without toxin treatment, since gene expression can be altered during the culture time, which would potentially help to identify the compound's safety (Bono et al, 2003; Novak et al, 2002; Pritchard et al, 2001). Primary hepatocytes isolated freshly from the liver by two step perfused methods (Segal, 1979) were extensively used for the toxicity study, and were considered as gold standard to assess the genomics studies. Gene expression is highly dependent on the condition of the culture (Sahu, 2007). Richert reported that basal gene expression from *in vivo* human liver tissue and freshly isolated hepatocytes was significantly different from one culture to another under the same culture conditions by using Affymetrix, assays with 8700 genes detected in total (Richert, 2006). Boess investigated gene expression comparison between two cell lines, rat primary hepatocytes with conventional monolayer culture, sandwich culture of different time points, together with gene expression of liver slice and tissue *in vivo*. The result demonstrates that the liver slice shows the strongest similarity to the *in vivo* gene expression, with some decrease in drug metabolism genes. Gene expression of primary

hepatocytes was not stable over time, even immediately after isolation, and was dramatically changed during the culture period. Gene expression of spheroids was evaluated on the Huh7 cell line cultured on polyurethane foam, also performed by cDNA microarray (Yamashita et al, 2004).

2.4.5 Functional Imaging

Fluorescent labelling and staining with multicoloured probes in conjunction with an appropriate microscope can be useful as an analytical tool for toxicological endpoints. Fluorescent microscopes contain two filters, excitation and emission filters, to make sure specimens are excited and detected under the correct wavelengths. The standard fluorescent microscope enables the specimen to be excited at the same time and monitored evenly on the stage. The cellomics microscope (Cellomics Arrayscan VTI HCS Reader, Thermo Fisher Scientific, UK) is a traditional fluorescent microscope, but combines high content screen technology with multi-parameter quantitative image analysis. It allows users to target samples for different characteristics, for example cytoplasma intensity or size of nuclei eyes, within a short period of time. Meanwhile the confocal microscope introduces a spatial pinhole which eliminates the light out of focus on the focal plane. This does not just improve the quality of images, it also offers a stack of images in Z direction with different focus on the plane, which allows 3D imaging (Helmchen F. and Denk W., 2005). The two photon or multi-photon fluorescent microscope uses pulsed long-wavelength light to excite the samples, which results in the

energy level being twice as high as with the single/traditional fluorescent microscope. (So, et al, 2000). There is a similarity between the confocal microscope and multiphoton microscope as they both generate images in 3 different depths. However, the longer wavelength of MPM offers less damage to the cells for continuing examinations and confocal microscope is more invasive of the two technologies.

2.5 Three Dimensional Cell Culture

However, cell growth in traditional monolayer culture (called 2D culture in this thesis) has many limitations. For example, cell morphology is different from that in vivo, in that it lacks the structure and cell-cell contacts and cells dedifferentiated with time (Bhadriraju and Chen, 2002). Three dimensional architecture provides a place for better cell attachment and increased surface area with designed structures (Kazemnejad, 2009). Gene expression in monolayer and 3D also shows different results (Birgersdotter, Sandberg and Ernberg, 2005), with 3D gene expression highly up-regulated compared with 2D (Ghosh et al., 2005). Evidence indicates that conventional methods failed to predict organ-specific toxicity (Mazzoleni et al, 2009). The disadvantages of monolayer culture would hamper the development of toxicity testing, and 3D culture would improve the predictivity and accuracy in preclinical trials (Pampaloni and Stelzer, 2009).

2.5.1 Scaffolds

Three dimensional matrices ensure that the natural microenvironment of cells can be reproduced more accurately. They have porous architectural structures, allowing cells to

grow and differentiate within the structure (Lee, 2008，Grayson, 2004; Wang, 2005). Cells in three dimensions are capable of adopting their native morphology, facilitating cell to cell contact as well as making contact with the extracellular matrix (ECM) and increasing signal processing and cell development (Abbott, 2003; Levenberg S, 2003).

Cell cultures in three dimensions can be constructed from natural and synthetic scaffold biomaterials (Freed LE, 1994), cells aggregate into spheroids without scaffolds. Whether synthetic or natural, all these scaffold materials have to meet required criteria such as non-toxicity or non-inflammatory, porosity, permeability, biocompatibility, biodegradability and bioresorbability. Also similar mechanical properties to natural tissue and good cell adhesion need to be taken into consideration (Lorenz Meinel, 2004, Huntmacher, 2000).

2.5.1.1 Natural Scaffold materials

Natural polymer scaffolds facilitate cell interaction. The most frequent by used ones are collagen, chitosan, collagen/chitosan composites, alginate and its composites, biomatrix, peptides, hyaluronic acid, fibrin and gelatin. However, batch-to-batch variation following isolation from biological tissue and poor mechanical strength are major limitations of these natural polymers (Badylak, 2009).

Alginate Hydrogel

According to the previous section, when biomaterials match the selection criteria, they can be used for scaffolding the cells. A variety of biomaterials are widely used for scaffolds, for example, alginate, collagen type I, II, and some synthetic polymers.

Alginates are derived from seaweed polysaccharides which consist of blocks of co-polymer of β-D-Mannuronic acid (M units) and α-L-Guluronic acid (G units) (Martinsen, 1989) (See Figure 2.3).

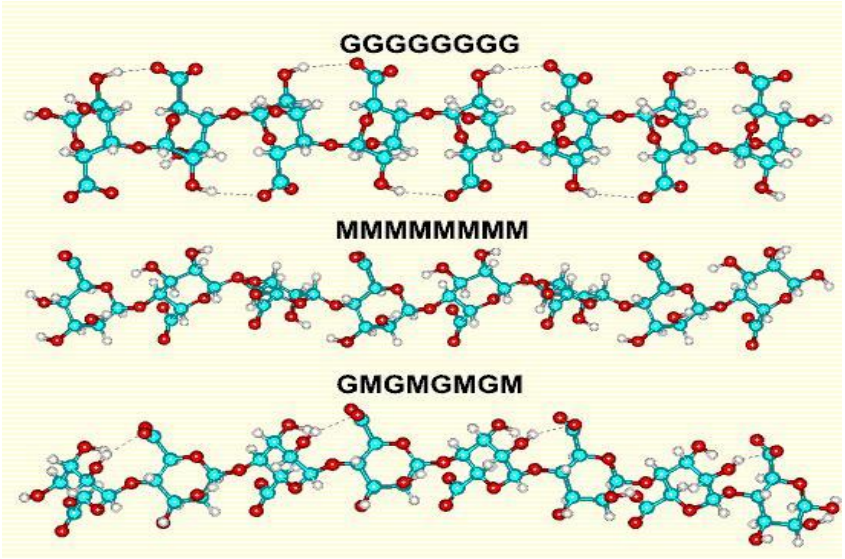

Figure 2.3 Molecular Structure of Alginates (Fabia, 2005)

The molecular structure of alginates varies depending on their source. They may have a structure which is composed only of M units or G units, and may also have alternating residues which is a G-M-G-M unit sequence. The di-cations like Ca^{2+}, Mg^{2+} corporately bind the alginate chains which make alginate jelly (Shoichet, 1996; Fabia, 2005). Hydrogels are commonly used as biomaterials to synthesise ECMs because of their biological properties (Smidsrod O, 1990). The only success of sole use of alginate gel has been reported for rat MSCs growth. Human MSCs do not attach or proliferate in it (Lawson MA, 2004) Covalent modification of alginate with RGD-peptide would significantly improve the cell attachment compared to alginate alone when used as scaffolds (Rowley, 1999; Kreeger, 2003).

Collagen

Of the various three-dimensional scaffold materials, collagen has been reported as the more suitable one for research *in vitro* and *in vivo*. It is the main protein in connective tissue in animals and humans, and accounts for about 25-30% of all the protein in the body by weight, especially in extracellular matrix (ECM) and cartilage which contain more than 95% collagen. There are several types of collagen, for instance, collagen type I, collagen type II, etc. Collagen type I is the most abundant type among 28 identified types overall. It regulates cell growth due to its plasticity and mechanical properties, and it also provides the relevant physiological stiffness of tissues. The basic structure of collagen is left-hand triple helix. It is composed of a 300 nm-long, 1.5nm thin protein, which consists of 2 α1 (I) and 1 α2 (I) subunits (see Figure 2.4).

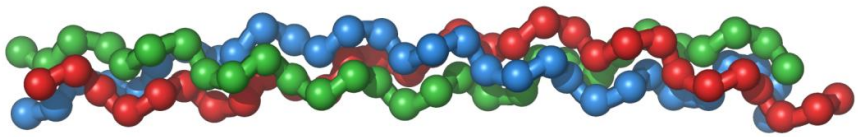

Figure 2.4 Triple Helix Structure of Collagen

(http://en.wikipedia.org/wiki/File:Collagentriplehelix.png)

Fibrous collagen type I can be exacted and dissolved in an acidic solution (Pampaloni and Stelzer, 2009). The highly fibrillar order of collagen can be controlled by adjusting the concentration of the collagen solution (Bessea et al. 2002). The more fibrous component collagen gel contains, the more rigid the cyto-architecture is (Handel et al. 2005).

However, when pure collagen is used as scaffold material, it is reported to degrade

rapidly at concentrations below 2mg/ml (Trainer, 2007). Due to its degradable property, collagen type I scaffolds need to be used in higher concentrations.

Matrigel™

Matrigel™, a commercial available hydrogel from BD, is a protein extract from basement membrane derived from Engelbreth-Holm-Swarm (EHS) mouse sarcoma (Kleinman and Martin, 1989). Basement membrane consists of various proteins and growth factors. The majority of the proteins are lamin which was isolated from a glycoprotein (Timpl et al, 1979), collagen Type IV, a high percentage of glycosylated molecules, and perlecan, heparin sulphate proteoglycan core protein (Kleinman and Martin, 2005). Growth factors, such as TGF-β, FGF, EGF, are also important components of basement membrane. One of the most important components, laminin, has been reported to promote epithelial and endothelial cell attachment but not for fibroblasts (Terranova et al, 1986).

Matrigel also supports cell differentiation. Hepatocytes for instance, grown in a sandwich between a collagen pre-coated plate and matrigel gelled on top, maintained their morphology and functions for a longer period than when only grown on pre-coated plates (Sawada et al. 1987; Scheutz et al 1988).

2.5.1.2 Synthetic Scaffold Materials

Synthetic polymers can be designed and prepared with specific chemical and physical properties (Oh et al, 2007). Degradation also can be modified as needed by altering the chemical properties. There are various sources of synthetic polymers that are commonly used in tissue engineering. They include polyglycolic acid (PGA), poly (l-lactic acid) (PLLA) and polylactic acid (PLA), poly lactic-co-glycolic acid (PLGA) and polycaprolactone (PCL) (Lanza et al. 2007). Synthetic polymers can be used as sole or mixed as copolymer. Copolymer PLGA is composed of PLLA and PGA with increased degradability of each component (Yang et al, 2001). Synthetic polymers show the advantages of good mechanical performance, degradation, no variation between batches. However, they lack cell recognition signals and good cell attachment property (Kazemnejad, 2009).

2.5.1.3 Hybridisation of Natural and Synthetic Scaffold Materials

Hybridisation of natural polymers and synthetic polymers overcomes the problems that both pose. Different techniques can be employed for hybridisation. Hybridisation of PLGA-collagen, for instance, involves grafting collagen onto the surface of PLGA fibres. After lyophilisation, collagen sponges were reinforced by PLGA fibres (Wen, 2007). Another example of using similar materials but different technology is electrospinning. A mixed solution of PLGA and solvent with a certain ratio produces nanofibres by electrospinning; then immersing nanofibres into collagen solution gives a

hydrophilic surface (Feng, 2010). Both technologies were applied to rat hepatocytes culture, and the results positively indicated that hybridisation of natural and synthetic polymers improve the cell attachment and maintain the cellular functions.

2.5.2 Self-Assembly Spheroids

Cells also can be self-assembled into spheroids without scaffolding materials. The conception of spheroid culture was originally generated by Holtfreter in 1944 and Moscona in 1952 (Holtfreter, 1944; Moscona, 1952; Moscona, 1961). They discovered that chicken embryonic cells aggregated together into a spherical shape, which aroused great interest in academia as a whole as the new technology challenged the traditional monolayer culture, reflecting a more complex culture system that was closer to the appearance *in vivo*. Shortly after that, tumour spheroid formation was reported successful in the mid 1970s (Sutherland, 1976). Then rat hepatocyte spheroids (Guigoz, 1987; Landry, 1985; Koide et al, 1989; Wu, 1999; Abu-Absi et al. 2002), cardiomyocyte spheroids (Decker et al, 1991; Akins, 1999), chondrocytes (Guo, 1989; Bonavent 1994) models were created with differentiation capacity (Altmann et al, 2009). Spheroid culture offers the three-dimensional cyto-architecture for cells to retain their *in vivo* like morphology and cell-cell contacts, as well as distribution of cytoskeleton.

Spheroid liver culture method was first investigated in the mid 1980s. When cultured, liver cells either spontaneously aggregated into spheroids, with a diameter of 150 μm,

on top of a non-adherent plastic surface or through rotation under appropriate conditions. Liver cell spheroids gradually developed polarity and bile canaliculi (Abu-Absi, 2002), and closer morphological structures to the *in vivo* situation (Lazar, 1995; Harada, 2003; Lu, 2005). They also maintained a differentiated phenotype, metabolic capacity and hepatic gene expression (Guigoz, 1987; Landry, 1985; Glicklis, 2000; Hamamoto et al, 1998).

Spheroid Formation Methods

Freshly isolated hepatocytes, ideally with more than 90% viability were placed on a bacteriological dish or on a rotary shaker with a specific time and a constant speed (Yagi et al, 1993) or rotational stirrers (Bilodeau and Mantovani, 2006; Moscona, 1961). Alternatively, a cell suspension droplet hang from the top of the petri-dish lid, the 'hanging-drop' method, can be applied for spheroid formation (Kelm et al, 2003; Timmins, 2004). Apart from rocking, rotational and hanging-drop methods, spheroids can also be formatted to a specific size and arrangement with scaffolds. Rat hepatocytes were encapsulated in alginate beads for spheroid formation (Miranda, 2010). Alternatively, spheroids formed within lyophilised PLGA-collagen sponges (Wen, 2007) or collagen coated PLGA fibres (Feng, 2010) or on top of pre-coated surface Poly(2-hydroxyethyl methacrylate) (PHEMA) or PLA (Riccalton-Banks et al, 2003). Furthermore, 3D inverted colloidal crystal in conjunction with a hydrogel, poly (acrylamide) for example, support spheroid formation with controlled uniform sizes and unique hierarchical porosity (Cuddihy, 2008; Kotov, 2004; Lee, 2006; Shanbhag, 2005).

Listed all spheroid formation techniques, spheroid size control needs to be taken into consideration. Research has shown that necrotic cells accumulate in the centre of spheroids due to inadequate oxygen and nutrition or accumulated waste products. A diameter greater than 250μm may lead to hypoxia and necrosis in central hepatocytes (Atala and Lanza 2002; Lu, 2005).

2.5.3 Effect of Perfusion

Three dimensional methods mimic the cell growth environment with similar properties to ECM. However, it is not similar enough to imitate the natural ECM. Conventionally, the cell culture medium needs to be manually replaced every two or three days in static culture. This may influence cell proliferation either in monolayer or three dimensions, in terms of pH changes, insufficient nutrition supply, oxygen level, and mass transfer, and may also lead to contamination. Bioreactors are designed to support a complicated cell culture in a perfused system, which continuously supplies fresh culture medium to keep cells at a stable value of pH, temperature and oxygen. This also improves the culture efficiency since it facilitates cultures with small volumes and multi-parallel operation for preclinical high throughput testing (Kostov et al., 2001; Maffia et al., 1999; Huh, 2005; Brischwein, 2003; Hung; 2005; Torisawa, 2007; Khademhosseini, 2005; Taylor, 2005). The continuous flow supplies the homogenous distribution and increased mass transfer that ensure a stable environment and meet the metabolic demand for the cells (Powers, 2002). Meanwhile, the flow can be monitored and manipulated for creating *in*

vivo like cellular physiologic culture environment, improving the culture efficiency (Walker, 2004; Raty, 2004; Kaji, 2003; Viravaidya, 2004; Tourovskaia; 2005; Allen, 2005; Song, 2005); more specifically, for drug testing, the perfused system would give a more stable environment, because even small changes affect the cell biological and physiological functions (M.H. Wu, 2007). Application of perfused bioreactors has already been used to design Lab-on-a-chip (Ong, 2008;Toh; 2007; Figallo, 2007) and hollow fibre bioreactors (Ellis, 2006) etc.

2.5.4 Multiple Parallel Microbioreactors

Multiple parallel microbioreactors are designed to manipulate small volumes of simultaneous parallel flow for high throughput toxicity testing in a miniaturised scale. The sections below described the bioreactors materials and the microbioreactors that were utilised in the study.

Microbioreactor Materials

There are several materials that are widely used for bioreactors such as silicon, elastomer and synthetic polymers which are biocompatible (Vozzi, 2002; Ciaravella, 2002; Leclerc, 2003; Leclerc, 2004). Silicon elastomer polydimethylsiloxane (PDMS) is widely used for casting the bioreactors (Leclerc, 2004; Wu MH, 2004). PDMS is prepared by combining 10 parts of tetra(trimethylsiloxy)silane as a polysiloxane base and 1 part of curing agent, tetramethyltetravinylcyclotetrasiloxane, by weight. After curing and polymerising, pieces of clean and flat PDMS can be manually stuck together in a reversible fusion to form a closed environment without bubbles. Alternatively, if PDMS needs to be sealed on a piece of glass or layers of PDMS need to be bound as

reversibly, oxygen plasma treatment can be employed before bringing them into contact within a short period of time (Lawton et al, 2005; Berrea, 2006).

Silicon elastomer polydimethylsiloxane (PDMS) was also treated and used successfully for long term cell culture of endothelial cells, Escherichia coli, ovary cells, hepatocyte spheroid culture (King, 2001; Walker G M, 2002, Yu H, 2005, Chang W J, 2003, Powers, 2002) with perfused fluids (Borenstein, 2002; Powers, 2001). One of the most notable examples is called the 'liver on a chip' device, originated at Massachusetts Institute of Technology (MIT), Boston. It used PDMS for surface printing to construct the multi channel chip, applied with continuous media to support hepatocyte culture (Powers, 2001; Powers, 2002). As one of the most favourable materials, PDMS shows the advantages of high biocompatibility, non toxicity, high oxygen and carbon dioxide permeability, optical transparency which is useful for microscopic observation, as well as construction of closed cell culture chamber to avoid contamination (Charati, 1998; Szita, 2002; Zanzotto, 2003; M.H. Wu, 2007).

TissueFlex^{TM} Microbioreactors

The TissueFlex^{TM} microbioreactor is one of the platforms which combined both three dimensional cell culture technology and perfusion technology and was aimed to improve the measurement of drug efficacy and toxicity. The system was invented by a group of biomedical engineers from the University of Oxford. Multiple channels support 3D cultures with parallel flow with continuous flow input and waste supernatant

as output for constant nutrient supply, as well as requiring no labour. A PDMS made microbioreactor lid and bottom can be easily sealed and removed as a ready-to-use feature without the risk of contamination and with high gas permeability for gas exchange and pH maintenance, and high transparency property for imaging purposes. Applications using the TissueFlex^{TM} system have been described in publications across the various cell types and scaffold materials; bone marrow mesenchymal stem cells within collagen and matrigel (Cui, 2007), chondrocytes encapsulated in micro alginate beads, HepG2 cells for spheroid culture trapped in alginate beads and Ntera2/clone D1 human teratocarcinoma cell culture within Hystem and Matrigel (Hart T, 2011).

Micro-patterned Microbioreactors

The micro-patterned bioreactor, modified from TissueFlex^{TM} microbioreactors, is particularly designed for spheroid culture. With the same dimensions as TissueFlex^{TM} microbioreactors, the only difference is that the micro-patterned bioreactor is composed of 500 inverted pyramidal mini wells with the same length, width and depth of 250µm. Kloss et al in 2008 already described a similar design for spheroid formation, but with 300 micron dimensions, and 25 mini wells in total (Kloss et al, 2008). The functions of spheroids are directly related to their size (Griffth, 2006). Spheroid formation needs more oxygen than other cell types, and the oxygen diffusion is between 150-200µm (Curcio 2007). Diameters greater than 250µm may lead to hypoxia and necrosis in central hepatocytes (Atala and Lanza 2002; Lu, 2005) Therefore, spheroid formatting devices need to be designed for that purpose.

2.6 Summary

In vitro toxicity testing of compounds is important for pre-clinical trials during drug development, which includes cellular based drug testing together with animal trials. Therefore, using better cell sources with more efficient toxicity approaches would contribute to drug efficacy and safety, and ultimately reduce the use of animals. Stem cells are self renewal cells which maintain their own phenotype and proliferation ability, and also can be differentiated into various types of cells under certain circumstances. Use of stem cells for drug testing would overcome the limitations of the abnormal genotype of cell lines and batch to batch variation of primary cells, as well as leading to less animal usage. Organ specific toxicity is also one of the main concerns for drug testing, since when compounds fail the clinical trials, this is mainly due to organ specific toxicity such as hepatotoxicity. Stem cells can be differentiated into hepatocytes. However, current techniques can only differentiate hepato-like cells; therefore, primary hepatocytes as one of the main cell sources show the advantages of better gene expression and reasonable resemblance to *in vivo* liver phenotype during sandwich culture, as compared to cell lines and cryopreserved hepatocytes. By creating a three dimensional cell culture with natural or synthetic scaffolds, cell-cell contacts, *in vivo* like cell morphology and closer gene expression can be increased. By applying perfused medium in gas permeable bioreactors, together with the three dimensional system, the cell culture maintains a stable pH and sufficient nutrition supply, as well as requiring

less time consuming work. All of these advantages would contribute to the development of toxicity testing, which potentially improves the predictivity and accuracy of drugs in preclinical trials. Cellular toxicity may be evaluated by standard techniques such as viability assays, functional assays, genomics studies, as well as optical imaging.

Chapter 3 Development of 3D MSC-Based Model for Toxicity Testing

3.1 Introduction

This chapter focuses on the development of a three dimensional perfused model for testing toxicity of drugs, reagents and scaffold materials. Mesenchymal stem cells, sourced from bovine, mouse and human tissue, were used as the model cell type. For three dimensional cultures, it is desirable that scaffold materials meet certain criteria. They must be non-toxic, shown not to promote inflammation, and have adequate porosity and permeability to permit diffusion of metabolites and removal of waste products. If the scaffolds are to integrate with the host tissue, they must be biocompatible, and in many situations, the scaffold must also degrade at a controlled rate into materials that can be metabolised or quickly removed from the scaffold without causing damage. Also, it may be desirable to match the scaffolds mechanical properties to natural tissue and ensure the scaffold can provide the necessary adhesive ligands for cell binding (Lorenz Meinel, 2004, Huntmacher, 2000).

Alginate and collagen I have been commonly used as scaffolds that support cell culture and both materials are investigated in this chapter. The rate at which gels of Collagen I degrade depends on a number of parameters which affect the scaffold biomechanical properties, and an optimisation of collagen biomechanical properties has been carried

out. A non-toxic viability dye, alamarBlue®, was used to report on cell viability throughout the culture period. Prior to performing drug testing, the effects of cell culture medium supplements, such as fetal bovine serum and phenol red, on the alamarBlue® assay were isolated , and the volume of alamarBlue® solution, incubation time and standard curve were calculated. Human mesenchymal stem cells encapsulated in collagen I, with perfused medium in bioreactors were employed to test two compounds, Trimethoprim and pyrimethamine. Trimethoprim is a bacterial antibiotic, which blocks the pathway of folate synthesis by inhibiting the dihryofolate reductase enzyme in bacteria (Lampert, 1992). Pyrimethamine interferes with folic acid and widely used as anti-malarial drug and HIV drug (Verhoeff, 1999). Both compounds are known to be toxic to cells (Kmat and Lamm, 2004; Abou-Eisha and Afifi, 2004). This study was designed to establish the 3D culture system, and test if the system can be used at drug testing rather than being used to investigate drug mechanisms of action. Optimisation of human MSCs culture was performed before drug testing, and species differences were investigated for both trimethoprim and pyrimethamine.

3.2 Materials and Methods

3.2.1 Materials

The materials used in the presented experiments are listed in Table 3.1

Materials	Purchased from
Dulbecco's Modified Eagle Medium (DMEM), α- Modified Eagle Medium (αMEM) trypsin/EDTA solution penicillin (100 U/ml) and streptomycin (100 mg/ml), Calcein acetoxymethyl (Calcein-AM) Propidium Iodide (PI)	Gibco BRL, Invitrogen Ltd., Paisley, UK
MSCGM bullet kit Human Mesenchymal Stem Cells (HMSCs)	Lonza, workingham, UK
Foetal bovine serum(FBS)	M. B. Meldrum Ltd. Bourne End, UK
alamarBlue®	Biosource, UK
Cell culture flask, 24-well plates, 96-well-plates, tubes, 21 gauge needle, 31 gauge needle	FALCON Fahrenheit, Milton Keynes, UK
Collagen rat tail type I Dimethyl sulfoxide (DMSO) Trimethoprim Pyrimethamine Hoechst 33342	Sigma-Aldrich Chemical Company Ltd., Dorset, UK
Syringe pump	Harvard Apparatus, UK
Desktop incubator/ normal air incubator	Fisher Scientists, Loughborough, UK
Polydimethylsiloxane (PDMS)	Dow Corning Limited, Belgium

Table 3.1 Materials Used in Present Experiments

3.2.2 Mesenchymal Stem Cells

3.2.2.1 Preparation of Human MSCs

Human Mesenchymal Stem Cells (Human MSCs) were originally obtained from Lonza, Wokingham, UK, with 0.5×10^6 cells per vial. On arrival frozen vial was warmed in a water bath at 37ºC for 2 minutes. After thawing, the cells were immediately transferred and centrifuged for five minutes with complete medium composed of MSCGM (Lonza, UK), which contains 10% MCGS (mesenchymal cell growth supplement, Lonza, UK), 2% L-Glutamine (Lonza, UK), and GA-1000 (Gentamicin-sulphate, amphotercin-B, Lonza, UK) . The supernatant was removed, and cells resuspended in complete medium. The cells suspension was placed in a 75 cm^2 flask with 15ml of complete medium. The medium was changed every three days until the cells reached confluence. After several passages (performed as per Mouse MSCs passage, described in the section 3.2.2.2), the human MSCs were ready to use.

3.2.2.2 Harvest and Isolation of Mouse MSCs

Mouse mesenchymal stem cells (Mouse MSC) were obtained from the bone marrow of a 2-month old mouse (from Oxford Ludwig Institute). Primary mouse bone mesenchymal stem cells (MSCs) were prepared as follows. Both femora and tibias were removed and soft tissues were detached. Metaphysis from both ends were resected and bone marrow cells were collected by flushing the disphysis with 2ml of Dulbecco's Modified Eagle Medium (DMEM; GIBCO, UK) per bone. A suspension of bone marrow cells was obtained by repeated aspiration of the cell preparation through a 25

gauge needle. Cells were centrifuged (300g) for 5 minutes at 1500 rpm and resuspended in 8 ml DMEM medium containing 10% FBS (M. B. Meldrum Ltd. Bourne End, UK), penicillin (100 U/ml) and streptomycin (100 mg/ml), $NaHCO_3$ 3.7 g/L, plated in a 25 cm^2 polystyrene tissue culture flask (FALCON Fahrenheit, Milton Keynes, UK) and cultured in a humidified atmosphere with 5% CO_2 at 37ºC. After 4 days, the culture medium was removed and new medium was added. The medium was changed every second or the third day and the floating cells were removed. After 10 days of culture, cells were passaged by trypsinisation (0.05 % trypsin / 1mM ethylenediaminetetraacetic acid (EDTA) solution) into 75 cm^2 tissue culture flasks, with the seeding density 10^4cells /cm^2. As the culture reached almost complete confluence, cells were passaged or plated for subsequent experiments. All these cells in the experiments were used before the tenth passage, most commonly at the sixth or seventh passage.

3.2.2.3 Harvest and Isolation of Bovine MSCs

Bone marrow was obtained from the tuber coxae of two 6-month-old calves. The marrow was drawn into 21 gauge needle syringes containing heparin (1000 units) following aseptic preparation of the harvesting fields and infiltration with local anesthetic. Bovine MSCs were isolated using the following brief steps: firstly, one volume of bone marrow sample was mixed with two volumes of 1× phosphate-buffered saline (PBS); The mixture was then centrifuged (300g) for 10 minutes, and washed twice by discarding the supernatant. Afterwards, the cell suspension was washed two more times with phenol red-free Dulbecco's Modified Eagle Medium (DMEM). Cells

were added into 15 ml DMEM medium supplemented with 10% FBS, penicillin (100 U/ml) and streptomycin (100 mg/ml), $NaHCO_3$ 3.7 mg/ml, plated in a polystyrene 75 cm^2 tissue culture flask and cultured in a humidified atmosphere with 5% CO_2 at 37ºC. After being cultured for 4 days, the old culture medium was removed, together with non-adherent cells. After a further 3 to 4 days, essential to allow for cell attachment the flask, media was changed 2 to 3 times a week. Cells were found to be confluent on days 12 to 13. They were detached (using 0.05 % trypsin/1mM EDTA solution) and replated using standard procedures at 1:3 to 1:4 ratio for the first passage. The second passage of the cells was performed at a seeding density of 1×10^5cells/cm^2 (Darko B, 2004). Cells were primarily harvested at passage 2 or 3.

3.2.3 Scaffolds Preparation

3.2.3.1 Collagen Preparation

Conventional Collagen Preparation

Collagen I scaffolds were typically produced as follows. One part of 10x concentrated DMEM/αMEM was combined with two parts of dH_2O or one part of 10x concentrated PBS. Collagen type I from rat tail was gently added into solution to a final concentration of 5mg/ml and mixed thoroughly by pipetting up and down. All solutions were kept on ice at 4 ºC to prevent premature gelation. The pH was checked using pH indicator paper to ensure that it was between 7.2 - 7.4. If the pH was not correct, 0.4 mM NaOH was added drop by drop until expected the pH was reached. The cell pellet

was added with seeding density 0.5×10^6 cells/ml in collagen, and the solution was gently mixed by pipetting up and down. Finally, 100µl of the prepared collagen and cell suspension was slowly pipetted into each well of a 96-well-plate, making sure that no bubbles were formed. The samples were then placed in an incubator at 37℃ for 3 hours to allow the solution to polymerize before adding culture medium.

Modified Collagen Preparation

This method varies due to the addition of culture media during cell-resuspension. Preparation of collagen mixed with 10x concentrated DMEM/αMEM or PBS was the same as before, however, when mixing cells with 5mg/ml collagen solution, the cell pellet was first resuspended in culture medium to half of the final volume. The remaining half volume of collagen solution was gently added and mixed well with the cell suspension. The final collagen concentration in solution is 2.5mg/ml. 100µl of prepared collagen solution was placed into each well of a 96-well-plate without bubbles. The samples were placed in an incubator at 37℃ for 3 hours to allow the solution to polymerize before adding culture medium. The key point is the pH value of collagen solution. It has to be between 7.2-7.4.

Collagen Compressor

The mechanical strength of collagen can be increased by applying an external force to extract a large amount of the liquid content. The idea was initially proposed by Prof. Robert Brown of University College London, whereby collagen gels were sandwiched

between two pieces of nylon mesh, and compressed by an equally distributed mass. Extracted fluid was absorbed by filter paper (Brown, 2005). An adaption of this method was investigated. Collagen I, seeded with human MSCs was incubated for 3 hours at 37°C to form a gel. Compression was subsequently applied using a syringe plunger wrapped with autoclaved filter paper. However, the edge of the collagen gel in a 96-well-plate was found to adhere to the filter paper during compression. Upon removal of the syringe plunger, the compressed collagen gel was also removed from the 96-well plate. On removal from the plunger, some collagen stuck to the filter paper and the gel pellet lost its cylindrical shape. In addition, the quantity of collagen that remained on the plunger varied. This was because each well was manually compressed and so the load applied was not consistent and neither, therefore, was the resulting shape or quantity of remnant collagen. To resolve this issue, a modified compression device was designed to fit the 96-well plate.

The modified device consisted of three different components: a compressor top, a set of compressor necks, and a set of compressor tips (see figure 3.1). The compressor top was made of Perspex plastic and had 4 holes bored to accommodate the compressor necks, the fit of which is adjustable by screws. The distance between the necks is the same as the distance between wells in the 96-well plate. The compressor neck is a hollow steel tube, the inner diameter of which matches that of the compressor tips. The compressor top does not need to be sterilised, however the neck and tips must be sterilized before use.

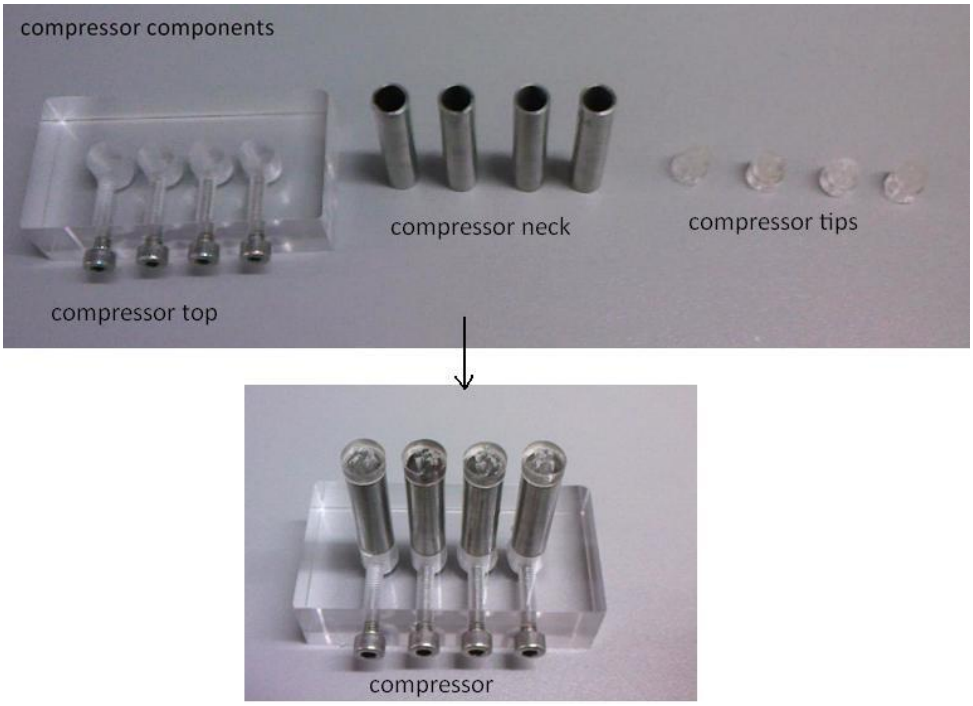

Figure 3.1 Compressor Components

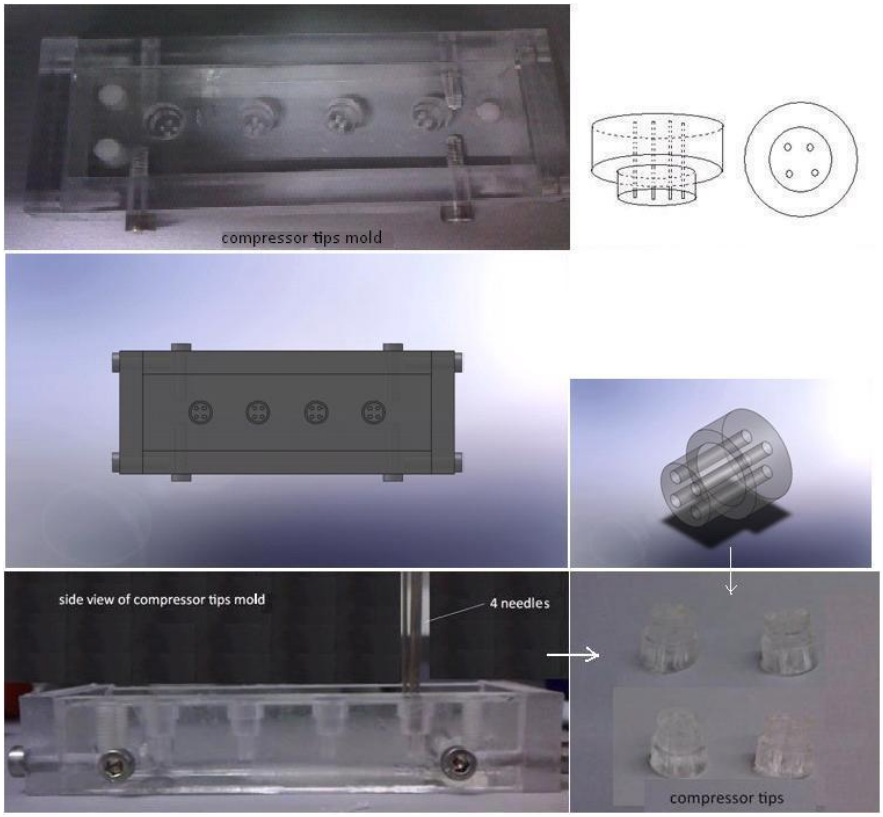

Figure 3.2 Compressor Tips

Figure 3.2 shows how the compressor tips are made. The perspex compressor tip mould has four inner recesses for casting the PDMS compressor tips (top left of figure 3.2). A schematic of the resultant casting is shown on the top right of the figure. It is cylindrical in shape, but with two different diameters. The diameter of the lower section is 1mm less than the upper section, which is designed fit into the compressor neck. In order to allow liquid from the collagen to exit up through the compressor, four channels were made by inserting 25 Gauge needles in the compressor tip mould (bottom left of figure 3.2). PDMS was poured after needles were inserted into the Perspex. Six hours later, the compressor tips were removed from the mould and sterilized (bottom right of figure 3.2).

3.2.3.2 Alginate Preparation

Two solutions are used in production of alginate gels: 0.9% NaCl solution and 1.2% Alginate solution. 0.9% NaCl solution was prepared by adding 1.8g NaCl powder in 200 ml of distilled water. 102mM $CaCl_2$ was prepared by dissolving 3 g $CaCl_2$ powder in 200ml distilled water. These solutions were filter sterilised through a 0.22µm syringe filter and then stored at room temperature until required. 1.2% Alginate solution was prepared by slowly adding 120 mg of alginate into pre-warmed 0.9% NaCl solution, and stirred using a magnetic stirrer. The beaker was covered with parafilm and stirred continuously at 37℃ for 1 to 2 hours. The resultant alginate solution was filter sterilised through a 0.22µm syringe filter and stored at room temperature until required.

Before encapsulation, the cells were spun down by a centrifuge at 1000rpm for 5 minutes, and the supernatant was removed. The cell pellet was resuspended in 1.2% alginate solution at two different densities, 3×10^6 cells/ml and 1.5×10^6cells/ml. After mixing, the cell alginate solution was aspirated into a 1ml syringe, and then slowly dropped into 102mM $CaCl_2$ solution through a 30 Gauge needle to create alginate beads, and left for 10 minutes to gel. The $CaCl_2$ solution was then removed and replaced with a 0.9% NaCl solution wash for 10 minutes.

3.2.4 Static Cell Culture

3.2.4.1 2D Cell Culture

For 2D culture, bovine MSCs, mouse MSCs and human MSCs were respectively seeded at 1×10^4 cells/cm^2, 1×10^4 cells/cm^2 and 0.5×10^4 cells/cm^2 in 75 cm^2 flasks. Culture medium was replaced every three days by fresh medium. When cell growth reached 80-90% of confluence in the flask, cells were passaged into the new flasks. The cells were rinsed twice with PBS, and detached from the flasks by exposure to 0.05% trypsin / 1mM EDTA solution, and incubated for 5 minutes at 37°C. The trypsin solution was deactivated by adding fresh culture medium containing serum. 10µl was removed and plated into a haemocytometer and the cell number was counted by trypan blue. The cell suspension was transferred to a centrifuge tube and centrifuged for five minutes at 1000rpm. The supernatant was discarded and fresh culture medium was added. The cells were resuspended and pipetted into 75cm^2 flasks at the same seeding density of the

previous passage and 15 ml of medium was added. The plates were then incubated at 37°C with 5% CO_2 at 100% relative humidity.

3.2.4.2 3D Cell Culture

For 3D culture, bovine MSCs were seeded at 0.5×10^6/ml, 1×10^6/ml, 2×10^6/ml and 3×10^6/ml into alginate beads, and cultured in a 96-well plate to observe cell growth for 7 days. Culture medium was replaced every second day. Alginate beads were dissolved by citrate buffer at the end of experiments to recover the cells. Human MSCs were seeded at 0.4×10^6/ml in collagen in a 96-well plate. After incubation 3 hours to allow for gelation, Lonza complete medium was added, and replaced every second day. The plates were incubated in a 37°C humidified atmosphere containing 5% CO_2.

3.2.5 Perfused Cell Culture

Fabrication of Bioreactors

PDMS is prepared by combining 10 parts of tetra(trimethylsiloxy)silane and 1 part of curing agent, tetramethyltetravinylcyclotetra-siloxane by weight, and placing it into 4-well bioreactor mould, then leaving it in a 60 °C oven for 4 hours to polymerise. In its native state, the external surface of solid PDMS presents hydrophobic methyl groups (McDonald, 2002), and for this reason, the PDMS surface expels water, and adsorbs proteins. Placing a glass cover slip coated with 0.1% (w/v) gelatin at the bottom of the PDMS overcame this problem. 0.1% (w/v) gelatin was therefore added in double

distilled H_2O at room temperature after autoclaving. A piece of 13mm diameter glass cover slip was placed at the bottom of each bioreactor well, and 250µl of gelatin solution added on top of the cover slips. The bioreactor was then left in an incubator for 30 minutes and then removed and washed using PBS before use.

Perfusion System

The objectives of this study were to compare the cell culture in different culture system, static and perfusion culture. Static culture was described in section 3.2.4, cells were cultured in four-well-plates, with a surface area of $2cm^2$. For perfused system, cells were cultured in four-well-bioreactors with the same surface areas or 96-well format size bioreactors. As describe above, a 0.1% gelatin coated glass cover slip was placed in the bottom of the wells of both the four-well-plates and four-well bioreactors. Culture media were supplied to the chamber wells by syringe pump at the rate of 16.7µl/hr. The perfusion rate was calculated by the medium changing rate from static culture, which is 0.8ml /change. Culture medium was changed every second day. The perfused system is shown in figure 3.3

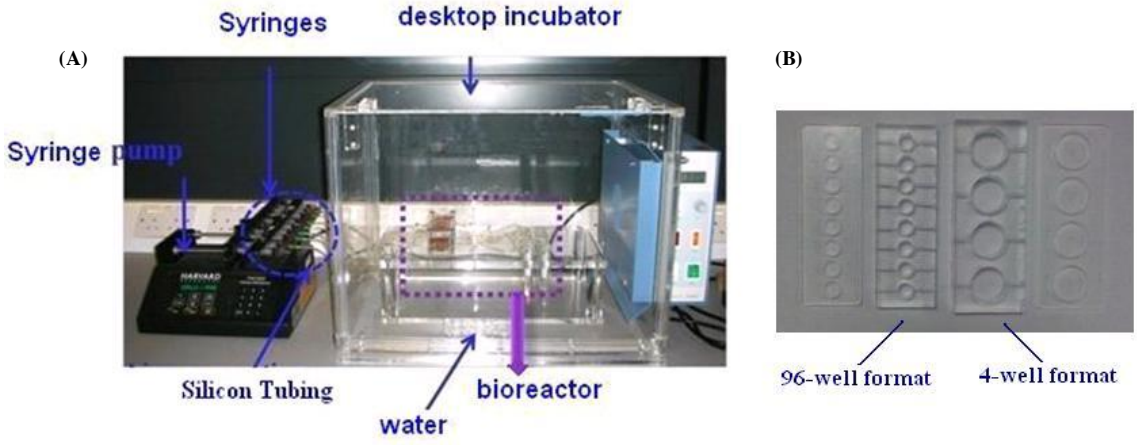

Figure 3.3 Perfused Culture System

Figure 3.3 displays the perfused culture system (A) and two types of bioreactors (B). (A) shows the perfused system, which contains syringe pump and desktop incubator. Bioreactors were placed inside of desktop incubator. Medium input for bioreactors were supplied by syringes driven by syringe pump. (B) image shows two different bioreactors used in the study, 96-well format bioreactor and 4-well bioreactor. The surface area of 96-well format bioreactor is the same with 96-well plates', 0.3196 cm^2. The 4-well bioreactor has the same surface area with 4-well plate, which is 2 cm^2.

3.2.6 Functional Assays

3.2.6.1 AlamarBlue® Assay

Cell Proliferation

For quantification of cell metabolism, and indirectly, cell number, the alamarBlue® assay was used. AlamarBlue® solution was added into the medium with the final concentration 5% in normal culture medium [DMEM/ αMEM, 10%FBS, penicillin (100 U/ml) and streptomycin (100 mg/ml), without phenol red]. Cell growth in the presence and absence of the added drugs was compared in monolayer culture. As a negative

control, alamarBlue® was added to the medium without cells. The medium was placed in an incubator for four hours at 37 ^{o}C, and then transferred to a 96-well-plate for measurement. Accumulation of reduced alamarBlue® in the culture medium was determined using a spectrophotometer (microplate reader). In the method, the dye resazurin which appears dark blue in colour is reduced into resorufin which is pink in colour by metabolically active cells. The maximum absorption of resazurin is 605nm and the maximum absorption of resorufin is 573nm (Technical bulletin). The absorbance of the test and control wells was selected and read at wavelengths of 570nm and 600nm. The number of viable cells correlates with the magnitudes of dye reduction and is expressed as percentage of alamarBlue® reduction (Ahmed et al., 1994; Goegan et al;, 1995; Nociari et al., 1998). The calculation of the percentage of alamarBlue® reduction (%AB reduction) is shown in Equation 3.1.

$$\%\text{AB reduction} = \frac{(\varepsilon_{ox}600\text{ nm}*\text{A}570\text{ nm} - \varepsilon_{ox}570\text{ nm}*\text{A}600\text{ nm})\text{ of treated sample}}{(\varepsilon_{red}570\text{ nm}*\text{A}'600\text{ nm} - \varepsilon_{red}600\text{ nm}*\text{A}'570\text{ nm})} \times 100$$

Equation 3.1 %AB Reduction for Cell Quantification Assay

In this equation % alamarBlue® reduction is equal to the value of treated sample divided by the value of negative control. The constants ε_{ox} and ε_{red} represent the molar extinction coefficient of alamarBlue® at specified wavelengths. Where ε_{ox} 600 nm = 117,216 (molar extinction coefficient of oxidized alamarBlue® reagent at 600 nm), ε_{ox} 570 nm = 80,586 (molar extinction coefficient of oxidized alamarBlue® reagent at 570 nm), A570 nm represents the absorbance of the sample at 570 nm, while A600 nm represents the absorbance of the sample at 600 nm. Three repeat tests were performed

for each data point. ε_{red} 570nm =155,677 (molar extinction coefficient of reduced alamarBlue® at 570 nm), ε_{red} 600 nm = 14,652 (molar extinction coefficient of reduced alamarBlue® at 600 nm), A'600 nm = absorbance of negative control wells which contained media plus alamarBlue® but no cells at 600 nm, and A'570nm = absorbance of negative control wells that contained media plus alamarBlue® but no cells at 570 nm (S.Al-Nasiry, et al., 2007).

Cytotoxicity

MSCs were prepared as previously described. alamarBlue® reagent (at concentration 5%) was directly added into culture medium and incubated for 2 to 3 hours for both monolayer and three dimensional culture. Reduced alamarBlue® was transferred to a new blank 96-well-plate, and absorbance was measured using a microplate reader at 570nm and 600nm. The formula used is shown in Equation 3.2.

$$\%AB\ reduction = \frac{(\varepsilon_{ox}600\ nm * A570\ nm - \varepsilon_{ox}570\ nm * A600\ nm)\ of\ treated\ sample}{(\varepsilon_{ox}600\ nm * A570\ nm - \varepsilon_{ox}570\ nm * A600\ nm)\ of\ untreated\ control} \times 100$$

Equation 3.2 %AB Reduction of Cytotoxicity Assay

In this equation % alamarBlue® reduction is equal to the value of treated sample divided by the value of untreated control and then multiplied by 100 (S.Al-Nasiry, et al., 2007). ε_{ox} and ε_{red} are constants representing the molar extinction coefficient of alamarBlue® at specified wavelengths. The constants are defined in last section. Three repeat tests were performed for each data point.

Standard Curves

A standard curve of % alamarBlue® reduction was calibrated and plotted. This is to establish a standard curve to use for measurement of cell numbers. alamarBlue® measures the collective metabolic activity (cell number x metabolic rate). The method is non-destructive and can be applied repeatedly to growing cells and tissue. It was tested by seeding different cell densities. By using this standard curve, it is possible to indicate cell proliferation and viability. The densities of species of MSCs' that were selected at 8×10^5 cells/ml, 6×10^5 cells/ml, 4×10^5 cells/ml, 2×10^5 cells/ml, 1×10^5 cells/ml, and 0.5×10^5 cells/ml. The effect of absence or presence of phenol red and FBS was tested and plotted, as well as optimal culture medium for alamarBlue® Assay.

Live and Dead Assays

Calcein-AM and propidium iodide (PI) were used to stain for live and dead cells respectively. Calcein-AM is green fluorescent cell marker, which is transported through the cell membrane and becomes active through removal of the acetomethoxy group by intracellular esterases found only in living cells. PI does not permeate the membrane of live cells. It is widely used to identify dead cells by passing through the damaged cell membrane, where on binding to DNA, its red fluorescence is significantly enhanced. 4',6-diamidino-2-phenylindole (DAPI), a blue fluorescent cell marker, was also used as cell nuclei stain.

Prior to staining, media was removed and discarded from wells containing the matrices

with cells, and the gels were washed twice with PBS, The live-dead solution contained 1µl of calcein-AM (Gibco BRL, Invitrogen Ltd., Paisley, UK), with 1µl of propidium iodide (PI) (Gibco BRL, Invitrogen Ltd., Paisley, UK) and 1µl of 4',6-diamidino-2-phenylindole (DAPI),added to 1mL of PBS in a dark environment. This solution was added to wells and incubated for 30 minutes at 37 ^{o}C and 5% CO_2. The solution was then removed and the cells were washed once with PBS. The wells were filled with PBS for fluorescence microscope and multi-photon microscope imaging.

3.2.7 Test Compounds

Two compounds, Trimethoprim and Pyrimethamine, were screened in these experiments. Stock solutions at the concentration of 1mg/ml were prepared with a 70% volume of alcohol(Cui, 2007). Both Trimethoprim and Pyrimethamine were prepared in a series of concentrations from 10^{-10}g/ml to 10^{-4}g/ml. Chemicals were diluted into complete medium, DMEM/ αMEM, containing 10% FBS (M. B. Meldrum Ltd. Bourne End, UK), penicillin (100 U/ml) and streptomycin (100 mg/ml). Drug response on mouse MSCs and human MSCs were performed in monolayer and three dimensional culture, in a desktop (normal air, 0.03% CO_2) incubator at 37°C.

Cells were seeded into wells at a seeding density of 10^4cell/cm^2 in a 100µl cell suspension and cultured for 24 hours before being exposed to the series of drug

concentrations. Subsequently, cell proliferation was determined by alamarBlue® assay at day 2 and day 3. 5% alamarBlue®was added for 2 hours incubation. Untreated cells with no drug exposure were considered as the positive controls, and wells with no cells and only alamarBlue® with culture medium was defined as the negative control.

For cytotoxicity testing, cells were respectively seeded at 10^4cell/cm^2 in monolayer culture, and into 50µl of collagen at 0.2×10^6 cells/ml and cultured in static and perfused systems. Cells were cultured for 24 hours before adding drugs, and after this, culture medium was replaced with fresh medium containing the different drugs every second day. For the perfused system, the pump rate was set as 16.7µl/hr. alamarBlue® assay was performed on days 3 and 7.

3.2.8 Statistical Analysis

The data is presented as the mean ± standard deviation from three separate experiments. Data were analysed by one way ANOVA non-parametric analysis for comparisons, and statistical significance was accepted at $P<0.05$.

3.3 Results and Discussion

3.3.1 Optimisation of Scaffold Materials

3.3.1.1 Alginate Beads

Bovine MSCs were seeded at four different densities, 0.5×10^6cells/ml, 1×10^6cells/ml, 2×10^6cells/ml and 3×10^6cells/ml to observe cell growth over 7 days. Live/dead assay was performed and observed under fluorescent microscope.

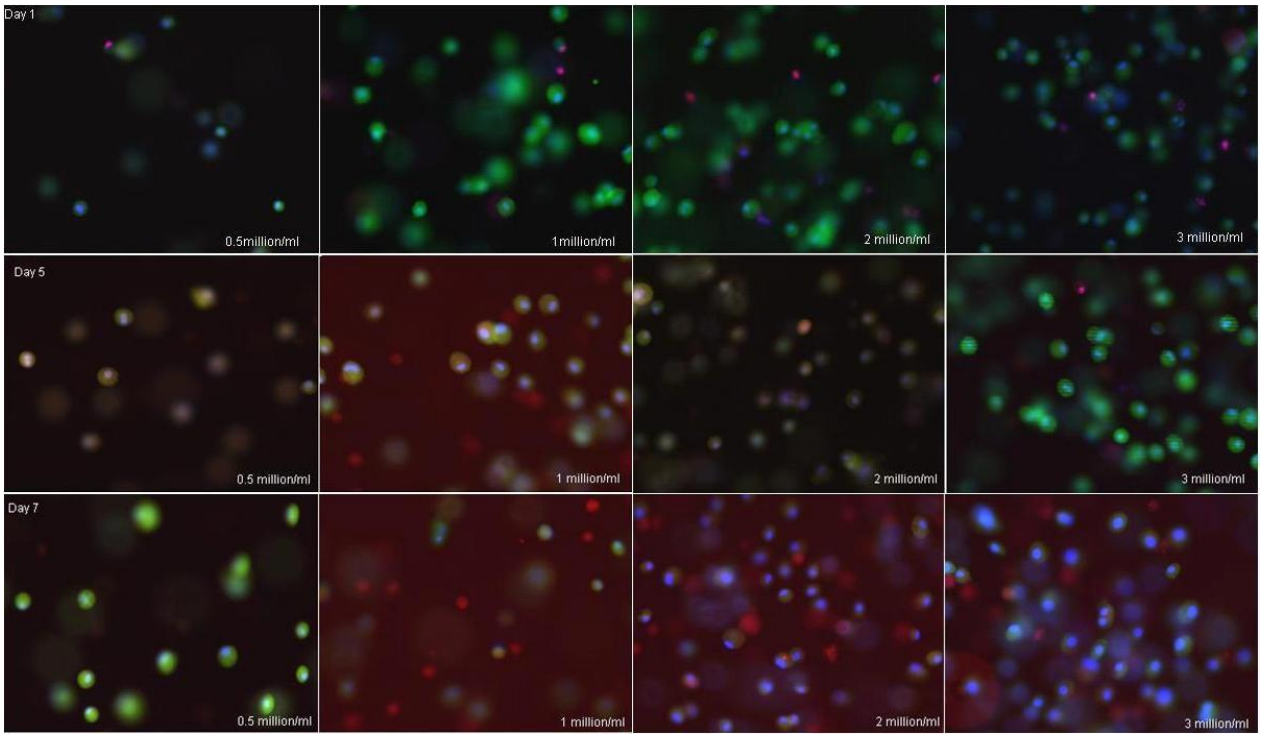

Figure 3.4 MSCs Morphology and Live/Dead Staining in Alginate Beads

Figure 3.4 MSCs Morphology and Live/Dead Staining in Alginate Beads. Red dye is PI, which stains nuclei of dead cells, blue dye is DAPI, which stains nuclei of alive cells and green dye is Calcein-AM, which stains the cytoplasm of live cells.

Figure 3.4 shows the MSCs morphologies with different seeding densities on days 1, 5 and 7. For the same seeding density, one observes that cells number increases as time

progresses. However, the differences among day 1, 5 and 7 are minor. Also, by the end of day 7, at densities of 1, 2 and 3×10^6cells/ml, dead cells were observed more than day 5 and day 1. The morphology of the MSCs in alginate scaffolds was observed to be spherical rather than the cells adopting extended or long, thin, fibroblast like shapes. This was thought to indicate that the alginate beads, as 3D scaffold, did not provide adequate binding sites for MSCs attachment.

3.3.1.2 Collagen

An investigation of cell growth and cell morphology was performed to test the suitability of collagen for MSCs culture., Human MSCs were seeded in triplicate into 96-well-plates at two different cell densities (0.5×10^4cells/well and 1×10^4cells/well) and with 5mg/ml collagen at 100µl per well. After gelation, 250µl of complete αMEM medium was added to each well. The medium was changed every second day and alamarBlue® assay was performed with a 3 hours incubation time.

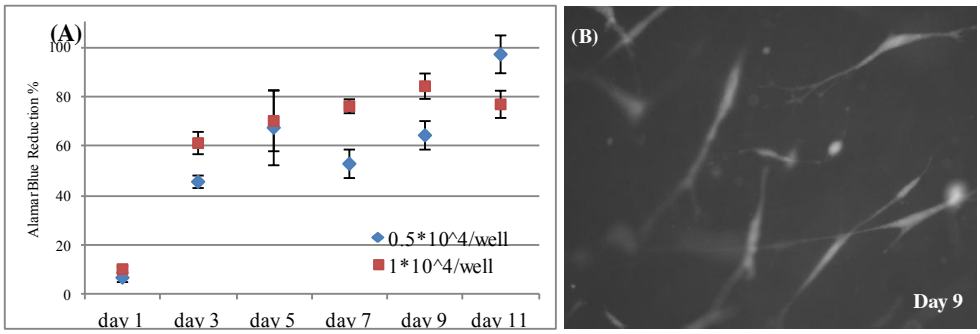

Figure 3.5 Human MSCs Growth and Morphology

Figure 3.5 Human MSCs growth and Morphology. (A) shows the growth of human MSCs up to

11 days in collagen, with two different seeding densities 0.5×10^4cells/well and 1×10^4cells/well. (B) shows the human MSCs morphology at day 9.

From Figure 3.5 (A), shows the growth of human MSCs up to 11 days in collagen. Figure 3.5 (B) shows the morphology taken by fluorescent microscope. In Figure 3.5 (A), the red square markers present the cells growth with seeding density 1×10^4cells/well, where blue diamond markers present cells growth with seeding density 0.5×10^4cells/well. For 1×10^4/well density, human MSCs grew Increased in number rapidly from day 1 to day 3, then steadily from day 3 to day 9. After day 9, cell growth slowed, and it was thought that the cells had reached confluence by day 11, decreasing in metabolism, if not in cell number. For 0.5×10^4cells/well, human MSCs grew similar with higher seeding densities from day 1 to day 5. However, the metabolic activity was seen to decrease at day 7, then increase again at day 9, with the same growth speed of 1×10^4cells/well. At day 11, the highest metabolic activity was seen. In general, human MSCs growth with 1×10^4cells/well was fast and more stable than for the lower seeding density, before reaching confluence after day 9. Also, cell morphology at day 9 can be seen in figure 3.5 (B). This shows the better cell attachment in collagen environments than alginate beads. For this reason, collagen was selected for the study.

3.3.1.3 Collagen Compression

Sterilised compressor tips were inserted into to compressor necks and the compressor top, and experiments were performed in 96-well plates (see Figure 3.6).

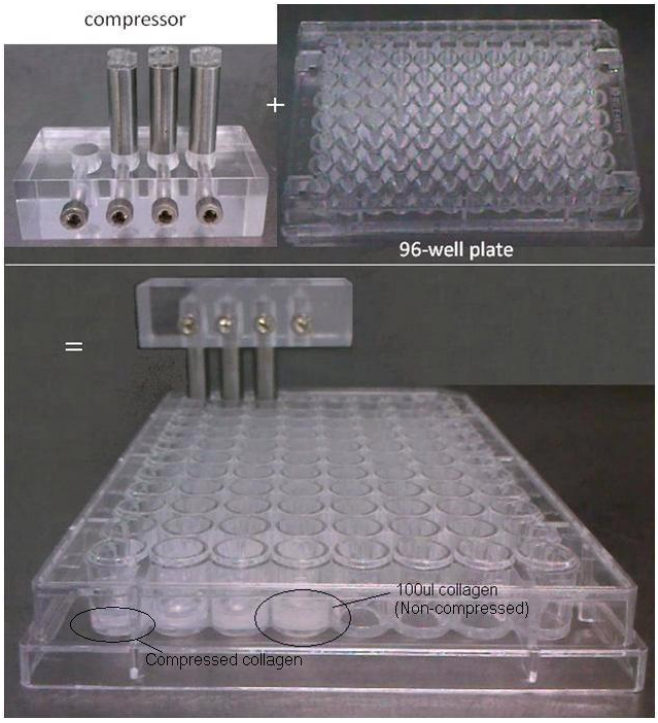

Figure 3.6 Collagen Compression Apparatus

Figure 3.6 shows the process of how compressor works. 100µl collagen was seeded as control in a 96-well plate. Compressed collagen was demonstrated. It is evident that the compressed collagen occupies less volume, when compared with the non-compressed collagen. Subsequent experiments were carried out to investigate cell proliferation between compressed and non-compressed collagen.

The advantages of the compressor are that it provides an equal load to the collagen being compressed in three wells. The use of PDMS to form the compressor tips prevents the collagen from sticking to the bottom of the compressor tips.

Experiments were performed to identify the optimal collagen concentration for compression. The collagen concentrations used ranged from 2mg/ml to 7 mg/ml. It has been found that the collagen concentrations from 4mg/ml to 5mg/ml are optimal in this

experiment. For concentrations higher than 5mg/ml, a larger loading force was required, which resulted in collagen also being squeezed through the compressor tips with the liquid. Concentrations lower than 4mg/ml were found to be too weak to retain the required structure. This was because collagen was mixed with 10×PBS, and lower collagen concentrations contained more liquid with little collagen left after compressing.

As described previously, human MSCs seeded at 0.5×10^6cell/ml were mixed with 5mg/ml collagen, and cultured in 96-well-plates for up to 7 days. Medium was changed every day, and cell proliferation was tested by use of the alamarBlue® assay, as described above. Figure 3.7 plots the difference between alamarBlue® reduction for the compressed and non-compressed collagen cell seeded scaffolds. Non compressed collagen (blue diamonds) was found to support a slightly larger number of cells than the compressed collagen (red squares), but not significantly different, and the cell growth rates were found to be similar. This indicates that compression method can be useful and investigated more in future work.

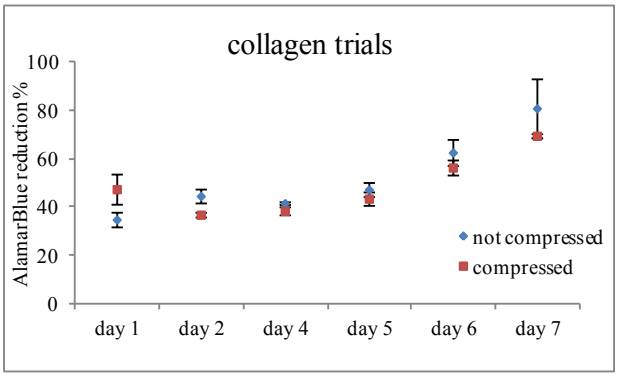

Figure 3.7 Human MSCs for Collagen Trials

3.3.2 Optimisation of AlamarBlue® Assay

3.3.2.1 Presence of FBS and Phenol Red

The effects of FBS and phenol red in the culture medium on the alamarBlue® assay was studied with following four conditions:

1. DMEM with phenol red and FBS (D++)
2. DMEM with phenol red, without FBS (D+-)
3. DMEM without phenol red with FBS (D-+)
4. DMEM without phenol red and FBS (D--)

5µl alamarBlue® was added in different 100µl culture mediums, with cell densities of 10,000cells/ml, 20,000cells/ml, 40,000cells/ml and 60,000cells/ml. Negative control was performed without cells. After 2 hours incubation, absorbance was measured at 570nm and 600nm.

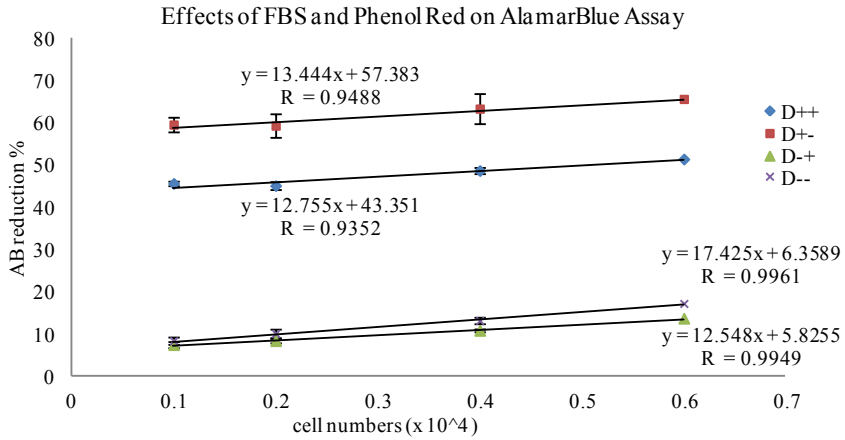

Figure 3.8 Effects of FBS and Phenol Red on alarmarBlue® Assay

Effect of FBS and phenol red on alamarBlue®assay. Tests performed under different conditions namely D++ (+phenol red, +FBS), D+- (+Phenol red, -FBS), D-+(-phenol red, +FBS) and D- -(-phenol red, -FBS)

Figure 3.8 demonstrates the difference of alamarBlue® reductions among culture medium with the presence and absence of phenol red and FBS. Results show the linearity of increasing concentrations. Linear regression was analysed in all four conditions. The top two lines show the results for media containing DMEM with phenol red (D++ and D+-), while bottom two lines show the effect of the absence of phenol red (D-+ and D--). Although Phenol red affects the background absorbance which could be significant, the presence of phenol red does not affect the slope of the reduction rate versus cell numbers. As a result, the calibration curve with phenol red is simply shifted to a higher level, which is almost the identical slope with the one without phenol red. However, for the linear regression equations of both D++ and D+-, taken from the figure, the R^2 values are both smaller than D-+ and D--, the addition of phenol red in the medium needs to be further investigated. For cells cultured in media in the presence of FBS and but without phenol red (D-+), a smaller slope is seen, in comparison to the absence of FBS for the same condition (D--).Therefore, later alamarBlue® assay in monolayer experiments have been performed in DMEM without phenol red and without FBS.

3.3.2.2 Culture Medium Volume

Cell suspension was prepared for a series dilution of seven cell densities from 7×10^4 cells/ml to 1×10^4 cells/ml. After 4 hours cell of attachment, culture medium was replaced with 5% alamarBlue® in basal DMEM without phenol red and with FBS. Two different volumes were investigated, 100µl and 200µl. For the negative controls, the same medium without cells was investigated. Absorbance was measured at 570nm and 600nm after 2 hours of incubation time.

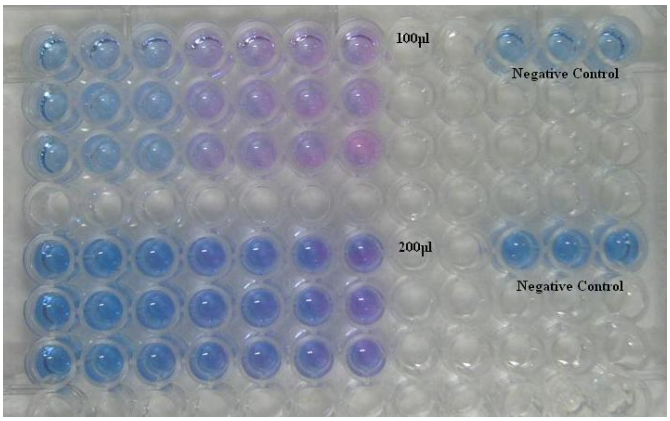

Figure 3.9 Effect of Culture Volume for the alarmarBlue® Assay

When the alamarBlue® assay was performed using 200µl of solution per well, the colour changes were found to be less prominent (see Figure 3.9, bottom set), and a light pink hue was evident for only the highest concentrations. In contrast, for the alamarBlue® assay performed using 100µl of solution per well (see Figure 3.9, top set), it was observed that colour changed gradually from blue to pink, which shows the reduction of alamarBlue® by live cells was gradually increasing. Using linear regression, when using 100µl of solution per well, $y = 4.4676x + 6.0345$, and $R^2 = 0.9969$; and when using 200µl of solution per well, $y = 2.92x + 1.7992$, and $R^2 = 0.9607$.

The gradient of the slope found in the first equation (100µl of media) was steeper; illustrating that metabolic reduction was more concentrated in 100µl of media than in 200µl. Results indicated that the alamarBlue® assay had a better dynamic range when incubated in the 100µl of media.

3.3.2.3 Incubation Time

Cell suspension was prepared at 5 different densities, 0.1×10^5 cells/ml, 0.5×10^5 cells/ml, 1×10^5 cells/ml, 2×10^5 cells/ml and 4×10^5 cells/ml. 100µl of each density was seeded into 96-well plate in triplicate. Four hours after seeding, cell culture medium was replaced with 5% alamarBlue® in basal αMEM without FBS. Cells were cultured for 2 or 3 hours to determine an optimal incubation time. Wells with the same media, but without cells were used as negative controls. Absorbance was measured at 570nm and 600nm.

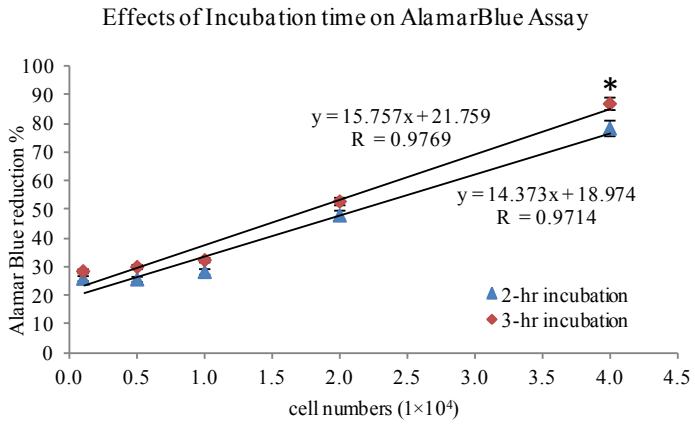

Figure 3.10 Effect of Incubation Time on alarmarBlue® Assay

Results are displayed in figure 3.10. Both results for 2 hours and 3 hours incubation

times show good linearity in the figure, with R^2 greater than 0.95.The difference between 2 hours and 3 hours was found to be minor, only significant different in the highest cell numbers. It was found that for both the two hour and three hour incubation times, alamarBlue® reduction increased in a similar manner and in line with cell density. The difference between the slopes of the regression equations was small, and cellular metabolic activity for two and three hours was found to be similar. To keep the assay time short, 2 hours incubation time was selected for the experiments that followed.

3.3.2.4 Standard Curves

Standard curves relating the % alamarBlue® reduction in different culture mediums to the number of cells were investigated, and it was found that alamarBlue® could be used within a certain range of cell densities. The four different plots shown in Figure 3.11 describe monolayer cultures with $NaHCO_3$ (+αMEM) and without $NaHCO_3$ (-αMEM), and three dimensional cultures with $NaHCO_3$ (+αMEM) and without $NaHCO_3$ (-αMEM). Investigations were performed by seeding a known numbers of cells and assayed by alamarBlue®. Cell densities of 8×10^5, 6×10^5, 4×10^5, 1×10^5, 0.5×10^5 and 0.1×10^5cells/ml were investigated. 5% alamarBlue® in 100µl of αMEM with phenol red (αMEM medium without phenol red is not commercial available), without FBS and with 25mM HEPES was added to each well. The samples were incubated for two hours at 37°C, 5% CO_2 in a 100% humidified environment before being read as described above.

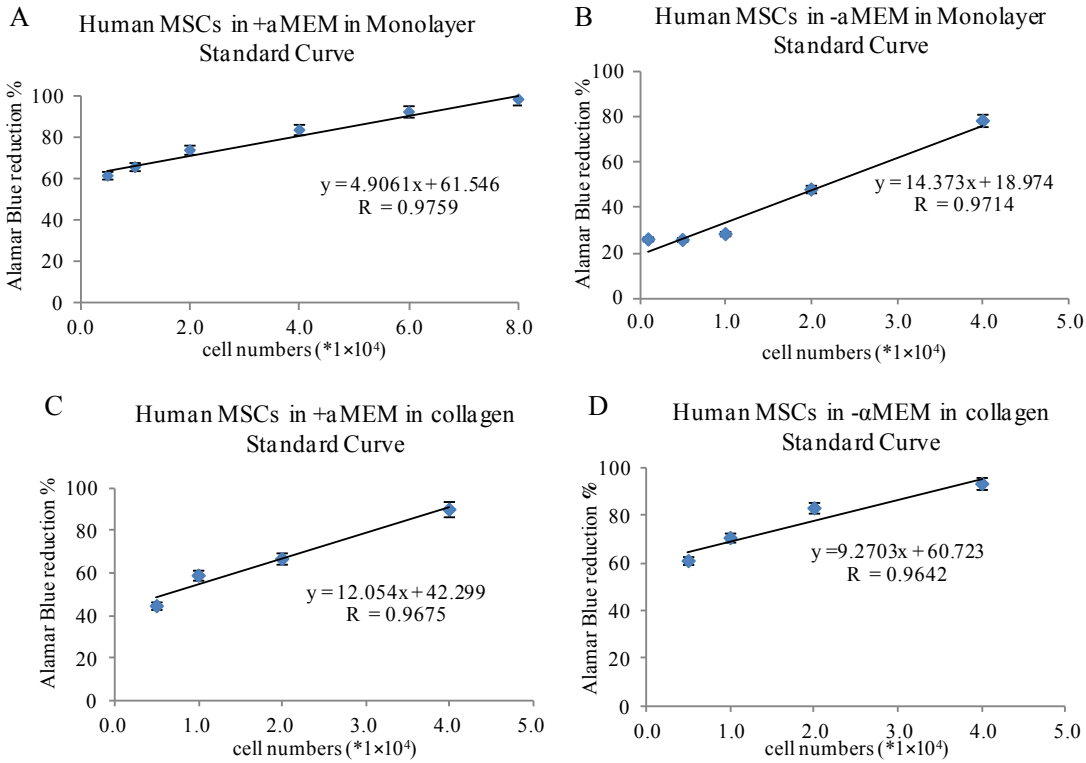

Figure 3.11 Human MSCs' Standard Curves

Figure 3.11 Standard curves of human MSCs in αMEM with $NaHCO_3$ (A) and without $NaHCO_3$ (B) in Monolayer culture. Standard curves of human MSCs in αMEM with $NaHCO_3$ (C) and without $NaHCO_3$ (D) in collagen.

As seen in Figure3.11, there is a high linear reduction rate of alamarBlue®. Within two hours, the reduction percentage changed significantly, and the physical colour changed from purple (because αMEM contains phenol red) to pink. The slope equations, performed in monolayer with or without $NaHCO_3$, shown in figure 3.11, are respectively given as $y = 4.9061x + 61.546$, with $R^2 = 0.98$, and $y = 14.373x + 18.974$, with R^2 equals 0.9714. Similar reduction rates were seen in collagen within two hours, with $y = 12.054x + 42.299$ with $R^2 = 0.9675$ in +αMEM and $y = 9.2703x + 60.723$ with $R = 0.9642$ in –αMEM.

3.3.3 Optimisation of Human MSCs Growth Condition

For routine culture of MSCs, MSCGM (mesenchymal stem cell growth medium, Lonza, UK) was utilized. This contains 10% MCGS (mesenchymal cell growth supplement, Lonza, UK), 2% L-Glutamine (Lonza, UK), and GA-1000 (Gentamincin-slufate, amphotercin-B, Lonza, UK). As present study utilised a desktop incubator with culture performed under normal air conditions (0.03% CO_2), it was decided that complete medium from Lonza would not be suitable because of absence of HEPES buffer. The basal medium, αMEM, which contains HEPES was consider more suitable. Previous cell culture experience in the lab has demonstrated that MSCs divide more slowly in αMEM supplemented with FBS and penicillin and streptomycin (AA), than in MSCGM during passaging. Therefore, optimisation of human MSCs growth was carried out by investigating supplements FBS, AA, MCGS, GA-1000 and $NaHCO_3$.

Four groups of factors combinations in different culture mediums were tested as below.

Group 1. Four subgroups were selected in αMEM without $NaHCO_3$

(a) No_$NaHCO_3$_αMEM_MCGM+GA-1000

(b) No_$NaHCO_3$_αMEM_MCGM+AA

(c) No_$NaHCO_3$ _αMEM_FBS+GA-1000

(d) No_$NaHCO_3$ _αMEM_FBS+GA-1000

Group 2. Two subgroups were selected in DMEM without $NaHCO_3$

(a) No_$NaHCO_3$_DMEM_MCGM+GA-1000

(b) No_$NaHCO_3$_DMEM_MCGM+AA

Group 3. Two subgroups were selected in αMEM with $NaHCO_3$

(a) with $NaHCO_3$_αMEM_MCGM+GA-1000

(b) with $NaHCO_3$_αMEM_MCGM+AA

Control: Lonza complete medium with supplement of MCGS and GA-1000

Human MSCs were equally seeded at 10^4 cell numbers/cm^2 into 96-well plates and cultured in 95% air and 5% CO_2 incubator or normal air incubator (desktop incubator). alamarBlue® assay was evaluated every second days for 7 days duration. Fresh medium was replaced after alamarBlue® assay.

The figure 3.12 shows the optimal cell growth in the different media. The top line is the Lonza control, which shows the highest reduction rate for cells cultured in MSCGM medium. Generally speaking, cells grew better in αMEM with presence of $NaHCO_3$ than αMEM without $NaHCO_3$. With the absence of $NaHCO_3$, cells grew better in αMEM than in DMEM. Cells cultured in DMEM appear to show a significantly lower reduction of alamarBlue® than cells cultured in αMEM. This was because the DMEM used did not contain phenol red, which was shown above to increase the overall background level in the alamarBlue® assay. However, DMEM shows less advantage for human MSCs culture. The reduction rate difference between day 1 to day 7 is much

smaller than any other medium formulation in this experiment, illustrating that cells grew more slowly in DMEM. With the presence of $NaHCO_3$ in αMEM, it is observed that cells proliferated more rapidly in MCGS than in FBS according to alamarBlue® reduction rates at day 7. Meanwhile, all αMEM medium formulations, with or without $NaHCO_3$ show AA improved cell proliferation. In conclusion, the combination of MCGS and AA, together with $NaHCO_3$ in αMEM was found to be most suitable for human MSCs growth.

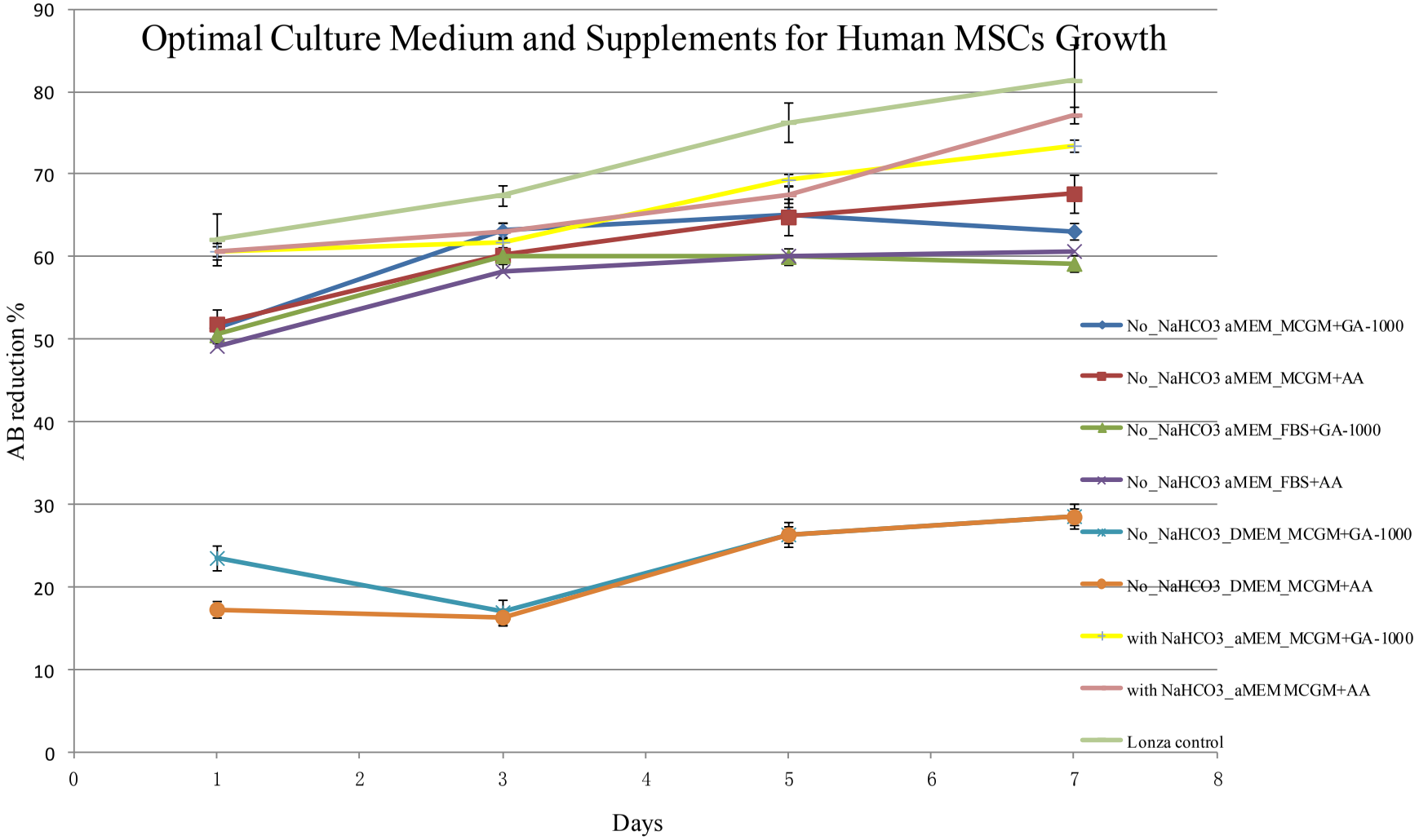

Figure 3.12 Optimal Culture Medium and Supplements for Human MSCs Growth

3.3.3 2D Static Culture Responses to Compounds

The response of human MSCs and mouse MSCs was investigated when exposed to Trimethoprim and Pyrimethamine in 2D static culture conditions. Both trimethoprim and pyrimethamine were prepared in a series of concentrations from 10^{-10}g/ml to 10^{-4}g/ml. Chemicals were diluted into complete medium , αMEM, which contains 10% FBS, 1% penicillin (100 U/ml) and streptomycin (100 mg/ml), 2.2g/L $NaHCO_3$ and 25mM HEPES. 100µl of cell suspension at 10^4cell/cm^2 seeding density was seeded into the wells of a 96-well plate and incubated overnight before treatment. Culture media was replaced with a series of drug concentrations after 48hrs. Cell proliferation was determined by alamarBlue® assay at days 2 and 3. 5% alamarBlue® was added for a two hour incubation period in the desktop incubator at 37ºC. Wells seeded with cells and media containing no drugs were used as positive control (untreated cells), and alamarBlue® with culture medium and no cells was defined as the negative control.

3.3.3.1 Human MSCs Response to Compounds

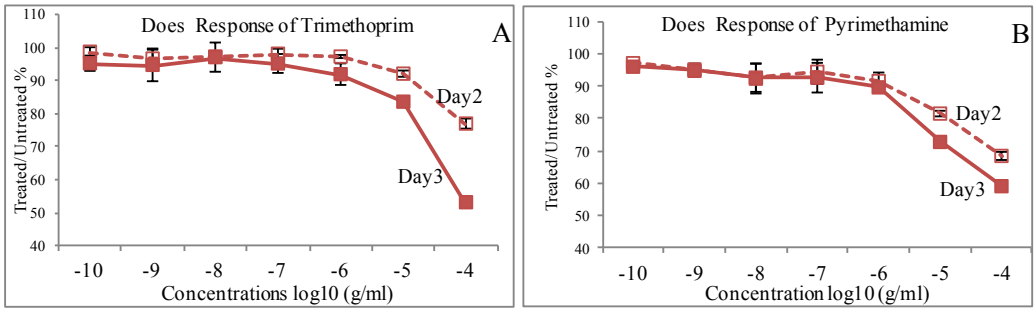

Figure 3.13 Dose Response of Trimethoprim and Pyrimethamine using Human MSCs

Dose responses of trimethoprim and pyrimethamine were investigated by using

human MSCs at days 2 and 3, as shown in figure 3.13. The red solid line represents a dose response at day 2 and the red dashed line represented the dose response at day 3 for both figures. The results were normalised by dividing the untreated dose by the untreated control. At day 2, trimethoprim was found to be non-toxic to human MSCs at lower concentrations between 10^{-10} g/ml and 10^{-6} g/ml. When the dose was increased from 10^{-6} g/ml to the highest dose of 10^{-4} g/ml, the ratio of alamarBlue® reduction in treated/untreated cells decreased gradually from 97.13% to 76.82%. At day 3, lower doses from 10^{-10} g/ml to 10^{-5} g/ml showed no toxic to cells, the ratio dropped dramatically at 10^{-5} g/ml with 83.46% viable cells and 52.98% at 10^{-4} g/ml. For pyrimethamine dose response, presented in figure 3.13 (B), the compound did not show toxicity to human MSCs when the doses were lower than 10^{-6} g/ml. The ratio of treated/untreated cells was 91.65% at day 2 and 89.69% at day 3. For the higher dose, 10^{-5} g/ml, the ratio was 81.58% at day 2 and 72.80% at day 3. Dose response at 10^{-4} g/ml dropped from 68.47% at day 2 to 59.10% at day 3.

3.3.3.2 Mouse MSCs Response to Compounds

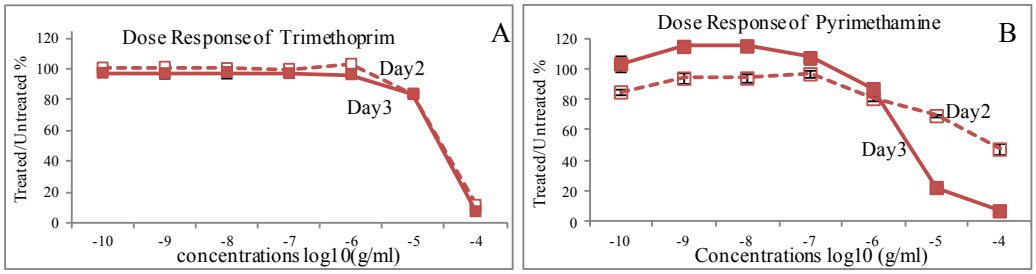

Figure 3.14 Dose Response of Trimethoprim and Pyrimethamine using Mouse MSCs

Similarly, Mouse MSCs were utilised to test the dose response of trimethoprim and pyrimethamine at day 2 and 3, shown in figure 3.14. The red solid line represents dose

response at day 2 and the red dashed line represents dose response at day 3 for both figures. Mouse MSCs response to doses lower than 10^{-6} g/ml showed similar results at day 2 and day 3. The cell viability ratio dropped to 83.20% when treated with 10^{-5} g/ml trimethoprim, and the highest dose of 10^{-4} g/ml was found to be lethal to cells. For dose response to pyrimethamine, the viability ratio showed that 10^{-6} g/ml was the lowest concentration to lead to a reduction in cell metabolism, and the highest concentration, of10^{-4} g/ml, as also found to be toxic to cells.

In comparison, both human MSCs and mouse MSCs showed a similar dose response trend to these compounds, however, human MSCs were less sensitive in the higher doses. Table 3.2 lists both human and mouse MSCs dose response to trimethoprim/Pyrimethamine.

(g/ml)	Human Day 2	Mouse Day 3	Human Day 2	Mouse Day 3
10^{-7}	98.00 %±1.51%	99.71%±2.48 %	95.04%±2.87%	96.84%±2.09%
10^{-6}	97.13%±0.47%	103.00%±1.68%	91.80%±3.27%	96.12%±1.79%
10^{-5}	91.95%±0.95%	83.68%±0.74%	83.46%±1.23%	83.20%±1.36%
10^{-4}	76.82%±1.53%	11.62%±0.13%	52.98%±0.95%	7.36%±0.07%

Table 3.2 Dose Response of Human and Mouse MSCs for Trimethoprim

The dose response of trimethoprim shows that when human MSCs were treated at 10^{-5} g/ml, the treated/untreated proliferation ratio was 91.95% at day 2, but dropped down to 83.68% at day 3, while mouse MSCs maintained the same proliferation at both day 2 and 3. When treated at 10^{-4} g/ml, human MSC proliferation ratio was 76.82% at day 2, and dropped to 52.98% at day 3, while mice proliferation ratios changed from 11.62% to 7.36% between days 2 and 3, which is much lower than human MSCs at

the same drug concentration. This indicates that Trimethoprim at higher concentrations is more toxic to mice MSCs than human MSCs.

(g/ml)	Human Day 2	Human Day 3	Mouse Day 2	Mouse Day 3
10^{-7}	94.53%±3.75%	92.69%±4.59%	96.82%±2.31%	107.25%±4.04%
10^{-6}	91.65%±2.64%	89.70%±0.26%	80.67%±1.50%	87.13%±3.04%
10^{-5}	81.58%±0.87%	72.80%±0.64%	69.48%±0.83%	22.50%±2.04%
10^{-4}	68.47%±1.26%	59.10%±0.88%	47.65%±3.62%	7.28 %±0.26%

Table 3.3 Dose response of Human and Mouse MSCs for Pyrimethamine

Likewise, when the pyrimethamine dose exponentially increased from 10^{-7}g/ml to 10^{-4}g/ml, the human MSCs proliferation ratio decreased from 92.69% to 59.08% at day 2 and from 94.52% to 68.47% at day 3, while for mouse MSCs, the ratio dropped from 96.82% to 47.65% at day 2 and 107.25% to 7.28% at day 3. This indicates that the same dose of pyrimethamine is more toxic to mouse MSCs than to human MSCs.

3.3.5 Effect of 3D and Perfused Culture

Human MSCs were seeded at $1x10^4$cells/well in 24-well plates for monolayer culture, and 50µl of 0.2×10^6cells/ml in final concentration of 2.5mg/ml collagen in 96-well format bioreactor three dimensional culture. Cells were cultured for 24 hours before the addition of drugs. The medium with drugs was replaced every second day in static, monolayer and three dimensional culture. For the perfused culture system, the pump rate was set as 16.7µl/hr. alamarBlue® assay was performed at days 3 and 7. Data was normalised by dividing the readings from drug treated cells with readings from untreated cells. Results of 2D static and 3D static at 10^{-5}g/ml, and all culture methods at 10^{-4}g/ml at day 7 are not available.

Comparison of 2D static & 3D static

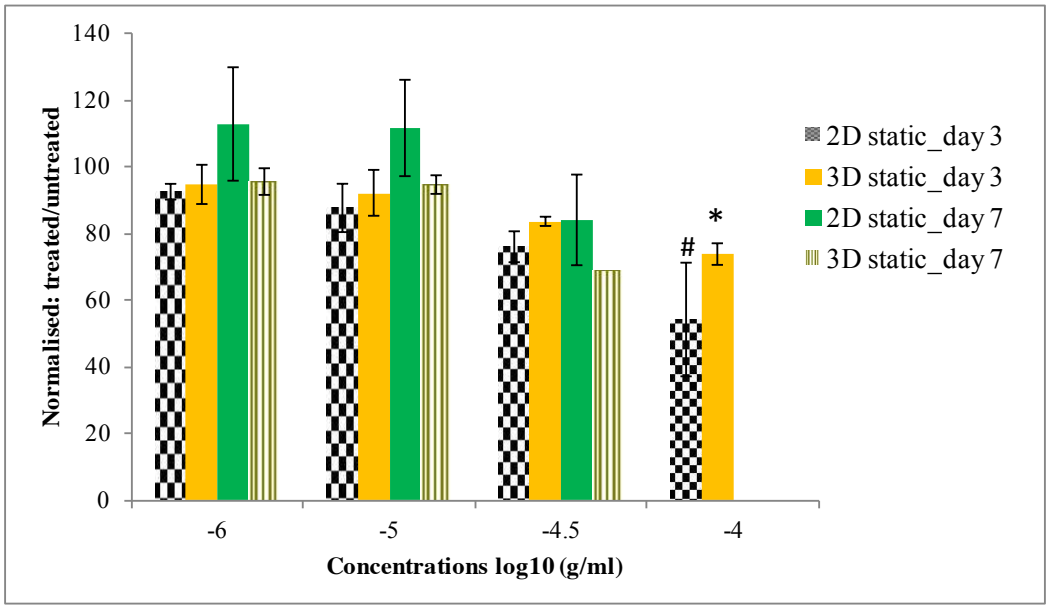

Figure 3.15 Static Comparison: 2D & 3D. Cells in both 2D static culture and 3D static culture were treated with Trimethoprim at 10^{-6}g/ml, 10^{-5}g/ml, $10^{-4.5}$g/ml and 10^{-4}g/ml for 3 days and 7 days. Data is shown as treated dose/untreated control. Bars represent the mean values with standard deviation from three separate experiments with triplicates per subject plotted as error bars. #P<0.05 statistically significant compared to the values of 10^{-6}g/ml and 10^{-5}g/ml for 2D static culture at day 3, *P<0.05 comparing 10^{-6}g/ml and 10^{-5}g/ml for 3D static culture at day 3. There is no significant difference between the values of different time points under the same culture methods at the same treatment. And there is no significant difference between the values of the same dose under different culture methods at the same time points.

Figure 3.15 presents the results of the comparison of the static 2D and 3D on alamarBlue® assay. In general, clear dose responses were observed for both culture methods at day 3 and day 7. At day 3, the cell proliferation ratio of 2D static culture at 10^{-6}g/ml and 10^{-5}g/ml was similar to that of 3D static culture. When drug concentration was increased to half log dose, $10^{-4.5}$g/ml, the viability ratio was dropped to 75.91% for 2D static culture, and 83.53% for 3D static culture. At day 7, there was a clear difference between 2D static culture and 3D static culture at 10^{-6}g/ml, 10^{-5}g/ml and $10^{-4.5}$g/ml. This was thought to be due to the proliferation ratio

increasing faster for 2D culture than for 3D culture within same amount of time.

Comparison of 2D Perfusion and 3D Perfusion

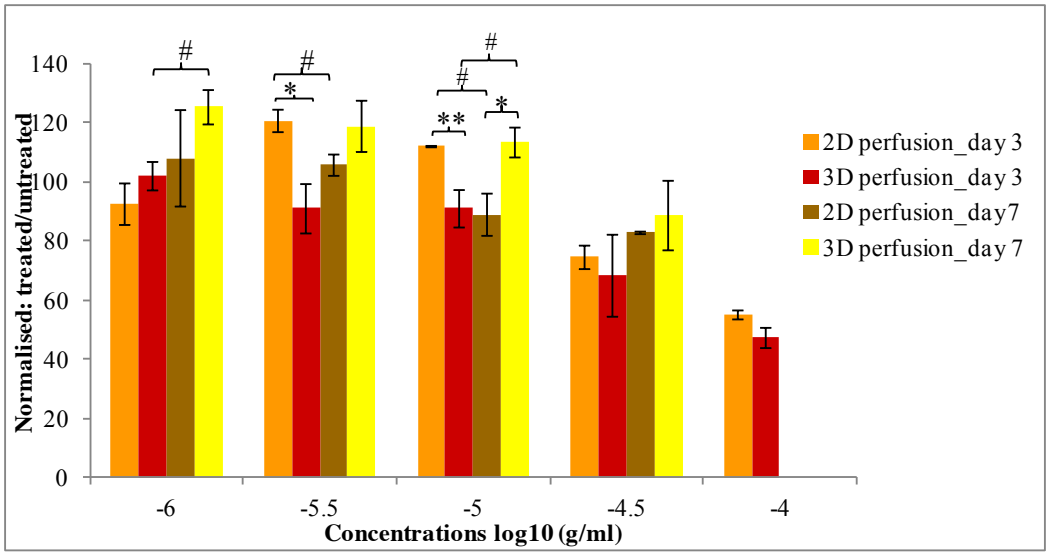

Figure 3.16 Perfusion Comparison: 2D & 3D. 2D & 3D. Cells in both 2D perfused culture and 3D perfused culture were treated with Trimethoprim at 10^{-6}g/ml, $10^{-5.5}$g/ml,10^{-5}g/ml, $10^{-4.5}$g/ml and 10^{-4}g/ml for 3 days and 7 days. Data is shown as treated dose/untreated control. Bars represent the mean values with standard deviation from three separate experiments with triplicates per subject plotted as error bars. #P<0.05 statistically significant compared to the values of each treatment under same culture method day 3 versus day 7. *P<0.05, **P<0.01 statistically significant compared to the values of same dose 2D perfused culture versus 3D perfused culture at each time point.

Figure 3.16, demonstrates the difference in results between perfusion culture in 2D and 3D. Again, both culture methods show the clear dose response, although the response of 2D perfusion culture at 10^{-6}g/ml was lower than for $10^{-5.5}$g/ml and 10^{-5}g/ml on day 3. On day 3, the proliferation ratio in 3D perfused culture was higher than for 2D culture only for 10^{-6}g/ml. However, for day 7, 3D culture showed the opposite results, with proliferation ratios at all doses showing larger values than for 2D culture. When comparing the same culture method at the different time points, 3D

perfused culture shows consistently higher proliferation at the same dose that 2D perfused culture on day 7.

Comparison of 2D Static and 2D Perfusion

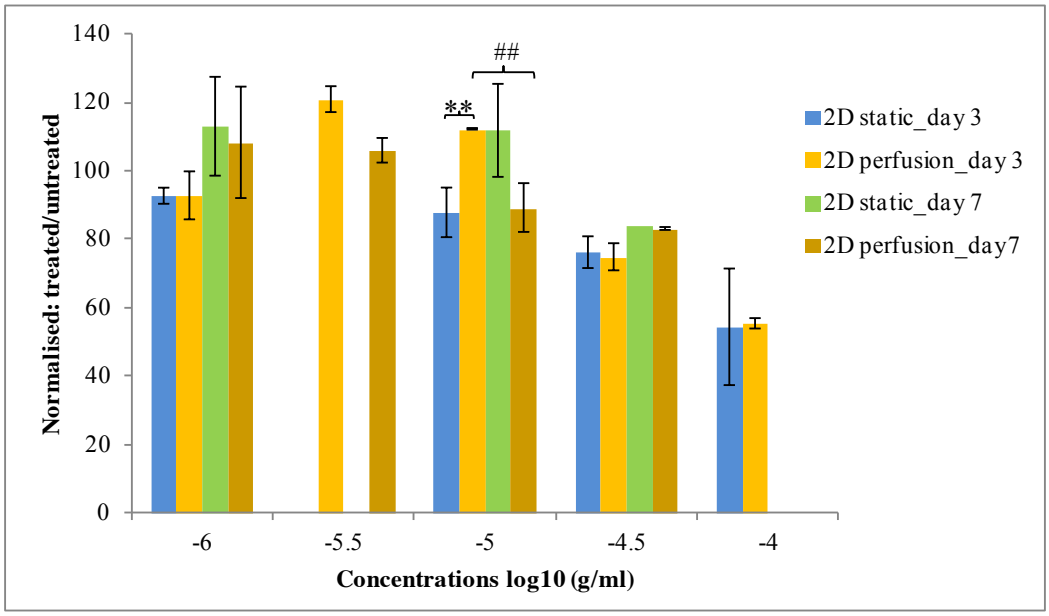

Figure 3.17 Comparison in 2D Static and 2D Perfused System. Cells in both 2D static culture and 2D perfused culture were treated with Trimethoprim at 10^{-6}g/ml, $10^{-5.5}$g/ml,10^{-5}g/ml, $10^{-4.5}$g/ml and 10^{-4}g/ml for 3 days and 7 days. Data is shown as treated dose/untreated control. Bars represent the mean values with standard deviation from three separate experiments with triplicates per subject plotted as error bars. Hash marks (#) show the statistically significant comparison between values at the each treatment under same culture condition day 3 versus day 7. Only ##P<0.01 significantly different between day 3 and day 6 at 10^{-5}g/ml in 2D perfusion. Asterisks(*) donate statistically significant comparisons between 2D static versus 2D perfusion under the same treatment at the each time point. Only **P<0.01 shows the significantly difference between 2D static and 2D perfusion at 10^{-5}g/ml at day 3.

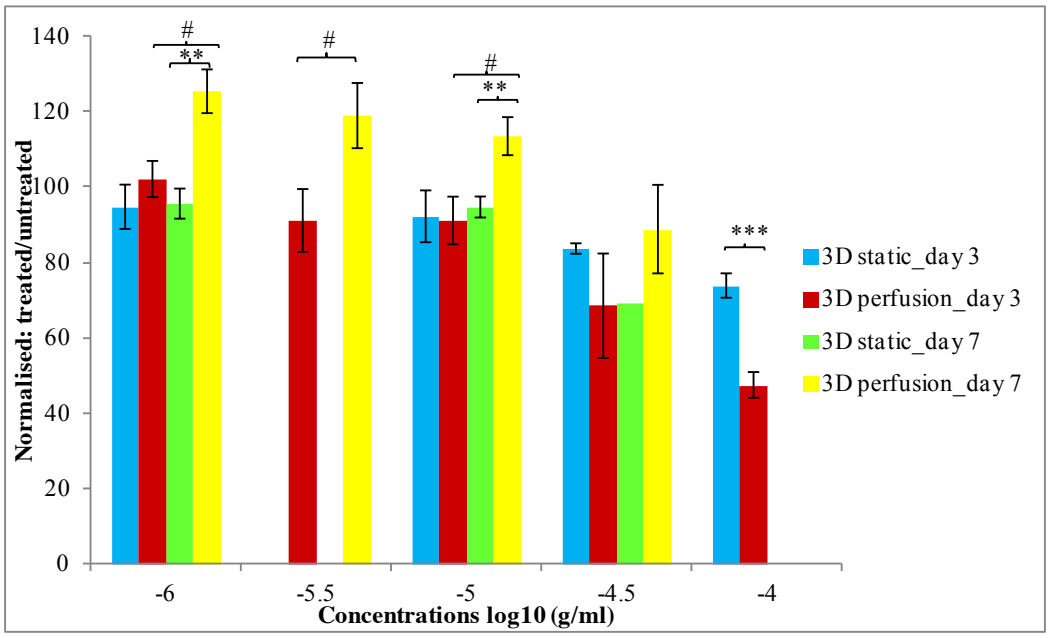

Figure 3.18 Comparison in 3D Static and 3D Perfused System. Cells in both 3D static culture and 3D perfused culture were treated with Trimethoprim at 10^{-6}g/ml, $10^{-5.5}$g/ml,10^{-5}g/ml, $10^{-4.5}$g/ml and 10^{-4}g/ml for 3 days and 7 days. Data is shown as treated dose/untreated control. Bars represent the mean values with standard deviation from three separate experiments with triplicates per subject plotted as error bars. Hash marks (#) show the statistically significant comparison between values at the each treatment under same culture condition day 3 versus day 7 (#P<0.01). Asterisks(*) donate statistically significant comparisons between 3D static versus 3D perfusion under the same treatment at the each time point (**P<0.01, ***P<0.001).

The figures 3.17 and 3.18 above compare trimethoprim response for static and perfused culture. In Figure 3.17, both static culture and perfused culture in 2D show clear dose response. For the doses: 10^{-6}g/ml and $10^{-4.5}$g/ml, both static culture and perfused culture show close proliferation ratios at day 3 and day 7. However, for 10^{-5}g/ml, perfused cultured show higher proliferation at day 3, but lower ratios at day 7. Figure 3.18 illustrates the difference between static and perfused culture in three dimensions. It was found that in 3D on day 7, the cell treated/untreated ratios were greater than for static culture. The dose response in perfused monolayer culture was found to be not as great as in that seen in 3D culture. This may be because perfused

3D systems create an environment with a continuous drug medium flow, which provides cells with stable pH, drug concentrations, and mass transfer. However the reason why cells exposed to trimethoprim in 3D perfused culture show higher proliferation remains unclear.

In conclusion, trimethoprim drug testing was performed in both 2D and 3D, static and perfused culture system. It was found that cells displayed a different sensitivity of response in the different culture system. The dose response curve of the drugs tested indicates that cell response was dose-independent and the lowest dose investigated in the present experiments had a stimulatory response.

3.4 Summary

The objective of this chapter was to investigate an in-vitro, perfused, 3D MSCs culture based system for cytotoxicity testing. The results acheived are summarised below.

(a) Protocols for the culture and isolation of bovine and mouse MSCs were established.

(b) Before the cells could be grown in 3D, an appropriate scaffold had to be selected that would support their growth. Alginate beads and collagen were investigated for this purpose. Cell morphology and cell proliferation at different seeding densities in

the two scaffold types was compared. Collagen was ultimately selected and utilised as the more suitable scaffold for this study.

(c) A novel collagen compressor system was established for increasing the mechanical property of the resulting collagen scaffold. It was shown that cell proliferation was not significantly adversely affected by compressing the collagen scaffold.

(d) Due to the availability of 5% CO_2 incubator, the perfusion system was maintained inside a desktop incubator with a normal gas mix atmosphere, and the selection of culture medium for drug testing using this setup was investigated. Result suggested that αMEM with MCGS and AA would be the most suitable combination for cell growth in this study.

(e) alamarBlue® was selected as the indicator of viable cells. The protocol was optimised for this study, and the most suitable incubation time, cell seeding density, as well as the effects of FBS and phenol red were determined.

(f) Both dose responses of human MSCs and mouse MSCs were performed on trimethoprim and pyrimethamine. Mouse MSCs were found to be more sensitive to higher concentrations of the drugs investigated than human MSCs.

(g) For human MSCs, a dose response investigation was performed with Trimethoprim. Comparison between static and perfusion culture in 2D and 3D was investigated. It was found that the perfusion system was more sensitive than static culture system. The sensitivity were thought to be related to continuous supply of fresh culture medium to keep cells in the stable pH value, temperature, oxygen, and or simply more in-vivo like environment. Also the difference could be the unclear drug interaction with cells. The purpose of this chapter was to build up the 3D perfused system, rather than the drug mechanism study.

Chapter 4 Three Dimensional Rat ADMSCs Perfused Culture for Drug Discovery

4.1 Introduction

Chapter three described the development of a three dimensional perfused model for toxicity testing. This chapter describes experiments using the same perfused bioreactors with rat adipose derived mesenchymal stem cells and two compounds (compounds A and B), supplied confidentially by Pfizer, UK.

Cytotoxicity of oxazolidinones via inhibition of mitochondrial protein expression is induced by isomers with cis (Compound A), but not trans (Compound B), stereo chemistry on the heterocycle. Collagen type I was used as a scaffold material after being successfully used in the experiments described in chapter 3. AlamarBlue® was used as a cell viability index. Since alamarBlue® was used with different cells and media, characterisation was carried out before toxicity testing. The cytotoxicity of the two stereoisomers was assessed in 2D vs. 3D culture formats, with and without media flow.

4.2 Methodology

4.2.1 Rat Adipose-derived Mesenchymal Stem Cells and Cell Expansion

Cryopreserved rat adipose derived mesenchymal stem cells (ADMSCs) were obtained directly from the Tissue Engineering Lab, Oxford University with density of 0.5×10^6 cells/vial. After thawing, 1 vial of ADMSCs was placed in a 75 cm^2 polystyrene tissue culture flask (FALCON Fahrenheit, Milton Keynes, UK) with 20 ml of pre-warmed, fresh, and complete high-glucose Dulbecco's Modified Eagle Medium (DMEM; GIBCO, UK), which contains 10% FBS (M. B. Meldrum Ltd. Bourne End, UK), penicillin (100 U/ml) and streptomycin (100 mg/ml), 3.7 g/L $NaHCO_3$ and 25mM HEPES. The medium was changed every three days until the cells reached confluence. ADMSCs were subsequently passaged or plated for the experiments.

4.2.2 Collagen Scaffolds Preparation

Ten times concentrated PBS was combined with collagen type I from rat tail to make a final collagen solution concentration of 5mg/ml. All solutions were kept at 4 ºC. The pH was checked to ensure that it was between 7.2 - 7.4. If the pH was not correct, 0.4 mM NaOH was added drop by drop until the expected pH was reached. The cell pellet was added with seeding density 0.4×10^6 cells/ml in collagen, and the solution was gently mixed. Cells were mixed with the 5mg/ml collagen solution. The cell pellet was

re-suspended in culture medium to reach the half of the final expected volume, and the other half volume of collagen solution was gently added and mixed well with the cell suspension. The final cell-collagen solution was 2.5mg/ml. 50µl of prepared collagen solution was placed into each well of a 96-well-plate without bubbles. The samples were placed in an incubator at 37℃ for 3 hours to allow the solution to polymerise before adding culture medium.

4.2.3 Bioreactor Fabrication

Bioreactor fabrication protocol was described fully in Section 3.2.5.1. PDMS was prepared by combining 10 parts of tetra(trimethylsiloxy)silane with 1 part of curing agent, tetramethyltetravinylcyclotetra-siloxane by weight, and placing the solution into a 4-well /96-well format bioreactor mold before being left in a 60 °C oven for 4 hours to polymerise.

4.2.4 Cell Culture Methods

For 2D culture, a 13mm diameter round glass cover slip was placed at the bottom of each well of a 24-well plate and 4-well format bioreactor. Both wells of 24-well plate and 4-well bioreactors have the same surface area, 2cm^2. 200µl of gelatin solution was added on top of the cover slips with 30 minutes incubation time at 37 ºC. The gelatin solution was then removed and the glass coverslips were washed with sterilised PBS

twice before cell seeding. ADMSCs were seeded at 0.5×10^4 cells/cm^2 ($2cm^2$) in a 24-well-plate and bioreactor for 2D static culture and in a 4-well bioreactor for 2D perfused culture. For static culture, 1.2 ml of fresh complete high-glucose DMEM was used, which contains 10% FBS (M. B. Meldrum Ltd. Bourne End, UK), penicillin (100 U/ml), streptomycin (100 mg/ml), 3.7 g/L $NaHCO_3$ and 25mM HEPES. The culture medium was changed every three days. For perfused culture, the culture media were supplied by a syringe pump at a rate of 16.7µl/hr. The perfusion value was calculated from the medium changing rate used with the static culture. Both 2D static and perfused cultures were kept in a humidified atmosphere with normal air which contained around 0.033% CO_2 by volume, at 37ºC. Cell proliferation/cytotoxicity was characterized by alamarBlue® assay at day 3 and day 6.

For 3D Culture, ADMSCs initial seeding numbers were kept the same as in the 2D culture system. 50µl of ADMSCs was seeded at 0.2×10^6/ml in collagen gel in both 96-well pate and 8-well bioreactors. After 3 hours of polymerization time, for 3D static culture, cell-collagen gel was transferred from 96-well plate into a 24-well plate for the addition of a larger volume of medium, 1.2 ml of fresh medium. Culture medium was replaced every three days. For perfused culture, culture media were supplied by syringe pump at the rate of 16.7µl/hr. Both 3D static and perfused culture were kept in a humidified atmosphere with normal air which contains around 0.033% CO_2 by volume, at 37ºC. Cell proliferation/cytotoxicity was characterized by alamarBlue® assay at day 3, and day 6.

4.2.5 AlamarBlue® Assay

4.2.5.1 Proliferation

100μl of alamarBlue® solution was added to the medium with a final concentration 5% of the normal culture medium [high-glucose DMEM, 10%FBS, penicillin (100 U/ml) and streptomycin (100 mg/ml), without phenol red]. Cell growth in the presence and absence of the added drugs was compared in the monolayer. As the negative control, alamarBlue® was added to the medium without cells. The medium was placed in an incubator for two hours at 37℃, and then transferred to a 96-well-plate for measurement (see Section 3.2.6.1)

4.2.5.2 Standard curves

A standard curve of % alamarBlue® reduction was calibrated and plotted for the measurement of cell numbers. With a standard curve, it is possible to obtain the cell proliferation and viability for a given alamarBlue® reduction. The alamarBlue® reduction was tested over a range of different cell densities; 4×10^5 cells/ml, 3×10^5 cells/ml, 2×10^5 cells/ml, 1×10^5 cells/ml, and 0.5×10^5 cells/ml.

4.2.5.3 Optimisation of alamarBlue® Assays

According to the alamarBlue® product information sheet from Arcus Biological, the use of phenol red, 10% FBS does not interfere with alamarBlue® Assay. However, Page et

al in 1995 stated that the serum may cause the interference on the assay. From previous experiments, with presence of phenol red, culture medium buffer could also have an impact on the assay due to the pH changing rapidly if the culture medium is exposed to a different environment. Therefore the effect of phenol red, serum, HEPES and $NaHCO_3$ on alamarBlue® assay was investigated.

The complete culture medium usually contains phenol red, 25mM HEPES, 3.7g/L $NaHCO_3$, 10% (v/v) serum in high glucose DMEM. Each component was kept the same concentration in the experiments. Experiments were divided into 2 parallel groups, with phenol red (+ Phenol Red) and without phenol red (- Phenol Red). Each group consists of 3 sub groups; and the names are listed in Table 4.1

1. contains HEPES, with/without serum (+/- serum);
2. contains only $NaHCO_3$, with/without serum (+/- serum)
3. contains both HEPES and $NaHCO_3$ (+/- serum).

symbol	Description		
H1+S	+ Phenol Red	+ HEPES	+ serum
H1-S	+ Phenol Red	+ HEPES	- serum
H2+S	+ Phenol Red	+ $NaHCO_3$	+ serum
H2-S	+ Phenol Red	+ $NaHCO_3$	- serum
H3+S	+ Phenol Red	+ HEPES + $NaHCO_3$	+ serum
H3-S	+ Phenol Red	+ HEPES + $NaHCO_3$	- serum
H4+S	- Phenol Red	+ HEPES	+ serum
H4-S	- Phenol Red	+ HEPES	- serum
H5+S	- Phenol Red	+ $NaHCO_3$	+ serum
H5-S	- Phenol Red	+ $NaHCO_3$	- serum
H6+S	- Phenol Red	+ HEPES + $NaHCO_3$	+ serum
H6-S	- Phenol Red	+ HEPES + $NaHCO_3$	- serum

Table 4.1 Names of Testing Groups for AlamarBlue® Assay

The ADMSCs cell suspension was diluted into 5 different densities; 0.25× 10^5 cells/ml, 0.5× 10^5 cells/ml, 1× 10^5 cells/ml, 2× 10^5 cells/ml and 3× 10^5 cells/ml, and cultured in 96-well plates for 4 hours at 37ºC in a humidified atmosphere with normal air (which contains around 0.033% CO_2 by volume). After cells were attached to the bottom of the well, the old culture medium was replaced by 5% alamarBlue® in 100µl of each medium condition listed in the table 4.1 Plates were covered with aluminium foil and incubated at 37ºC, 0.033% CO_2 for 1and 2 hour time points. Absorbance was measured at 570nm and 600nm.

4.2.6 Drug Candidates*[1]

Two compounds CONA-04806 (Drug A) and CONA-04807 (Drug B), obtained from Pfizer. Ltd confidentially, were used in these experiments. Stock solutions at the concentration of 10mM were prepared with DMSO, and DMSO vehicle is kept constantly at 0.5% for all treatment. Treatment doses were suggested by Pfizer. Three doses were ultimately utilised in the later experiments, which were 5µM, 15.8µM and 50µM.

4.2.7 Statistical Analysis

The data is presented as the mean ± standard deviation from three separate experiments. Data were analysed by one way ANOVA non-parametric analysis for comparisons, and statistical significance was accepted at $P<0.05$.

[1] The compounds were provided by Pfizer ltd (Sandwich, UK), under confidentiality agreement.

4.3 Results and Discussions

4.3.1 Optimisation of AlamarBlue® Assay

The effects on alamarBlue® assay of phenol red, HEPES, $NaHCO_3$ and serum within high glucose DMEM were investigated. 5 different densities of ADCSs were used; 0.25×10^5 cells/ml, 0.5×10^5 cells/ml, 1×10^5 cells/ml, 2×10^5 cells/ml and 3×10^5 cells/ml, with two different incubation time courses, 1 hour and 2 hours. Results are discussed below.

4.3.1.1 $NaHCO_3$ and Phenol Red Addition on AB Assay

$NaHCO_3$ was the only pH buffer in the culture medium presented in the normal air condition. To establish the effect of medium contains $NaHCO_3$ only on the phenol red influence on the alamarBlue® assay, two groups of assay conditions were examined; with phenol red (H2+Serum/-Serum) and without phenol red (H5+Serum/-Serum). Results are displayed in Figure 4.1.

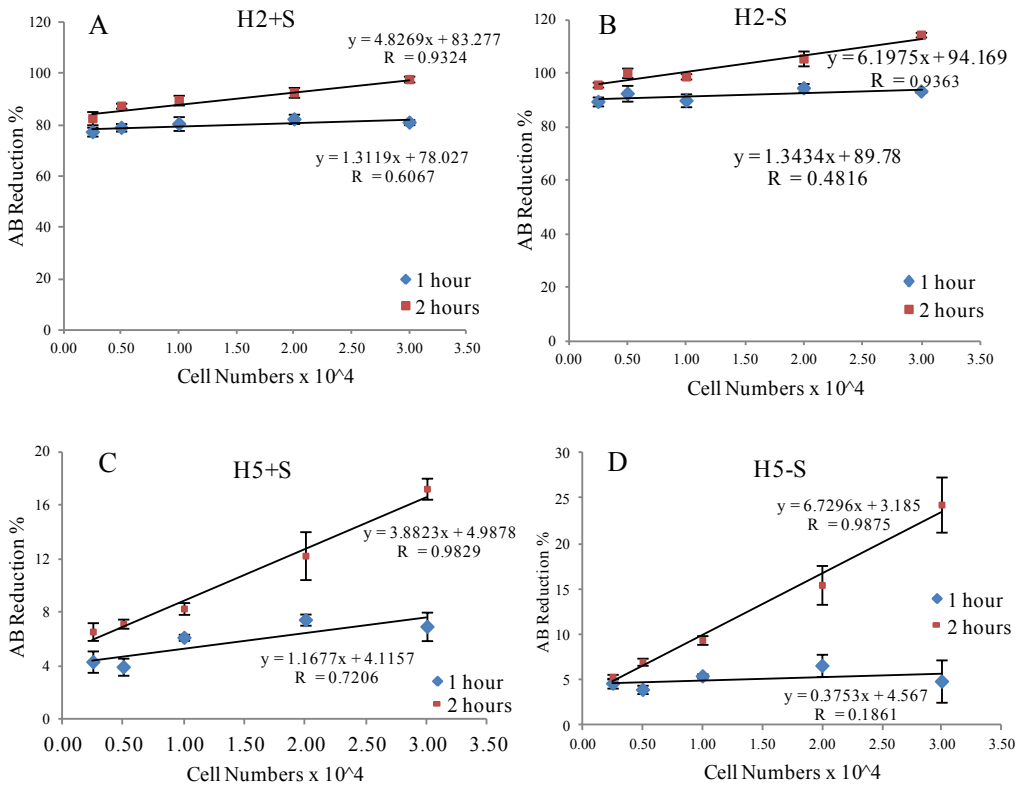

Figure 4.1 Effect of $NaHCO_3$ on AlamarBlue® Assay

Effect of $NaHCO_3$ on alamarBlue® assay. Tests performed under four different conditions: H2+S: +Phenol red, +$NaHCO_3$, +serum; H2-S: +Phenol red, +$NaHCO_3$, -serum; and H5+S: -Phenol red, +$NaHCO_3$, +serum; H5-S: -Phenol red, +$NaHCO_3$, -serum

3.7g/L $NaHCO_3$ was added to the culture medium as suggested by the product sheet. However, this concentration of $NaHCO_3$ is for use when cells are cultured under 5% CO_2, rather than 0.03% CO_2 (normal air). The equation governing the effect of CO_2 on

the solution acidity is; $CO_2+H_2O \rightleftharpoons H^+ + HCO_3^-$. In normal air, the CO_2 concentration is much lower than 5% so, in order to maintain equilibrium within the culture medium, the reaction proceeds backwards, reducing the concentration of H^+ ions and therefore solution acidity. Phenol red, a pH indicator present in the medium, turned pink which gave the AB assay a strong background colour, see figure 4.1 (A and B) H2+S, H2-S. Apart from shifting the whole AB reduction values up, both R^2 of 1 hour and 2 hours' are smaller than 0.95, that is, the linear regression is not significantly different. With the absence of phenol red the results are as shown in Figure 4.1 (C) and (D). Both 1 hour incubation time of +S media and –S media also present R^2 vaules less than 0.95; only 2 hours' linear regression was greater than 0.95. Also, 1 hour incubation had less than 10% of reduction with all tested cell numbers. At the same time, since the pH was changed because of the change in CO_2 concentration, the colorimetric assay could be affected by instable pH. So even though the linear regression of 2 hour line in both +S and –S is greater than 0.98, the results are still not reliable. Therefore, using $NaHCO_3$ as the sole buffer is not suitable for alamarBlue® assay when the CO_2 concentration is that of normal air. Other buffers (HEPES and HEPES conjunction with $NaHCO_3$) are discussed in section 4.3.1.4.

4.3.1.2 Phenol Red Effect

The effect of phenol red in the assay medium with a different pH buffer is considered in this section. H1 represents the medium + phenol red + HEPES; H4 represents the

medium - phenol red + HEPES; while H3 represents + phenol red + HEPES + $NaHCO_3$, and H6 represents - phenol red, + HEPES and $NaHCO_3$.

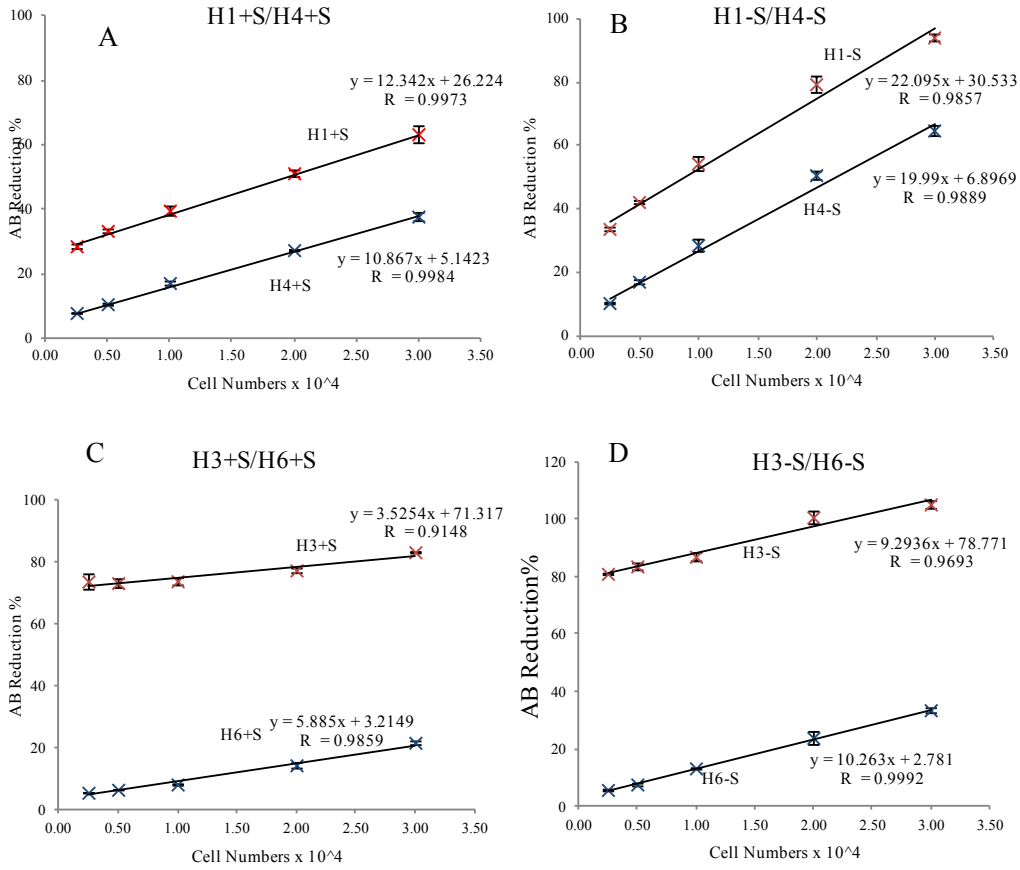

Figure 4.2 Effect of Phenol Red on AlamarBlue® assay

Effect of phenol red on alamarBlue® assay. Tests were performed under four different conditions. (A) and (B) show with/without phenol red (H1/H4) in HEPES buffered medium, both with (+) and without (-) serum. (C) and (D) show with/without phenol red (H3/H6) in HEPES and $NaHCO_3$ together buffered medium, both with (+) and without (-) serum.

It can be seen from the Figure 4.2 that with the presence of phenol red (red cross points of each figure), keeping others conditions unchanged, the AB reduction was much higher than without phenol red (blue cross of each figure) for all cell densities.

Furthermore, the tested range of AB reduction% from the smallest cell densities to highest cell densities with phenol red were significantly smaller than that of the range without phenol red.

With the presence of phenol red, shown in Figure 4.2 (B),for H1-S (red cross points), AB reduction rate at 3 x 10^4 cells/well was more than 100%, similarly, for H3-S (red cross points in figure4.2 (C), AB reduction rate at 2 x 10^4 cells/well and 3 x 10^4 cells/well were both more than 100%. With the absence of phenol red, shown by H4-S (blue cross points in Figure 4.2(B)) and H6-S (blue cross points in Figure 4.2(D)), AB reduction at the highest cell number 3 x 10^4 cells/well was 70% and 40% respectively. This effect is seen because phenol red itself has a strong background colour. It is the pH indicator of the culture medium, it turns yellow if the pH goes below 6.8 and turns pink if the pH goes higher than 8.2. The culture medium pH would not change significantly within 2 hours so any erroneous reading is the result of the strong background colour of the phenol red. Since alamarBlue® itself is a colorimetric assay the presence of a strong background colour, even with the negative control which had no cell contact, will cause an increase in AB reduction rate. Indeed, the reduction rate of the highest cell density was over 100%. 100% alamarBlue® reduction rate indicates that alamarBlue® has been completely reduced during assay. Such a result is therefore inaccurate and so phenol red is not to be used for alamarBlue® assay if a medium without phenol red is available.

4.3.1.3 Serum Effect

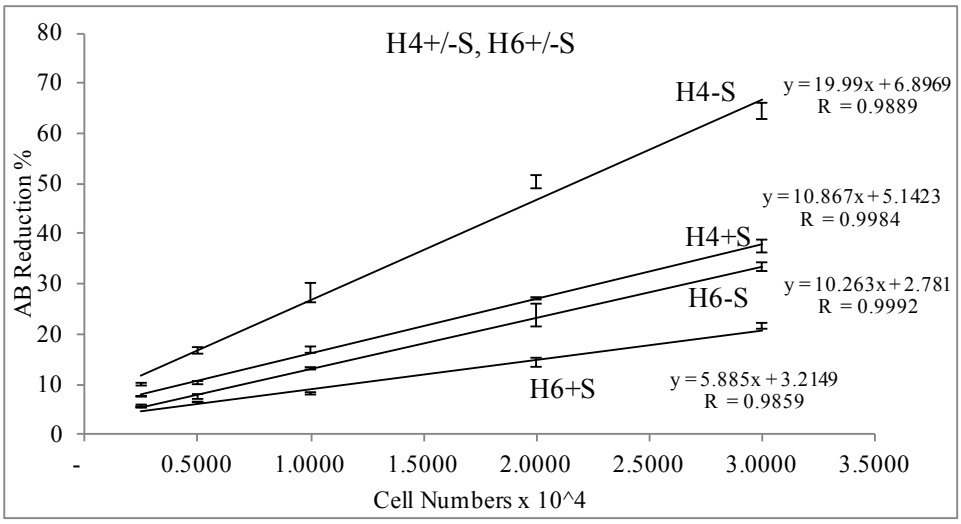

Figure 4.3 Effect of Serum on AlamarBlue® assay

Effect of serum on alamarblue® assay. Tests performed under two different conditions namely H4 (HEPES only), and H6 (HEPES and $NaHCO_3$), both with (+) and without (-)serum.

The effect of serum on alamarBlue® assay is considered in this section. All groups were compared in pairs with/without serum (eg. H4+S and H4-S). Figure 4.3 shows the effect of serum on alamarBlue® assay for H4 and H6. H4 represents the medium -phenol red, +HEPES; and H6 represents -phenol red, +HEPES and $NaHCO_3$. In this figure, the range of AB reduction rate with the absence of serum (H4-S or H6-S) is much bigger than that of the same condition with the presence of serum (H4+S or H6+S). This suggests the cellular metabolic rate in the medium without serum for 2 hours is higher than the medium containing serum. This may because temporarily removing the serum causes the cells metabolic rate to increase for prolonged survival. This effect could also be the result of the serum depressing the reduction of alamarBlue®, or quenching the absorbance (Geogan, 1995). Therefore, serum should be excluded when performing alamarBlue® assay.

4.3.1.4 Buffer Effects

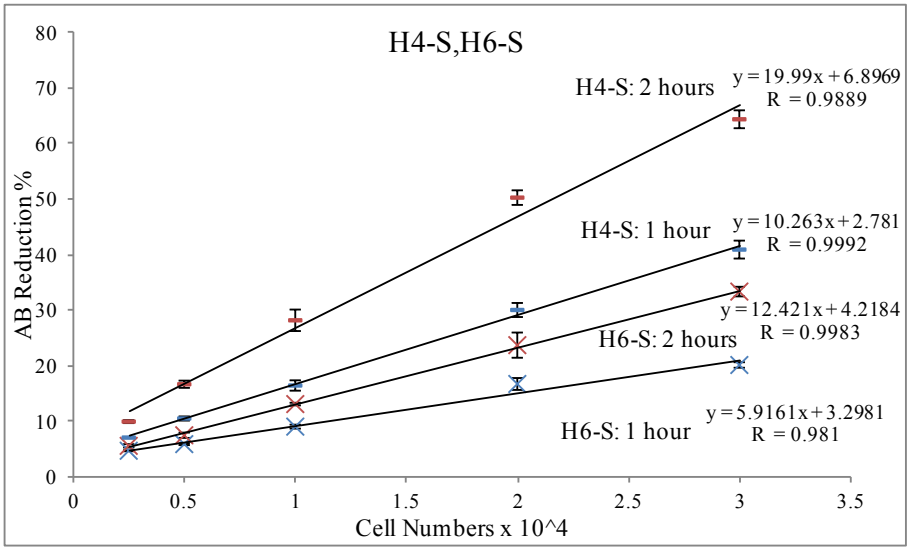

Figure 4.4 Buffer Effect on alamarBlue® assay

Effect of different buffers on alamarBlue® assay. Tests were performed under two different conditions namely H4 (HEPES only), and H6 (HEPES and $NaHCO_3$), both with without (-) serum.

The effects $NaHCO_3$, phenol red and serum were discussed in the previous sections, leaving two other conditions; with HEPES (H4-S) and with both HEPES and $NaHCO_3$ (H6-S) in the culture medium for alamarBlue® assay (shown in figure 4.4) Red bar points represent the 2-hour incubation time for H4-S, blue bar points represent 1-hour incubation time for H4-S. Red cross points represent the 2-hour incubation time for H6-S, blue cross points represent 1-hour incubation time for H6-S. Both H4-S and H6-S at 1 and 2 hours showed good linearity, however, the optimal assay condition is to have the biggest linear range within shortest incubation time. Figure 4.4 suggests that H4-S 2 hours give the optimal metabolic rate with 2 hours incubation time (curve with the steepest gradient) which has the regression equation: Y=19.99 x +6.8969 and R^2=0.9889.

Since most commercial culture media are designed for the presence of 3.7g/L $NaHCO_3$ and to be used under 5% CO_2, having HEPES as an additional pH buffer allows a lower CO_2 level to be used. If the culture medium does not contain $NaHCO_3$, then HEPES can be used as the sole pH buffer for the culture medium. The current study used high glucose DMEM formula without $NaHCO_3$, therefore HEPES can be used as the sole buffer. Furthermore, for the reasons discussed above, for effective use of alamarBlue® assay, both serum and phenol red were not used in the medium.

4.3.1.5 Standard Curves

After optimisation of alamarBlue® assay, calibration of cells numbers and AB reduction rate was determined. Figure4.5 shows two different plots, which are standard curve for monolayer cultures (A) and three dimensional culture (B) in high glucose DMEM (see figure4.5). 100 µl ADMSC suspensions with serial dilution of stock cell density 4×10^4/ml, diluted to 1×10^4/ml, 0.25×10^4/ml and 0.5×10^4/ml solutions were prepared. Then 5% alamarBlue® was added before incubating for 2 hours for monolayer culture, and 3 hours for three dimensional culture.

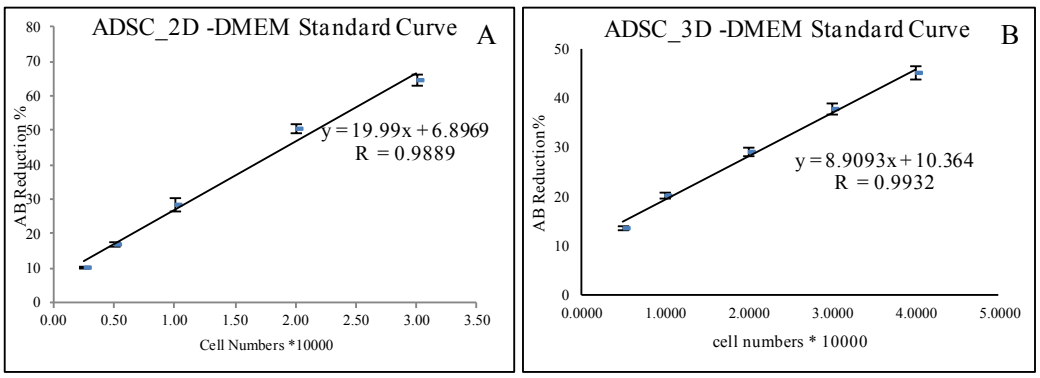

Figure4.5 ADMSCs' Standard Curves

4.3.2 Dose Response to Compounds

Both compound A and B, obtained from Pfizer ltd confidentially, were investigated at three doses concentrations, 5μM, 15.8μM and 50μM. ADMSCs numbers were seeded the same initially for 2D static, 2D perfusion, 3D static and perfusion systems, the different culture methods were described in section 4.2.4. Cells were left overnight to recover before applying the doses of compounds. Cell proliferation/cytotoxicity was characterised by alamarBlue® assay at day 3, and day 6. Results are shown below. Cell proliferation was normalised by treated doses/untreated control. The 2S, 2P, 3S and 3P abbreviations refer to 2D static system, 2D perfused system, 3D static system and 3D perfused system respectively.

4.3.2.1 Dose Response to Compound A

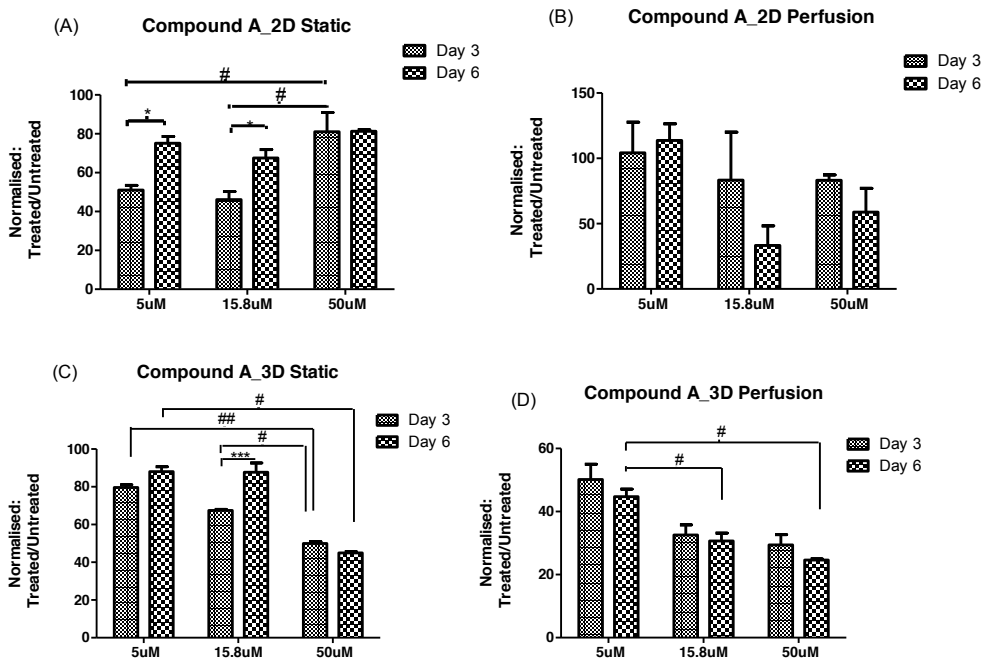

Figure 4.6 Comparison of Each Compund A Dose Treatment for ADMSCs at Day 3 and Day 6 of each Culture Systems

ADMSCs were treated with compound A at 5μM, 15.8μM and 50μM for 6 days (where cells were plated at day -1, and treated at day 0) in 2D Static culture system (A), 2D perfused culture system (B), 3D static culture system (C) and 3D perfused culture system (D). alamarBlue® assay was performed at day 3 and 6. Data is expressed by treated dose/untreated control. Asterisks(*) donate statistically significant comparisons among doses at day 3 and day 6. Hash marks (#) donate the comparison between each time point at the same doses. Statistics were analysed by one-way ANOVA, where *$p<0.05$, **$p<0.01$ and ***$p<0.001$. error bars= SD, n=3

Figure 4.6 A shows the results of compound A tested in 2D static culture system, cell proliferation at day 6 was significantly greater than day 3 at 5μM and 15.8μM concentrations, but not at 50μM. 50μM results in both time points exhibiting higher proliferation, which indicates lower toxicity. Figure 4.6 B shows the results of compound A tested in 2D perfused culture system. There is no significant difference

between different time points at the same dose and, no significant difference among doses at the same time point. The 5μM treatment of compound A has shown better proliferation than 100%, because under low doses of toxin, cells compete to survive, and therefore proliferate faster than that without toxin. ADMSCs under 15μM and 50μM treatments showed lower proliferation than at 5μM treatment at each time point, but did not show dose-dependency at either time point. Figure 4.6 C shows the results of compound A tested in 3D static culture system. Each dose was significantly different at day 3 compared with day 6. For the highest dose (50μM), toxicity were higher at day 6 than day 3, but for lower doses, toxicity at day 6 were less toxic than day 3. At day 3, half log dose treatments showed clear dose response, the higher the dose treatment, the greater toxicity presented to the cells. However at day 6, cell proliferation was similar at 5μM and 15.8μM of compound A, 88.01% and 87.67% respectively. Figure4.6 D shows the results of compound A tested in 3D perfused culture system. Toxicity was clearly observed in this system at both time points. Further analyses based on the same experiments among different systems were shown as follows.

Comparison of 2D Static vs 2D Perfusion System

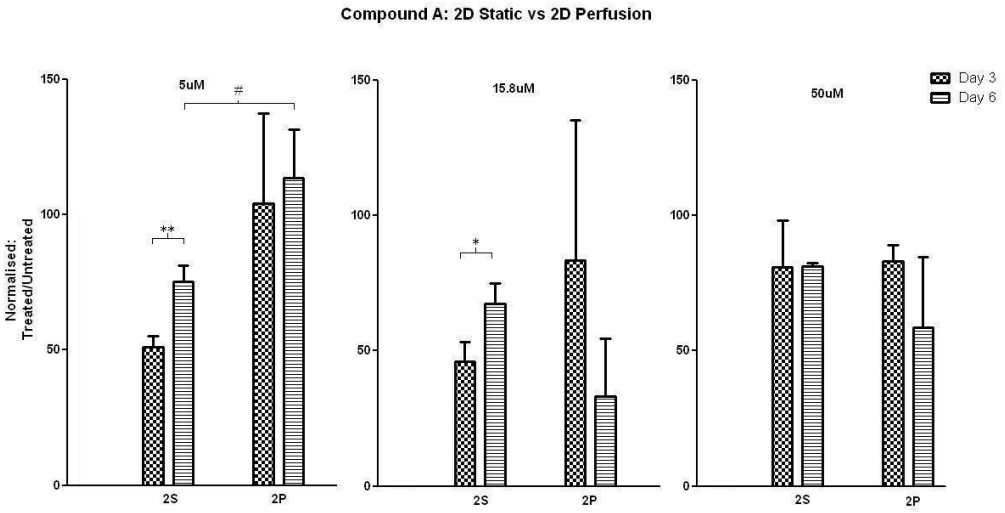

Figure 4.7 Comparison of 2D Static and 2D Perfused Culture Systems for Dose Response to Compound A Data is expressed by treated dose/untreated control. Asterisks(*) donate statistically significant comparisons between day 3 and day 6 at the same doses for the same culture method (*p<0.05, **p<0.01). Hash marks (#) show the significant difference between 2D static versus 2D perfusion under same treatment at each time point. Only #P<0.05 significantly different compared between 2D static and 2D perfusion at day 6 under 5μM treatment. Error bars= SD, n=3

The results of compound A tested in 2D static system and 2D perfused system are presented in figure 4.7. For the 5μM treatment, ADMSC proliferation was greater at day 6 than day 3 in both systems, with the perfused system showing higher values than static system for both time points. For the 15.8μM treatment, the perfused system at day 6 displayed greater toxicity compared with day 3, which was opposite to the static system. With the highest dose treatment, the perfused system shows greater toxicity at day 6 than day 3 and again greater toxicity than 2D static at day 6. Results indicate that the 2D perfused systems with lower dose treatments promote cell proliferation, but not with higher doses, because with continuous flow, cells are supplied with fresh medium which delivers the nutrition and removes the metabolite of cells without interfering cell

proliferation.

Comparison of 2D Static vs 3D Static System

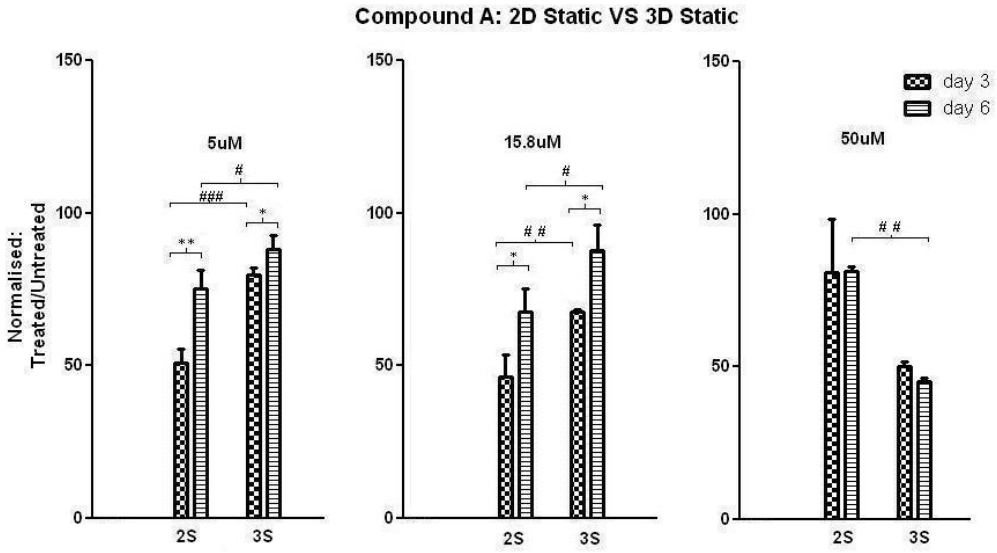

Figure 4.8 Comparison of 2D Static and 3D Static Culture Systems for Dose Response to Compound A. Asterisks(*) donate statistically significant comparisons between day 3 and day 6 for the same culture method at the same doses (*p<0.05, **p<0.01). Hash marks (#) show the significant difference between 2D static versus 3D static under same treatment at each time point (#P<0.05, ##P<0.01 and ###P<0.001). Error bars= SD, n=3

The results of compound A tested in 2D static system and 3D static system are presented in figure 4.8. Under 5μM and 15.8μM treatments, ADMSC proliferation was significantly greater in 3D static system than 2D static system at both day 3 and day 6. While under 50μM treatment, cell proliferation in 3D system was less than in 2D at both day 3 and 6, so the observed toxicity at day 3 and day 6 is higher in the 3D system. Results demonstrate that 3D static culture system promotes cell growth at lower toxin treatment, and improves the toxicity in higher toxin treatment. When cells grow in a three dimensional environment, the cell-cell contact is different from cells grown in

monolayer such that the physiological environment is closer to in vivo conditions. In terms of higher dose testing in these two systems, the 3D system is more sensitive than the 2D system.

Comparison of 3D Static vs 3D Perfusion System

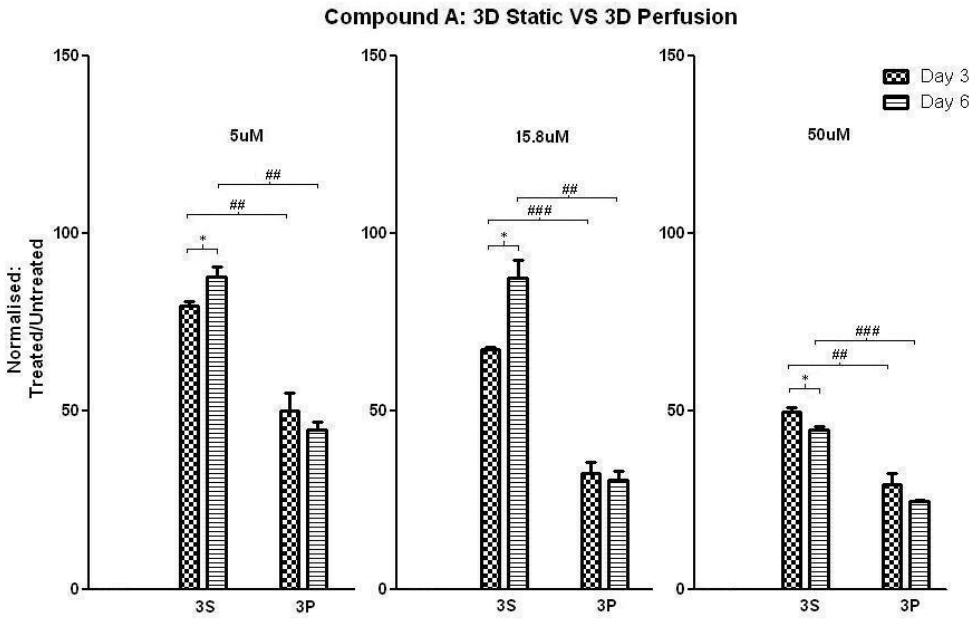

Figure 4.9 Comparison of 3D Static and 3D Perfused Culture Systems for Dose Response to Compound A. Asterisks(*) donate statistically significant comparisons between day 3 and day 6 for the same culture method at the same doses (*$p<0.05$). Hash marks (#) show the significant difference between 3D static versus 3D perfusion under same treatment at each time point (##$P<0.01$ and ###$P<0.001$). Error bars= SD, n=3

A comparison of 3D static and 3D perfused systems tested with compound A is presented in figure 4.9. Cell proliferation in the 3D perfused system was significantly less than that of 3D static system for all treatments at both day 3 and day 6, which indicates that under same dose treatment, the 3D perfused system predicts higher toxicity than the 3D static system. Furthermore, only in the 3D perfused system, has compound A shown dose-dependency from day 3 to day 6.

Comparison of 2D Perfusion vs 3D Perfusion System

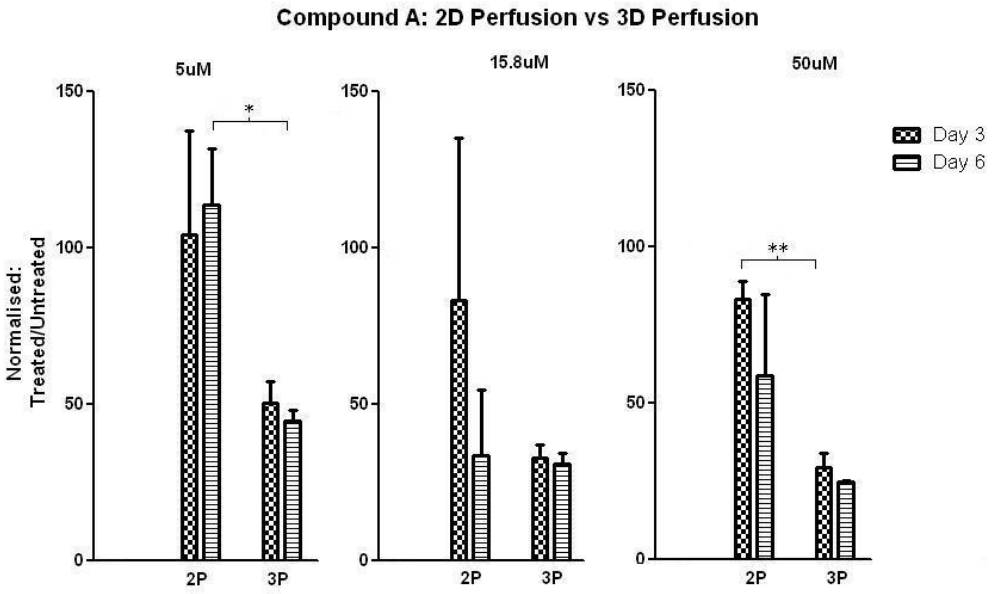

Figure 4.10 Comparison of 2D Perfused and 3D Perfused Culture Systems for Dose Response to Compound A. Asterisks(*) show the significant difference between 3D static versus 3D perfusion under same treatment at each time point (*P<0.05 and **P<0.01). Error bars= SD, n=3

A comparison of 2D perfused and 3D perfused systems is shown in figure 4.10. In general, the 3D perfused system has shown greater toxicity for all treatments at day 3 and 6. The perfused system has already shown better toxicity prediction when compared with static system. For the different perfused systems, the 3D system again shows greater sensitivity to toxins than the 2D system for all treatments. The 2D system was less sensitive to toxicity at the lowest treatment, this may be because cells in 2D were lacking the physiological structure provided by a 3D environment.

Comparison of 2D Static and 3D Perfusion System

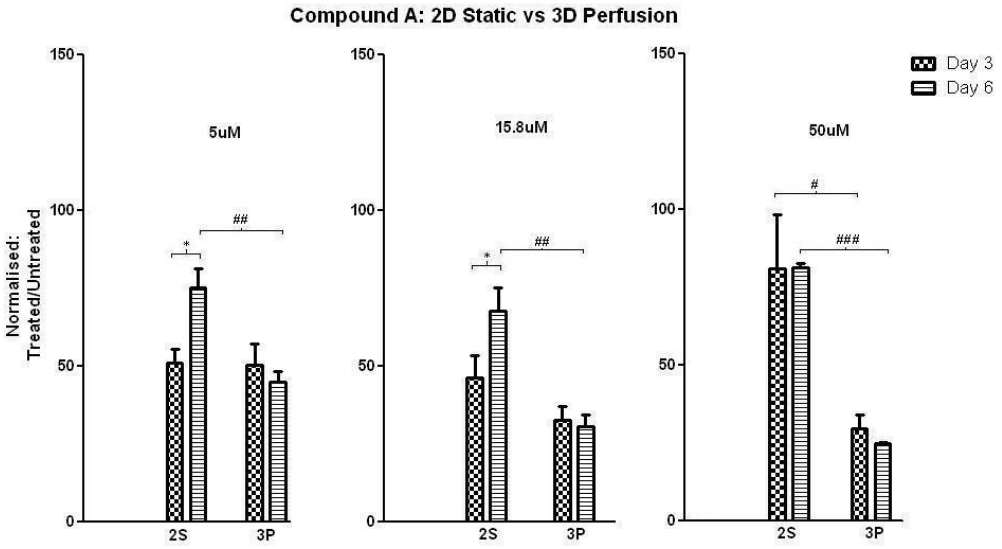

Figure 4.11 Comparison of 2D Perfused and 3D Perfused Culture Systems for Dose Response to Compound A. Asterisks(*) donate statistically significant comparisons between day 3 and day 6 for the same culture method at the same doses (*p<0.05). Hash marks (#) show the significant difference between 2D static versus 3D perfusion under same treatment at each time point (#P<0.05, ##P<0.01 and ###P<0.001). Error bars= SD, n=3

A comparison of 2D static and 3D perfused systems tested with compound A is shown in figure 4.11. Having already compared 2D static vs 2D perfusion, 2D static vs 3D static, 3D static vs 3D perfusion and 2D perfusion vs 3D perfusion, this final comparison is between 2D static and 3D perfusion. Previously, it was observed that the perfused system shows greater sensitivity than the static system. Since the 3D systems have shown to have advantages over the 2D systems, the 3D perfused system would be expected to show greater sensitivity than the 2D static system for toxicity testing. As shown in figure 4.11, cell toxicity was significantly higher in the 3D perfused system than the 2D static system for all treatments at day 6, especially for the highest dose treatment, for which the 3D perfused system showed an especially large difference to the 2D static system.

4.3.2.1 Dose Response to Compound B

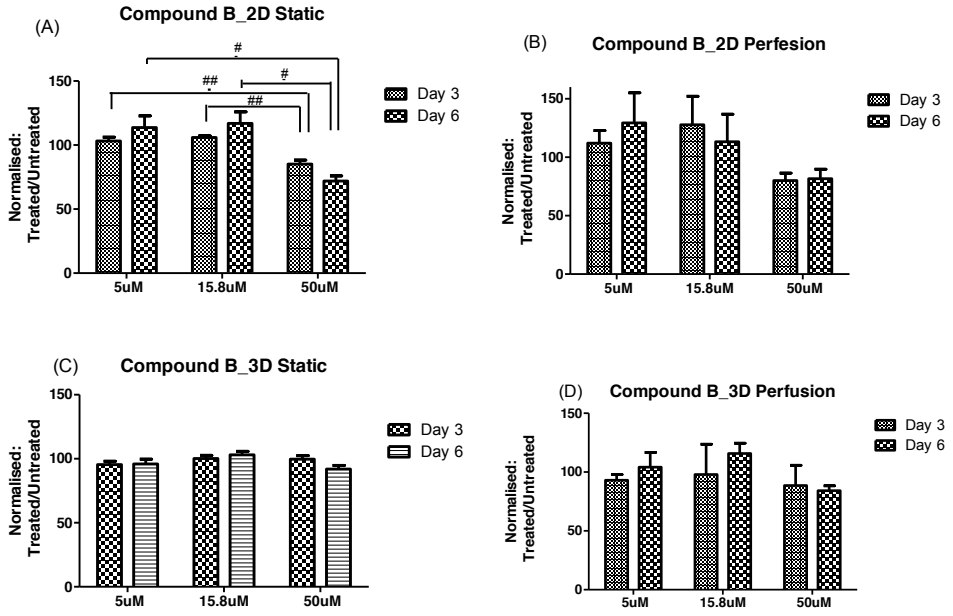

Figure 4.12 Comparison of Each Compound B Dose Treatment for ADMSCs at Day 3 and Day 6 of each Culture Systems

ADMSCs were treated with compound B at 5μM, 15.8μM and 50μM for 6 days (where cells were plated at day -1, and treated at day 0) in 2D Static culture system (A), 2D perfused culture system (B), 3D static culture system (C) and 3D perfused culture system (D). Alarmar Blue assay was performed at day 3 and 6. Asterisks(*) donate statistically significant comparisons among doses at day 3 and day 6. Hash marks (#) donate the comparison between each time point at the same doses. Only in 2D static system, different doses showed the significant differences at the same time point. Statistics were analysed by one-way ANOVA, where #$p<0.05$, ##$p<0.01$ and Error bars= SD, n=3

As presented in Figure 4.12 in the 2D static system (A), cells grew better under lower compound treatments than control (100%), with 3.14% more at day 3 and 13.62% more at day 6 for the 5μM treatment, and 5.93% more at day 3 and 16.95% more at day 5 for the 15.8μM treatment. Under the highest dose, cell viability reduction was observed with 14.81% at day 3 and 28.11% at day 6. Similarly, in 2D perfused systems (B), cells grew better under 5μM and 15.8μM treatments, with 12.11% more at day 3 and 29.33%

more at day 6 under 5μM treatment, 27.77% more at day 3 and 13.32% more at day 6 under 15.8μM treatment. For the highest dose (50μM) cells grew 19.11% less at day 3 and 18.34% less at day 6. For both 3D static system (C) and 3D perfused system (D), cell proliferation shows a similar pattern to the 2D systems; cell viability was higher than control under lower dose treatments, 5μM and 15.8μM and for the highest treatment, a proliferation reduction of 91.96% was observed for the 3D static system and and 84.15% for the 3D perfused system. The data was statistically analysed with the student T-test which showed no significant changes in each system with dose factor and time factor. Further analyses based on the same experiments among different systems treated under the same doses were shown in Figure 4.13.

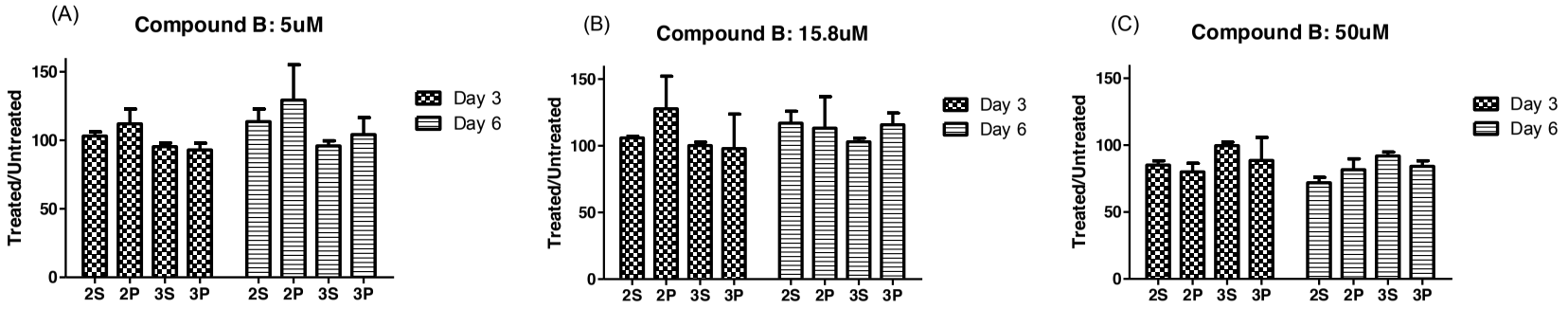

Figure 4.13 Dose Response for Compound B

ADMSCs were treated with compound B of a series of half log concentration at 5μM (A), 15.8μM (B) and 50μM (C) for 6 days (where cells were plated at day -1, and treated from day 0) in 2D Static culture system (2S), 2D perfused culture system (2P), 3D static culture system (3S) and 3D perfused culture system (3P). AlamarBlue® assay was performed at day 3 and 6. Data is expressed by treated dose/untreated control, statistical comparison among different culture system at the same doses and the comparisons between different time point for the same system at the same dose were performed by one-way ANOVA. Error bars= SD, n=3. There is no significant difference between compared groups.

In general, all systems demonstrated toxicity on ADMSCs for compound A testing. For the 2D static system, all treatments were toxic to cells at day 3 without obvious dose response, while at day 6, the effect of the compound on the cells was less toxic in all doses. For the 2D perfused system, 15.8μM and 50μM of compound A shows greater toxicity when compared to the 2D static system at day 3 and day 6. However, 5μM treatment of ADMSCs shows better proliferation. This is possibly because at lower doses of toxin, cells compete to survive, and therefore exhibit greater proliferation than in the absence of toxins. For 3D static and 3D perfused systems, the toxicity was observed much more clearly in both systems than that of the 2D systems, as well as dose-response. Similarly, for 3D static culture, lower doses (5μM and 15.8μM) show less toxicity at day 6 than day 3. The same result was observed for the 2D static system. All treatments in the 3D perfused system demonstrate greater dose-response when compared with the other systems, and cell proliferation at day 6 is lower than at day 3, suggesting toxicity at day 6 is greater than day 3, but this is not statistically significant. Figure 4.13 shows the results for a series of half log concentrations of compound B that were tested in 4 different systems. The testing with compound B did not show the same toxicity as compound A. Apart from at the highest dose (50μM) the cells did not exhibit the effects of the toxin. Compound A and B are both oxazolidinones compounds which are cis-trans stereoisomers. The choice of these two compounds was based on the fact that compound A (cis isomer) has well demonstrated toxicity via inhibition of protein expression within mitochondria while compound B, which is trans isomer of the stereo chemistry on the

heterocycle, does not show the same toxicity.

4.4 Summary

Cytotoxicity of oxazolidiones via inhibition of mitochondrial protein expression is induced by isomers with cis (Compound A), but not trans (Compound B), stereo chemistry on the heterocycle. Alamar blue was used as a viability index. Optimisation was carried out before drug testing. The optimal assay condition for ADMSCs was to use a FBS in high glucose DMEM medium with HEPES and phenol red, and without $NaHCO_3$. Cytotoxicity of the two stereoisomers in 2D vs. 3D culture formats was then investigated with and without media flow. The isomer with cis stereochemistry was significantly more cytotoxic than the trans isomer in both 2D and 3D perfused or 3D static culture compared to 2D static culture. This effect was seen after three days of treatment and continued to six days of treatment. 3D static and perfusion data shows time and dose dependence. The data indicates that perfusion and 3D culturing contribute to a better toxicity prediction. Although a reduction in cell viability was observed in both 2D static 2D perfused culture for Compound B, this is was only at the highest dose 50μM. The results demonstrate that the 3D perfused system improves the prediction of drug toxicity over the 2D culture formats suggesting 3D culture is preferable for preclinical drug toxicity testing.

Chapter 5 Development and Characterisation of *In Vitro* Liver Models

5.1 Introduction

Organ specific toxicity is also one of the main concerns during toxicological testing. The majority of compounds that fail the clinical trials do so due to organ specific toxicity, such as hepatotoxicity. In industry, the standard method to test hepatotoxicity is to use hepatocyte sandwich culture, where hepatocytes are cultured between a layer of collagen and a layer of matrigel. In this chapter, a novel three dimensional perfused micro-patterned bioreactor was developed to facilitate primary hepatocytes culture. Freshly isolated rat hepatocytes self assembled into multicellular structure without scaffolds within micro-patterned bioreactors due to gravity. The functions of these self-assembly cultures were compared with sandwich culture using a variety of analytical techniques. This included analysis of cell viability, expression of biomarkers, biochemical functional testing, immunocytochemistry, gemone wide mRNA analysis. Light microscopy, cellomics and confocal microscopy were also utilised as imaging approaches. Apart of the novel bioreactor without scaffold support for hepatocyte culture, TissueFlex^{TM} bioreactor, previously used in chapter 3 and 4, was also assessed with a variety of scaffolds. Scaffold selections included collagen type I, alginate beads, poly acid fibres, and algimatrix^{TM}.

5.2 Methodology

5.2.1 Primary Hepatocytes Isolation*[1]

Male Wistar-Han rats between the ages of 6-8 weeks and 200-250g were used for hepatocyte isolations, using a modified form of the two step collagenase perfusion method (Seglen, 1976). Cell viability regularly approached 90-95% with an average yield of approximately $4x10^8$ cells/liver. Briefly, the hepatic portal vein of anaesthetised animals was cannulated using a 20 Gauge needle. This was followed by the insertion of a second cannula in to the right atrium using an 18 Gauge needle. The liver was then perfused with 200 ml of HBSS (without Ca^{2+} or Mg^{2+} and phenol red) at 37 ℃ at a rate of 25ml/min. After the blood had been cleared from the liver, the second perfusion was preceded with digestion buffer for approximately 10-30 minutes. The digestion buffer consisted of pre-warmed HBSS (without Ca^{2+} or Mg^{2+} and phenol red) containing 5mM $CaCl_2$, and 120 units/ ml of Collagenase type II (Worthington, UK). (Performed by Pfizer).

The 'perfused' liver was temporarily placed into a petridish containing HBSS with 5 mM $CaCl_2$, and 10,000 units DNase on ice. Hepatocytes were gently released from the liver by agitation and filtered through 100 micro nylon mesh (Falcon, UK). The filtered

[1] Isolation of rat liver was performed by Kathryn Hedley in Pfizer ltd, Sandwich, UK

cells were centrifuged once for 5 minutes at 30 x g, and followed by 3 x wash with the Attachment Media with the same centrifuge rate at 4 ℃. Media composition is described in Section 5.2.2. The dead cells were then removed by discarding the supernatant. After three times of centrifugation, hepatocytes were re-suspended and overlaid onto a layer of 25 ml percoll solution (sigma), which consists 90% (v/v) original percoll, 9.6% (v/v) of 10 x HBSS (without Ca^{2+} and Mg^{2+}) and 0.4% (v/v) of 1M HCl. The tubes were inverted 3 times before centrifugation at 60 x g for 10 minutes at 4 ℃. Dead cells and debris were visible as floating layer on the top of the centrifuge tubes and was subsequently removed. Cells were washed three times with Attachment Media with a centrifugation at 30 x g between each wash. Cells were counted using a haemocytometer. Cell viability and cell number was determined using the Guava Viacount method, described in the appendix, fluoresces labelled live/dead cells count machine.

5.2.2 Culture Media

Attachment medium was mainly used for hepatocyte isolation and inoculation. The basal medium was Williams' medium E without phenol red (Sigma, UK) with supplements of 10% (v/v) of Foetal Bovine Serum (PAA, UK), 2mM Glutamax (Gibco, UK), 100 Units/μg/ml Penicillin Streptomycin (Gibco, UK), 0.17μM Human Insulin (Sigma, UK), 0.03μM Dexamethasone (Sigma, UK), 10μM HEPES (Gibco, UK), and 50μg/ml Gentamycin (Gibco, UK). The serum-free medium was then used for culturing

purposes. Basement medium has exactly the same formula as that used for the attachment medium, but with the absence of FBS. Basement medium + consisted of basement medium with the supplement of 10 ng/ml of Epidermal Growth Factor (EGF) (Sigma, UK) and 10 ng/ml Hepatocytes Growth Factor (HGF) (Sigma, UK), which was used after 24 hours culturing.

5.2.3 Sandwich Culture

Freshly isolated hepatocytes were re-suspended to a final density of 4×10^5 cells/ml with an average viability of 93%. 0.5 ml of cell suspension/Attachment media was immediately inoculated into pre-coated 24-well collagen type I plates (BD Falcon, UK) at 4 ℃. After 2 hours, the attachment media was replaced with pre-warmed basement media, and then incubated overnight at 37 ℃ with 5% CO_2.

Matrigel was left on ice at 4℃ to thaw overnight. The next morning, pre-thawed matrigel was diluted into basement medium to reach the final concentration of 500 μg/ml on ice. The overnight medium was replaced from the 24-well plates with fresh ice-cold matrigel solution/ basement media + for 24 hours at 37℃ incubator. The culture media was changed every day with basement media +.

5.2.4 Hepatocyte Self-assembly Culture

Hepatocytes can aggregate together and from self-assembled structures without scaffolding materials. The micro-patterned bioreactor is a platform which was initially designed by Zyoxel, ltd. It is the modified version of the TissueFlex^{TM} bioreactor. The difference of modified version is in the bottom design of each well. The bottom of the MP bioreactor is composed of around 500 inverted pyramid-like mini wells, with the dimension of 250 μm for length, width and the depth (see figure 5.1). The advantage of this MP bioreactor is to create an environment for cells to naturally self-assemble together within each mini-wells due to gravity.

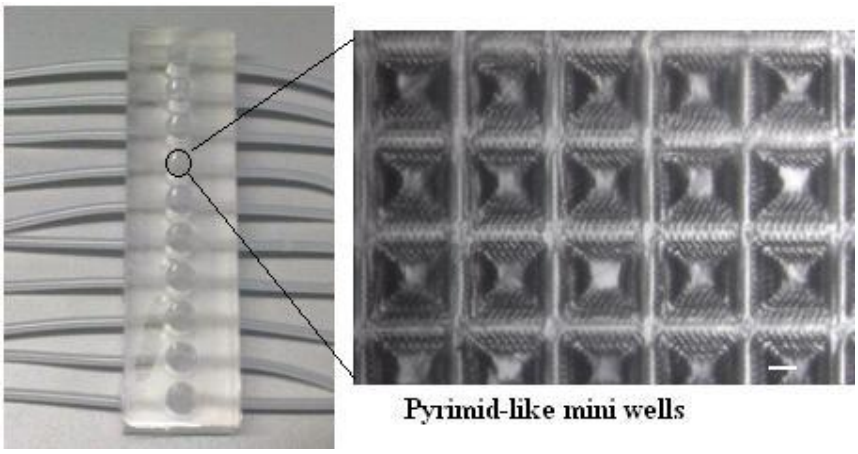

Figure 5.1 Micro-patterned Bioreactor [obtained from Zyoxel Ltd, UK]

5.2.4.1 Optimisation of Surface Condition

MP bioreactors are made of Polydimethylsiloxane (PDMS), which is highly hydrophobic. Therefore, when wetting the surface of bioreactors before inoculation, or

directly inoculating the cell suspension into each well, bubbles can become trapped into each mini-well. If these bubbles are agitated using a pipette tip, the structure of the inverted pyramids can be easily damaged. Therefore, it was necessary to preserve the surface integrity of each mini well. A method was developed to minimise this issue. By autoclaving MP bioreactors with distilled water at 121 ℃, and then exchanging the distilled water with culture media after cooling down this problem could be avoided. The images of MP before and after autoclaving were monitored under light microscope.

5.2.4.2 Optimisation of Seeding Densities

The optimal seeding density of primary hepatocytes was determined. A number of different densities were selected, 2 $\times 10^6$ cells/ ml, 1 $\times 10^6$ cells/ml, 0.4 $\times 10^6$ cells/ml, 0.25 $\times 10^6$ cells/ml and 0.01 $\times 10^6$ cells/ml/. 100µl of each cell suspension at each density were seeded separately into individual MP bioreactor wells, and then MP bioreactors were transferred to a plate shaker at 300 rpm for 30 minutes at 37 ℃. Cells distribution was monitored before placing the MP bioreactors into an incubator. MP bioreactors were applied with perfused basement media + from the second morning, and the culture duration was 7 days, with 20µl/hour.

5.2.5 Scaffold-Based 3D Hepatocytes Culture

As previously used in Chapter 3 and Chapter 4, TissueFlex^{TM} again was employed to support scaffolding in the current chapter. A varity of scaffolding materials were taken into consideration, since the cells were different from those analysed in chapters 3 and 4.

5.2.5.1 Collagen Type I

Pure collagen solution was prepared according the manufacturer's instructions (BD Falcon). Briefly, a high concentration of rat tail collagen type-I, 10 x PBS, sterile dH_2O and sterile 1M NaOH were kept at 4 ℃. Each component was prepared as follows. Determine A) the volume of high concentration collagen that was needed to make 6mg/ml collagen solution. B) the volume of 10 x PBS was determined by 10% of final collagen solution (v/v). C) the volume of 1M NaOH was 0.023 times the volume of high concentration of collagen. D) the volume of dH_2O was determined by subtracting all the other contents from the total volume. After preparation, B, C and D were mixed gently, and then added to A gently without bubbles. The pH was confirmed to be between 7.2-7.4.

A solution was prepared that consisted of 50% freshly isolated hepatocytes (starting concentration of 8 $\times 10^6$ cells/ml) and 50% collagen solution (6mg/ml). The final concentration of hepatocytes was therefore 4 $\times 10^6$/ml in a final collagen concentration

of 3mg/ml. 50µl of this cell/collagen solution was inoculated into single wells of bioreactors. The final cell number per well was 2×10^5. After 3 hours polymerisation at 37 ℃, basement media was placed on top of the collagen scaffold. The second morning, basement media + was applied to bioreactor at a perfusion rate of 20 µl/hr for 7 days.

At the end of culture, cells were stained with live/dead assay: Syto 10 and Dead Red were observed under confocal microscopy (10 x), together with bright field, and the images merged.

5.2.5.2 Collagen/Matrigel

Collagen solution preparation is described in Section 5.2.5.1, and matrigel (BD Falcon) was directly diluted into collagen solution to reach a final collagen concentration of 6mg/ml and a final matrigel concentration of 5mg/ml.

A solution was prepared that consisted of 50% freshly isolated hepatocytes (starting concentration of 8×10^6 cells/ml) and 50% matrigel/collagen mix solution (6mg/ml)

The final concentration of each component was reduced to half, and total cell number per well was 2×10^5. The culture conditions and analytical microscopy were identical to those used in Section 5.2.5.1.

5.2.5.3 Collagen/Matrigel/Poly Lactic Acid (PLA) Fibre

Poly Lactic Acid (PLA) fibres were purchased from Ingeo^{TM} (MN, USA). The fibres were minced into very fine fragments and sterilised in 70% ethanol for 2 hours before drying in a sterilised safety cabinet with air circulation overnight (Cui, 2007). PLA fibres were then placed into sterilised bioreactors before cell/collagen/matrigel solution (described in Sections 5.2.5.1 and 5.2.5.2) was added.

50µl of cell/collagen/matrigel solution was inoculated into pre-placed PLA fibres of each well by pipetting up and down gently for mixing purpose. The total cell number per reactor was 2×10^5. The culture conditions and analytical microscopy were identical to those used in Section 5.2.5.1.

5.2.5.4 PLA Fibres

The preparation of PLA fibres is described in Section 5.2.5.3. 50µl of 2×10^6/ml cells was inoculated into each well of bioreactor with pre-placed PLA fibres underneath. The culture conditions and analytical microscopy were identical to those used in Section 5.2.5.1, and morphology was examined by light microscope.

5.2.5.5 Alginate Beads

High guluronic acid (High G) content sodium alginate powder was obtained from Pronova, Norway. Following sterilisation, solutions were prepared of 0.9% (w/v) NaCl and 102mM $CaCl_2$ and stored at room temperature. A 1.2% Alginate solution was prepared by slowly adding 120 mgs of alginate into pre-warmed 0.9% NaCl solution, and stirred using a magnetic stirrer. The beaker was covered with parafilm and the solution inside was stirred at 37℃ for 1 to 2 hours. The resultant alginate solution was sterilized by 0.22 μm syringe filter and then stored at room temperature until use. Citrate buffer was also prepared to dissolve the alginate beads, which consisted of 55 mM Sodium Citrate, 50 mM EDTA and 0.15M NaCl, adjusted to pH 7.4 by HCl.

3×10^6 /ml of freshly isolated hepatocytes were encapsulated in 1.2% alginate solution, and 75 beads/ml were generated in 102mM $CaCl_2$ solution using a 26 Gauge needle (13.3μl /bead). Beads were formed within 10 minutes and subsequently washed by 0.9% NaCl solution twice, with first wash not exceeding 15 minutes and second wash not exceeding 5 minutes. The culture conditions were identical to those used in Section 5.2.4.1. Alginate beads were dissolved using citrate buffer with a volume ratio of 1:3 at the end of culture. Cell viability was determined by Guava Viacount assay and morphology was examined by confocal microscope with live/dead assay.

5.2.5.6 Algimatrix™

Alginatrix™ sponge is commercial product from Invitrogen, UK. It is made of lyophilised alginate gel, with pore size between 50 and 200μm, and 5 mm thickness within 96-well plates. The standard protocol of using Algimatrix™ sponge was supplied by Invitrogen. Briefly, hepatocyte suspension was combined with 10% (v/v) of firming buffer, which was mainly $CaCl_2$ solution, to reach a density of 1×10^6 cells/ml. 100μl of cell suspension was then inoculated in the centre of the sponges. The creation of gas bubbles was avoided. If bubbles were found to be present they were released using a pipette tip gently to push the sponge against the wall. The seeded plate was centrifuged at 100 × g for 4 minutes, and then allowed to rehydrate for 5 minutes before topping up the culture media up to 200μl. The plate was then incubated at 37 ℃ with 5% CO_2. The next morning, the basement media + was applied to bioreactor at a perfusion rate of 20 μl/hr for 12 days. Cells were stained with Calcein-AM, To-pro 3 and Hoechst at the end of the culture period. Calcein-AM stains the nucleic acid of alive cell, To-pro 3 stains nucleic acid of dead cells and Hoechst stains nuclei of alive cells. Cell viability and morphology were determined by using confocal microscopy.

5.2.6 Functional Assays

5.2.6.1 Adenosine Triphosphate Measurement

Adenosine triphosphate (ATP) provides the energy for all living organisms. It is primarily synthesised within mitochondria of eukaryotic cells. The quantitation of the ATP content of cells can be used to determine viability. CellTiter-Glo® Luminescent Cell Viability Assay was utilised in this experiment (Promega, UK). It is luciferase reaction, with the participants of luciferin, product itself, oxygen and ATP, which was released from lysed membrane. With the Mg^{2+} catalysed, oxyluciferin was produced, together with AMP, Pi, CO_2, and the energy/light (See Reaction Equation 2.2). The luminescence light was measured by using a luminometer. The content of ATP is proportional to the number of living cells (Promega manufacture sheet). The protocol is described briefly as follows. 20µl of pre-mixed CellTiter-Glo® buffer and CellTiter-Glo® Substrate was added into the wells contained cells and 100µl supernatant. Plates were left on a plate shaker at 450 rmp for 2 minutes at room temperature. After shaking, the plate was left in the dark for 10 minutes before reading using a luminometer. The ATP assay was performed every day for 6 days.

5.2.6.2 Quantitative Evaluation of Hepatocytes Related Biomarkers

All biomarker kits were ready to use solution and purchased from ADVIA, Ireland. Supernatant samples of both sandwich culture and self-assembly culture were collected

every 24 hours post initial seeding, and stored at -20 ℃ before measurement. Absorbance was measured by ADVIA Chemistry systems at 340nm.

(a) Alanine Aminotransferase Measurement

Alanine Aminotransferase (ALT) is predominantly located within heptocytes, therefore, measuring the quantity of ALT released into the bloodstream, serum or plasma can be used to accurately diagnose hepatic diseases. The protocol was followed according to the manufacturers instructions. Briefly, Reagent 1 and reagent 2 of the ALT kit were combined before the addition of serum samples. The mixed solution contains L-Alanine, lactate dehydrogenase (LDH), sodium azide, α-Ketoglutarate, NADH. 0.5ml of each samples were added into the mixed solution. ALT leaks from the damaged cell membranes into plasma, with the presence of L-Alanine and α-Ketoglutarate, pyruvate and L-glutamate were then formed during catabolism. LDH catalysed the second reaction; pyruvate was reduced to lactate, NADH was oxidised to NAD. The resulting rate, which is NADH oxidation rate, is proportional to the ALT activity rate directly (See Reaction Equation 2.3). The absorbance was measured at 340 nm using a spectrophotometer.

(b) Aspartate Aminotransferase Measurement

Aspartate Aminotransferase (AST) is unlike ALT, not a specific-liver enzyme. It can be found in many different tissues, including the liver, heart, skeleton muscles, and red blood cells. However, AST measurement is more sensitive then ALT measurement, due

to the large amount of AST in liver (Talwar and Srivastava, 2004). The assay is also able to measure cellular integrity. Similar to the quantitation of ALT, the measurement of AST requires the pre-mixing of 2 reagents included within the kit. These reagents contain L-Aspartic acid, malate dehydrogenase (MDH), LDH, solium azide, α-Ketoglutarate, and NADH. AST catalysed the amino acid transferred from L-Aspartic acid to α-Ketoglutarate, resulting in the formation of oxalacetate and L-glutamate. Meanwhile, NADH and oxalacetate were catalysed by MDH and yield NAD and Malate (See Reaction Equation 2.4). The resulting rate is proportional to AST activity under absorbance of 340 nm.

(c) Lactate Dehydrogenase Measurement

Lactate Dehydrogenase (LDH) Measurement is also based on quantitative determination of amount of enzyme released from the loss of cellular membrane integrity. 0.5 ml of each sample was added into the mixture of reagent 1 and 2, which contains NADH, pyruvate and sodium azide. LDH catalyses the reduction of pyruvate to l-lactate, resulting the oxidation of NADH to NAD. The oxidation rate, which is from NADH to NAD, was measured by evaluating the decrease in absorbance ay 340nm, and it is directly proportional to LDH activity (See Reaction Equation 2.1).

(d) Glutamate Dehydrogenase Measurement

Glutamate Dehydrogenase (GLDH) is a liver-specific enzyme predominantly found in mitochondria of liver cells. Increasing GLDH values can therefore indicate the direct

damage of hepatocytes. Unlike AST and ALT, GLDH deaminate from amino acid as a free ammonia, rather than the transfer of an amino group from one to another. The reaction is also highly reversible depending on the concentration of each of the substrates. Briefly, Reagent 1 was mixed with samples which contained NADH and ammonium acetate in Triethanolamine buffer. α-Ketoglutarate / Triethanolamine buffer as reagent 2 was added to initiate the reaction. GLDH catalyses the conversion of α-Ketoglutarate, NH_4^+ to glutamate, and the oxidation of NADH to NAD. The decrease in NADH is proportional to the GLDH activity directly (See Reaction Equation 2.5).

(e) Microalbumin Secretion

Albumin is a protein produced specifically in the liver, and circulates in the veins and arteries to maintain the oncotic pressure. If the albumin secretion level drops, the oncotic pressure decreases, the fluid in the bloodstream leaks into to the surrounding tissues to cause swelling, and can induce liver cirrhosis. It also can be detected in renal disease when albumin leaks into urine. A Microalbumin assay kit was used to measure albumin. The kit contains a ready to use solution and was purchased from ADVIA chemistry (USA). The assay is capable of measuring very small quantities of albumin from the sample using the ADVIA chemistry system, which is the trademark of Siemens Medical Solution Diagnostics. The Microalbumin evaluation method is based on a PEG enhanced immunoturbidimetric assay. The protocol was performed according to the manufacturer's instructions; reagent 1, containing polyethylene glycol was mixed with each sample to initiate the first reaction at 37 ^oC for 5 minutes, before the subsequent

addition of reagent 2, containing a goat anti-human albumin antibody. The reaction was incubated for 5 minutes. The turbidity in the final reaction was then measured at 340 nm using a spectrophotometer. Samples from culture medium supernatant were collected from both sandwich culture and self-assembly culture every day post to 24 hours seeding.

5.2.7 Functional Imaging

Primary hepatocytes were cultured in collagen type-I coated plates, with matrigel for 6 days. Culture conditions were described in Section 5.2.4. Cells were stained with 6 μM Calcein-AM, 1μM To-Pro3, 1μg/ml Hoechst at day 3 and day 6. Hepatocyte morphology was monitored using Cellomics microscopy at 20 x magnification, in conjunction with bright field analysis.

5.2.8 Immunocytochemistry

All primary antibodies were purchased from Abcam, UK. All secondary antibodies were purchased from Invitrogen, UK. At the end of both sandwich culture and self-assembly culture, immunostaining was evaluated. Cells grown in both 24-well plates and self-assembly grown in MP bioreactors were washed twice with PBS and then fixed using 4% paraformaldehyde in PBS at room temperature for 30 minutes. 0.1% (v/v)

Triton X-100 in PBS was used for permeabilisation for 10 minutes, followed by washing with PBS once before blocking. 2% (w/v) Bovine Serum Albumin (BSA) and 0.05% (v/v) Triton X-100 in PBS was utilised for blocking for 1 hour at room temperature. Primary antibodies were diluted into 2% (w/v) BSA + 0.05% (v/v) Triton X-100 / PBS and incubated with cells at 4 ℃ overnight. Cells were rinsed in 2% (w/v) BSA + 0.05% (v/v) Triton X-100 / PBS twice, each time 5 minutes at RT. Secondary antibodies were incubated on cells for 2 hours at RT, then rinsed with 2% (w/v) BSA + 0.05% (v/v) Triton X-100 / PBS twice before adding Hoechst at 1:10,000.

Primary antibodies used were Mouse monoclonal Cytokeratin 18 (CK-18), 1:500; Mouse monoclonal Zonula Occludens Protein 1 IgG1 (Zo-1), 1:500; Mouse monoclonal Hepatocyte Nuclear Factor 4 (HNF4), 1:500; Mouse monoclonal Multi-drug resistance protein 2 IgG_{2a} (Mrp2), 1:500; Albumin, 1:500; Sheep polyclonal to Human Serum Albumin, 1:500. Secondary antibodies used were Alexa Fluor® 647 F(ab')2 fragment of goat anti-mouse IgG (H+L) for CK18, HNF4 and Mrp2 ; Alexa Fluor® 488 goat anti-mouse IgG1 (γ1) for Zo-1; and Alexa Fluor® 488 donkey anti-sheep IgG (H+L) for Albumin.

The morphology of cells in sandwich culture was examined using a Cellomics microscope and the morphology of self-assembly was examined using confocal microscopy.

5.2.9 Gene Expression Profiling

5.2.9.1 RNA Isolation

RNA was isolated from both hepatocytes in sandwich cultures and self-assembly cultures. Cells were lysed at 3 and 6, as well as fresh isolated hepatocytes and liver slices. Each sample was collected with three different animals from three separate experiments, with total number of 18. After washing twice with ice cold PBS, cells were lysed. The total RNA from all samples was extracted using an RNeasy Mini Kit from Qiagen, UK. Breifly, cells were washed in ice cold PBS twice, followed by lysing with mixed solution of ß-mercaptoethanol and the RLT buffer (1:100,v/v). Homogenised cells were applied to a silica-gel based membrane in a spin column, which binds to RNA molecules exceeding 200 nucleotides in length in the presence of ethanol. Column were then washed three times to remove contaminants and then eluted in 30µl RNase-free water. The concentration of RNA was quantified by NanoDrop spectrophotometer (NanoDrop Technologies, USA). Extracted RNA samples were stored at -80 ℃ for up to 6 months prior to further analysis.

5.2.9.2 Microarray*[2]

Extracted RNA samples were used to produce biotin labelled cRNA targets. These targets were then hybridised to Affymetrix GeneChip Rat Genome 230 2.0 Arrays,

[2] Microarray was performed by AROS ltd, Denmark

which consists of more than 31,000 gene probes. The GeneChips were washed and stained with an Affymetrix Fluidics station and scanned by Affymetrix GeneChip Scanner 3000, according to manufacturers instructions. The work was supported by Pfizer ltd, Sandwich, UK. All data was analysed in R using the online open source: BioConductor packges; 'affy' for data import & manipulation, 'arrayQualityMetrics' for quality assessment, 'limma' for differential expression analysis, 'GOstats' for functional enrichment analysis, and 'rat2302.db' for probe annotations. The R script is attached in the Appendix.

5.2.9.3 Differential Expression and Functional enrichment*[3]

All arrays that passed quality control were taken forward into the analysis. The raw data were normalised with RMA. In order to mitigate the multiple testing issue, results from probes demonstrating no variance in RNA abundance across all samples tested were discarded, as were probes without any additional annotations (e.g. an Entrez ID). This resulted in 9754 probe sets for subsequent analysis. Differentially expressed genes were identified using the moderated t-test from Limma and were considered significant if the FDR corrected (Benjamini Hochberg) p-value is <0.05.

It is of interest to know the biological functions of those genes demonstrating differential expression between the sandwich and self-assembly culture models. The online Gene Ontology software was used (GO, http://www.geneontology.org/) to

[3] The Programme code for differential expression and functional enrichment were written by Ben Sidder, Pfizer, Cambridge, UK

classify genes according to their involvement in biological processes. This technique employs a hyper-geometric test that compares the number of genes from a GO category that are found in target gene lists with the number in the category as a whole, taking into account the total number of genes (the "universe") to test for those categories which are over represented within our self-assembly vs sandwich gene list. All of the genes that passed filtering were used as universe for variance and annotation criteria.

5.2.10 Statistical Analysis

The data is presented as the mean ± standard deviation from three separate experiments. Data were analysed by one way ANOVA non-parametric analysis for comparisons, and statistical significance was accepted at $P<0.05$.

5.3 Results and Discussions

5.3.1 Sandwich Culture

Freshly isolated hepatocytes were placed into sandwich culture (see Section 5.2.3) for 6 days. Cell viability was analysed at day 3 and at the end of 6 days by live/dead assay (see Figure5.2 and 5.3): The for both days 3 and 6, images show no dead cells, and a far greated proportion of live cells (B). It was found that hepatocytes showed good viability in sandwich culture at the end of day 6 (see Figure 5.3).

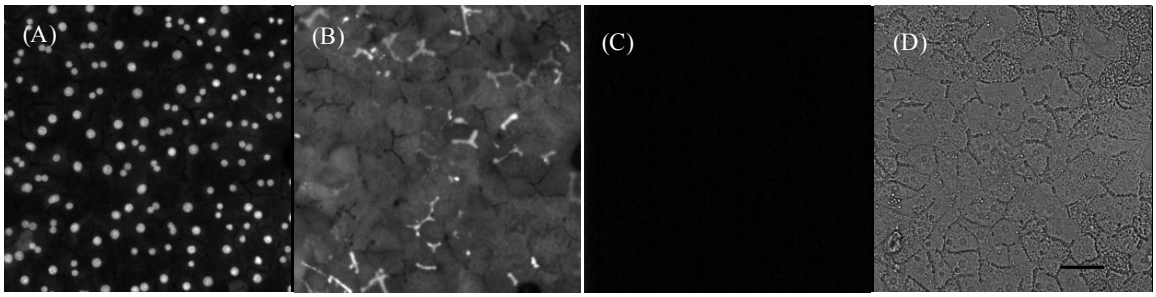

Figure 5.2 Hepatocytes Sandwich Culture at Day 3.

Figure 5.2 display the hepatocytes sandwich culture at day 3. Hepatocytes were stained with (A): Hoechst, which stained the nuclei eyes of alive cells; (B): Calcein-AM, which stains the living cells; (C): To-Pro3 stains the dead cells. It cannot be seen from the figure which indicates that no dead cells were found in the culture (D): Bright Field. Scale bar = 50μm

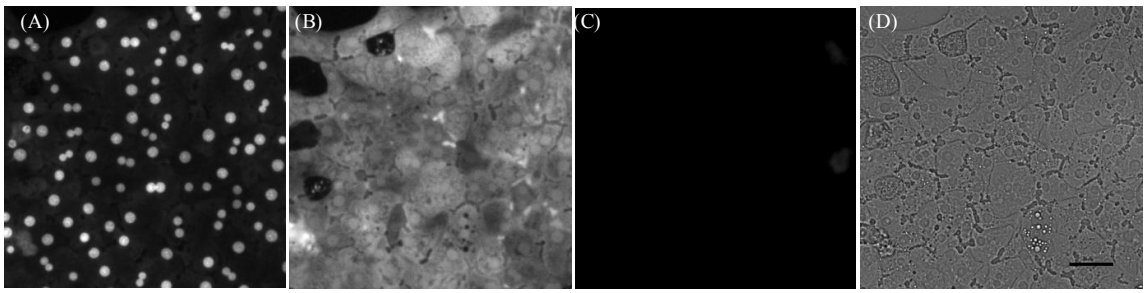

Figure 5.3 Hepatocytes Sandwich Culture at Day 6

Figure 5.3 display the hepatocytes sandwich culture at day 6. Hepatocytes were stained with (A): Hoechst, which stained the nuclei eyes of alive cells; (B): Calcein-AM, which stains the living cells; (C): To-Pro3 stains the dead cells. It cannot be seen from the figure which indicates that no dead cells were found in the culture (D): Bright Field. Scale bar = 50μm

5.3.2 Hepatocytes Self-assembly Culture

In the inverted-pyramid mini-well MP bioreactors, hepatocytes were self-assembled together without the requirement to add extra scaffold materials. A similar principle has also been used by other researchers previously. Torisawa designed a 4 x4 array which consisted of trapezoidally pyramid-like microholes (Figure 5.4 (A)). These square holes had 800μm long sides at the top, narrowing to 200μm sides at the base, and a depth of

400µm (Torisawa, 2007). The human cancer cell line, MCF-7, and hepatoma cell, HepG2, were used in this study and cultured under perfused conditions. As mentioned in the literature, size control is important for hepatocyte spheroid culture. If a spheroids is greater than 250µm in diameter, diffusion constraints may lead to a hypoxic core and necrosis of the central hepatocytes (Atala and Lanza 2002; Lu, 2005). Moreover, only a single spheroid can form in each microhole, resulting in the total capacity of the 4 x 4 array of 16 spheroids. This is considerably low in regard to high-throughput drug testing. Nakamura used a micro-space cell culture system for human primary hepatocytes in culture (Nakamura, 2011). Spheroids were formed onto 200µm x 200µm x 50µm micro-space plate (Figure5.4 (B)). However, the cells appear to be attached to the bottom of the plate, and no support data was shown to demonstrate that the assembled hepatocytes maintained a spheroid structure.

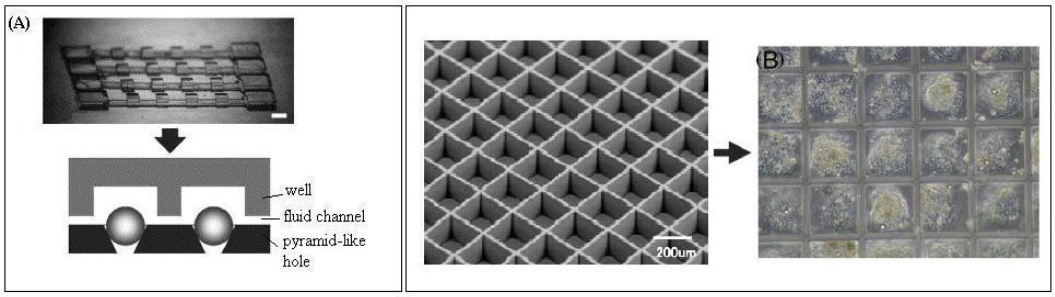

Figure 5.4 Self-assembly spheroids Concepts ((Nakamura, 2011))

The design of MP bioreactor differs from these two similar designs, because each single well of the bioreactor is capable of forming up to 500 self-assemblies, which is suitable for high throughput drug screening. The inverted pyramid-like mini-wells trap cells towards the centre of the cavity, which avoids hepatocytes self-assembled elsewhere in the chamber.

5.3.2.1 Optimisation of MP Bioreactor Surface

MP bioreactors are made of PDMS. Hydrophobicity is the main property of PDMS. Using a chemical solvent to change it into hydropholicity, may have negative affects in long term cell culture. However if the wetting MF bioreactor surfaces after sterilisation, bubbles may trapped into the inverted-pyramids, and cells could not be innoculated evenly into each mini-well. In Figure 5.5 (A), the red circle shows the trapped bubbles in a MF bioreactor mini-well while the yellow circle shows the mini-well without bubble. Scale bar is 100µm.

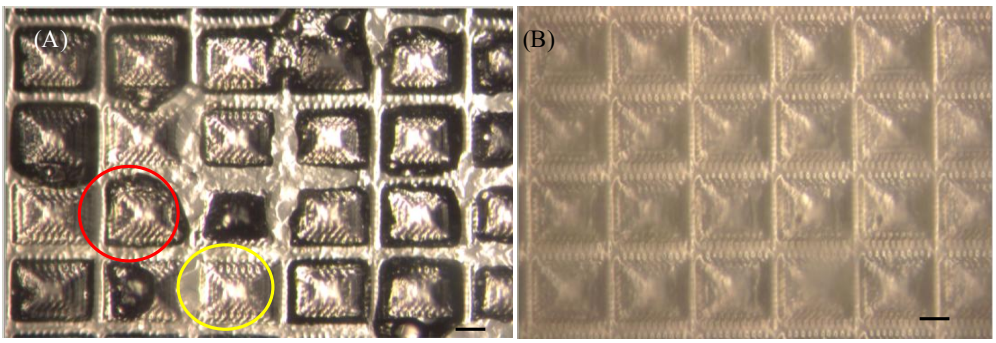

Figure 5.5 Trapped Bubbles in Mini-wells of MP Bioreactor. (A) shows the bubbles trapped into the inverted-pyrimids while wetting the surefaces of sterilised MF bioreactor. The red circle showed the bubble trapped inside of mini-well while the yellow circle showed no bubbles trapped. (B) shows the no bubbles trapped after autoclaving the MF bioreactors with addied water in the wells. Scale bar= 100µm

Sterilising the MP bioreactor with pre-loaded water would discard the bubbles in the mini-wells. Because increasing the temparature of PDMS would result in decreasing the surface tension temporarily. Result of this procedure is shown in Figure 5.5 (B) with 100µm scale bar. After autoclaving the MF bioreactors, mini-wells were sterilised without trapped bubbles. After cooling down to room temperature, cell culture media were changed several times before inoculation.

5.3.2.2 Optimisation of Hepatocyte Seeding Density

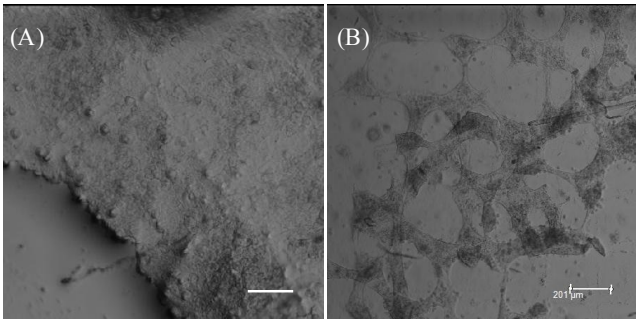

Figure 5.6 Different Seeding Densities of Hepatocytes in MP Bioreactors

Brightfield images of different seeding densities of hepatocytes seeded in MP bioreactors and cultured for 6 days. (A) Cell morphology of 100µl 2 $\times 10^6$/ml hepatocytes, with 100µm scale bar (B) Cell morphology of 100µl 1 $\times 10^6$/ml hepatocytes

When seeded at a higher density of 2x10^6cells/ml, hepatocytes were seen to join together and merge into a sheet of cells that covered the whole surface of bioreactor well (see Figure 5.6 (A)). When seeded at half this seeding density (1x10^6cells/ml), hepatocytes were also found to join together and covered parts of bioreactor well (see Figure 5.6 (B)).

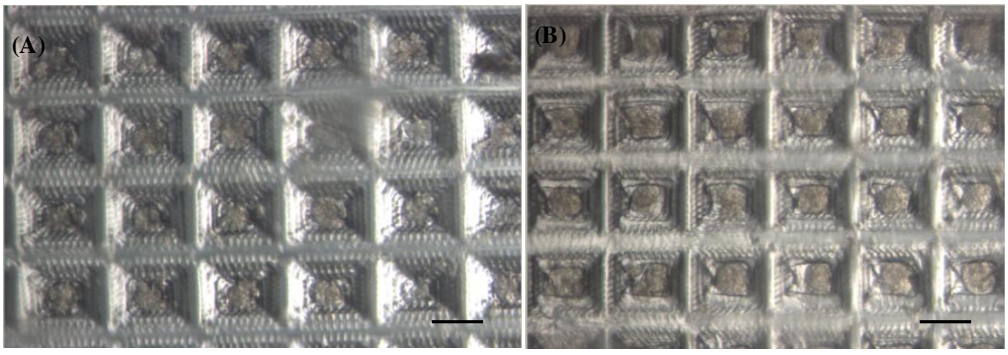

Figure 5.7 Hepatocytes Self-assembly Formation at 12 and 36 Hours

When seeded at the lower density of 100µl at 0.4x10^6cells/ml, hepatocytes formed self-assembly in each MP bioreactor mini-well. (A) shows the self-assembly morphology after 12 hours, (B) shows the self-assembly morphology after 36 hours. Scale bars for both (A) and (B) are 200µm.

Unlike higher seeding densities of $2x10^6$cells/ml and $1x10^6$cells/ml, hepatocytes seeded at $0.4x10^6$cells/ml formed self-assembly, rather than a sheet of cells across the top of the mini-wells (see Figure 5.6). During dynamic seeding, hepatocytes were initially trapped in the inverted pyramid-like mini-wells, and unable to contact cells in other wells. At 12 hours after seeding, hepatocytes aggregated together to form self-assembly (see Figure. 5.7 (A)). At 36 hours, self-assembly showed a distinctive spherical boundary with an average diameter between 100µm to 150µm (see Figure 5.7(B)).

5.3.2.3 Viability of Hepatocytes Self-assembly Culture

The viability of the self-assembly in micro-bioreactors was examined on days 3 and 6 using a confocal microscope. In comparison, the viability of hepatocytes placed into sandwich culture was examined by Cellomics assay and is described in Section 5.2.3. The self-assembly was found to have good viability, and no dead cells were found at day 3 (see Figure 5.8), where as only a few dead cells were seen on day 6 (see Figure 5.9).

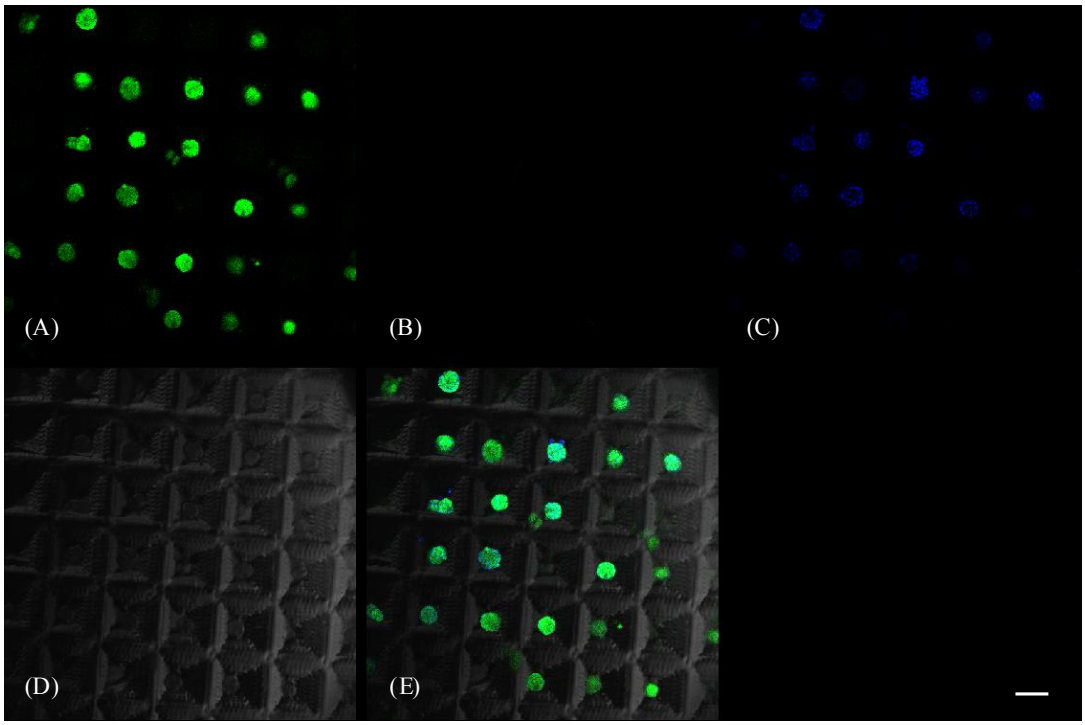

Figure 5.8 Hepatocyte Self-assembly Culture in MP Bioreactor at day 3

The green florescence dye is Calcein-AM. The blue dye is Hoechst 33324. (A) shows live cells (green); (B) shows a lack of To-Pro3 staining (red), indicating no dead cells were seen; (C) shows Hoechst which stains all nuclei; (D) shows the brightfield image and (E) is a composite image of all 4 channels. Scale bar is 200μm.

100μl 0.4 $\times 10^6$/ml hepatocytes were inoculated into each micro-bioreactor well and perfused for 3 days. At the end of day 3, cells were stained with live/dead dye, and imaged using a confocal microscope (see Figure5.8).

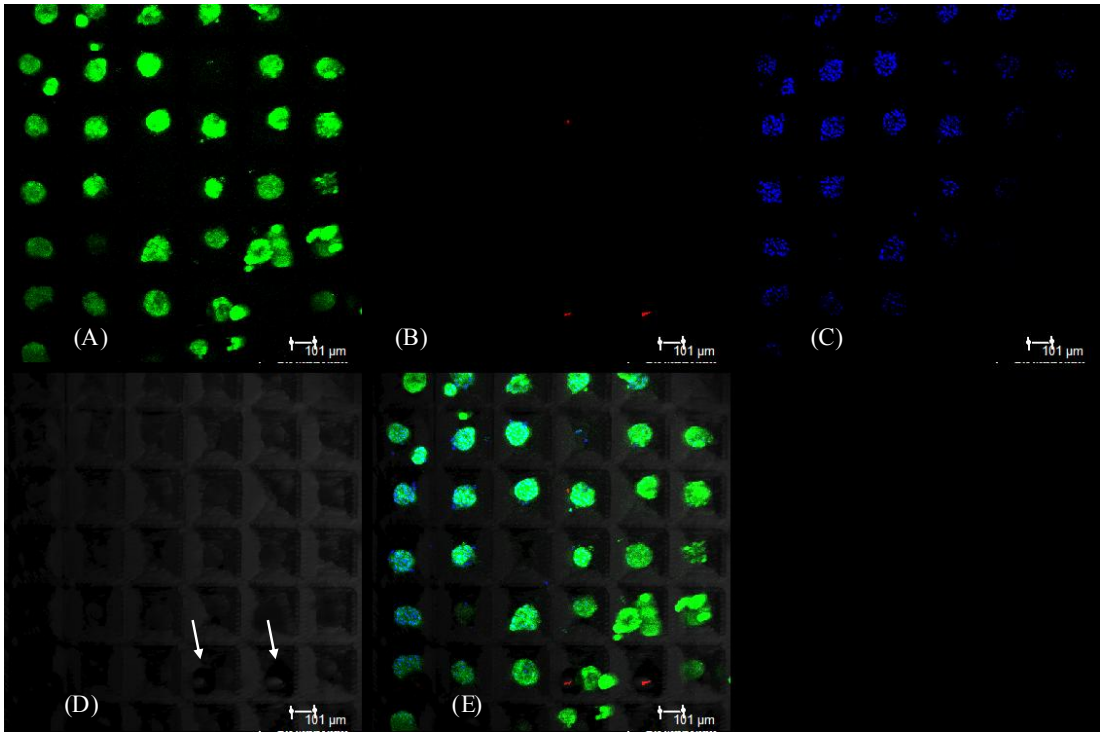

Figure 5.9 Hepatocyte Self-assembly Culture in MP Bioreactor at day 6

The green florescence dye is Calcein-AM. The blue dye is Hoechst 33324. (A) shows live cells (green); (B) shows a lack of To-Pro3 staining (red), indicating no dead cells were seen; (C) shows Hoechst which stains all nuclei; (D) shows the brightfield image and (E) is a composite image of all 4 channels. Scale bar is 101 µm.

At the end of the culture period, self-assembly were stained with the same live/dead assay used on day 3 and imaged (see Figure5.9), and good cell viability was found. Although a small amount of red can be seen in figure5.9 (B), it is thought that the red dots were not dead cells, but instead were the refection of the bubbles trapped in the wells when the dye was added (see Figure5.9 (D) white arrow).

5.3.3 Scaffold-Based 3D models

Different types of scaffolds for hepatocyte culture were investigatied in this section.

5.3.3.1 Collagen Type I

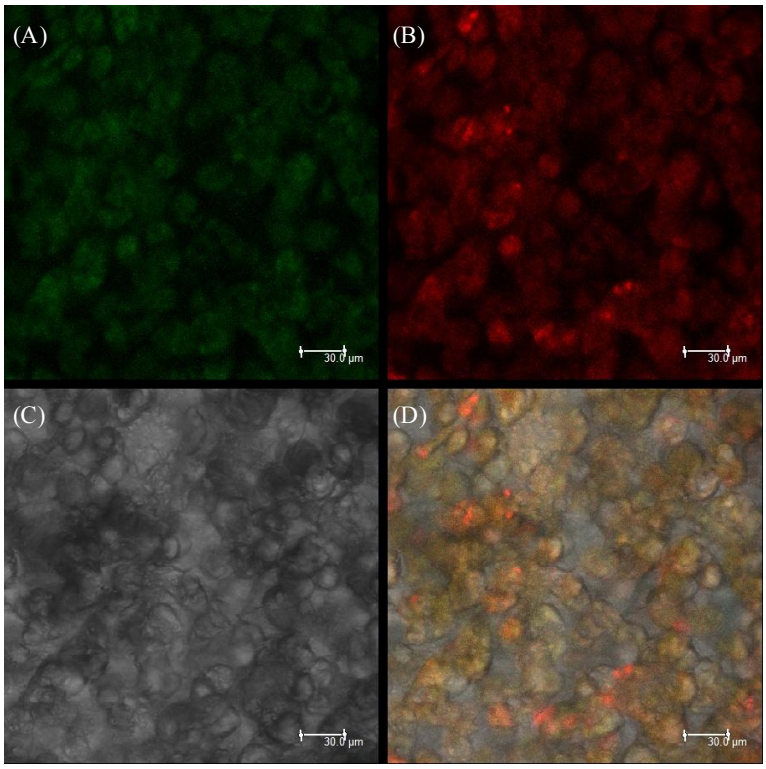

Figure 5.10 7-day Culture of Primary Hpatocytes in Collagen Type I

Syto 10 (A), Dead Red (B), bright field (C) and merged figure (D), (10 x magnification)

Hepatocytes were inoculated into 50µl of 3mg/ml collagen solution, at a density of $2x10^5$ cells/ml, and cultured for 7 days in a perfued TissueFlex^{TM} bioreactor. Cells were stained with live/dead assay and imaged under confocal microscope (Figure 5.10). From DEAD Red ^{TM} staining, it was observed that the majority of cells were dead after 7 days.

5.3.3.2 Collagen/Matrigel™

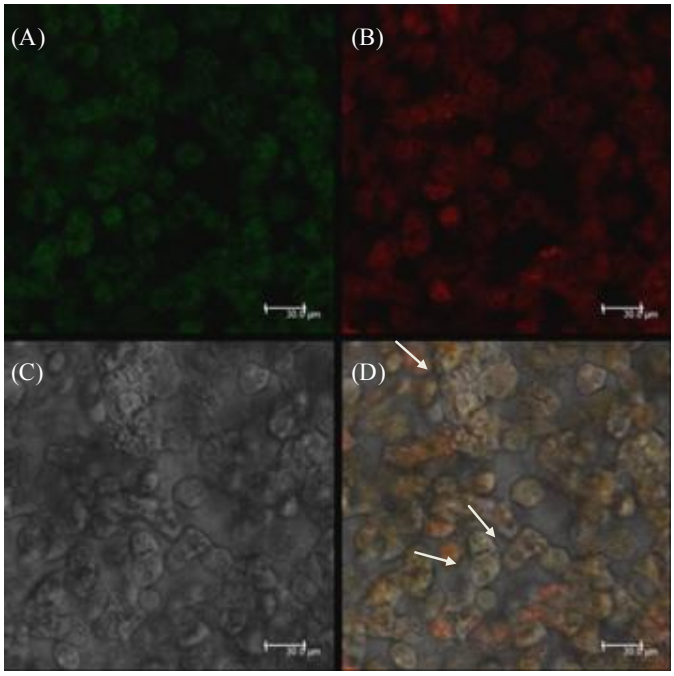

Figure5.11 7-day Culture of Primary Hepatocytes in Collagen Type I/Matrigel™
Syto 10 (A), Dead Red (B), bright field (C) and merged figure (D). White arrows denote moporlogy of hepatocyte monolayer culture

Hepatocytes were inoculated into a 50µl mixture of 3mg/ml collagen and 5mg/ml matrigel™ solution, at a density of 2 $\times 10^5$, and cultured for 7 days in a perfued bioreactor. Cells were stained with live/dead assay, and imaged under confocal microscope (10x). From DEAD Red™ staining, it is evident that the majority of cells were dead after 7 days. In the merged image (see Figure 5.11 (D)), the morphology of some cells is similar to the morphology of cells that grew in sandwich culture (see white arrows). Cells positioned in the flat bottom part of the scaffold were found to take on a spread morphology. Cells that were suspended in the scaffolds were found to take ona rounded morphology.

5.3.3.3 Collagen/Matrigel™/PLA Fibres

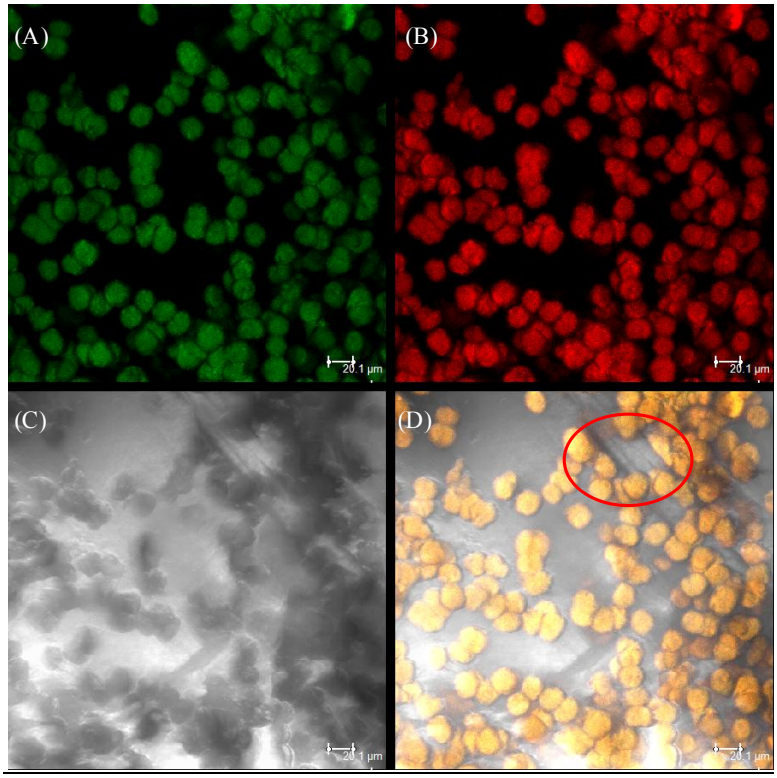

Figure 5.12 7-day Culture of Primary Hepatocytes in Collagen type I/Matrigel™/PLA fibres

Syto 10 (A) and Dead Red (B), bright field (C) and merged figure (D). Red circle denotes PLA fibre was surrounded by cells.

Hepatocytes were inoculated into a 50µl mixture of 3mg/ml collagen, 5mg/ml Matrigel, at a density of $2x10^5$cells/ml. The mixed cell/collagen/matrigel™ solution was seeded onto finely minced PLA fibres for a 7-day culture period in a perfused bioreactor. After 7 days, cells were found dead (See figure 5.12) PLA fibres were located under the collagen/matrigel scaffolds, and imaging was performed to investigate whether the fibres supported cell adhesion. From the merged image (see Figure 5.12 (D), red circle), it can be seen that the PLA fibre was surrounded by cells, however, it is difficult to distinguish whether the cells were attached to it or randomly distributed next to it. Cells

were also seeded onto PLA fibre alone, without the collagen/Matrigel^{TM} support scaffold (see Figure 5.13). The red arrow denotes a piece of PLA fibre where no cells were found attached. It was also observed that at the edge of the cells sheet (white arrow) the cells had no interaction with PLA fibres. These results indicate that PLA fibres do not significantly support cell attachment.

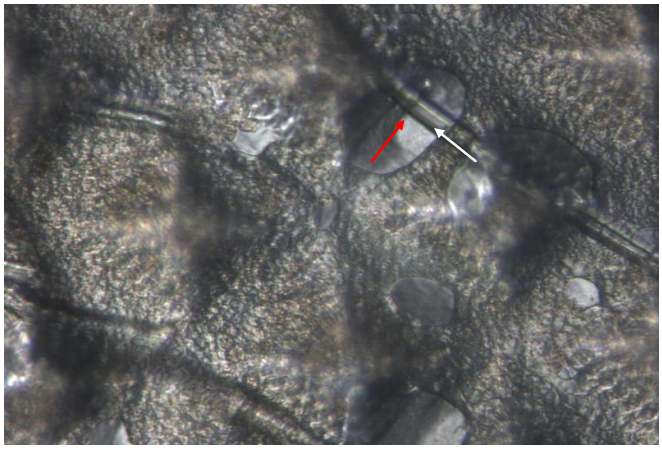

Figure 5.13 7-day Culture of Primary Hepatocytes on PLA Fibres

Collagen, matrigel and PLA as scaffold materials are commonly used for hepatocytes culture. Self-assembly have been observed to form within lyophilised PLGA-collagen sponges (Wen, 2007) or with collagen coated PLGA fibres (Feng, 2010) or on top of surface pre-coated with Poly (2-hydroxyethyl methacrylate) (PHEMA) or PLA (Riccalton-Banks et al, 2003). Formation of spheroids with a specific uniform size and unique hierarchical porosity has also been achieved (Cuddihy, 2008; Kotov, 2004; Lee, 2006; Shanbhag, 2005). The approach taken here uses a single scaffold material, based on studies complete in chapter 3 and 4. Using only collagen as the scaffold material for the formation of hepatocyte spheroids has also been reported elsewhere by Wang et al (Wang, 2004). Wang used mixture of collagen type I and IV, in ratio of 4:1, to

accommodate hepatocyte culture in static conditions. Culture medium was changed daily, and cells were cultured for a period of 9 days. They found that that collagen gel supported fine three dimensional growth of hepatocytes. However, in the current section, collagen, matrigel^{TM} and PLA fibres were investigated individually and together, and were found not to support to hepatocyte culture. In contrast, cells were found to be dead after 7 days in culture. Wang's work also showed the hepatocyte morphological changes after 24 hours and 72 hours in culture. Spheroid shape was seen to change from having a spherical clear boundary to flattened joined patches. In this section, cell morphology was monitored at day 7, and hepatocytes in collagen/matrigel^{TM} scaffolds were seen to display a similar phenomenon, with some cells spreading towards the bottom of the collagen scaffold, and displaying a similar morphology to cells found in monolayer culture. In the remainder of the scaffold, cells were observed to be rounded in shape and suspended in the scaffold. This may be because the cells traumatised during seeding, and died early in culture, and for this reason the morphology did not change. It may also be because cells died from the middle of the scaffold due to insufficient mass transport thorough the scaffold. In conclusion, it was found that mixing hepatocytes with collagen, matrigel^{TM} or PLA alone did not support viable cell culture.

5.3.3.4 Alginate Beads

Hepatocytes were encapsulated in alginate solution to reach $3x10^6$cells/ml density. Beads were generated by as described in Section 5.2.5.5. Viability of initial seeding was 85.7%, by day 3, the viability had dropped to 29.42% and by day 4 cell viability had again dropped to 15.78%. At the end of day 6, live/dead assay was performed. Cells were stained and examined under a confocal microscope. Cells were found to be dead by day 7 (See Figure 5.14 and 5.15).

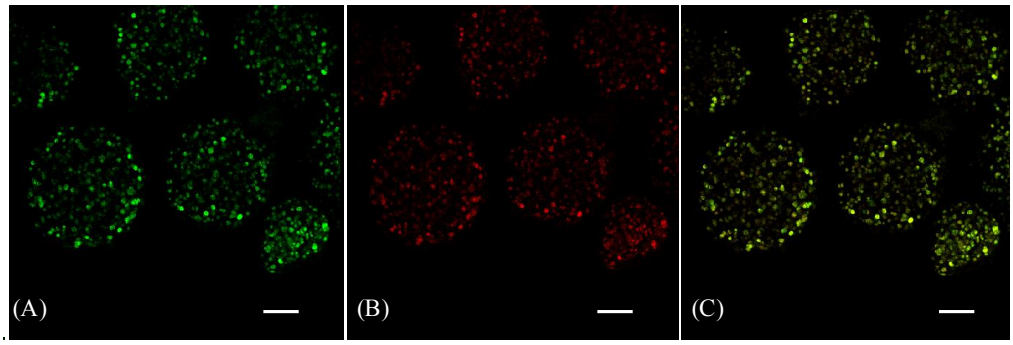

Figure 5.14 Hepatocytes Culture in Alginate Beads at the End of Culture (low power) (A) Syto 10 and (B) DEADRed™ and (C) merged image. Scale Bar = 1mm

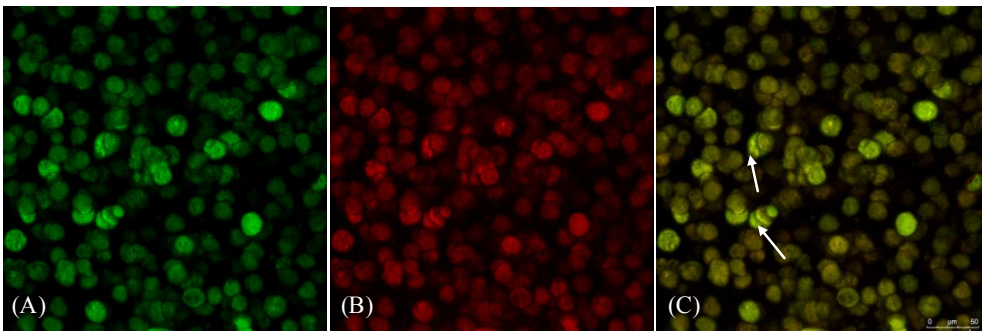

Figure 5.15 Hepatocytes Culture in Alginate Beads at the End of Culture (high power) Syto 10 and (B) DEADRed™ and (C) merged image. White arrow shows the aggregation of hepatocytes, which may indicate that before cells were dead, hepatocytes were trying to form into spheroids. Scale Bar = 50µm

5.3.3.5 Algimatrix™

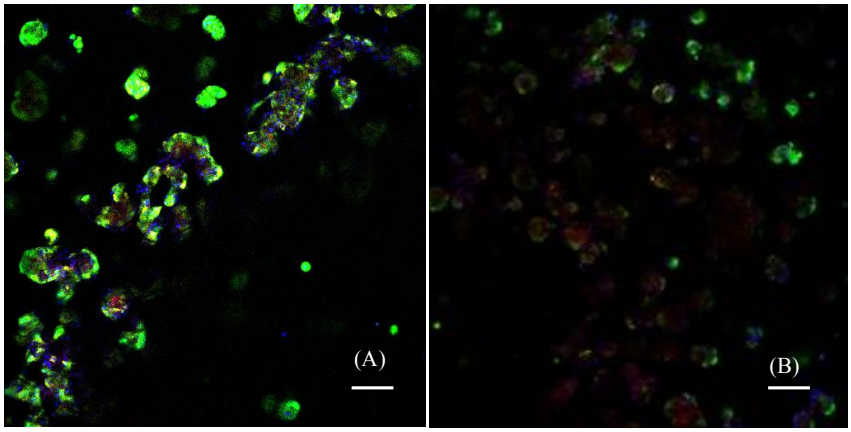

Figure 5.16 Hepatocytes Spheroid Culture in Algimatrix™

The merged image (A) shows the culture at day 5 while (B) shows the culture at day 8. Cells were stained with live/dead stain and examined under confocal microscope, Calcein-AM was used to stain live cells (green), whilst To-Pro3 was used to visualise dead cells (red) and Hoechst was used to stain the nuclei (blue). Scale bar = 100µm

Freshly isolated hepatocytes were seeded into each algimatrix sponge at a density of $1x10^6$cells/ml, and cultured for up to 12 days within a perfused bioreactor, at speed of 20µl/hour. . At day 5, live cells were seen throughout the matrix (see Figure 5.16 (A)) with only a few dead cells apparent, however at day 8, the majority of cells found in the scaffold were dead (see Figure 5.16 (B)).

Traditionally, hepatocytes spheroid formation is performed using a bacteriological dish or on a rotary shaker (Yagi et al, 1993) or rotational stirrers (Bilodeau and Mantovani, 2006), employing a specific time and a constant speed. Alternatively, in the 'hanging-drop' technique, droplets of cell suspension are pipetted onto the lid of a

petri-dish, which is carefully inverted and plated into the incubator. Cells cluster together at the bottom of the drop and spheroids are formed (Kelm et al, 2003; Timmins, 2004).

Alginate is one of the most popular scaffolds used to facilitate spheroid formation. Yang and Miranda have demonstrated that primary hepatocytes aggregated into spheroids under 400µm in size can be subsequently immobilised in alginate beads by by passing through a fine gauge syringe, followed by culture in a stirred bioreactor (Yang , 2000; Miranda, 2010). Falasca also entrapped freshly isolated hepatocytes in alginate beads with a size of around 200µm, and then placed these into culture in bioreactor with 1 litre/min medium flow rate (Falasca, 2001). In the current chapter, hepatocytes were entrapped in alginate beads directly after isolation and passage through syringe. The size of alginate beads were around 2mm, which was much larger than Falasca's (0.2mm), and it was found that the cell viability decreased gradually over time. This may have been due to the absence of a high medium flow rate, which would have affected the rate of diffusion of nutrients and reduced mass transfer within alginate beads. It is concluded that reducing the size of the alginate beads used in this study should increase cell viability at day 7.

Algimatrix^{TM} is a commercial available product sourced from Invitrogen. It is made of lyophilised alginate gel, with a pore size between 50µm and 200µm, and 5mm thickness within 96-well plates. It has been reported that primary hepatocytes can be seeding

dynamically into well-defined pores of the scaffold to form spheroids (Sams, 2010). The entire culture lasted 14 days with high cell viability. In the study described, hepatocytes were inoculated and cultured in Algimatrix^{TM} in perfused bioreactors. By the end of day 12, it was found that the majority of cells had died. This may have been due to differences in procedure and the constituents of the perfused medium. However, the results indicate after further investigation that Algimatrix^{TM} holds promise as a scaffold for spheroid culture.

5.3.4 Comparison between Hepatocyte Sandwich Culture and Self-assembly Culture

5.3.4.1 ATP content

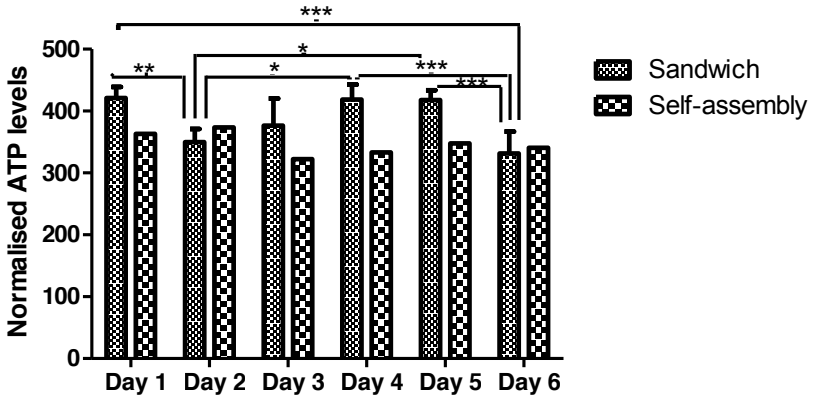

Figure 5.17 Comparison of ATP level between Sandwich Culture and Self-assembly Culture. ATP content was measured every day for 6 days. Asterisks (*) donate statistically significant comparisons among ATP content at different days for Sandwich culture. ATP content measurement were only performed once for self-assembly culture Statistics were analysed by one-way ANOVA, where *p<0.05, **p<0.01 and ***p<0.001. Error bars= SD, n=3

For sandwich culture, from day 1 to day 6, ATP level was reduced to 83.14% at day 2,

then gradually increased to 99.38% at day 4, by day 6, it dropped down to 78.93%. For self-assembly culture, ATP level was dropped to 88.75% at day 3, then kept stable around 95%. By day 5, both cultures were kept the good viability, however, hepatocytes in sandwich culture presented lower ATP level than in self-assembly culture at day 6.

5.3.4.2 ALT Measurement

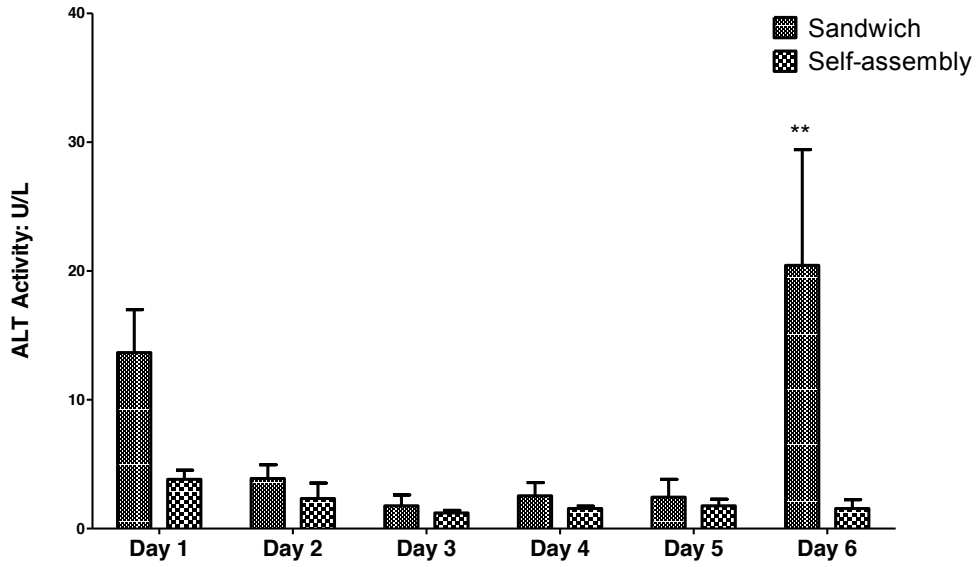

Figure 5.18 Comparison of Measurement of Biomarkers between Sandwich Culture and Self-assembly Culture-ALT. ALT was measured every day for 6 days. Asterisks(*) donate statistically significant comparison of the ALT activity for sandwich culture at day 6 with 4 other different time points for the same culture method, day 2, 3, 4 and 5, **$p<0.01$. For self-assembly culture, there is no significant difference throughout culture period. Error bars= SD, n=3

ALT activity was measured to assess hepatocyte viability in sandwich culture and self-assembly culture for 6 days (see Figure 5.18) ALT is liver specific enzyme, mainly found in cytoplasm. For self-assembly culture, ALT release was the highest at day 1. It then dropped on day 2, and maintained low levels up to day 6. For sandwich culture,

from days 2 to 5, ALT leakage was low and stable, but found to increase significantly at day 6, which is thought to be indicated a decrease in hepatocyte viability.

5.3.4.3 AST Measurement

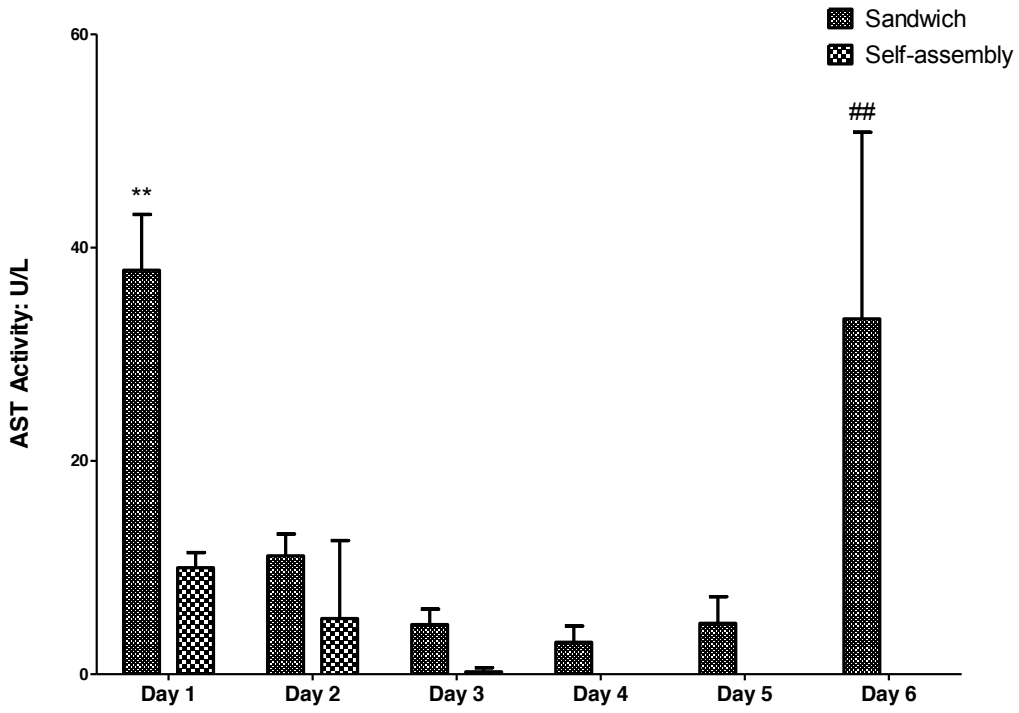

Figure 5.19 Comparison of Measurement of Biomarkers between Sandwich Culture and Self-assembly Culture-AST. AST was measured every day for 6 days. Asterisks(*) donate statistically significant comparison of the AST activity for sandwich culture at day 1 with 4 other different time points for the same culture method, day 2, 3 4 and 5, **p<0.01. Hash marks # donates donate statistically significant comparison of the AST activity for sandwich culture at day 6 with 3 other different time points for the same culture method, day 3, 4 and 5, ##p<0.01.For self-assembly culture, there is no significant difference throughout culture period. Error bars= SD, n=3

AST is not a liver specific biomarker. In live cells, it locates inside the mitochondria. AST activity is shown in figure 5.19, like ALT activity, for sandwich culture, ALT activity was high on day 2, and then decreased. It was seen to increase significantly

again at day 6 (P<0.01). However for self-assembly culture, after day 4, the leakage of AST was too small to be detected.

5.3.4.4 GLDH Measurement

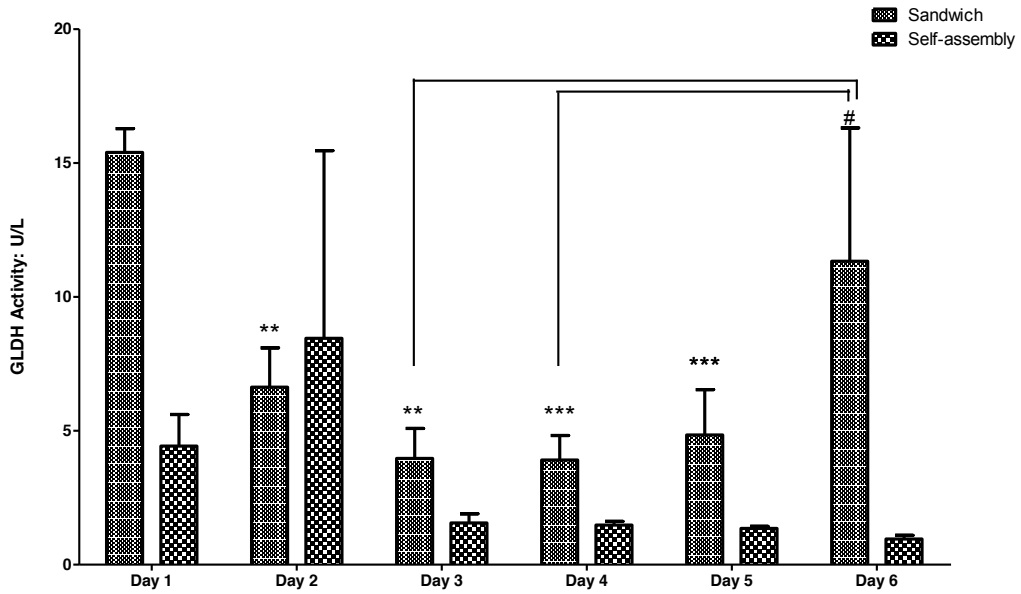

Figure 5.20 Comparison of Measurement of Biomarkers between Sandwich Culture and self-assembly Culture-GLDH. GLDH was measured every day for 6 days. Asterisks(*) donate statistically significant comparison of the GLDH activity for sandwich culture at day 1 with 4 other different time points for the same culture method, day 2, 3, 4 and 5, **p<0.01, ***P<0.005. Hash marks # donates donate statistically significant comparison of the GLDH activity for sandwich culture at day 6 with day 3, 4 #p<0.05.For self-assembly culture, there is no significant difference throughout culture period. Error bars= SD, n=3

Figure5.20 shows the GLDH activity. GLDH is liver specific enzyme that predominantly exists inside mitochondria. A rise in GLDH level can indicate mitochondrial damage (Dunn. J 1999). For sandwich culture, GLDH release followed the same pattern as for ALT and AST release. For self-assembly culture, GLDH displayed higher leakage at day 2 than the day 1, and subsequently remained low and stable.

5.3.4.5 LDH Measurement

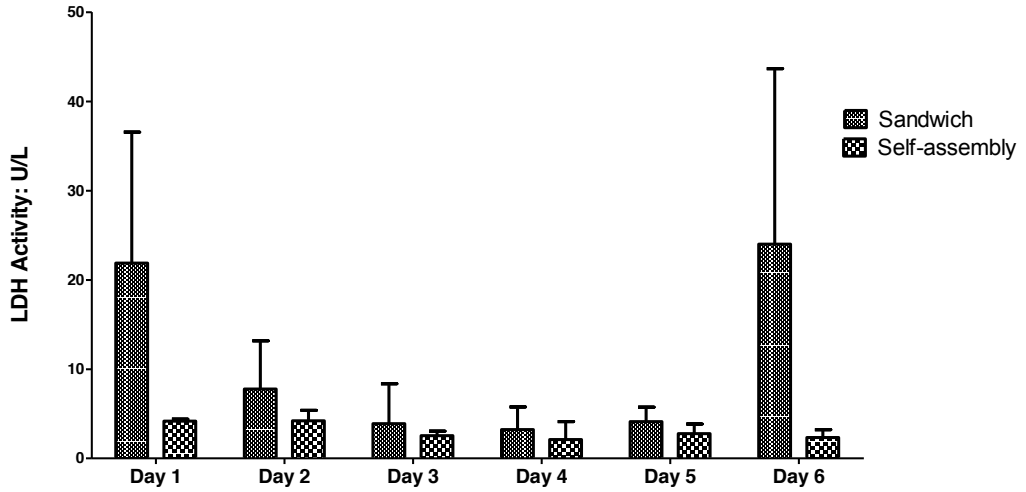

Figure 5.21 Comparison of Measurement of Biomarkers between Sandwich Culture and self-assembly Culture-LDH. LDH was measured every day for 6 days. For both sandwich culture and self-assembly culture, there is no significant difference throughout culture period. Error bars= SD, n=3

LDH is not a liver specific enzyme. LDH leakage was also found to present the same trend, with an increase in LDH leakage at day 6 for sandwich culture, but low levels of leakage in self-assembly culture. The results of enzymes leakage suggest that hepatocyte spheroid culture were more stable over time than the sandwich culture technique.

5.3.4.6 Microalbumin Secretion

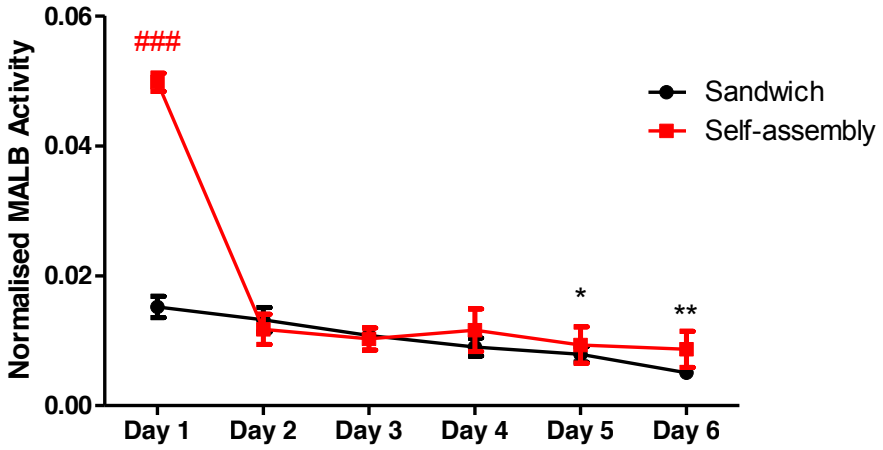

Figure 5.22 Comparison of MALB Secretion between Sandwich culture and Self-assembly Culture

Microalbumin secretion (MALB) was measured daily for both hepatocytes sandwich culture and self-assembly culture (Figure5.22). Asterisks(*) donate statistically significant comparison of the MALB activity for sandwich culture at day 1 with 2 different time points for the same culture method, day 5 and 6, *P<0.05, and *P<0.01. Hash marks # donate statistically significant comparison of the MALB activity for sandwich culture at day 1 with 5 other different time points for the same culture method, day 2, 3,4, 5 and 6, ###P<0.005. Error bars= SD, n=3

For hepatocytes sandwich culture, MALB secretion was decreased gradually to 33.27% of its initial expression at day 6. For self-assembly culture, MALB secretion dropped rapidly from first day to second, with 46.68% decrease. However, from day 2 to day 6, MALB expression decreased slower than that of sandwich culture, with 73.86% of the expression at day 2.

5.3.4.6 Characterisation of Immunocytochemistry

(a) Immunocytochemistry for Self-assembly Culture

Albumin+CK18+Hoechst

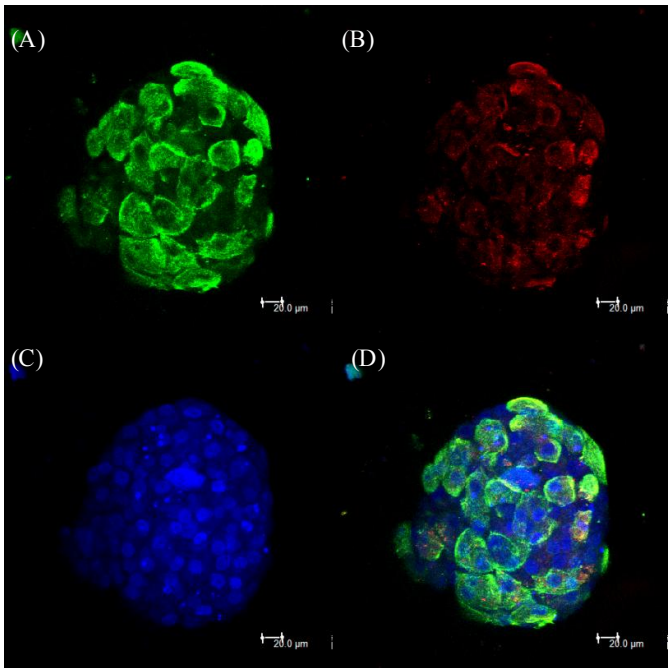

Figure5.23 Immunostaining of Albumin and CK18 for Self-assembly Culture at Day 6

Stains are for (A) albumin, (B) CK18, and (C) Hoechst. (D) Composite image of (A, B and C). Self-assembly were examined using a confocal microscope.

Figure 5.23 shows a single self-assembly immunostained to highlight hepatocyte function. Albumin and CK18 are both hepatic markers, where Albumin is the most abundant protein synthesised by functional hepatocytes (Baharvand, 2006), and CK18 is a constituent of the hepatocyte cytoskeleton (Moll, 1982). The positive fluoresce signal from Albumin secretion and CK18 expression demonstrates that self-assembly culture maintain the albumin and CK18 expression in MP bioreactors after 6 days in culture.

ZO-1+HNF-4+Hoechst

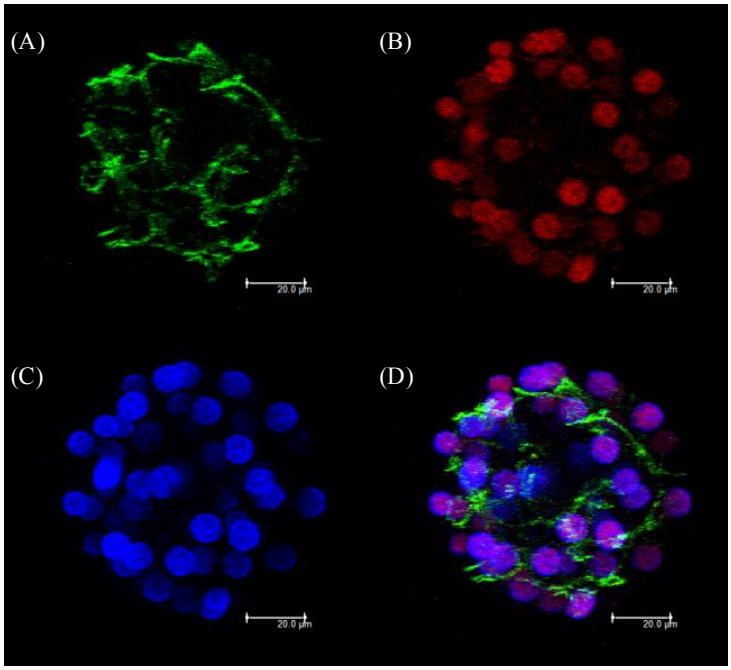

Figure 5.24 Immunostaining of ZO-1 and HNF-4 for Self-assembly Culture at Day 6

Spheroids after 6 days in culture were fixed and examined using a confocal microscope. The spheroids were stained for (A) ZO-1, (B) HNF-4, and (C) Hoechst. (D) Composite image of A, B, and C.

ZO-1 is a tight junction protein significant to bile canaliculi formation between hepatocytes in the liver. HNF-4 is a hepatocyte nuclear factor that contributes to hepatocytes transcription in live cells (Dean et al., 2010; Li et al., 2000; Lindros et al., 1997; Schrem et al., 2002). Positive expression of ZO-1 indicates that bile canaliculi reformed in spheroid culture after being isolated from liver tissue. It is also indicative of the bipolar configuration that consists of the apical and basolateral membranes (Abu-Absi et al., 2002; Fanning and Anderson, 2009). Also, hepatocytes in multicellular spheroid culture maintain positive expression of HNF-4 after 6 days in culture, again demonstrating a preserved cell phenotype.

Mrp2+Hoechst

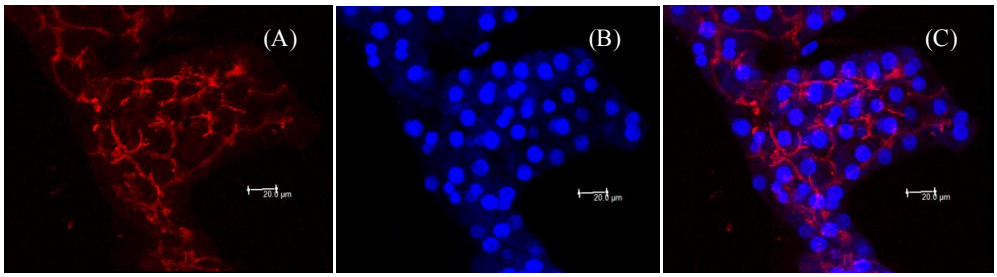

Figure 5.25 Immunostaining of Mrp-2 for Self-assembly Culture at Day 6

Spheroids in culture were fixed at day 6 and examined using a confocal microscope. Cells were stained for (A) Mrp-2 and (B) Hoechst. (C) Composite image of (A) and (B).

Mrp-2 (Multi-drug-resistance associated protein 2) is a drug transporter protein, and localises on the tubular structures of the bile canaliculi on the hepatocyte membrane (Sudo et al. 2005). The continued expression of Mrp-2 after 6 days in culture demonstrates that the function as efflux transport was preserved at day 6.

(b) Immunocytochemistry for Sandwich Culture

To directly compare self-assembly culture with the industry standard technique of sandwich culture, the same hepatocyte markers were chosen for sandwich culture and staining was carried out on day 6 (see Figure 5.26). The same conservation of hepatocyte markers was found, indicating that spheroid culture is equivalent to sandwich culture, in terms of the expression of markers investigated. Specifically, hepatocytes within spheroid and sandwich culture were both seen to positively express HNF-4 (see Figure 5.26, (H)), indicating a preserved cell phenotype. Albumin, cytokeratin 18, ZO-1 and Mrp-2 expression were also seen to be expressed in sandwich culture (see Figure5.26, (B,C,G,L,M)).

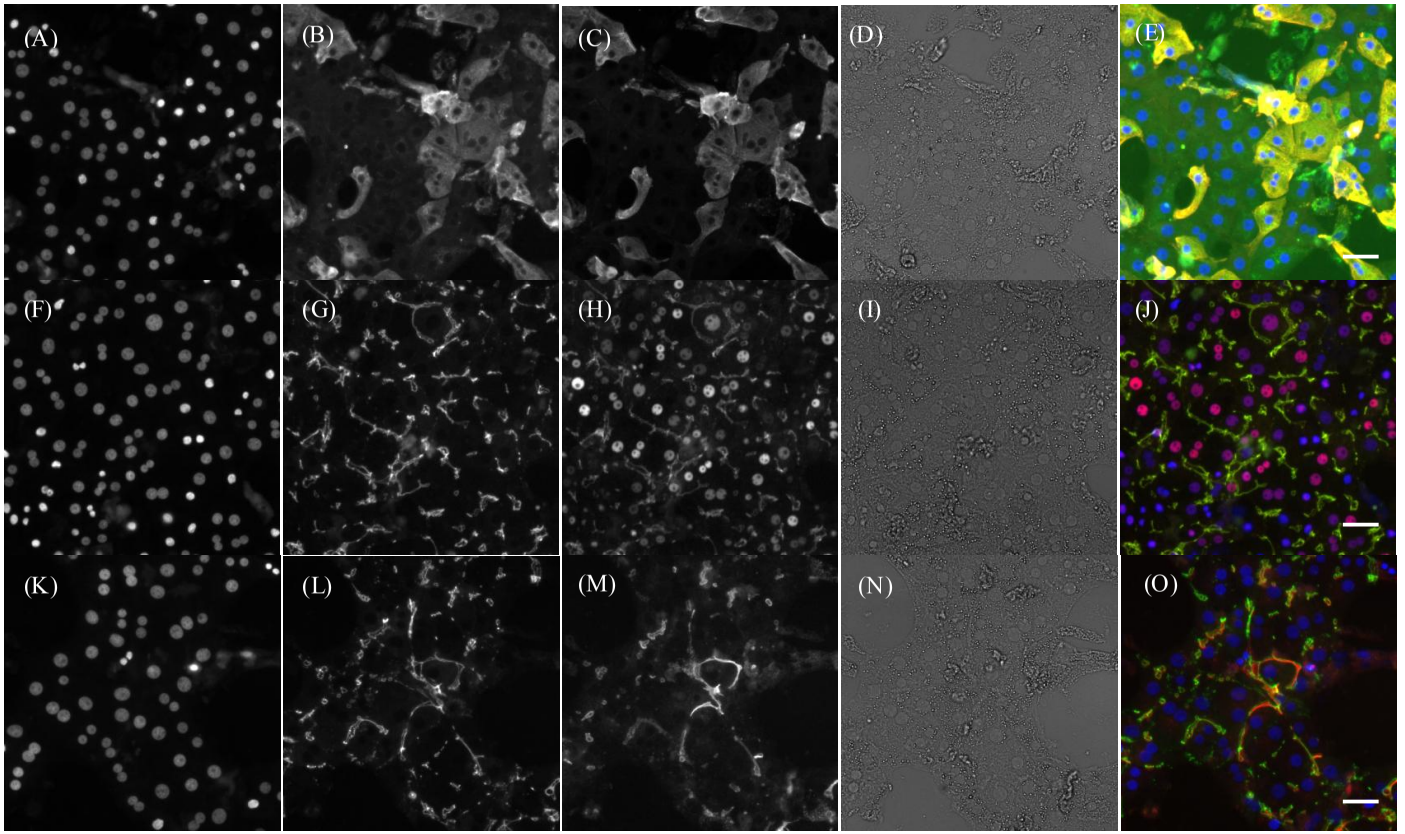

Figure5.26 Immunostaining of hepatocyte markers in sandwich cultured for 6 days. Cells were stained for (A, F and K) Hoechst, (B) Albumin (C) CK18 (G and L) ZO-1, (H) HNF-4 and (M) Mrp-2; (D, I and N) are bright field images; (E, J and O) show composite image of (A, B and C), (F, G and H) and (K, L and M) respectively. Scale bars = 50µm.

5.3.4.7 Gene Expression Profiling

Principle Component Analysis of All genes

Tissue and culture samples were sent to Affymetrix for gene expression array. Principle component analysis (PCA) was used to highlight differences in the gene expression profile of primary rat hepatocytes exposed to the culture methods investigated, and compared with normal (uncultured) rat liver tissue. The 'PCA methods' utility in the BioConductor package (online open source) was used to perform the analysis on the 9754 differentially expressed probe sets in the normalised dataset ($P<0.05$), and also to visualise the results (see Figure 5.27). Uncultured tissue samples provided from animals used in our experiments were found to be unreadable by Affymetrix. For this reason, results for normal (uncultured) tissue were obtained from a published experiment (GEO identifier: GSM495209) that used the same animal model, and reported expression from rat liver tissue on the same array platform used by Affymetrix. When all of the samples were included in the PCA analysis, it was clear that the sandwich culture and self-assembly culture expression results have similar principle components, whereas the freshly excised hepatocytes and the normal (uncultured) tissue samples displayed different expression profiles (Figure 5.27(A)). The large differences between the freshly excised hepatocytes and the normal (uncultured) tissue may have been due to experimental variation or directly due to unknown differences, given that the tissue samples compared are from

different laboratories.

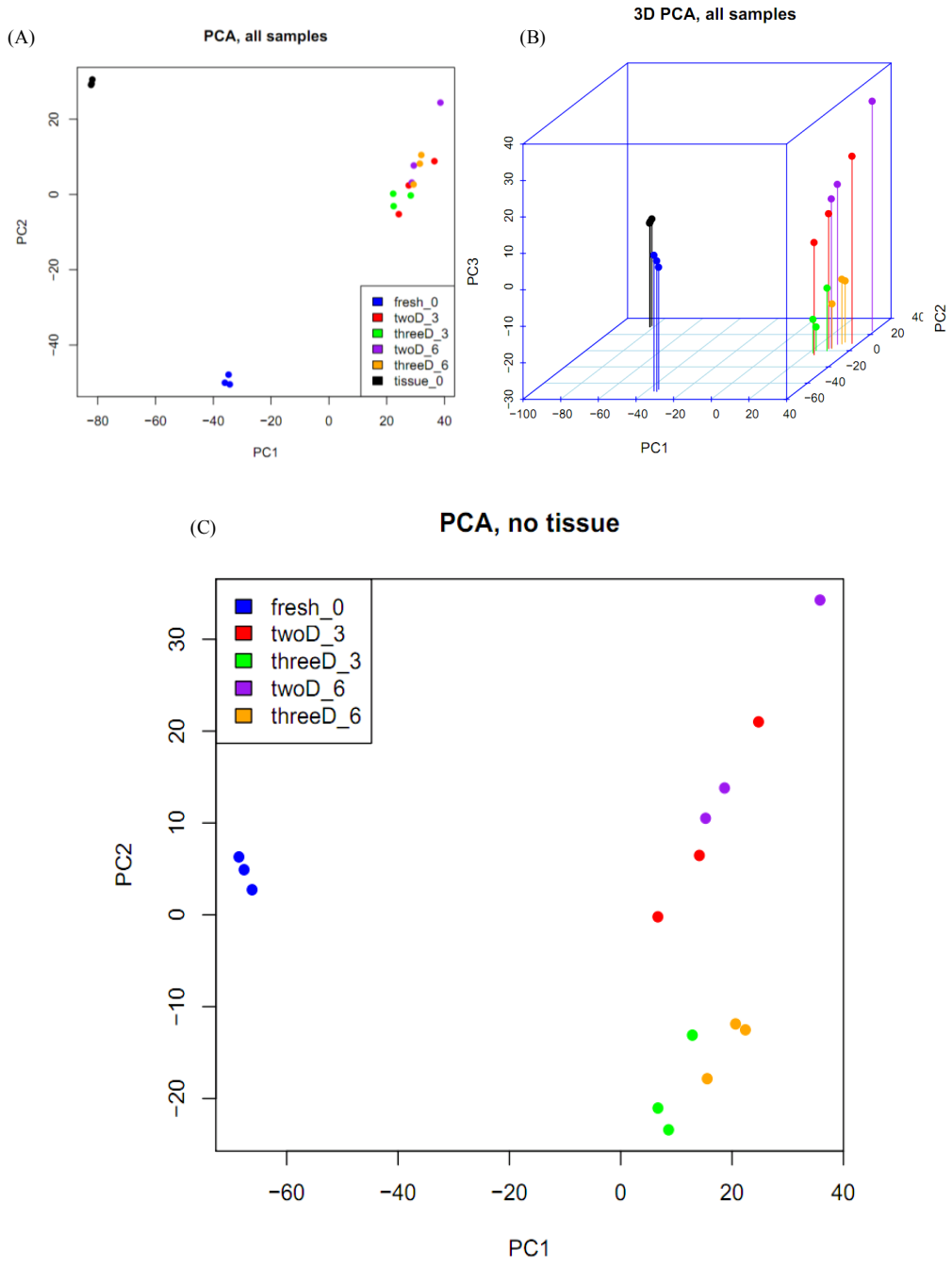

Figure 5.27 Principle Component Analysis using all the differential gene expression in tissue, freshly isolated hepatocytes, sandwich culture (only called '2D' in this occasion) and self-assembly culture (only called '3D' in this occasion) at day 3 and 6. Black spots represent normal (uncultured) tissue. Blue spots represent freshly isolated hepatocytes without culturing; red spots represent expression from cells in sandwich culture for 3 days and purple spots for 6 days, where green spots represent self-assembly culture for 3 days and orange spots for 6 days.

Figure 5.27 (B) compares the first and second principle components without the published (uncultured) tissue samples, which highlights the discrimination between the sandwich and self-assembly cultures more successfully. It is expected that the gene expression profiles of tissue and freshly isolated hepatocytes will be significantly different to sandwich culture and self-assembly culture. When the largest three principle components are visualised, it can be seen that gene expression for the sandwich and self-assembly culture techniques are distinct from each other (see Figure 5.27 (C)).

Boess et al. compared gene expression profiles for liver slice, uncultured freshly isolated hepatocytes, with hepatocytes in sandwich culture and monolayer culture at different time points (Boess, 2003). The gene expression data showed that liver slice expression was the most similar to the whole liver expression in vivo, as the slices contain all the lived cell types in a maintained three dimensional structure. For sandwich culture within 6 hours, expression was similar to liver slices, but after 24 hours the expression profile showed large divergence. In current study, it is to be expected that hepatocytes after isolation, or culture in sandwich or as self-assembled clusters will show a different expression profile to freshly isolated hepatocytes and liver slice tissue. However, it is also useful to compare the cultured hepatocyte expression profiles directly to distinguish the gene expression and the functional difference between sandwich culture and self-assembly.

Differentially Gene Expression and Functional Enrichment

Differentially expressed genes of self-assembly culture in contrast to sandwich culture were identified at both day 3 and 6. There were 155 differentially expressed genes at day 3 with 74 upregulated and 81 down regulated. There were 144 differentially expressed genes at day 6 were 57 upregulated genes and 87 downregulated genes (See Appendix B, table1 and table 3). The expression of albumin, CK18, ZO-1,HNF-4 and Mrp-2 were unchanged for both sandwich culture and self-assembly culutre, which support the immunocytochemistry in section 5.3.4.6. All differentially expressed genes were clustered by biological process functions. Most of functions that are involved with upregulated genes for both day 3 and 6 were related to metabolic processes (See Appendix B, table 2 and 4). Metabolism functions were significantly enhanced by involving oxidation reduction processes, carboxylic acid metabolic processes, fatty acid metabolic processes, lipid metabolic processes, cholesterol and steroid processes, as well as transport of cholesterol and steroid, which suggest, potentially, increases in the hepatocytes' metabolic functions and detoxification. For biological process functions that were involved with down regulated genes at day 3 were mainly related to three dimensional structures, for day 6, biological process functions were including hydrostatic pressure, epithelial cell development, regulation of collagen metabolic process and peptide activity. It is not clear that what caused the downregulated genes involved in those processes. Future investigation should be carried out in future work. Overall, self-assembly sphenoid culture in micro-patterned

bioreactor provide a novel tool, that maintains cell viability, and metabolising activity, which can be potentially used for improving hepatotoxicity testing.

5.4 Summary

The aim of chapter 5 was to develop a novel method to prepare a hepatocyte model for in vitro hepatotoxicity testing. Development and characterisation were carried out. Sandwich culture as a standard method has been wildly used in industry. Freshly isolated hepatocytes were cultured in sandwich for 6 days. Maintained viability was observed at day 3 and day 6 by cellomics microscope. Hepatocytes' self assembly culture method was introduced by using micro-patterned bioreactors, which consist of 500 inverted pyramid like mini wells at the bottom of each well. The MP bioreactors were made of PDMS. Due to the hydrophobic property, hepatocytes could not be inoculated evenly in mini-wells since bubbles were trapped within. Sterilising the MP bioreactor with pre-loaded dH_2O could discard the bubbles and allow even cell distribution in the mini-wells. Hepatocyte seeding density was investigated. 0.4×10^6 cells/ml was the optimal seeding density for self-assembly spheroid culture. Scaffold based 3D methods also evaluated. Collagen, collagen/matrigel, collagen/matrigel/PLA fibres, PLA fibres, alginate and algimatrix^{TM} were utilised to examine if the scaffold material was suitable to support hepatocyte growth. Algimatrix^{TM} was the only material in the study that showed the high viability of hepatocytes culture at day 5, but a majority of dead cells were presented at day 8. The rest of the materials studied were

not suitable for hepatocyte culture in the conditions presented. Algimatrix^{TM} should be investigated more in the future for longer culture period.

Comparisons between hepatocyte sandwich culture and self-assembly culture were carried out. ATP content, ALT, AST, GLDH, LDH and Microalbumin secretion were measured for both cultures daily. ATP result indicates that self-assembly culture showed the stable ATP level throughout the culture period, but for the sandwich culture, the there was a drop at day 6. ALT, AST, GLDH and LDH measurements all illustrated similar trends. Initially the enzyme leakage was high in both cultures, due to stress of isolation. The enzymes leakage decreased, and stayed stable throughout the culture for self-assembly culture, while for sandwich culture, there was an increase at day 6. However, there was a large error bar at day 6. It could be caused by the variation of isolation or operation differences during the culture. Microalbumin secretion for hepatocytes sandwich culture was decreasing with the time, however, for self-assembly culture, it dropped at day 2, but kept stable till the end of culture. Immunocytochemistry was examined both culture. Hepatocytes within the self-assembly culture and sandwich culture all expressed positive HNF-4, which indicates highly preserved cell differentiation. Meanwhile, albumin, cytokeratin 18, ZO-1 and Mrp-2 expression were all confirmed. CK 18 shows the liver-specific cytoskeleton, ZO-1 shows the formation of tight junctions and Mrp-2 is the drug transporter. Microarray was performed at day 3 and day 6 to compare self-assembly culture and sandwich culture. 155 differentially expressed genes at day 3 with 74

upregulated and 81 down regulated. 144 differentially expressed genes at day 6 were 57 upregulated genes and 87 downregulated genes. All differentially expressed genes were categorised by biological process functions. Most the functions that are involved with the upregulated genes for both day 3 and 6 were related to metabolic process, such as Metabolism functions were dramatically enhances by involving oxidation reduction process, carboxylic acid metabolic process, fatty acid metabolic process, lipid metabolic process, cholesterol and steroid process, as well as transport of cholesterol and steroid, etc., which suggest potentially increase the hepatocytes metabolic functions and detoxification. For biological process functions that were involved with down regulated genes at day 3 were mainly related to three dimensional structures, for day 6, biological process functions were including hydrostatic pressure, epithelial cell development, regulation of collagen metabolic process and peptide activity. It is not clear that what caused the downregulation of the genes involved in those processes. Investigation should be carried out in future. Overall, self-assembly spheroid culture in micro-patterned bioreactor provides a novel tool, that maintains cell viability, and metabolising activity, which can be potentially used for improving hepatotoxicity testing.

Chapter 6 Conclusions and Future Work

6.1 Conclusions

The aim of the thesis is to employ perfused bioreactors as a novel tool to improve the predictivity and accuracy of drugs in preclinical trials, which would ultimately reduce animal use. The main achievement is composed of several aspects as listed below.

An in-vitro perfused 3D MSCs culture-based system for cytotoxicity testing was developed. Alginate and collagen as widely used scaffolds were investigated for MSCs culture. Cell growths with different seeding densities, as well as cell morphology were compared. Alginate without any modification does not support cell attachment. Collagen was ultimately selected and utilized as the more suitable scaffold for the whole study. A novel protocol using a collagen compressor was established for increasing the mechanical properties. It has been experimentally proved that the cell growth which did not change significantly was in non-pressed collagen Alamarblue was used as the cell viability index. 5% alamarblue in 100µl culture medium with the presence of FBS and phenol red, for 2 hours incubation time in monolayer was found to be the optimal assay condition. The optimal human MSCs growth was found with the supplements of MCGS, AA, together with $NaHCO_3$ and HEPES in αMEM, culture in normal air condition (0.03% CO_2). Human MSCs for trimethoprim dose response was performed. Comparisons between 2D and 3D, static and perfusion demonstrated that the perfusion system

showed different results from the static system.

After the perfused 3D MSCs model for drug testing was established, two compounds (compounds A and B), supplied confidentially by Pfizer, UK were evaluated by using adipose-derived mesenchymal stem cells. Cytotoxicity of oxazolidiones via inhibition of mitochondrial protein expression is induced by isomers with cis (Compound A), but not trans (Compound B), stereo chemistry on the heterocycle. Alamarblue was used as a viability index. Optimisation was carried out before drug testing. With the presence of HEPES, absence of $NaHCO_3$, phenol red, FBS in high glucose DMEM medium was the optimal assay condition for ADMSCs. Cytotoxicity of the two stereoisomers in 2D vs. 3D culture formats was then investigated with or without media flow. The isomer with cis stereochemistry was significantly more cytotoxic than the trans isomer in both 2D and 3D perfused or 3D static culture compared to 2D static culture. This effect was seen after three days' treatment and continued to six days of treatment. 3D static and perfusion data shows the time and dose dependent effects. The data indicate that perfusion and 3D culture conditions contribute to a better toxicity prediction. However, a reduction in cell viability was observed at the highest dose tested (50μM) in both 3D static and 3D perfused culture for Compound B. The results demonstrate that the 3D perfused system improved the prediction of drug toxicity over 2D culture formats thereby recommending 3D culture for preclinical drug toxicity testing.

The aim of chapter 5 was to develop a novel method for the hepatocyte model for *in*

vitro hepatotoxicity testing. Development and characterisation were carried out. Sandwich culture as a standard method has been widely used in industry. Freshly isolated hepatocytes were cultured in sandwich for 6 days. Maintained viability was observed at day 3 and day 6 by the cellomics microscope. The hepatocyte self-assembly culture method was introduced by using micro-patterned bioreactors, which consist of 500 inverted pyramid-like mini wells at the bottom of each well. The MF bioreactors were made of PDMS. Due to its hydrophobic property, hepatocytes would not be inoculated evenly inside the mini-wells since bubbles were trapped within. Sterilising the MF bioreactor with pre-loaded dH_2O would eliminate the bubbles and allow even cell distribution in the mini-wells. Hepatocyte seeding density was investigated. 0.4 x 10^6 cells/ml was the optimal seeding density for self-assembly culture. Scaffold-based 3D methods were also evaluated. Collagen, collagen/matrigel, collagen/matrigel/PLA fibres, PLA fibres, alginate and algimatrix were utilised to examine if the scaffold material was suitable to support hepatocyte growth. Algimatrix was the only material in the study which showed a high viability of hepatocyte culture at day 5, but a majority of dead cells were present at day 8. The remaining materials were not suitable for hepatocyte culture in the conditions presented. Algimatrix can be investigated more in the future.

Comparisons between hepatocyte sandwich culture and self-assembly culture were carried out. ATP content, ALT, AST, GLDH, LDH and microalbumin secretion were measured for both cultures daily. The ATP result indicates that self-assembly culture

showed a stable ATP level throughout the culture period, but for the sandwich culture, there was a drop at day 6. ALT, AST, GLDH and LDH measurements all illustrated similar trends. Initially, enzyme leakage was high in both cultures, due to the stress of isolation. The enzyme leakage decreased, and remained stable throughout the culture for self-assembly culture, while for sandwich culture, there was an increase at day 6. However, there was a big error bar at day 6. It could be caused by the variation of isolation or operation difference during the culture. Microalbumin secretion for hepatocyte sandwich culture was decreasing with time; however, for spheroid culture, it dropped at day 2, but kept stable till the end of culture. Immunocytochemistry was examined in both cultures. Hepatocytes within the self-assembly culture and sandwich culture all expressed positive HNF-4, which indicates highly preserved cell differentiation. Meanwhile, albumin, cytokeratin 18, ZO-1 and Mrp-2 expression were all confirmed. CK 18 shows the liver-specific cytoskeleton, ZO-1 shows the formation of tight junctions and Mrp-2 is the drug transporter. Microarray was performed at day 3 and day 6 to compare spheroid culture and sandwich culture. There were 155 differentially expressed genes at day 3 with 74 upregulated and 81 downregulated. 144 differentially expressed genes at day 6 comprised 57 upregulated genes and 87 downregulated genes. All differentially expressed genes were categorised by biological process functions. Most of the functions involved with upregulated genes for both day 3 and 6 were related to metabolic processes. Metabolism functions were dramatically enhanced by involving oxidation reduction process, carboxylic acid metabolic process, fatty acid metabolic process, lipid metabolic process, cholesterol and steroid process, as

well as transport of cholesterol and steroid, etc., which suggests a potential increase in the hepatocytes' metabolic functions and detoxification. Biological process functions that were involved with down regulated genes at day 3 were mainly related to three dimensional structures; for day 6, biological process functions included hydrostatic pressure, epithelial cell development, regulation of collagen metabolic process and peptide activity. It is not clear what caused the downregulated genes involved in those processes. Investigation should be carried out in future. Overall, self-assembly spheroid culture in micro-patterned bioreactor provided a novel tool, that maintains cell viability, and metabolising activity, which can be potentially used for improving hepatotoxicity testing.

6.2 Future Work

The aim of this study was to provide a novel platform for toxicity testing. MSCs from different species were utilised as cell sources in perfused bioreactors for toxicity prediction. The perfused flow rate was determined by the total volume change of the static culture. The flow rate would have an effect on cell proliferation and differentiation. In *in vivo* ECMs, cells are proliferating under assured blood flow and need shear stress to enhance their growth. In *in vitro* perfusion systems, cells are cultured by continuous flow to mimic the *in vivo* environment, the surface of the cells, either in 2D or 3D has been surrounded by dynamic flow, and shear stress affected by perfusion rate therefore is the one of the key parameters to regulate cell proliferation and differentiation

(Hosseinkhani, 2005). The amount of maximal media flow which cells can tolerate varies among cell lines (Walker, 2004). The comparison of media flow in terms of shear stress should be performed shortly to examine the cell growth properties.

Scaffold material selection for hepatocyte spheroid culture should be carried out by using algimatrix. Algimatrix is a commercially available product from Invitrogen. It has been reported that primary hepatocytes can seed dynamically into well-defined pores of scaffolds to form spheroids. The entire culture lasted 14 days with high cell viability (Sams, 2010). In the current study, hepatocytes were inoculated and cultured in algimatrix in perfused bioreactors, and by the end of day 8, the majority of cells were dead. The dead cells were mainly located in the central of scaffolds, this may be caused by uneven cell distribution at inoculation or inefficient mass transfer during culture. Seeding efficiency can be conducted by dynamic seeding twice with different speeds. Mass transfer can be conducted by different perfused rate.

Gene expression profiling was performed by using microarray, and the differentially expressed genes were analysed and categorised into biological process functions. Most biological functions that were involved in upregulated genes were related to drug metabolism enzyme activity, which only suggests that the self-assembly spheroid model would potentially increase metabolising xenobiotics and drugs. Further toxicity testing using such a model should be conducted to prove the hypothesis. Also, the biological functions that were involved with downregulated genes at the end of the culture should

be taken into account for future study. Identifying the genes and investigating the reason would help to understand the self-assembly spheroid model. Prolonging the self-assembly spheroid culture also should be conducted to facilitate the chronic effect of drug testing.

References

Abbott et al., Cell culture: Biology's new dimension. Nature,2003,424: 870-872.

Abou-Eisha, A., Afifi, M., 2004. Genotoxic evaluation of the antimalarial drug, fansidar, in cultured human lymphocytes. Cell Biol. Toxicol. 20, 303–311.

Abpi: Stem cells in predictive toxicicology. A report of Stem cell for safer medicine, 2006

Abu-Absi SF, Friend JR, Hansen LK, Hu WS. 2002. Structural polarity and functional bile canaliculi in rat hepatocyte spheroids. Exp Cell Res 274(1):56–67.

Aden, D. P., Fogel, A., Plotkin, S., Damjanov, I. & Knowles, Controlled synthesis of HBsAg in a differentiated human liver carcinoma-derived cell line. 1979 Nature (London) 282, 615-616

Ahmed SARM, Walsh JE.Gogal. (1994). A new rapid and simple non-radioactive assay to monitor and determine the proliferation of lymphocytes: an alternative to thymidine incorporation assay. . J Immunol Meth, 170: 211-224.

Ahuja YR, Vijayalakshmi V, Polasa K. Stem cell test: A practical tool in toxicogenomics[J]. Toxicology, 2007, 231(1): 1-10.

Akhtar A, The Rise of In-Vitro Toxicity Testing, Veterinary World 2008 Vol. 1(5): 150-151

Akins RE, Boyce RA, Madonna ML, Schroedl NA, Gonda SR, McLaughlin TA, Hartzell CR. Cardiac organogenesis in vitro: reestablishment of three-dimensional tissue architecture by dissociated neonatal rat ventricular cells. Tissue Eng 1999; 5: 103-118

Allen JW, Khetani SR, Bhatia SN. In vitro zonation and toxicity in a hepatocyte bioreactor. Toxicol Sci 2005;84:110–9.

Altmann B, Welle A, Giselbrecht S, Truckenmüller R, Gottwald E. The famous versus the inconvenient - or the dawn and the rise of 3D-culture systems. World J Stem Cells. 2009 Dec 31;1(1):43-8

Alvarez-Dolgado, J.M. Garcia-Verdugo, J.R. Fike, H.O. Lee, K. Pfeffer, C. Lois, S.J. Morrison and A. Alvarez-Buyla, Fusion ofbone-marrow-derived cells with Purkinje neurons, cardiomyocytes and hepatocytes, Nature 425 (2003), pp. 968–973.

Améen C, Strehl R, Björquist P, Lindahl A, Hyllner J, Sartipy P. Human embryonic stem cells: current technologies and emerging industrial applications. Crit Rev Oncol Hematol. 2008, 65(1):54-80.

Aninat C et, al 2006Expression of cytochromes P450, conjugating enzymes and nuclear receptors in human hepatoma HepaRG cells. Drug Metab Dispos. 2006 Jan;34(1):75-83

Atala and Lanza. Methods of tissue Engineering, Gulf Professional Publishing, 2002

Badylak SF, Freytes DO, Gilbert TW. Extracellular matrix as a biological scaffold material: Structure and function. Acta Biomaterialia 2009;5 (1):1-13.

Baharvand H, Hashemi SM, Kazemi Ashtiani S, Farrokhi A. Differentiation of human embryonic stem cells into hepatocytes in 2D and 3D culture systems in vitro. Int J Dev Biol. 2006; 50(7):645-52.

Balls Michael, Goldberg Alan M, et. al. The three Rs: the way forward: the report and recommendations of ECVAM Workshop 11. Altern Lab Anim. 1995 Nov–Dec;23(6):838–866.

Banas A, Teratani T, Yamamoto Y, Tokuhara M, Takeshita F, Quinn G, Okochi H, Ochiya T: Adipose tissue-derived mesenchymal stem cells as a source of human hepatocytes. Hepatology 2007;46: 219–228.

Barhoumi R, et al, 2002 Characterization of Calcium Oscillations in Normal and Benzo[a]pyrene-Treated Clone 9 Cells. Toxicological Sciences Volume68, Issue2 Pp. 444-450

Batzakis KG and Briere RO, Interpretive enzymology, Thomas, Springfield, Illinois (1979).

Berg JM, Tymoczko JL, Stryer L Biochemistry textbook. Publisher: W. H. Freeman; 6 edition, May, 2006

Berrea ML, Crozatiera C. , Casquillasa GV and Chen Y. Reversible assembling of microfluidic devices by aspirationMicroelectronic Engineering Volume 83, Issues 4-9, April-September 2006, Pages 1284-1287

Bessea, L., Coulomb, B., Lebreton-Decoster,C. & Giraud-GuillE, M. M. (2002). Production of ordered collagen matrices for three-dimensional cell culture. Biomaterials 23, 27-36.

Bhadriraju, K. & Chen, C. S. (2002). Engineering cellular microenvironments to improve cell-based drug testing. Drug Discov. Today 7, 612-20.

Birgersdotter, A., Sandberg, R. & Ernberg, I. (2005). Gene expression perturbation in

vitro--a growing case for three-dimensional (3D) culture systems. Semin Cancer Biol. 2005 Oct;15(5):405-12.

Boess, F., Kamber, M., Romer, S., Gasser, R., Muller, D., Albertini, S., Suter, L. (2003). Gene expression in two hepatic cell lines, cultured primary hepatocytes, and liver slices compared to the in vivo liver gene expression in rats: possible implications for toxicogenomics use of in vitro systems. Toxicol. Sci. 73(2):386–402.

Bonavent ure J, Kadhom N, Cohen- Solal L, Ng KH, Bourguignon J, Lasselin C, Freisinger P. Reexpression of cartilage-specific genes by dedifferentiated human articular chondrocytes cultured in alginate beads. Exp Cell Res 1994; 212: 97-104

Bono H, Yagi K, Kasukawa T, Nikaido I, Tominaga N, Miki R, Mizuno Y, Tomaru Y, Goto H, Nitanda H, Shimizu D, Makino H, Morita T, Fujiyama J, Sakai T, Shimoji T, Hume DA,Hayashizaki Y, Okazaki Y; RIKEN GER Group; GSL Members. Systematic expression profiling of the mouse transcriptome using RIKEN cDNA microarrays. Genome Res. 2003 Jun;13(6B):1318-23.

Borenfreund, E., and Puerner, J. A. (1984). A simple quantitative procedure using monolayer cultures for cytotoxicity assays. J. Tissue Cult. Methods 9, 119–124.

Borenstein, J. T.; Terai, H.; King, K.; Weinberg, C.; Kaazempur-Mofrad, M.; Vacanti, J. P. Microfabrication technology for vascularized tissue engineering. Biomed. Microdevices 2002, 4 (3), 167-175.

Bremer S et al., Development of a Testing Strategy for Detecting Embryotoxic Hazards of Chemicals In Vitro by Using Embryonic Stem Cell Models 30 ALTERNATIVES TO LABORATORY ANIMALS 107, 107-109 (2002).

Brischwein M, Motrescu ER, Cabala E, Otto AM, Grothe H, Wolf B. Functional cellular assays with multiparametric silicon sensor chips. Lab Chip 2003;3:234–40.

Brown RA, Wiseman M, Chuo CB, Cheema U, Nazhat SN (2005) Ultrarapid engineering of biomimetic materials and tissues: fabrication of nano- and microstructures by plastic compression. Adv Funct Mater 15:1762–1770

Cai J, Zhao Y, Liu Y, Ye F, Song Z, Qin H, Meng S, Chen Y, Zhou R, Song X, Guo Y, Ding M, Deng H. Directed differentiation of human embryonic stem cells into functional hepatic cells. Hepatology 45, 1229-39.

Carakostas MC, Gossett KA, Church GE, Cleghorn BL (1986) Evaluating toxin-induced hepatic injury in rats by laboratory results and discriminant analysis. Veterinary Pathology 23, 264-9

Cezar GG, Quam JA, Smith AM, Rosa GJ, Piekarczyk MS, et al.. Identification of small

molecules from human embryonic stem cells using metabolomics. STEM CELLS AND DEVELOPMENT 16:869–882 (2007)

Chandra P, Lecluyse EL, Brouwer KL.Optimization of culture conditions for determining hepatobiliary disposition of taurocholate in sandwich-cultured rat hepatocytes. In Vitro Cell Dev Biol Anim. 2001 Jun;37(6):380-5.

Chang W JD, Sedlak M, Ladisch M R and Bashir RAkin. (2003). Poly(dimethylsiloxane) (PDMS) and silicon hybrid biochip for bacterial culture . Biomed. Microdev.,5 281–90.

Charati, S. G.; Stern, S. A. Diffusion of gases in silicone polymer: molecular dynamics simulations. Macromolecules, 1998, 31, 5529-5535.

Cho MH, Niles A, Huang R, Inglese J, Austin CP, Riss T, Xia MH, A bioluminescent cytotoxicity assay for assessment of membrane integrity using a proteolytic biomarker, Toxicology in Vitro 22 (2008) 1099–1106

Ciaravella, G.; Vozzy, G.; Bianchi, F.; Rosi, M.; Costanza, C.; Madeddu, P.; Ahuwalia, A. Microfabricated fractal trees as scaffolds for capillary morphogenesis: applications in therapeutic angiogenesis and vascular tissue engineering. IEEE-EMBS MCTE Conference, Genova, Italy, 2002, 46-47.

Clampitt RB (1978) An investigation into the value of some clinical biochemical tests in the detection of minimal changes in liver morphology and function in the rat. Archives of Toxicology Supplement 1, 1-13

Combes, R., Balls, M., Bansil, L., Barratt, M., Bell, D., Botham, P., Broadhcad, C., Clothier, R., George, E., Fentem, J., Jackson, M., Indans, I., Laozou, G., Navaratnam, V., Pentreath, V., Phillips, B.,Stemplewski, H., Stewart, J., 2002. An assessment of progress in the use of alternatives in toxicity testing since the publication of the report of the Second FRAME Toxicity Committee (1991). ATLA, 1211–1271.

Combes, R.D., 2005. Assessing risk to humans from chemical exposure by using non-animal test data. Toxicol. In Vitro 19, 921–924.

Corey MJ, Kinders RJ, Brown LG, Vessella RLA very sensitive coupled luminescent assay for cytotoxicity and complement-mediated lysis. J Immunol Methods. 1997 Aug 22;207(1):43-51.

Cuddihy MJ, Kotov NA. Poly(lactic-co-glycolic acid) bone scaffolds with inverted colloidal crystal geometry. Tissue Eng A 2008;14(10):1639–49.

Cui et al., (2007). Application of multiple parallel perfused microbioreactors and three-dimensional stem cell culture for toxicity testing. Toxicology, 21(7):1318-24

Curcio E, Salerno S, Barbieri G, De Bartolo L, Drioli E, Bader A. 2007. Mass transfer and metabolic reactions in hepatocyte spheroids Biomaterials. 2007 Dec;28(36):5487-9

Darko Bal.et. (2004). Chondrogenic differentiation of bovine bone marrow mesenchymal stem cells in pellet cultural system. Experimental Hematology, 32: 502-509.

Davila et al., 2004 J.C. Davila, G.G. Cezar, M. Thiede, S. Strom, T. Miki and J. Trosko, Use and application of stem cells in toxicology, Toxicol. Sci. 79(2004), pp. 214–223.

Davila JC, Rodriguez RJ, Melchert RB, Acosta D Predictive value of in vitro model systems in toxicology. Annual Review of Pharmacology and Toxicology, Vol. 38, No. 1. (1998), pp. 63-96.

Davila JC, Morris DL.Analysis of cytochrome P450 and phase II conjugating enzyme expression in adult male rat hepatocytes. In Vitro Cell Dev Biol Anim. 1999 Mar;35(3):120-30.

De Boo, J. & Hendrik S En, C. (2005). Reduction strategies in animal research: a review of scientific approaches at the intra-experimental, supra-experimental and extraexperimental levels. altern. Lab. anim. 33, 369-77

Dean S, Tang JI, Seckl JR, Nyirenda MJ. 2010. Developmental and tissue specific regulation of hepatocyte nuclear factor 4-alpha (HNF4-alpha) isoforms in rodents. Gene Expr 14(6):337–344.

Decker ML, Behnke-Barclay M, Cook MG, La Pres JJ, Clark WA, Decker RS. Cell shape and organization of the contractile apparatus in cultured adult cardiac myocytes. J Mol Cell Cardiol 1991; 23: 817-832

Delongchamp R, Velasco C, Dial S, Harris AJ. Genome-wide estimation of gender differences in the gene expression of human livers: Statistical design and analysis BMC Bioinformatics (2005) Volume: 6, Issue: Suppl 2, Pages: S2-S13

Drew B and Leeuwenburgh C. Method for measuring ATP production in isolated mitochondria: ATP production in brain and liver mitochondria of Fischer-344 rats with age and caloric restriction, 2003. Am J Physiol Regul Integr Comp Physiol 285: R1259–R1267.

Dunn J. Textbook of Small Animal Medicine. WB Saunders, Toronto, 1999. 1065 pp. ISBN 0-7020-1582-2.

Dunn, J. C. Y., Tompkins, R. G., and Yarmush, M. L. (1991). Long-term in vitro function of adult hepatocytes in a collagen sandwich configuration.Biotechnol. Prog. 7, 237–245.

Ellis M.J., Chaudhuri J.B.: Poly(lactic-co-glycolic acid) hollow fibre membranes for use as a tissue engineering scaffold. Biotechnol. Bioeng.(2006) 96, 177-187.

Ezzell, R. M., Toner, M., Hendricks, K., Dunn, J. C. Y., Tompkins, R. G., and Yarmush, M. L. (1993). Effect of collagen gel configuration on the cytoskeleton in cultured rat hepatocytes. Exp. Cell Res. 208, 442–452.

Fabia J. and Slusarczyk,Cz. (2005). supermolecular structure of alginate fibres for medical application studies by means of WAXS and SAXS methods. Fibres and textlines in east europe, 5: 114-117

Falasca L. Miccheli A, Sartori E, Tomassini A, Devirgiliis LC.Hepatocytes Entrapped in Alginate Gel Beads and Cultured in Bioreactor: Rapid Repolarization and Reconstitution of Adhesion Areas. Cells Tissues Organs 2001;168:126-136

Fanning AS, Anderson JM. 2009. Zonula occludens-1 and -2 are cytosolic scaffolds that regulate the assembly of cellular junctions. Ann N Y Acad Sci 1165:113–120.

Fautz, R., Husein, B., Hechenberger, C., 1991. Application of the neutral red assay (NR assay) to monolayer cultures of primary hepatocytes: Rapid colorimetric viability determination for the unscheduled DNA synthesis test (UDS). Mutat. Res. 253, 173–179.

Feng ZQ, Chu XH, Huang NP, Leach MK, Wang G, Wang YC, Ding YT, Gu ZZRat hepatocyte aggregate formation on discrete aligned nanofibers of type-I collagen-coated poly(L-lactic acid). Biomaterials. 2010 May;31(13):3604-12. Epub 2010 Feb 9.

Fielder RJ, Atterwill CK, Anderson D, Boobis AR, Botham P, Chamberlain M, Combes R, Duffy PA, Lewis RW, Lumley CE, Kimber I, Newall DR. BTS working party report on in vitro toxicology. Hum Exp Toxicol. 1997 Nov;16 Suppl 1:S1-40.

Fields RD and LancasterMV. (1993). Dual-attribute continuous monitoring of cell proliferation/cytotoxicity. Am Biotechnol Lab, 11,48–50.

Figallo E, Cannizzaro C, Gerecht S,. Burdick JA, Langer R, Elvassore N and Vunjak-Novakovic G. Micro-bioreactor array for controlling cellular microenvironments Lab Chip, 2007, 7, 710-719

Fotakis G , Timbrell JA. In vitro cytotoxicity assays: Comparison of LDH, neutral red, MTT and protein assay in hepatoma cell lines following exposure to cadmium chloride. Toxicology Letters. Volume 160, Issue 2, 5 January 2006, Pages 171-177

Freed LEG, Biron RJ, Eagles DB, Lesnoy DC, Barlow SK, Langer R.Vunjak-Novakovic. (1994). Biodegradable polymer scaffolds for tissue engineering. Biotechnology; 12: 689-693

Gad SC. Recent developments in replacing, reducing, and refining animal use in toxicologic research and testing. Fundam. Appl. Toxcol 1990; 15:8-16

Ghosh, S., Spagnoli, G. C., Martin, I., Ploeger t, S., Demougin, P., Heberer, M. & Reschner, A. (2005). Three-dimensional culture of melanoma cells profoundly affects gene expression profile: a high density oligonucleotide array study. J. Cell physiol. 204, 522-31.

Gimble JM, Guilak F, Nuttall ME, Sathishkumar S, Vidal M, Bunnell BA. In vitro Differentiation Potential of Mesenchymal Stem Cells, Transfus Med Hemother 2008;35:228–238

Glenn M. WalkerHenry C. Zeringueb and David J. Beebea. (2004). Microenvironment design considerations for cellular scale studies,. LabChip, 4:91-97

Glicklis R, Shapiro L, Agbaria R, Merchuk JC, Cohen S. Hepatocyte behavior within three dimensional porous alginate scaffolds. Biotechnol Bioeng 2000;67(3):344-353.

Goegan P, Johnson G, Vincent R. Effects of serum protein and colloid on the alamarBlue assay in cell cultures. Toxicol In Vitro. 1995 Jun;9(3):257-66.

Gómez-Lechón MJ, Jover R, Donato T, Ponsoda X, Rodriguez C, Stenzel KG, Klocke R, Paul D, Guillén I, Bort R, Castell JV. Long-term expression of differentiated functions in hepatocytes cultured in three-dimensional collagen matrix. J Cell Physiol. 1998 Dec;177(4):553-62.

Gómez-Lechón MJ, Lahoz A, Gombau L, Castell JV, Donato MT In vitro evaluation of potential hepatotoxicity induced by drugs. Curr Pharm Des. 2010 Jun;16(17):1963-77.

Gómez-Lechón, M.J., Larrauri, A., Donato, T., López, P., Montoya, A. and Castell, J.V., 1988. Predictive value of the in vitro test for hepatotoxicity of xenobiotics. In: Guillouzo, A., Editor,, 1988. Liver Cells and Drugs, Colloque INSERM/John Libbey Eurotext Ltd, Paris, pp. 371–377.

Grayson WL, Ma T, Bunnell B. Human mesenchymal stem cells tissue development in 3D PET matrices. Biotechnol Prog 2004; 20: 905-912

Griffth. LG. and Swartz, M. A. Capturing complex 3D tissue physiology in vitro. Nature Rev. Mol. Cell Biol. 7, 211–224 (2006)

Guigoz Y, Werffeli P, Favre D, Juillerat M, Wellinger R, Honegger P.Aggregate cultures of foetal rat liver cells: development and maintenance of liver gene expression. Biol Cell. 1987;60(3):163-71.

Guillouzo A,1999 Survival and function of isolated hepatocytes after

cryopreservation,Chemico-Biological Interactions Vol(121), Issue 1, Pages 7-16

Guo JF, Jourdian GW, MacCallum DK. Culture and growth characteristics of chondrocytes encapsulated in alginate beads. Connect Tissue Res 1989; 19: 277-297

Hamamoto R, Yamada K, Kamihira M, Iijima S. Differentiation and proliferation of primary rat hepatocytes cultured as spheroids. J Biochem 1998;124(5):972-979.

Hamilton, G. A., Jolley, S. L., Gilbert, D., Coon, D. J., Barros, S., and LeCluyse, E. L. (2001). Regulation of cell morphology and cytochrome P450 expression in human hepatocytes by extracellular matrix and cell-cell interactions. Cell Tissue Res. 306, 85–99.

Handel TM, Johnson Z, Crown SE, Lau EK, Proudfoot AE Regulation of protein function by glycosaminoglycans--as exemplified by chemokines. Annu Rev Biochem. 2005;74:385-410.

Harada K, Mitaka T, Miyamoto, Sugimoto S, Ikeda S, Takeda H, et al. Rapid formation of hepatic organoid in collagen sponge by rat small hepatocytes and hepatic nonparenchymal cells. J Hepato 2003;39(5):716-723.

Hart T, Hughes D, Li Z, Anderton J, Williams C, Sceats E, Hill E, Cui Z, Three Dimensional Perfused Tissue Culture: a platform for acute and chronic toxicity testing. Poster, 2011 SOT

Hart, A.B., Lee, H.C., Shukla, S.G., Shukla, A., Osier, M., Eneman, D.J., Chiu, J.-F., 1999. Characterization of cadmium-induced apoptosis in rat lung epithelial cells: evidence for the participation of oxidant stress. Toxicology 133, 43–58.

Hay DC, Zhao D, Ross A, Mandalam R, Lebkowski J, Cui W. (2007): Direct differentiation of human embryonic stem cells to hepatocyte-like cells exhibiting functional activities. Cloning Stem Cells 9, 51-62.

Helmchen F. Denk W. and Deep tissue two-photon microscopy Nature Methods - 2, 932 - 940 (2005)

Hengstler, J. G., Brulport, M., Schormann, W., Bauer, A., Hermes, M., Nussler, A. K., Fandrich, F.,Ruhnke, M., Ungefroren, H., Griffin, L., Bockamp, E., Oesch, F., von Mach, M.-A. (2006).Generation of human hepatocytes by stem cell technology: definition of the hepatocyte.Expert Opin. Drug Metab. Toxicol. 1:61–74.

Henningson CT Jr, Stanislaus MA, Gewirtz AM. Embryonic and adult stem cell therapy. J Allergy Clin Immunol. 2003 Feb;111(2 Suppl):S745-53.

Hewitt NJ, Lechón MJ, Houston JB, Hallifax D, Brown HS, Maurel P, Kenna

JG, Gustavsson L, Lohmann C, Skonberg C, Guillouzo A, Tuschl G, Li AP, LeCluyse E, Groothuis GM, Hengstler JG.Primary hepatocytes: current understanding of the regulation of metabolic enzymes and transporter proteins, and pharmaceutical practice for the use of hepatocytes in metabolism, enzyme induction, transporter, clearance, and hepatotoxicity studies. Drug Metab Rev. 2007;39(1):159-234.

Holtfreter J. A study of the mechanics of gastrulation: Part II. J Exp Zool 1944; 95: 171-212

Hosseinkhani HY, Hiraoka Y, Inoue S, Tabata Y.Inatsugu. (2005). Perfusion culture enhances osteogenic differentiation of rat mesenchymal stem cells in collagen sponge reinforced with poly(glycolic acid) fiber. Tissue Eng , 11:1476–1488

Huh D, Gu W, Kamotani Y, Grotberg JB, Takayama S. Microfluidics for flow cytometric analysis of cells and particles. Physiol Meas 2005;26:R73–98

Hung PJ, Lee PJ, Sabounchi P, Lin R, Lee LP. Continuous perfusion microfluidic cell culture array for high-throughput cell-based assays. Biotechnol Bioeng 2005;89:1–8.

HuntmacherW.Dietmar. (2000). Scaffolds in tissue engineering bone and cartilage. Biomaterials, 21: 2529-2543

Jones D.L. and Fuller M.T., Stem cell niches. In: R. Lanza, Editor, Handbook of Stem Cells vol. 23, Elsevier Academic Press (2004), pp. 59–72.

Kadiyala SRG, Thiede MA, Bruder SPYoung. (1997). Culture expanded canine mesenchymal stem cells possess osteochondrogenic potential in vivo and in vitro. Cell Transplant., 6:125–134.

Kaji H, Nishizawa M, Matsue T. Localized chemical stimulation to micropatterned cells using multiple laminar fluid flows. Lab Chip 2003;3:208–11.

Kajsa P. Kanebratt and Tommy B. Andersson, 2008 Evaluation of HepaRG Cells as an in Vitro Model for Human Drug Metabolism Studies DRUG METABOLISM AND DISPOSITION Vol. 36, No. 7:1444-1452

Kazemnejad S, Allameh A, Gharehbaghian A, Soleimani M, Amirizadeh N, Jazayeri M,Efficient replacing of fetal bovine serum with human platelet releasate during propagation and differentiation of human bone-marrow-derived mesenchymal stem cells to functional hepatocyte-like cells. Vox Sanguinis (2008) Volume: 95, Issue: 2, Pages: 149-158

Kazemnejad et. al, Heapatic tissue engineering using scaffolds: state of the art Avicenna Journal of Medical Biotechnology, Oct. –Dec. 2009 Vol. 1, No. 3: 135-145

Kelm JM. Method for generation of homogeneous multicellular tumor spheroids applicable to a wide variety of cell types. Biotechnol. Bioeng. 83, 173-180. Methuen, 1959.

Kelm, J. M., TimminS, N. E., Brown, C. J., Fussenegger, M. & Nielsen, L. K. (2003).

Kern, A., Bader, A., Pichlmayr, R., and Sewing, K. F. (1997). Drug metabolism in hepatocyte sandwich cultures of rats and humans. Biochem. Pharmacol 54, 761–772.

Kevin C. KempHows, Craig DonaldsonJill. (2005). Bone marrow-derived mesenchymal stem cells. Leukemia&Lymphoma,, (11): 1531-1544

Kew MC, Serum aminotransferase concentration as evidence of hepatocellular damage Lancet. 2000 Feb 19;355(9204):591-2.

Khademhosseini A, Yeh J, Eng G, Karp J, Kaji H, Borenstein J, et al. Cell docking inside microwells within reversibly sealed microfluidic channels for fabricating multiphenotype cell arrays. Lab Chip 2005;5: 1380–6.

Kienhuis AS, Wortelboer HM, Hoflack JC, Moonen EJ, Kleinjans JC, van Ommen B, van Delft JH, Stierum RH.Comparison of coumarin-induced toxicity between sandwich-cultured primary rat hepatocytes and rats in vivo: a toxicogenomics approach. Drug Metab Dispos. 2006 Dec;34(12):2083-90.

King, K.; Terai, H.; Wang, C.; Vacanti, J. P.; Borenstein, J. T. Microfluidics for tissue engineering microvasculature: endothelial cell culture. Micro total analysis system conference, Monterrey, CA, 2001, 247-249.

Kleinman, HK. & Martin, G. R. (1989). Reconstituted basement membrane complex with biological activity. US Patent 4,829,000, 198)

Kleinman,HK. & Martin, G. R. Matrigel: Basement membrane matrix with biological activity. Seminars in Cancer Biology 15 (2005) 378–386

Kloss, D., Fischer, M., Rothermel, A., Simon, J. C. & Robitzki, A. A. (2008). Drug testing on 3D in vitro tissues trapped on a microcavity chip. Lab Chip 8, 879-84.

Kmat, A.M., Lamm, D.L., 2004. Antitumor activity of common antibiotics against superficial bladder cancer. Urology 63, 457–460.

Kmat, A.M., Lamm, D.L., 2004. Antitumor activity of common antibiotics against superficial bladder cancer. Urology 63, 457–460.

Knasmüller S et. al, Use of human-derived liver cell lines for the detection of environmental and dietary genotoxicants; current state of knowledge Toxicology

Volume 198, Issues 1-3, 20 May 2004, Pages 315-328

Knight, A. (2007a). Animal experiments scrutinised: systematic reviews demonstrate poor human clinical and toxicological utility. altex 24, 320-5.

Knight, A. (2007b). Systematic reviews of animal experiments demonstrate poor human poor human clinical and toxicological utility. Altern Lab Anim 2007; 35(6): 641-659.

Koide N, Shinji T, Tanabe T, Asano K, Kawaguchi M, Sakaguchi K, Koide Y, Mori M, Tsuji T. Continued high albumin production by multicellular spheroids of adult rat hepatocytes formed in the presence of liver-derived proteoglycans. Biochem Biophys Res Commun 1989; 161: 385-391

Kostov Y, Harms P, Randers-Eichhorn L, Rao G. 2001. Low-cost microbioreactor for high-throughput bioprocessing. Biotechnol Bioeng 72:346 – 352.

Kotov NA, Liu Y, Wang S, Cumming C, EghtedariM, Vargas G, et al. Invertedcolloidal crystals as three-dimensional cell scaffolds. Langmuir 2004;20(19):7887–92.

Kreeger PK, Woodruff TK, Shea LDMurine granulosa cell morphology and function are regulated by a synthetic Arg-Gly-Asp matrix. Mol Cell Endocrinol. 2003 Jul 31;205(1-2):1-10.

Lampert, H.P., O'Grady, F.W., 1992. Diaminopyrimidines. Antibiotic and Chemotherapy. Churchill Livingstone, Edinburgh, pp. 148–153

Landry J, Bernier D, Ouellet C, Goyette R, Marceau N. Spheroidal aggregate culture of rat liver cells: histotypic reorganization, biomatrix deposition, and maintenance of functional activities. J Cell Biol. 1985 Sep;101(3):914-23.

Lanza R, Langer, R and Vacanti J. Principles of Tissue Engineering (Third Edition) Chapter 48. 2007 P722

Lavon N, Yanuka O, Benvenisty N. (2004): Differentiation and isolation of hepatic-like cells from human embryonic stem cells. Differentiation 72, 230-8.

Lawrence JN, Benford DJ, Development of an optimal method for the cryopreservation ofhepatocytes and their subsequent monolayer culture. Toxicol In Vitro. 1991;5(1):39-50.

Lawson MAJE, Wang L, Shelton RM, Triffitt JT.Barralet. (2004). Adhesion and growth of bone marrow stromal cells on modified alginate hydrogels. Tissue Engineering, 10(9-10):1480-91

Lawton R.A., Price CR, Runge AF, Doherty WJ, Saavedra SS. Air plasma treatment of

submicron thick PDMS polymer films: effect of oxidation time and storage conditionsColloids and Surfaces A: Physicochemical and Engineering Aspects Volume 253, Issues 1-3, 1 February 2005, Pages 213-215

Lazar A, Peshwa MV, Wu FJ, Chi CM, Cerra FB, Hu WS. Formation of porcine hepatocyte spheroids for use in a bioartificial liver. Cell Transplant 1995;4(3):259-268.

Leclerc E, Sakai Y, Fujii TBiotechnol Prog. Microfluidic PDMS (polydimethylsiloxane) bioreactor for large-scale culture of hepatocytes. 2004 May-Jun;20(3):750-5.

Leclerc, E.; Sakai, Y.; Fujii, T. Fabrication of microstructures in photosensitive biodegradables polymers for tissue engineering applications. Biomaterials 2004 Aug;25(19):4683-90

LeCluyse E, Bullock P, Madan A, Carroll K, Parkinson A Influence of extracellular matrix overlay and medium formulation on the induction of cytochrome P-450 2B enzymes in primary cultures of rat hepatocytes. 1999 Drug metabolism and disposition Vol. 27, No. 8: 909-915

LeCluyse EL, Alexandre E, Hamilton GA, Viollon-Abadie C, Coon DJ, Jolley S, Richert L. Isolation and culture of primary human hepatocytes. Methods Mol Biol. 2005;290:207-29.

LeCluyse EL. Human hepatocyte culture systems for the in vitro evaluation of cytochrome P450 expression and regulation Eur J Pharm Sci. 2001 Jul;13(4):343-68.

Lee J, Shanbhag S, Kotov NA. Inverted colloidal crystals as three-dimensional microenvironments for cellular co-cultures. J Mater Chem2006;16(35):3558–64.

Lee KD, Kuo TK, Whang-Peng J, Chung YF, Lin CT, Chou SH, Chen JR, Chen YP, Lee OK: In vitro hepatic differentiation of human mesenchymal stem cells. Hepatology 2004;40:1275–1284.

LeeJooWoo. (2008). Three-dimensional cell culture matricx: state of the art. Tissue Engineeing, 14:61-86

Levenberg SNF, Lavik E, Rogers AB, Itskovitz-Eldor J, Langer R.Huang. (2003). Differentiation of human embryonic stem cells on three-dimensional polymer scaffolds. Proc Natl Acad Sci , 100: 12741-12746

Li J, Ning G, Duncan SA. 2000. Mammalian hepatocyte differentiation requires the transcription factor HNF-4alpha. Genes Dev 14(4):464–474.

Lindena J, Friedel R, Rapp K, Sommerfeld U, Trautschold I, Deerberg F (1980) Long-term observation of plasma and tissue enyzme activities in the rat. Mechanisms of

Ageing and Development 14, 379-407

Lindros KO, Oinonen T, Issakainen J, Nagy P, Thorgeirsson SS. 1997. Zonal distribution of transcripts of four hepatic transcription factors in the mature rat liver. Cell Biol Toxicol 13(4–5):257–262.

Lorenz Meinelal.et. (2004). Bone Tissue Engineering Using Human Mesenchymal Stem Cells: Effects of Scaffold Material and Medium Flow. Annals of Biomedical Engineering, Vol. 32, No. 1, pp.,112–122

Lu HF, Chua KN, Zhang PC, Lim WC, Ramakrishna S, Leong KW, et al. Three-dimensional coculture of rat hepatocyte spheroids and NIH/3T3 fibroblasts enhances hepatocyte functional maintenance. Acta Biomater 2005;1(4):399-410.

Lucena MI, García-Cortés M, Cueto R, Lopez-Duran J, Andrade RJ. Assessment of drug-induced liver injury in clinical practice. Fundam Clin Pharmacol. 2008 Apr;22(2):141-58.

Maffia AM 3rd, Kariv II, Oldenburg KR. 1999. Miniaturization of a mammalian cell-based assay: luciferase reporter gene readout in a 3 microliter 1536-well plate. J Biomol Screen 4:137 – 142.

Martinsen A, Skjbk-Braek, G, and SmidsrØd O. (1989)Alginate as Immobilization Material: I. Correlation between Chemical and Physical Properties of Alginate Gel Beads. Biotechnology and Bioengineering, Vol. 33, Pp.79-89

Marx-Stoelting P, Adriaens E, Ahr H, et. al, A Review of the Implementation of the Embryonic Stem Cell Test (EST) ATLA 37, 313–328, 2009

Mazzoleni G, Di Lorenzo D, Steimberg N. Modelling tissues in 3D: the next future of pharmaco-toxicology and food research? Genes nutr. 2009 (4), 13-22.

Mazzoleni, G., Di Lorenzo, D. & Steimberg, N. (2009). Modelling tissues in 3D: the mechanical constraints. A comparative review. Tissue Eng. 12, 2367-2383.

Mineault M, Batra SK, Recent insights into the moleculat mechanisms involved in aging and the maligmant transformation of adult stem/progenitor cells and their therapeutic implications. Ageing Res Rev. 2009 Apr;8(2):94-112.

Miranda JP, Rodrigues A, Tostões RM, Leite S, Zimmerman H, Carrondo MJ, Alves PM. Extending hepatocyte functionality for drug-testing applications using high-viscosity alginate-encapsulated three-dimensional cultures in bioreactors. Tissue Eng Part C Methods. 2010 Dec;16(6):1223-32.

Miyamoto Y, Suzuki S, Nomura K, and Enosawa S, Improvement of Hepatocyte

Viability After Cryopreservation by Supplementation of Long-Chain Oligosaccharide in the Freezing Medium in Rats and Humans. Cell Transplantation, Vol. 15, pp. 911–919, 2006

Moccona, A. (1961). Rotation-mediated histogenetic aggregation of dissociated cells. A quantifiable approach to cell interactions in vitro. Exp. Cell Res. 22, 455-475.

Moghe, P. V., Coger, R. N., Toner, M., and Yarmush, M. L. (1997). Cell-cell interactions are essential for maintenance of hepatocyte function in collagen gel but not on Matrigel. Biotechnol. Bioeng. 56, 706–711.

Moll, R., Franke, W.W., and Schiller, D.L. The catalog of human cytokeratins: patterns of expression in normal epithelia tumors and cultured cells. Cell 31, 11, 1982

Morgan, D.C., Mills, C.K., Lefkowitz, L.D., Lefkowitz, S.S., 1991. An improved colorimetric assay for tumor necrosis factor using WEHI 164 cells cultured on novel microtiter plates. J. Immunol. Meth. 145, 259–262.

Moscona A. Cell suspensions from organ rudiments of chick embryos. Exp Cell Res 1952; 3: 535-539

Moscona A. Rotation-mediated histogenetic aggregation of dissociated cells. A quantifiable approach to cell interactions in vitro. Exp Cell Res 1961; 22: 455-475

Moscona A. The development in vitro of chimeric aggregates of dissociated embryonic chick and mouse cells. Proc Natl Acad Sci USA 1957; 43: 184-194

MosmannT. (1983). Rapid colorimetric assay for cellular growth and survival: application to proliferation and cytotoxicity assays. Jounal of Immunol Meth, 65,55-63.

Nakamura K, Mizutani R, Sanbe A, Enosawa S, Kasahara M, Nakagawa A, Ejiri Y, Murayama N, Miyamoto Y, Torii T, Kusakawa S, Yamauchi J, Fukuda M, Yamazaki H, Tanoue A.Evaluation of drug toxicity with hepatocytes cultured in a micro-space cell culture system. J Biosci Bioeng. 2011 Jan;111(1):78-84.

Nguyen TH and N Ferry, Liver gene therapy: advances and hurdles ,Gene Therapy (2004) 11, S76–S84.

Novak JP, Sladek R, Hudson TJ.Characterization of variability in large-scale gene expression data: implications for study design. Genomics. 2002 Jan;79(1):104-13

O'Brien P. J., Slaughter M. R., Polley S. R. & Kramer K. Advantages of glutamate dehydrogenase as a blood biomarker of acute hepatic injury in rats, Laboratory Animals (2002) 36, 313–321

O'Brien PJ, Slaughter MR, Swain A, Birmingham JM,Greenhill RW, Elcock F, Bugelski PJ (2000)Repeated acetaminophen dosing in rats: adaptation of hepatic antioxidant system. Human and Experimental Toxicology 19, 277-83

Oh SH, Park IK, Kim JM and Lee JH In vitro and in vivo characteristics of PCL scaffolds with pore size gradient fabricated by a centrifugation method Biomaterials Volume 28, Issue 9, 2007, Pages 1664-1671

Okumoto K, Saito T, Hattori E, Ito JI, Adachi T, Takeda T, Sugahara K, Watanabe H, Saito K, Togashi H, Kawata S: Differentiation of bone marrow cells into cells that express liver-specific genes in vitro: implication of the Notch signals in differentiation. Biochem Biophys Res Commun 2003; 304:691–695

Olson H, Betton G, Robinson D, Thomas K, Monro A, Kolaja G, Lilly P, Sanders J, Sipes G, Bracken W, Dorato M, Van Deun K, Smith P, Berger B, Heller A. (2000). Concordance of the toxicity of pharmaceuticals in humans and in animals. Regul. Toxicol. pharmacol. 32, 56-67.

Olsson T, Gulliksson H, Palmeborn M, Bergström K, Thore ALeakage of adenylate kinase from stored blood cells. J Appl Biochem. 1983 Dec;5(6):437-45.

Ong SM, Zhang C, Toh YC, Kim SH, Foo HL, Tan CH, van Noort D, Park S, Yu H A gel-free 3D microfluidic cell culture system. Biomaterials. 2008 Aug;29(22):3237-44

Ouchi H, K. Otsu, T. Kuzumaki, Y. Iuchi and K. Ishikawa,Synergistic induction by collagen and fibronectin of liver-specific genes in rat primary cultured hepatocytes. Archives of Biochemistry and Biophysics Volume 358, Issue 1, 1 October 1998, Pages 58-62

Pampaloni, F. & Stelzer, E. H. K, Three-Dimensional cell cultures in toxicology. Biotechnology and Genetic Engineering Reviews - Vol. 26, 129-150 (2009)

Paquette JA, Kumpf SW, Streck RD, Thomson JJ, Chapin RE, Stedman DB. Assessment of the Embryonic Stem Cell Test and application and use in the pharmaceutical industry. Birth Defects Res B Dev Reprod Toxicol. 2008 Apr;83(2):104-11.

Parker DM and John J. Holbrook The oxaloacetate reductase activity of vertebrate lactate dehydrogenase, 1981 International Journal of Biochemistry Volume 13, Issue 10, Pages 1101-1105

Pittenger MFAM, Beck SC, Jaiswal RK, Douglas R, Mosca JD et al.Mackay. (1999). Multilineage potential of adult human mesenchymal stem cells. Science, 284: 143-147

Pouton CW, Haynes JM. Pharmaceutical applications of embryonic stem cells. Adv

Drug Deliv Rev. 2005, 57(13):1918-34

Pouton CW, Haynes JM: Embryonic stem cells as a source of models for drug discovery. Nat Rev Drug Discov 2007;6:605-616.

Powers, M.; Domansky, K.; Udapadhia, A.; KazempurMofrad, M.; Kursawky, P.; Janigan, D. M.; Wack, K.; Stolz, D.; Kamm, R.; Griffith, L. A. microarray perfusion bioreactor for 3D liver culture. Biotechnol. Bioeng. 2001, 78, 257-269

Powers, M.; Janigan, D.; Wack, K.; Baker, C.; Stolz, D.; Griffith, L. Functional behavior of primary rat liver cells in a three-dimensional perfused microarray bioreactor. Tissue Eng. 2002, 8 (3), 499-513..

Price, P.S., Keenan, R.E. and Swartout, J.C., (2008). Characterising interspecies uncertainty using data from studies of anti-neoplastic agents in animals and humans. Toxicology and Applied Pharmacology. Article in Press

Pritchard CC,Hsu L,Delrow J and Nelson PS. (2001) Project normal: Defining normal variance in mouse gene expression. Proc. Natl. Acad. Sci. USA98 (23), 13266–13271.

Rambhatla L, Chiu CP, Kundu P, Peng Y, Carpenter MK. (2003): Generation of hepatocyte-like cells from human embryonic stem cells. Cell Transplant 12, 1-11.

Raty S, Walters EM, Davis J, Zeringue H, Beebe DJ, Rodriguez-Zas SL, et al. Embryonic development in the mouse is enhanced via microchannel culture. Lab Chip 2004;4:186–90.

Rej R, Aspartate aminotransferase activity and isoenzyme proportions in human liver tissues, Clin Chem 24 (1978), pp. 1971–1979

Riccalton-Banks L, Liew C, Bhandari R, Fry J, Shakesheff K. Long-term culture of functional liver tissue: three-dimensional coculture of primary hepatocytes and stellate cells. Tissue Eng. 2003 Jun;9(3):401-10.

Richert L, Liguori MJ, Abadie C, Heyd B, Mantion G, Halkic N, Waring JF. Gene expression in human hepatocytes in suspension after isolation is similar to the liver of origin, is not affected by hepatocyte cold storage and cryopreservation, but is strongly changed after hepatocyte plating. Drug Metab Dispos. 2006 May;34(5):870-9. Epub 2006 Feb 10.

Richert, L., Liguori, M. J., Abadie, C., Heyd, B., Mantion, G., Halkic, N., Waring, J. F. (2006). Gene expression in human hepatocytes in suspension after isolation is similar to the liver of origin,is not affected by hepatocyte cold storage and cryopreservation, but is strongly changed after hepatocyte plating. Drug Metab. Dispos. 34(5):870–879.

Rolletschek, P. Blysczuk and A.M. Wobus, Embryonic stem cell-derived cardiac, neuronal and pancreatic cells as model systems to study toxicological effects, Toxicol. Lett. 149 (2004), pp. 361–369.

Rotunda et al . Detergent Effects of Sodium Deoxycholate Are a Major Feature of an Injectable Phosphatidylcholine Formulation Used for Localized Fat Dissolution Dermatol Surg 2004;30:1001–1008

Rowley JA, Madlambayan G, Mooney DJ. Alginate hydrogels as synthetic extracellular matrix materials. Biomaterials. 1999 Jan;20(1):45-53

Rubin LL: Stem cells and drug discovery: the beginning of a new era.Cell. 2008 Feb 22;132(4)

Russell WMS, Burch RL. The principles of humane experimental technique.1959

S.Al-NasiryM.Hanssens, C.Luyten and R.Pijnenborg,N.Geusens,.(2007). The use of AlamarBlue assay for quantitative analysis of viability, migration and invasion of choriocarcinoma cells,. Human Reproduction, Vol.22, No.5 pp.1304–1309,.

Sahu S, Michael W. O'Donnell Jr and Paddy L. Wiesenfeld Comparative hepatotoxicity of deoxynivalenol in rat, mouse and human liver cells in culture J. Appl. Toxicol. 2010; 30: 566–573

Sahu S. Hepatotoxicity. Wiley. 2007

Sams A.V, Li ZS and Powers J., The Application of 3D Alginate Scaffolds for Liver Tissue Modelling, Primary & Stem Cell Systems, Invitrogen Corporation, Frederick, MD, USA, 21704

Sawada N, Tomomura A, Sattler CA, Sattler GL, Kleinman HK, Pitot HC. Effects of extracellular matrix components on the growth and differentiation of cultured rat hepatocytes. In Vitro 1987;23:267–73.

Scheers et al., 2001 M.E. Scheers, Ba Ekwall and J.P. Dierickx, In vitro long-term cytotoxicity testing of 27 MEIC chemicals on HepG2 cells and comparison with acute human toxicity data, Toxicol. In Vitro 15(2001), pp. 153–161.

Scheutz EG, Li D, Omiencski C, Eberhard UM, Kleinman HK, Elswick B, et al. Regulation and gene expression in adult rat hepatocytes cultured on an extracellular basement membrane matrix. J Cellul Physiol 1988;134:309–23.

Schirmer K., Chan A.G.J., G.M. Greenberg, D.G. Dixon and N.C. Bols, Methodology for demonstrating and measuring the photocytotoxicity of fluoranthene to fish cells in culture, Toxicol In Vitro11 (1997), pp. 107–119.

Schmidt E and Schmidt FW, Enzyme diagnosis in diseases of the liver and biliary system. In: E Schmidt, FW Schmidt, I Trautschold and R Friedel, Editors, Advances in clinical enzymology vol 1, Karger, Basel (1979), pp. 239–292.

Schmidt ES, Schmidt FW (1988) Glutamate dehydrogenase: biochemical and clinical aspects of an interesting enzyme. Clinica Chimica Acta 43, 43-56

Schrem H, Klempnauer J, Borlak J. 2002. Liver-enriched transcription factors in liver function and development. Part I: The hepatocyte nuclear factor network and liver-specific gene expression. Pharmacol Rev 54(1):129–158.

Schuster D, Laggner C, Langer T. Why drugs fail--a study on side effects in new chemical entities.Curr Pharm Des. 2005;11(27):3545-59.

Schwartz RE, Reyes M, Koodie L, Jiang Y, Blackstad M, Lund T, Lenvik T, Johnson S, Hu WS, Verfaillie CM: Multipotent adult progenitor cells from bone marrow differentiate into functional hepatocyte-like cells. J Clin Invest 2002;109:1291–1302.

Senthil Kumar Pazhansamy, Vinu Jyothi Stem Cells in Drug Discovery: Current trends and Emerging Challenges.Hygeia.J.D.Med Vol2 (1), Mar-Aug 2010:1-13

Seo MJ, Suh SY, Bae YC, Jung JS: Differentiation of human adipose stromal cells into hepatic lineage in vitro and in vivo. Biochem Biophys Res Commun 2005;328:258–264

Sgodda M, Aurich H, Kleist S, Aurich I, Konig S, Dollinger MM, Fleig WE, Christ B: Hepatocyte differentiation of mesenchymal stem cells from rat peritoneal adipose tissue in vitro and in vivo. Exp Cell Res 2007;313:2875–2886

Shahan TAPD, et al.,Siegel. (1994). A sensitive new bioassay for turmor necrosis factor. J Immunol Meth, 170: 211-224.

Shanbhag S, Lee J, Kotov AN. Diffusion in three-dimensionally ordered scaffolds with inverted colloidal crystal geometry. Biomaterials 2005;26(27):5581–5.

Shi XL, Qiu YD, Li Q, Xie T, Zhu ZH, Chen LL, Li L, Ding YT Hepatocyte-like cells from directed differentiation of mouse bone marrow cells in vitro. Acta Pharmacologica Sinica (2005) 26, 469–476

Shirahashi H, Wu J, Yamamoto N, Catana A, Wege H, Wager B, Okita K, Zern MA. Differentiation of human and mouse embryonic stem cells along a hepatocyte lineage. Cell Transplant. 2004;13(3):197-211

Shoichet MS, Li H, White ML et. al. Winn SL. 1996 Stability of Hydrogels Used in Cell Encapsulation: An In Vitro Comparison of Alginate and Agarose. Biotechnol Bioeng. 1996 May 20;50(4):374-81

Sidney Green, Alan Goldberg, Joanne Zurlo TestSmart–High Production Volume Chemicals: An Approach to Implementing Alternatives into Regulatory Toxicology Toxicol. Sci. (2001) 63 (1): 6-14.

Slater K.Cytotoxicity tests for high-throughput drug discovery. Curr Opin Biotechnol. 2001 Feb;12(1):70-4.

So. PTC et al. Two-photon excitation fluorescence microscope. Annu. Rev. Biomed. Eng. 2000. 02:399–429

Song JW, Gu W, Futai N, Warner KA, Nor JE, Takayama S. Computer-controlled microcirculatory support system for endothelial cell culture and shearing. Anal Chem 2005;77:3993–9.

Strober W. Trypan blue exclusion test of cell viability. Curr Protoc Immunol. 2001 May;Appendix 3:Appendix 3B.

Sudo R. Mitaka T, Ikeda M,* and Tanishita K, Reconstruction of 3D stacked-up structures by rat small hepatocytes on microporous membranes *The FASEB Journal*. 2005;19:1695-1697.

Sutherland RM, Durand RE. Radiation response of multicell spheroids--an in vitro tumour model. Curr Top Radiat Res Q 1976; 11: 87-139

Szita, N.; Zanzotto, A.; Boccazzi, P; Sinskey, A.; Schmidt, M.; Jensen, K, Monitoring of cell growth, oxygen and pH in microfermentors. Micro Total Analysis System conference, Nara, Japan, 2002, 7-9.

Talens-Visconti R, Bonora A, Jover R, Mirabet V, Carbonell F, Castell JV, Gomez-Lechon MJ: Hepatogenic differentiation of human mesenchymal stem cells from adipose tissue in comparison with bone marrow mesenchymal stem cells. World J Gastroenterol 2006;12:5834–5845

Talwar G.P.and Srivastava L.M. The textbook of biochemistry and human biology third edition. PHI Learning Pvt. Ltd. 2004 Page 267
Taylor AM, Blurton-Jones M, Rhee SW, Cribbs DH, Cotman CW, Jeon NL. A microfluidic culture platform for CNS axonal injury, regeneration and transport. Nat Methods 2005;2:599–605.

Technical bulletin, CellTiter-Blue, Cell Viability assay instuctions

Terranova VP, Aumailley M, Sultan LH, Martin GR, Kleinman HK. Regulation of cell attachment and cell number by fibronectin and laminin. J Cell Physiol 1986;127:473–9.

Thiede. MA. And Tonkens R. Stem cell application and opportunities in drug discovery.

Spring 2009 issue of DDW

Timmins, N. E., Dietmair, S. & Nielsen L. K. (2004). Hanging-drop multicellular spheroids as a model of tumour angiogenesis. angiogenesis 7, 97-103.

Timpl R, Rohde H, Robey PG, Rennard SI, Foidart JM, Martin GR.Laminin-a glycoprotein from basement membranes. J Biol Chem 1979;254:9933–7

Tonkens, R., May. June. 2005. An overview of drug delopment process. The physician executive.

Torisawa YS, Takagi A, Nashimoto Y, Yasukawa T, Shiku H, Matsue T. A multicellular spheroid array to realize spheroid formation, culture, and viability assay on a chip. Biomaterials. 2007 Jan;28(3):559-66.

Torisawaa YS, Takagia A, Nashimotoa Y, Yasukawaa T, et. al A multicellular spheroid array to realize spheroid formation, culture, and viability assay on a chip Biomaterials 2007Volume 28, Issue 3, pages 559-566

Tourovskaia A, Figueroa-Masot X, Folch A. Differentiation-on-achip: a microfluidic platform for long-term cell culture studies. Lab Chip 2005;5:14–9.

Trainer, N. (2007). Transfer report. Novel methods for skeletal drug testing using human mesenchymal stem cells in a three dimensional scaffold. University of Oxford.

Tully, B.D., Collins, J.B., Overstreet, J.D., Smith, S.C., Dinse, E.G., Mumtaz, M.M., Chapin, E.R., 2000. Effects of arsenic, cadmium, chromium, and lead on gene expression regulated by a battery of 13 different promoters in recombinant HepG2 cells. Toxicol. Appl. Pharmacol. 168, 79–90.

Tunca, B., Egeli, U., Aydemir, N., Cecener, G., Bilaloglu, R., 2002.Investigation of the genotoxic effect in bone marrow of Swiss albino mice exposed long-term to pyrimethamine. Teratogen. Carcinogen.Mutagen. 22, 393–402.

Tuschl G, Lauer B, Mueller SO.Primary hepatocytes as a model to analyze species-specific toxicity and drug metabolism. Expert Opin Drug Metab Toxicol. 2008 Jul;4(7):855-70.

Ukelis, U., Kramer, P.J., Olejniczak, K. and Mueller, S.O., (2008). Replacement of in vivo acute oral toxicity studies by in vitro cytotoxicity methods: Opportunities, limits and regulatory status. Regulatory Toxicology and Pharmacology. 51:108-118

Verhoeff FH, Brabin BJ, Hart CA, Chimsuku L, Kazembe P, Broadhead RL.Increased prevalence of malaria in HIV-infected pregnant women and its implications for malaria control. Trop Med Int Health. 1999 Jan;4(1):5-12.

Viravaidya K, Shuler ML. Incorporation of 3T3-L1 cells to mimic bioaccumulation in a microscale cell culture analog device for toxicity studies. Biotechnol Prog 2004;20:590–7.

Vozzi, G.; Flaim, C.; Bianchi, F.; Ahluwalia, A.; Bhatia, S. Microfabricated, PLGA scaffolds: a comparative study for application to tissue engineering. Mater. Sci. Eng. C 2002, C20, 43-47.

Walker G MM S and Beebe D JOzers. (2002). Insect cell culture in microfluidic channels. Biomed Microdev, 4 161–6

Walker GM, Zeringue HC, Beebe DJ. Microenvironment design considerations for cellular scale studies. Lab Chip 2004;4:91–7

Wallace DC. Mitochondrial DNA in aging and disease. Sci Am 277: 40–47, 1997.

Wang LS et. al. Evaluation of MTS, XTT, MTT and3HTdR incorporation for assessing hepatocyte density, viability and proliferation. 1996 Methods in Cell Science 18: 249-255.

Wang Y, Kim UJ, Blasioli DJ, Kim HJ, Kaplan DL. In vitro cartilage tissue engineering with 3D porous aqueousderived silk scaf f olds and mesenchymal st em cells. Biomaterials 2005; 26: 7082-7094

Wang YJ, Liu HL, Guo HT, Wen HW, Liu J. Primary hepatocyte culture in collagen gel mixture and collagen sandwich. World J Gastroenterol. 2004 Mar 1;10(5):699-702.

Wen F., Chang S. Y.C. Toh, S.H. Teoh and H. YubDevelopment of poly (lactic-co-glycolic acid)-collagen scaffolds for tissue engineering Materials Science and Engineering: C Volume 27, Issue 2, March 2007, Pages 285-292

Wu FJ, Friend JR, Remmel RP, Cerra FB, Hu WS. Enhanced cyt ochrome P450 I A1 act ivit y of self - assembled rat hepatocyte spheroids. Cell Transplant 1999; 8: 233-246

Wu M.H. al.,et. (2007). Effect of extracellular pH on matrix synthesis by chondrocytes in 3D agarose gel. Biotechnol. Prog, 23: 430-434

Wu MH, Cai H, Xu X, Urban JP, Cui ZF, Cui Z A SU-8/PDMS hybrid microfluidic device with integrated optical fibers for online monitoring of lactate. Biomed Microdevices. 2005 Dec;7(4):323-9.

Wu X, Ding S, Ding Q, Gray NS, Schultz PG: Small molecules that induce cardiomyogenesis in embryonic stem cells. J Am Chem Soc 2004;126:1590-1591.

Yagi K, Tsuda K, Serada M, Yamada C, Kondoh A, Miura Y Rapid formation of

multicellular spheroids of adult rat hepatocytes by rotation culture and their immobilization within calcium alginate. Artif Organs. 1993 Nov;17(11):929-34.

Yamashita Y, Shimada M, Harimoto N, Tanaka S, Shirabe K, Ijima H, Nakazawa K, Fukuda J, Funatsu K, Maehara YcDNA microarray analysis in hepatocyte differentiation in Huh 7 cells. Cell Transplant. 2004;13(7-8):793-9.

Yang S, Leong KF, Du Z, Chua CK. The design of scaffolds for use in tissue engineering. Part I. Traditional factors. Tissue Eng. 2001 Dec;7(6):679-89.

Yang SM. Lee. DH. Park JK. 2000 Effects of Degree of Cell-Cell Contact on Liver Specific Functions of Rat Primary Hepatocytes .Biotechnol. Bioprocess Eng. 2000, 5: 99-105

Yi-Chin Toh, Chi Zhang, Jing Zhang, Yuet Mei Khong, Shi Chang, Victor D. Samper, Danny van Noort, Dietmar W. Hutmacher and Hanry Yu A novel 3D mammalian cell perfusion-culture system in microfluidic channels Lab Chip, 2007, 7, 302-309

Yu HI, Shkel I A and Beebe D JMeyvantsson. (2005). Diffusion dependent cell behavior in microenvironments. Lab Chip 5

Zambrowicz BP, Sands AT.Knockouts model the 100 best-selling drugs--will they model the next 100? New Rev Drug Discov.2003, 2(1): 38-51

Zanzotto, A.; Szita, N.; Boccazzi, P.; Sinskey, A.; Jensen, K. Growth and oxygenation in a membrane-aerated microbioreactor for high-throughput bioprocessing. AIChE Annual Meeting, San Francisco, CA, 2003, 206a.

Zuang V, Eskes C, Griesinger C and Hartung T. ECVAM key area topical toxicity: Update on activities AATEX 14, Special Issue, 523-528 Proc. 6th World Congress on Alternatives & Animal Use in the Life Sciences August 21-25, 2007, Tokyo, Japan

Appendix A: List of Publications

Conference Papers:

Use of Three Dimensional Perfused Liver Models to Study Drug Hepatotoxicity. Hart T., Yang J. Anderton J., Hughes D., Li Z., Sceats E., Williams C., Cui Z., Rossi A. the 47th Congress of the European Societies of Toxicology (EUROTOX 2011), Paris, France. Poster

3D Cell Culture Improves Detection of Oxazolidinone Toxicity, J. Yang; X. Xu; K. Howe; J. Dykens; Z. Cui. the 50th Annual Meeting of the Society of Toxicology, March, 2011 in Washington, D.C. the U. S.

TissueFlex®, an advanced cell culture system for toxicity testing. Li Z, Yang J, Urban J, Cui Z, Hart T. 49th Annual Meeting &ToxExpoTM March, 2010, Salt Lake City, the U.S. Poster

Improve the Mechanical Strength of Collagen Scaffolds by Mechanical Compression J.Yang, X. Xu, R.Field, Z.F.Cui, International Bioengineering Conference 2009, Oxford, UK. Presented Poster

Engineering postgraduates Poster presentation - second year DPhil, 2008, Oxford, UK

Appendix B: Guava ViaCount Protocol

Materials required:

1) The Guava Technologies, PCA 96, Millipore, UK
2) Guava bead kit, Millipore, UK
3) Guava ViaCount Reagent
4) 10% and 20% (v/v) bleach/dH_2O , dH_2O
5) 1ml Eppendorfs with lip/scroll cap
6) 1 × PBS

Guava Check

1) Turn the computer and the Guava Technologies on, and click Guava Check.
2) Replace 6 × 1ml eppendorfs. Fill up the each tube with water and 20% bleach into the right position, according to the schematic figure on the screening.
3) 'Back flash'→ 'Quick Clean' × 2
4) Make up guava beads (475µl PBS+ 25µl well mixed beads), then place in position 1→ 'check'
5) Only if the count results are less than 0.03% considered as the fail, the system needs to be checked again.

Guava ViaCount

1) Go back to the main menu, click 'Guava ViaCount'
2) Create new 'worklist', fill in the blanks with the right dilution ratio of the cells/Guava ViaCount reagent, sample numbers, and the positions where the sample will be placed. Then 'save'.
3) Make samples with 375µl Guava ViaCount reagent +25µl cells (1:16 dilution), select right guava worklist, then start with 'Adjust settings': adjust the PM1 and PM2 at 10e2.
4) Acquire samples→ start
5) Segment the samples population with alive and dead cells. Cells numbers/ cell densities will be shown on the screen after counting.

Appendix C: R Code for Analysis of Gene Expression

R code for the analysis of whole genome expression data either sandwich culture (2D) or self assembly spheroid culture (3D) in vitro cultures, as well as from freshly obtained ex vivo hepatocytes.

```
# load required packages:
library("affy")
library("arrayQualityMetrics")
library("limma")
library("rat2302.db")
library("pcaMethods")
library("scatterplot3d")
library("genefilter")
library("gplots")
library("GOstats")
library("GO.db")
library("Hmisc")

# set working directory:
setwd(getwd())

# load raw data from .cel files:
df<- read.delim("targets.txt",sep="\t")
filenames <- as.vector(df$SampleID)
pheno <- read.AnnotatedDataFrame(filename="targets.txt")
data <- read.affybatch(filenames=filenames,phenoData=pheno)

# rma normalise the data:
normdata <- rma(data)

# filter probes to remove those with small variance & those without an entrez ID
(control probes etc):
filtdata <- nsFilter(normdata,require.entrez=TRUE,var.filter=TRUE,var.cutoff=0.3)

# run QC on raw data:
qanorm_raw =
arrayQualityMetrics(data,outdir="QC_raw",force=TRUE,do.logtransform=TRUE,intgr
oup=as.character("Levs"),grouprep=TRUE)

#run QC on normalised data:
```

```
qanorm =
arrayQualityMetrics(normdata,outdir="QC_norm",force=TRUE,do.logtransform=TRU
E,intgroup=as.character("Levs"),grouprep=TRUE)

# compute differential expression with limma:
lev <- unique(df$Levs)
f <- factor(df$Levs,lev)
design <- model.matrix(~0+f)
colnames(design) = lev
fit <- lmFit(filtdata$eset, design)
cont.matrix <-
makeContrasts("threeD_3-twoD_3","threeD_6-twoD_6","twoD_3-fresh_0","threeD_3-f
resh_0",
            "twoD_3-tissue_0","threeD_3-tissue_0","(threeD_3-fresh_0)-(twoD_3-fresh_
0)",levels=design)
fit2 = contrasts.fit(fit, cont.matrix)
fit2 = eBayes(fit2)
results <- decideTests(fit2,adjust.method="fdr",p.value=0.05)
results_fc1 <- decideTests(fit2,adjust.method="fdr",p.value=0.05,lfc="1")

# output counds of differentially expressed genes:
write.table(summary(results),file="result_summary.txt",sep="\t",quote=FALSE,eol="\r"
)

# load microarray probe annotations:
entrez <- rat2302ENTREZID
mapped_probes <- mappedkeys(entrez)
entrez2 <- as.list(entrez[mapped_probes])

hugo <- rat2302SYMBOL
mapped_hugo <- mappedkeys(hugo)
hugo2 <- as.list(hugo[mapped_hugo])

# generate and save lists of differentially expressed genes for each comparison of
interest:
threeD3_twoD3 =
topTable(fit2,coef=1,adjust.method="fdr",p.value=0.05,number=Inf,lfc="1",sort.by="lo
gFC")
threeD3_twoD3 =
cbind(threeD3_twoD3,as.character(entrez2[threeD3_twoD3$ID]),as.character(hugo2[th
reeD3_twoD3$ID]))
write.table(threeD3_twoD3,file="threeD3_twoD3_FILT_results.txt",sep="\t",quote=FA
LSE,eol="\r")
```

```
threeD6_twoD6 =
topTable(fit2,coef=2,adjust="fdr",p.value=0.05,number=Inf,sort.by="logFC")
threeD6_twoD6 =
cbind(threeD6_twoD6,as.character(entrez2[threeD6_twoD6$ID]),as.character(hugo2[th
reeD6_twoD6$ID]))
write.table(threeD6_twoD6,file="threeD6_twoD6_FILT_results.txt",sep="\t",quote=FA
LSE)

twoD3_fresh0 =
topTable(fit2,coef=3,adjust="fdr",p.value=0.05,number=Inf,lfc="1",sort.by="logFC")
twoD3_fresh0 =
cbind(twoD3_fresh0,as.character(entrez2[twoD3_fresh0$ID]),as.character(hugo2[twoD
3_fresh0$ID]))
write.table(twoD3_fresh0,file="twoD3_fresh0_FILT_results.txt",sep="\t",quote=FALS
E)

threeD3_fresh0 =
topTable(fit2,coef=4,adjust="fdr",p.value=0.05,number=Inf,lfc="1",sort.by="logFC")
threeD3_fresh0 =
cbind(threeD3_fresh0,as.character(entrez2[threeD3_fresh0$ID]),as.character(hugo2[thr
eeD3_fresh0$ID]))
write.table(threeD3_fresh0,file="threeD3_fresh0_FILT_results.txt",sep="\t",quote=FA
LSE)

twoD3_tissue0 =
topTable(fit2,coef=5,adjust="fdr",p.value=0.05,number=Inf,lfc="1",sort.by="logFC")
twoD3_tissue0 =
cbind(twoD3_tissue0,as.character(entrez2[twoD3_tissue0$ID]),as.character(hugo2[two
D3_tissue0$ID]))
write.table(twoD3_tissue0,file="twoD3_tissue0_FILT_results.txt",sep="\t",quote=FAL
SE)

threeD3_tissue0 =
topTable(fit2,coef=6,adjust="fdr",p.value=0.05,number=Inf,lfc="1",sort.by="logFC")
threeD3_tissue0 =
cbind(threeD3_tissue0,as.character(entrez2[threeD3_tissue0$ID]),as.character(hugo2[th
reeD3_tissue0$ID]))
write.table(threeD3_tissue0,file="threeD3_tissue0_FILT_results.txt",sep="\t",quote=FA
LSE)

cul_fresh =
topTable(fit2,coef=7,adjust="fdr",p.value=0.05,number=Inf,sort.by="logFC")
cul_fresh =
cbind(cul_fresh,as.character(entrez2[cul_fresh$ID]),as.character(hugo2[cul_fresh$ID]))
```

```
write.table(cul_fresh,file="cul_fresh_FILT_results.txt",sep="\t",quote=FALSE)

# perform and plot PCA to understand the relationship between samples:
resPCA2 <- pca(filtdata$eset,method="svd",nPcs=2)
cols <-
c("blue","red","green","purple","orange","blue","red","green","purple","orange","blue",
"red","green","purple","orange","black","black","black")
PCAscores <- cbind(scores(resPCA2),cols)
plot(scores(resPCA2),type="p", pch=19,main="PCA, all samples",col=cols)
legend("bottomright",as.character(unique(df$Levs)),fill=c("blue","red","green","purple"
,"orange","black"))

resPCA <- pca(filtdata$eset,method="svd",nPcs=3)
cols <-
c("blue","red","green","purple","orange","blue","red","green","purple","orange","blue",
"red","green","purple","orange","black","black","black")
PCAscores <- cbind(scores(resPCA),cols)
scatterplot3d(PCAscores, pch=19,col.axis="blue",col.grid="lightblue",main="3D PCA,
all samples",lty.hplot=1,type="h")

resPCA3 <- pca(filtdata$eset[,c(-16,-17,-18)],method="svd",nPcs=2)
cols <-
c("blue","red","green","purple","orange","blue","red","green","purple","orange","blue",
"red","green","purple","orange")
PCAscores <- cbind(scores(resPCA3),cols)
plot(scores(resPCA3),type="p", pch=19,main="PCA, no tissue",col=cols)
legend("topleft",as.character(unique(df$Levs[-c(16,17,18)])),fill=c("blue","red","green"
,"purple","orange"))

# perform gene set enrichment to identify Biological Proces GO categories enriched in
the differentially expressed genes:
universe = as.character(entrez2[fit$genes[,1]])
hgCutoff <- 0.001

all_sig = as.character(cul_fresh[,8])
params <-
new("GOHyperGParams",geneIds=all_sig,universeGeneIds=universe,annotation="rat2
302",ontology="BP",pvalueCutoff=hgCutoff,conditional=TRUE,testDirection="over")
hgOver <- hyperGTest(params)
write.table(summary(hgOver),file="BP_all_3Dv2D.txt",sep="\t",quote=FALSE,eol="\r
")

up_sig = as.character(cul_fresh[cul_fresh$logFC > 0, 8])
```

```
params <-
new("GOHyperGParams",geneIds=up_sig,universeGeneIds=universe,annotation="rat2
302",ontology="BP",pvalueCutoff=hgCutoff,conditional=TRUE,testDirection="over")
hgOver <- hyperGTest(params)
write.table(summary(hgOver),file="BP_up_3Dv2D.txt",sep="\t",quote=FALSE,eol="\r
")

down_sig = as.character(cul_fresh[cul_fresh$logFC < 0, 8])
params <-
new("GOHyperGParams",geneIds=down_sig,universeGeneIds=universe,annotation="ra
t2302",ontology="BP",pvalueCutoff=hgCutoff,conditional=TRUE,testDirection="over"
)
hgOver <- hyperGTest(params)
write.table(summary(hgOver),file="BP_down_3Dv2D.txt",sep="\t",quote=FALSE,eol=
"\r")

# perform gene set enrichment to identify Molecular Function GO categories enriched
in the differentially expressed genes:
all_sig = as.character(cul_fresh[,8])
params <-
new("GOHyperGParams",geneIds=all_sig,universeGeneIds=universe,annotation="rat2
302",ontology="MF",pvalueCutoff=hgCutoff, conditional=TRUE,testDirection="over")
hgOver <- hyperGTest(params)
write.table(summary(hgOver),file="MF_all_3Dv2D.txt",sep="\t",quote=FALSE,eol="\r
")

up_sig = as.character(cul_fresh[cul_fresh$logFC > 0, 8])
params <-
new("GOHyperGParams",geneIds=up_sig,universeGeneIds=universe,annotation="rat2
302",ontology="MF",pvalueCutoff=hgCutoff,conditional=TRUE,testDirection="over")
hgOver <- hyperGTest(params)
write.table(summary(hgOver),file="MF_up_3Dv2D.txt",sep="\t",quote=FALSE,eol="\r
")

down_sig = as.character(cul_fresh[cul_fresh$logFC < 0, 8])
params <-
new("GOHyperGParams",geneIds=down_sig,universeGeneIds=universe,annotation="ra
t2302",ontology="MF",pvalueCutoff=hgCutoff,conditional=TRUE,testDirection="over
")
hgOver <- hyperGTest(params)
write.table(summary(hgOver),file="MF_down_3Dv2D.txt",sep="\t",quote=FALSE,eol
="\r")

# end of code.
```

Appendix D: Differentially Gene Expression and Functional Enrichment

Differentially expressed genes of self-assembly culture in contrast to sandwich culture were identified at both day 3 and 6, using the moderated t-test from limma, online Bioconduction package. Expressions were considered Significant if the $p<0.05$ and log2 fold change>1. Indentified genes were then clustered by biological function from Gene Ontology (GO). Results were plotted in table 2 and 4. The "GOBPID", is the official GO ID. The "P-value" is generated if <0.001. The "Count" is the actual number of genes from the category that were shown to be differentially expressed. "Term" is the descriptive name of the GO category.

At day 3, there were 74 upregulated genes and 81 downregulated genes, together with 9599 unchanged genes (see table 1) Differentially expressed genes were clustered according different phases of drug metabolism.

Expression of phase I:

Drug metabolising enzymens (DMEs) such as Cyp isoforms of Cyp3a2, Cyp2c12, Cyp3a18 were upregulated. Others such as aldehyde dehydrogenases (aldh1a1), Fads1 and Fads2 (fatty acid desatures), Fabp1, Fabp2, Fabp5 where upregulated, while fmo1 and fom5(flavin containing monooxygenases), Fasd3 were downregulated. **Expression of phase II**

DMEs such as Gsta5 Gstt3 Gstm2 (glutathione transferases), sulfortransferases Sult2a2,

Ephx1 (epoxidases) Glucuronosyl transferases (Ugt2b1) and Aox1 (detoxification) were upregulated.

Expression of drug transporters,

Drug transporters, efflux transporters abcc3 was upregulated, as well as influx transporter (slc17a3, slc23a1 and slco1a4). In contrast, efflux transporter abca8a was downregulated.

Each gene is responsible for different functions including biological process, molecular process and cellular process. Likewise, each GO function also involves different genes. Biological process results are also concordant to the differential gene expression (see table 2). Metabolic functions were dramatically enhanced by involving oxidation reduction process (GO: 0055114), carboxylic acid metabolic process (GO: 0019754), fatty acid metabolic process (GO: 0006631), lipid metabolic process(GO: 0006629), toxin response(GO: 0009636), xenobiotics process(GO: 0006805), cholesterol (GO: 0006695) and steroid process (GO: 0006694), as well as transport of cholesterol (GO: 0033344) and steroid (GO: 0015918), etc., which suggests potential increase in the hepatocytes metabolic functions and detoxification. For example, Cyp3a2 was associated with steroid metabolic process, drug metabolic process, oxidation reduction process, steroid metabolic process. Fads1 and Fads2 were involved in oxidation reduction process. Lipid metabolic process was increased by Fads1 and Apoa2. Sterol metabolic process was increase by cyp3a2 and sutl2a2. Gstp1 was responsible for xenobiotics metabolic process. Response to nutrition was increased by Gstp1 and Fads1.

Apoa2 was one of the genes that controlled the response for cholesterol metabolic process and transportation to keep the balance of intercellular cholesterol concentrations. Interestingly, the response to extracellular stimulus of self-assembly culture was enriched, compared with sandwich culture. This may be a result of perfused medium, or bioreactors itself, because when hepatocytes grown in two different environments, culture medium was kept the same, but hepatocytes self-assembly formation, both culture were static. By applying perfused medium initially in bioreactor, self-assemblies require sometime to adapt to the new environment.

For downregulated biological functions, 4/7 functions were related to 3D structure, cell-cell adhesion, biological adhesion, cellular component assembly and anatomical structure morphogenesis. More specifically, for instance, Egln3 expression was downregulated. It controls the response to hypoxia, and apoptosis. Crystallin, alpha B (Cryab) also control the response to hypoxia and apoptosis which involved in morphogenesis. Transforming growth factor bata 2 (Tgfb2) is responsible for cell morphogenenis and hypoxia. Connective tissue growth factor (Ctgf) was downregulated, which controls cell adhesion and cell matrix adhesion. Cldn1 also involves in apoptosis. Downregulated functions that associated with structural and apoptosis genes in self-assembly culture indicate that hepatocytes grown in spheroids culture at day 3 required less cell adhesion function.

	Probe ID	HUGO ID	logFC	AveExpr	P Value	Entrez ID
Upregulated	1370593_at	Cyp3a2	3.84571	8.617763	7.52E-05	266682
	1368453_at	Fads2	3.253292	7.460552	2.10E-05	83512
	1371089_at	Gsta5	3.136509	7.153731	4.61E-05	494500
	1387936_at	Sult2a2	3.003281	4.496772	0.013098	361510
	1367857_at	Fads1	2.940322	9.960973	2.10E-05	84575
	1388122_at	Gstp1	2.881063	8.679225	0.016329	24426
	1373544_at	Cxcl9	2.777999	5.680957	0.000104	246759
	1368155_at	Cyp2c12	2.700177	6.75284	0.000373	25011
	1374070_at	Gpx2	2.557955	5.526963	0.018878	29326
	1387094_at	Slco1a4	2.526163	6.926136	0.000522	170698
	1383315_at	Tsku	2.377386	7.959319	0.000186	308843
	1370870_at	Me1	2.350227	7.979574	0.000756	24552
	1387312_a_at	Gck	2.166381	6.773703	8.02E-05	24385
	1367856_at	G6pd	2.159567	7.506985	0.001466	24377
	1377885_at	LOC685203	2.124861	4.755706	0.005325	685203
	1368736_at	Tsx	2.100767	6.31254	0.000898	29391
	1369727_at	Apoa2	1.979544	12.0465	0.001759	25649
	1369698_at	Abcc3	1.960034	5.194999	0.003713	140668
	1387022_at	Aldh1a1	1.946146	9.598334	0.00028	24188
	1398260_a_at	Serpind1	1.896871	9.983663	0.001139	79224
	1371237_a_at	Mt1a	1.856975	10.02515	0.005325	24567
	1387316_at	Cxcl1	1.85521	5.397089	0.048066	81503
	1369111_at	Fabp1	1.824371	11.73058	0.002833	24360
	1380013_at	Pnpla3	1.81123	4.223505	7.52E-05	362972
	1389725_at	Tm7sf2	1.697012	9.308164	0.000557	293688
	1382579_at	Tox3	1.684814	3.893562	0.018383	291908
	1388271_at	Mt2A	1.659938	8.328637	0.013772	689415
	1387599_a_at	Nqo1	1.625242	8.961162	0.048181	24314
	1387118_at	Cyp3a23/3a1	1.625106	11.90485	0.000954	25642
	1371942_at	Gstt3	1.617202	10.08042	8.00E-05	499422
	1376051_at	Cryl1	1.614743	8.079252	0.00285	290277
	1387669_a_at	Ephx1	1.523295	11.13532	0.001302	25315
	1394401_at	Elovl6	1.519851	5.555999	0.032679	171402
	1367707_at	Fasn	1.508558	7.611498	0.048352	50671
	1375852_at	Hmgcr	1.502059	9.834714	8.18E-05	25675
	1368335_at	Apoa1	1.491458	12.27112	0.000112	25081
	1369162_at	Gucy2c	1.489726	6.464048	0.000756	25711
	1387376_at	Aox1	1.480753	9.834889	0.0028	54349
	1368121_at	Akr7a3	1.472277	10.26097	0.019882	26760
	1370281_at	Fabp5	1.414278	9.069307	0.000834	140868
	1372306_at	Ethe1	1.403671	9.581192	0.014361	292710
	1368953_at	Uggt1	1.388696	5.394883	9.78E-05	171129

	1378032_at	Nfkbiz	1.332721	6.500001	0.001457	304005
	1370220_at	Scpep1	1.324925	8.482761	7.52E-05	114861
	1369581_at	Pemt	1.323155	9.457878	0.047976	25511
	1369195_at	Fabp2	1.296383	5.601247	0.002713	25598
	1370688_at	Gclc	1.295225	6.583787	0.001759	25283
	1380262_at	Sgk2	1.294136	5.556112	0.001139	171497
	1384905_at	Cd209g	1.293911	4.463301	0.030648	688750
	1387830_at	Crp	1.264798	11.51495	0.005308	25419
	1390591_at	Slc17a3	1.252854	8.363529	0.002248	266730
	1388689_at	Acyp2	1.236952	5.71725	0.028253	364224
	1383379_at	LOC684112	1.231213	6.410175	9.78E-05	684112
	1369169_at	Slc23a1	1.205948	6.531558	0.004829	50621
	1386980_at	Apom	1.197442	10.31777	0.000522	55939
	1370952_at	Gstm2	1.15982	10.84153	0.007301	24424
	1371462_at	Igfbp4	1.154188	6.845813	0.002635	360622
	1382325_at	Gcat	1.140749	7.663532	0.000126	366959
	1370698_at	Ugt2b1	1.140308	11.42334	0.006742	286954
	1374524_at	Scly	1.126779	8.854126	0.001991	363285
	1372973_at	Lss	1.118828	7.079914	0.003243	81681
	1387323_at	Klkb1	1.093269	8.451978	0.013085	25048
	1391626_at	Mnd1	1.055294	5.503925	0.007405	295160
	1390851_at	Lactb2	1.046756	9.279305	0.000112	297768
	1398307_at	Cyp3a18	1.042076	10.52841	0.037628	252931
	1376976_at	Sectm1b	1.035619	6.029167	0.042463	287884
	1379411_at	RGD156382	1.032032	6.598908	0.018878	306366
	1389156_at	LOC498606	1.030286	7.585291	4.61E-05	498606
	1368270_at	Apobec1	1.027883	6.223581	0.011662	25383
	1380854_at	Vegfb	1.024764	6.263402	0.001472	89811
	1369671_at	Otc	1.022241	10.58549	0.001979	25611
	1387926_at	Sc5dl	1.011906	9.352712	0.005334	114100
	1368323_at	Tfpi	1.003836	6.155175	0.002752	29436
	1398286_at	Csad	1.001125	9.429573	0.002248	60356
Downregulated	1389857_at	Wbp5	-1.01049	7.683627	0.02931	680354
	1376157_at	Uba6	-1.01553	6.784264	0.037628	305268
	1397552_at	Eml4	-1.01643	6.810659	0.027229	313861
	1388456_at	S100a1	-1.01666	4.86333	0.018878	295214
	1392590_at	Arhgap24	-1.01686	6.331304	0.004019	305156
	1368429_at	Taf9b	-1.02622	3.030792	0.001767	171152
	1383047_at	Gas6	-1.02651	8.543171	0.003948	58935
	1368491_at	Dnase2b	-1.02758	6.740749	0.00371	59296
	1375870_a_at	Rbms1	-1.03026	6.591849	0.006738	362138
	1375933_at	Cldn2	-1.03367	6.540045	0.009398	300920
	1383248_at	Fmo5	-1.04666	8.454229	0.035151	246248

1389546_at	Amotl2	-1.05279	8.266365	0.00065	65157
1383732_at	RGD130760	-1.0623	6.474999	0.027229	293656
1388686_at	Rcan1	-1.06897	9.919079	0.026861	266766
1375367_at	Pdlim2	-1.07146	5.342893	0.034941	290354
1390783_at	Abca8a	-1.09055	7.845072	0.042948	303638
1367601_at	Cited2	-1.10603	7.923327	0.035811	114490
1393337_at	Tcfcp2l1	-1.12161	4.570225	0.004746	304741
1371537_at	B4galt5	-1.1808	7.016403	0.0264	362275
1370234_at	Fn1	-1.18117	11.52519	0.009351	25661
1394077_at	Rnd3	-1.18831	5.728511	0.001767	295588
1376100_at	Tubb6	-1.19248	6.226581	0.048181	307351
1398373_at	B3galnt1	-1.2176	5.023027	0.002833	310508
1372476_at	Fads3	-1.21794	6.644279	0.00285	286922
1380668_at	MGC72974	-1.21982	3.983899	0.000898	316976
1370778_at	Mup5	-1.22727	4.061135	0.042463	298107
1389034_at	Usp18	-1.22867	5.493412	0.037628	312688
1369732_a_at	St3gal2	-1.23571	3.521312	0.001929	64442
1389166_at	Cib2	-1.23695	3.747288	0.016593	300719
1384742_at	Atrx	-1.27235	4.207309	0.003713	246284
1383433_at	Klhl23	-1.30274	4.098631	0.002525	311114
1367794_at	A2m	-1.30672	6.659536	0.043942	24153
1367584_at	Anxa2	-1.33312	9.132349	0.004177	56611
1381533_at	Rnd1	-1.338	6.706573	0.023129	362993
1380536_at	RGD1305928	-1.35342	5.679896	0.000193	300207
1390455_at	Abhd2	-1.36625	8.164239	0.035811	293050
1375612_at	Hnrnpa1	-1.37522	6.468093	0.016824	29578
1370202_at	Pla2g16	-1.38188	8.28044	0.001139	24913
1385707_at	Lect2	-1.38821	10.38656	0.001685	361205
1391897_at	Rabgap1l	-1.39717	5.432859	0.001086	304914
1393902_at	Akr1c1	-1.40627	4.693265	0.003612	307092
1370479_x_at	Obp3	-1.40866	7.119273	0.00788	259247
1388718_at	Tmod1	-1.42999	6.119257	0.043542	25566
1379440_at	Fstl3	-1.43238	4.884127	4.61E-05	114031
1386994_at	Btg2	-1.44885	7.224075	0.001412	29619
1391935_at	Eif4e3	-1.46046	3.745651	0.001469	297481
1380515_at	Bbs7	-1.46843	5.608216	0.014411	361930
1371412_a_at	Nrep	-1.52647	6.217641	0.005841	338475
1377642_at	Cav2	-1.54286	7.290598	0.00257	363425
1384254_at	Otud1	-1.56744	7.785086	0.001991	498803
1380250_at	Sned1	-1.58955	5.422594	4.61E-05	316638
1386890_at	S100a10	-1.59433	8.956616	0.012953	81778
1385570_at	LOC10036228	-1.60579	4.56143	0.011559	1E+08
1392754_at	Adam8	-1.61936	4.584755	0.020666	499285

1397536_at	Camta1	-1.64732	2.659401	0.018878	500591
1385089_at	Grhl1	-1.66196	3.634912	0.00919	313993
1383743_at	Lrrc16a	-1.69336	4.514479	0.004177	306941
1369202_at	Mx2	-1.70371	4.15276	0.015273	286918
1367905_at	Enpp3	-1.72934	8.75484	7.52E-05	54410
1389270_x_at	LOC680367	-1.77777	9.26235	0.049867	680367
1388255_x_at	RT1-CE5	-1.81384	6.271707	0.000551	309607
1372316_at	Sgk493	-1.86671	8.151535	0.039155	313860
1368174_at	Egln3	-1.90623	4.969586	4.61E-05	54702
1370026_at	Cryab	-1.94243	8.651999	0.00098	25420
1368627_at	Rgn	-1.94815	7.205149	0.000316	25106
1371922_at	Car12	-1.95231	6.155915	0.00478	363085
1373378_at	Agtpbp1	-2.0336	5.813454	0.000112	290986
1392382_at	Tgfb2	-2.11201	3.729203	0.041857	81809
1387343_at	Cebpd	-2.11686	5.373323	0.032457	25695
1376646_at	Popdc2	-2.1815	5.741144	0.000112	360718
1375138_at	Timp3	-2.23993	4.080555	0.002713	25358
1387455_a_at	Vldlr	-2.302	3.251942	4.61E-05	25696
1367574_at	Vim	-2.38292	7.898508	0.000898	81818
1372111_at	Cav1	-2.44691	4.38686	0.040728	25404
1383946_at	Cldn1	-2.46822	7.10073	4.61E-05	65129
1387156_at	Hsd17b2	-2.6005	6.968024	0.04261	79243
1373654_at	Anxa8	-2.67149	5.478651	2.57E-05	306283
1393221_at	RGD1564865	-2.73263	6.295987	0.000172	498789
1367896_at	Car3	-2.92772	8.198576	0.01979	54232
1367631_at	Ctgf	-2.93509	8.74889	2.08E-06	64032
1387053_at	Fmo1	-4.07811	7.276036	0.000244	25256

Table 1 List of Differentially Expressed Gene in Self-assembly Culture Compared with Sandwich Culture at day 3

	GOBPID	P-value	Count	Term
Upregulated	GO:0055114	2.55E-17	52	oxidation reduction
	GO:0016125	1.20E-12	19	sterol metabolic process
	GO:0042180	4.04E-12	48	cellular ketone metabolic process
	GO:0006082	8.62E-12	47	organic acid metabolic process
	GO:0006694	6.24E-11	18	steroid biosynthetic process
	GO:0006695	3.40E-10	10	cholesterol biosynthetic process
	GO:0008654	1.37E-08	15	phospholipid biosynthetic process
	GO:0044281	2.21E-08	37	small molecule metabolic process
	GO:0046688	4.46E-08	9	response to copper ion

GO:0044255	1.59E-07	23	cellular lipid metabolic process
GO:0044106	1.88E-07	24	cellular amine metabolic process
GO:0009991	3.98E-06	27	response to extracellular stimulus
GO:0009410	4.07E-06	8	response to xenobiotic stimulus
GO:0045017	6.14E-06	11	glycerolipid biosynthetic process
GO:0044283	6.34E-06	32	small molecule biosynthetic process
GO:0010876	1.18E-05	15	lipid localization
GO:0006805	1.44E-05	7	xenobiotic metabolic process
GO:0008299	1.78E-05	6	isoprenoid biosynthetic process
GO:0006631	2.69E-05	19	fatty acid metabolic process
GO:0050896	3.30E-05	99	response to stimulus
GO:0009636	3.35E-05	11	response to toxin
GO:0006749	3.36E-05	7	glutathione metabolic process
GO:0006629	3.46E-05	16	lipid metabolic process
GO:0006656	3.67E-05	5	phosphatidylcholine biosynthetic process
GO:0050892	3.67E-05	5	intestinal absorption
GO:0006732	3.67E-05	10	coenzyme metabolic process
GO:0006767	4.35E-05	7	water-soluble vitamin metabolic process
GO:0019287	4.56E-05	3	isopentenyl diphosphate biosynthetic process, mevalonate pathway
GO:0046490	4.56E-05	3	isopentenyl diphosphate metabolic process
GO:0033344	5.08E-05	6	cholesterol efflux
GO:0015918	5.56E-05	7	sterol transport
GO:0019637	5.75E-05	15	organophosphate metabolic process
GO:0019218	6.93E-05	8	regulation of steroid metabolic process
GO:0009108	8.05E-05	10	coenzyme biosynthetic process
GO:0032787	8.83E-05	12	monocarboxylic acid metabolic process
GO:0007584	1.04E-04	18	response to nutrient
GO:0046395	1.09E-04	12	carboxylic acid catabolic process
GO:0006575	1.55E-04	12	cellular amino acid derivative metabolic process
GO:0043691	1.76E-04	4	reverse cholesterol transport
GO:0065005	1.76E-04	4	protein-lipid complex assembly
GO:0070189	1.78E-04	3	kynurenine metabolic process
GO:0007586	2.40E-04	7	digestion
GO:0042439	2.52E-04	6	ethanolamine and derivative metabolic process
GO:0045540	2.86E-04	4	regulation of cholesterol biosynthetic process
GO:0006725	2.91E-04	12	cellular aromatic compound metabolic process
GO:0009611	3.94E-04	26	response to wounding
GO:0034380	4.32E-04	3	high-density lipoprotein particle assembly
GO:0046394	4.63E-04	14	carboxylic acid biosynthetic process
GO:0019752	6.16E-04	10	carboxylic acid metabolic process
GO:0034367	6.37E-04	4	macromolecular complex remodeling
GO:0034369	6.37E-04	4	plasma lipoprotein particle remodeling

	GO:0006752	9.09E-04	5	group transfer coenzyme metabolic process
Downregulated	GO:0016337	7.44E-05	12	cell-cell adhesion
	GO:0031579	2.02E-04	3	membrane raft organization
	GO:0022610	4.46E-04	20	biological adhesion
	GO:0022607	4.70E-04	32	cellular component assembly
	GO:0009653	6.59E-04	38	anatomical structure morphogenesis
	GO:0070836	7.66E-04	2	caveola assembly
	GO:0070970	7.66E-04	2	interleukin-2 secretion

Table 2 List of GO biological process enriched in self-assembly culture and sandwich culture at day 3

At the end of culture, day 6, there were 57 upregulated genes and 87 downregulated genes (see table 3), together with 9610 unchanged genes. Similarly, majority phase I, II, and III DMEs from upregulated genes were remained upregulated at day 6. After enrichment for biological process of differentially expressed genes, 11 out of 25 functions were involved with metabolic process (see table 4), including or oxidation reduction process (GO: 0055114), fatty acid metabolic process (GO: 0006631), lipid metabolic process (GO: 0006629), cholesterol metabolic process (GO: 0008203), steroid metabolic process (GO: 0008202) etc. the rest of upregulated functions were include absorption (GO: 0050892), digestion (GO: 0007856), transportation (GO: 0015718), as well as response to chemical stimulus (GO: 0042221). All of the upregulated functions show the potential of capable of metabolism more xenobiotics or chemicals. Only 4 downregulated functions detected at day 6, response to hydrostatic pressure (GO: 0051599), epithelial cell development (GO: 0002064), regulation of collagen metabolic process (GO: 0010712) and regulation of peptidase activity (GO: 0052547). Bmp4 (bone morphogenetic protein 4) is partly associated with epithelial cell development. Adora2b (an adenosine receptor that is a member of the G protein-coupled

receptor superfamily), bmp4 and ctgf is involved in regulation of collagen metabolic process. Cav1 (caveolin 1, caveolae protein) is involved with peptidase activity. It is not clear that what caused the downregulated genes involved in those processes. Investigation should be carried out in future. Overall, self-assembly sphenoid culture in micro-patterned bioreactor provide a novel tool, that maintains cell viability, and metabolising activity, which can be potentially used for improving hepatotoxicity testing.

	Probe ID	HUGO ID	logFC	AveExpr	adj.P.Val	EntrezID
Upregulated	1370593_at	Cyp3a2	5.525839	8.617763	4.61E-06	266682
	1387936_at	Sult2a2	3.12118	4.496772	0.009934	361510
	1371089_at	Gsta5	2.992702	7.153731	5.63E-05	494500
	1369162_at	Gucy2c	2.546552	6.464048	5.95E-06	25711
	1387118_at	Cyp3a23/3a1	2.435363	11.90485	2.57E-05	25642
	1387094_at	Slco1a4	2.414695	6.926136	0.00068	170698
	1379411_at	RGD1563825	2.325986	6.598908	3.74E-05	306366
	1369727_at	Apoa2	2.267324	12.0465	0.000616	25649
	1371237_a_at	Mt1a	2.204803	10.02515	0.002177	24567
	1369921_at	Gstm3	2.142734	6.82948	0.009729	57298
	1370870_at	Me1	2.022065	7.979574	0.002677	24552
	1369660_at	Defb1	1.991498	4.458911	0.000542	83687
	1370698_at	Ugt2b1	1.95912	11.42334	0.000105	286954
	1368155_at	Cyp2c12	1.896901	6.75284	0.005695	25011
	1369698_at	Abcc3	1.885578	5.194999	0.005695	140668
	1368374_a_at	Ggt1	1.873373	5.051503	0.011245	116568
	1373975_at	Inmt	1.864836	5.576214	0.007106	368066
	1388014_at	Obp1f	1.838682	5.039916	0.002388	192267
	1367668_a_at	Scd	1.741589	3.192091	0.026239	83792
	1398307_at	Cyp3a18	1.732549	10.52841	0.002056	252931
	1385189_at	Duoxa1	1.714773	4.15228	0.002489	311374
	1373544_at	Cxcl9	1.709347	5.680957	0.005695	246759
	1378848_at	Asb5	1.658048	4.162042	0.006564	361187
	1383315_at	Tsku	1.650625	7.959319	0.00406	308843
	1368453_at	Fads2	1.640234	7.460552	0.003968	83512
	1375719_s_at	Cdh13	1.582737	4.037804	0.022033	192248
	1379275_at	Snx10	1.567586	3.636595	0.000636	297096

	1370464_at	Abcb1a	1.557513	5.639401	0.000393	170913
	1377885_at	LOC685203	1.45305	4.755706	0.040347	685203
	1385165_at	Cyp39a1	1.451729	8.163682	0.000573	301264
	1376973_at	Sdcbp2	1.416738	4.023587	5.95E-06	311532
	1369195_at	Fabp2	1.368829	5.601247	0.00229	25598
	1370390_at	Coro6	1.31439	4.291514	0.000245	245982
	1369581_at	Pemt	1.308058	9.457878	0.042221	25511
	1387376_at	Aox1	1.303003	9.834889	0.007106	54349
	1367648_at	Igfbp2	1.284252	5.452385	0.01482	25662
	1370220_at	Scpep1	1.280521	8.482761	0.000105	114861
	1369111_at	Fabp1	1.256641	11.73058	0.026357	24360
	1367857_at	Fads1	1.233687	9.960973	0.011669	84575
	1375852_at	Hmgcr	1.230419	9.834714	0.000555	25675
	1387323_at	Klkb1	1.223741	8.451978	0.006564	25048
	1376248_at	Sult2b1	1.189759	6.024827	0.016215	292915
	1378032_at	Nfkbiz	1.186656	6.500001	0.003746	304005
	1398551_at	Ttc25	1.178751	5.028401	0.041996	303534
	1387137_at	Comp	1.168853	2.974529	0.026157	25304
	1376051_at	Cryl1	1.153092	8.079252	0.022832	290277
	1387109_at	Por	1.131602	8.518513	0.001415	29441
	1370952_at	Gstm2	1.131392	10.84153	0.008451	24424
	1387830_at	Crp	1.127324	11.51495	0.010988	25419
	1398260_a_at	Serpind1	1.125806	9.983663	0.028758	79224
	1385901_at	Ptdss2	1.112003	4.508284	0.00882	293620
	1380504_at	Acaa2	1.058125	6.987991	0.041892	170465
	1391626_at	Mnd1	1.050295	5.503925	0.007528	295160
	1387312_a_at	Gck	1.022039	6.773703	0.020144	24385
	1383379_at	LOC684112	1.015123	6.410175	0.000602	684112
	1377662_at	Pir	1.006727	7.625273	0.044983	363465
	1390851_at	Lactb2	1.000267	9.279305	0.000226	297768
Downregulated	1376496_at	Apol9a	-1.01048	5.392064	0.005325	503164
	1390944_at	Chmp4c	-1.01214	6.179061	0.007106	361916
	1370243_a_at	Ptma	-1.03632	9.081609	0.023236	29222
	1373657_at	Slc31a2	-1.03736	6.706341	0.025915	298091
	1388456_at	S100a1	-1.04287	4.86333	0.01482	295214
	1370295_at	Nme1	-1.05403	7.832078	0.000536	191575
	1370855_at	Cst3	-1.05959	10.8354	0.000226	25307
	1370202_at	Pla2g16	-1.06724	8.28044	0.007137	24913
	1377307_at	Fam89a	-1.06945	6.485642	0.032259	361441
	1369450_at	Ust5r	-1.0765	6.86404	0.032235	171398
	1371542_at	Tuba4a	-1.0825	9.076921	0.005695	316531
	1389166_at	Cib2	-1.08656	3.747288	0.028461	300719
	1391611_at	Kif12	-1.08756	4.442988	0.042265	313254

1394616_at	Mesdc2	-1.09314	5.585738	0.034931	308796
1371436_at	Ddah2	-1.10398	5.072493	0.038514	294239
1387197_at	Omd	-1.10732	7.607428	0.00948	83717
1388403_at	Idh2	-1.13069	9.474528	0.000105	361596
1387455_a_at	Vldlr	-1.14012	3.251942	0.008765	25696
1375003_at	Serpinb6a	-1.15206	5.098335	0.030014	291085
1367601_at	Cited2	-1.16095	7.923327	0.025289	114490
1387816_at	Igfals	-1.17934	6.237179	0.006932	79438
1388666_at	Enc1	-1.18206	7.612483	0.048642	294674
1372476_at	Fads3	-1.18907	6.644279	0.003968	286922
1394077_at	Rnd3	-1.19753	5.728511	0.002177	295588
1387372_at	Slc6a13	-1.21016	6.968802	0.015461	171163
1371537_at	B4galt5	-1.21214	7.016403	0.020629	362275
1396820_at	Hdac1	-1.21272	5.5519	0.017065	297893
1391897_at	Rabgap1l	-1.21351	5.432859	0.003515	304914
1372205_at	Zfp278	-1.24991	3.467802	0.00483	305471
1372870_at	Kdelr3	-1.26012	5.562059	0.002831	315131
1384023_at	Spin2a	-1.26189	3.55122	0.006932	317395
1391059_at	Npw	-1.27279	3.415089	0.023877	259224
1379238_at	Ctdsp1	-1.3024	2.99332	0.00229	301056
1384742_at	Atrx	-1.32724	4.207309	0.003407	246284
1391022_at	Lamb3	-1.32867	4.384292	0.015866	305078
1387232_at	Bmp4	-1.3358	4.145717	0.042221	25296
1368174_at	Egln3	-1.3554	4.969586	0.000602	54702
1394960_at	Sdr42e1	-1.3588	6.669354	0.038014	307897
1384580_at	C6	-1.36561	7.298224	0.002788	24237
1385707_at	Lect2	-1.37881	10.38656	0.00229	361205
1373677_at	Slc39a10	-1.41451	4.004656	0.023609	363229
1377642_at	Cav2	-1.46444	7.290598	0.004017	363425
1368290_at	Cyr61	-1.47997	6.276799	0.03642	83476
1387395_at	Adora2b	-1.49813	5.789894	0.045925	29316
1369202_at	Mx2	-1.51032	4.15276	0.025814	286918
1387995_a_at	Ifitm3	-1.5363	9.236767	0.027413	361673
1368147_at	Dusp1	-1.53864	6.60475	0.005695	114856
1380250_at	Sned1	-1.53869	5.422594	5.63E-05	316638
1373970_at	Il33	-1.55588	6.086147	0.030516	361749
1367905_at	Enpp3	-1.55806	8.75484	0.00022	54410
1385570_at	LOC100362283	-1.56313	4.56143	0.012291	1E+08
1384824_at	Pcdh18	-1.56573	6.000039	0.026357	295027
1371083_at	LOC299282	-1.58708	7.585863	0.000573	299282
1391935_at	Eif4e3	-1.61188	3.745651	0.00068	297481
1371034_at	Onecut1	-1.61195	7.173121	0.032389	25231
1373378_at	Agtpbp1	-1.63525	5.813454	0.000916	290986

1374683_at	Sgcg	-1.64687	5.139667	0.024267	305941
1370157_at	Pln	-1.67066	3.33205	0.000113	64672
1379625_at	Fam164a	-1.68609	4.603996	0.013731	310244
1371412_a_at	Nrep	-1.74717	6.217641	0.002788	338475
1388686_at	Rcan1	-1.76653	9.919079	0.001077	266766
1367570_at	Tagln	-1.78403	4.424931	0.046611	25123
1367631_at	Ctgf	-1.813	8.74889	0.000114	64032
1375367_at	Pdlim2	-1.82675	5.342893	0.001315	290354
1383915_at	LOC686120	-1.83015	5.266248	0.002322	686120
1367574_at	Vim	-1.84287	7.898508	0.005731	81818
1392754_at	Adam8	-2.02907	4.584755	0.005695	499285
1368171_at	Lox	-2.06745	3.150072	0.010168	24914
1393902_at	Akr1c1	-2.16973	4.693265	0.000113	307092
1370026_at	Cryab	-2.1824	8.651999	0.000405	25420
1368627_at	Rgn	-2.2457	7.205149	0.000105	25106
1370479_x_at	Obp3	-2.2573	7.119273	0.000231	259247
1372316_at	Sgk493	-2.29842	8.151535	0.01175	313860
1374434_at	LOC498222	-2.32529	5.211738	0.019923	498222
1376646_at	Popdc2	-2.59111	5.741144	2.57E-05	360718
1383946_at	Cldn1	-2.61517	7.10073	2.21E-05	65129
1388255_x_at	RT1-CE5	-2.65149	6.271707	1.91E-05	309607
1392382_at	Tgfb2	-2.93928	3.729203	0.00665	81809
1372111_at	Cav1	-2.99528	4.38686	0.012891	25404
1373654_at	Anxa8	-3.00459	5.478651	5.95E-06	306283
1381557_at	Gna14	-3.0574	4.929507	0.008257	309242
1367896_at	Car3	-3.5147	8.198576	0.006712	54232
1389270_x_at	LOC680367	-3.63793	9.26235	0.000542	680367
1393221_at	RGD1564865	-3.7357	6.295987	1.21E-05	498789
1387053_at	Fmo1	-3.81539	7.276036	0.000536	25256
1387156_at	Hsd17b2	-4.11075	6.968024	0.003082	79243
1370396_x_at	Rup2	-4.21871	9.929823	0.000602	619560

Table 3 List of Differentially Expressed Gene in Self-assembly Culture Compared with Sandwich Culture at day 6

	GOBPID	P-value	Count	Term
Upregulated	GO:0042180	4.0719E-07	33	cellular ketone metabolic process
	GO:0019752	7.21E-07	32	carboxylic acid metabolic process
	GO:0006082	8.81E-07	32	organic acid metabolic process
	GO:0006631	3.91E-06	18	fatty acid metabolic process
	GO:0050892	1.20E-05	5	intestinal absorption
	GO:0051186	1.47E-05	17	cofactor metabolic process
	GO:0006629	1.81E-05	21	lipid metabolic process
	GO:0007586	5.65E-05	7	digestion
	GO:0008203	7.28E-05	9	cholesterol metabolic process
	GO:0008202	1.15E-04	14	steroid metabolic process
	GO:0016042	1.83E-04	12	lipid catabolic process
	GO:0007568	2.02E-04	13	aging
	GO:0034380	2.18E-04	3	high-density lipoprotein particle assembly
	GO:0006656	2.64E-04	4	phosphatidylcholine biosynthetic process
	GO:0030258	3.15E-04	10	lipid modification
	GO:0006752	3.16E-04	5	group transfer coenzyme metabolic process
	GO:0006575	3.31E-04	12	cellular amino acid derivative metabolic process
	GO:0015718	5.46E-04	7	monocarboxylic acid transport
	GO:0042221	5.70E-04	53	response to chemical stimulus
	GO:0043627	5.70E-04	12	response to estrogen stimulus
	GO:0055114	6.62E-04	23	oxidation reduction
	GO:0008654	7.08E-04	8	phospholipid biosynthetic process
	GO:0006635	7.36E-04	6	fatty acid beta-oxidation
	GO:0002740	8.07E-04	2	negative regulation of cytokine secretion involved in immune response
Downregulated	GO:0051599	1.63E-04	3	response to hydrostatic pressure
	GO:0002064	7.62E-04	7	epithelial cell development
	GO:0010712	9.11E-04	5	regulation of collagen metabolic process
	GO:0052547	9.14E-04	13	regulation of peptidase activity

Table 4 List of GO biological process enriched in self-assembly culture and sandwich culture at day 6